MATRUSRI ENGINEERING COLLEGE

(Sponsored by Matrusri Education Society, Estd.1980)
(Approved by AICTE & Affiliated to Osmania University)
#16-1-486, Saidabad, Hyderabad – 500 059. Ph: 040-24072764
Email: matrusri.principal@gmail.com, www.matrusri.edu.in

INDEX

3.3.3 Number of extension and outreach programs conducted by the institution through NSS/NCC/Red cross/YRC etc., (inclu the programmes such as Swachh Bharat, AIDS awareness, Gender issues etc. and/or those organised in collaboration with indu community and NGOs)

A.Y: 2018-19

Sl. No.	Name of the teacher	Title of the book/chapters published	Title of the paper	Title of the proceedings of the conference	Year of publication	ISBN/ISSN number of the proceeding	Whether at the time of publication Affiliating Institution Was same Yes/NO	Name of the publisher	Page No.
1	B.Udaya sree	-	Analysis of M20 Grade concrete using Silico Manganese Slag as a partial replacement of coarse Aggregate	Recent Advances in Civil engineering Infrastructure(RACEI-2019)	2018-19	978-93-8935-486-7	Yes	BS Publications	1-9
2	T.RajaRamanna	-	Analysis of M20 Grade concrete using Silico Manganese Slag as a partial replacement of coarse Aggregate	Recent Advances in Civil engineering Infrastructure(RACEI-2019)	2018-19	978-93-8935-486-7	Yes	BS Publications	10-18

3	K.Smitha	-	Evaluation of capacity of Roundabout at Necklace road using Gap Acceptance method	Recent Advances in Civil engineering Infrastructure((RACEI-2019)	2018-19	ISBN:978-93-8935-486-7	Yes	BS Publications	19-24
4	P.Dhanmma	-	A Design of Concrete Bridge	Recent Advances in Civil engineering Infrastructure((RACEI-2019)	2018-19	978-93-8935-486-7	Yes	BS Publications	25-40
5	T.RajaRamanna	-	A Design of Concrete Bridge	Recent Advances in Civil engineering Infrastructure((RACEI-2019)	2018-19	978-93-8935-486-7	Yes	BS Publications	41-56
6	S.lokeswari	-	Influence of velocity on Major lift irrigation projects	Recent Advances in Civil engineering Infrastructure((RACEI-2019)	2018-19	978-93-8935-486-7	Yes	BS Publications	57-61
7	M. Pratibha	-	Influence of velocity on Major lift irrigation projects	Recent Advances in Civil engineering Infrastructure((RACEI-2019)	2018-19	ISBN:978-93-8935-486-7	Yes	BS Publications	62-66
8	Mrs. M. Srividya	-	Analysis of liquefaction of soil using SPT data	Recent Advances in Civil engineering Infrastructure((RACEI-2019)	2018-19	ISBN:978-93-8935-486-7	Yes	BS Publications	67-73
9	P.Dhanamma	-	Analysis of liquefaction of soil using SPT data	Recent Advances in Civil engineering Infrastructure((RACEI-2019)	2018-19	ISBN:978-93-8935-486-7	Yes	BS Publications	74-80
10	P.Ashveen Kumar	-	A Review on Light Weight Vermiculite Concrete	Recent Advances in Civil engineering Infrastructure((RACEI-2019)	2018-19	ISBN:978-93-8935-486-7	Yes	BS Publications	81-85

11	S.lokeswari	-	Evaluation studies of Existing Aqueduct on Kalwakurthy Main Canal of Mahatma Gandhi Lift Irrigation Scheme in Mahabubnagar District	Recent Advances in Civil engineering Infrastructure((RACEI-2019)	2018-19	ISBN:978-93-8935-486-7	Yes	BS Publications	86-91
12	T.RajaRamanna	-	Evaluation studies ofExisting Aqueduct on Kalwakurthy Main Canal of Mahatma Gandhi Lift Irrigation Scheme in Mahabubnagar District	Recent Advances in Civil engineering Infrastructure((RACEI-2019)	2018-19	978-93-8935-486-7	Yes	BS Publications	92-97
13	M. Pratibha	-	Evaluation studies ofExisting Aqueduct on Kalwakurthy Main Canal of Mahatma Gandhi Lift Irrigation Scheme in Mahabubnagar District	Recent Advances in Civil engineering Infrastructure((RACEI-2019)	2018-19	978-93-8935-486-7	Yes	BS Publications	98-103
14	T.Vishnu	-	Green synthesis and characterization of silver nanoparticles by using mango leaf extract	National seminar on Recent advances in materials and chemical sciences	2018-19		Yes	Dept of Chemistry, Sri Venkateshwara University	104-111
15	K.Aruna	-	Book detection using Deep learning	3rd International Conference on Computing Methodologies and Communication (ICCMC 2019)	2018-19	978-1-5386-7808-4	Yes	IEEE Explorer	112-116
16	A S Keerthi Nayani	-	Design and implementation of Uart protocol for avionics applications	ICICCS-2019,IEEE conference	2018-19	978-1-5386-8113-8	Yes	IEEE Explorer	117-125

17	T.Vishnu	-	Synthesis and Characetrzation of Bio nano Composite Films and their Antimicribial studies	Emerging trends in chemical sciences	2018-19		Yes	Dravidian University sponsored by UGC	126-135
18	Dr. Pallavi Khare	-	QWERTY Keyboard in Virtual Domain Using Image Processing	3rd International Conference on Intelligent Computing and Control systems (ICICCS 2019) IEEE	2018-19	978-1-5386-8112-1	Yes	IEEE Explorer	136-142
19	Dr.M.Sushanth Babu	-	PS-DCT Image Functioned Framework for Steganography	IEEE International Conference on Recent Innovations in Electrical, Electronics and Communication Engineering	2018-19	ISBN: CFP18P98-PRT/978-1-5386-5994-6	Yes	School of Electrical EngineeringKIIT	143-152
20	Mr. C. Venkateshwar Reddy	-	Effect of Benzoxazine on Epoxy Based Carbon Fabric Reinforced Composites for High Strength Applications	Proceedings of International Conference on Intelligent Manufacturing and Automation	2018-19		Yes	Dwarkadas J. Sanghvi College of Engineering	153-168
21	A S Keerthi Nayani	-	Prevention of Gas Leakage Hazards in home	Smart DSC2018(Research on smart technologies in data science and communications)	2018-19	978-0-9876174-5-3	Yes	VIIT	169-175
22	Dr. Ashok Kumar K	-	Improvement of Code Utilization CDMA for On-Chip Communication Architecture using Orthogonal Gold Code	International Conference on Inventive Computation Technologies	2018-19	978-1-5386-4984-8	Yes	IEEE	176-183

23	V.Karunakar Reddy	Coding Theory	Combined Crosstalk Avoidance Code With Error Control Code For Detectionof Random And Burst Errors	-	2018-19	978-1-78984-443-6	Yes	Intech Open	184-195
24	Dr.M.Sushanth Babu	MuplitpleInputs Multiple Output Basic Concept for Research	-	-	2018-19	978-1-365-69776-0	Yes	LULU Publisher	196-197
25	Dr.M.Sushanth Babu	Low Power Transmission System Based on Smart Technologies	-	-	2018-19	978-1-365-69777-7	Yes	Barnes & Noble Press	198-200
26	Dr. Ashok Kumar K	Coding Theory	Combined CrossTalk avoidance Code With error Control Code for detection of Random and bursts error	-	2018-19	978-1-78984-443-6	Yes	Intech Open	201-212
27	Dr. G.Shyama Chandra Prasad	C Programming coding and aptitude approach	C Programming coding and aptitude approach	-	2018-19	978-81-920425-5-8	Yes	UMA Publishers	213-215

Principal

Principal
Maturi Engineering College
Saidabad, Hyderabad.

RACEI 2019

Proceedings

International Conference on

Recent Advances in Civil Engineering Infrastructure

(With a Focal theme of Sustainable Development Goals)

16-18 December 2019

Organized by

DEPARTMENT OF CIVIL ENGINEERING

MUFFAKHAM JAH COLLEGE OF ENGINEERING AND TECHNOLOGY, HYDERABAD, INDIA

International Conference on Recent Advances in Civil Engineering Infrastructure (RACEI-2019)
Department of Civil Engineering, Muffakham Jah College of Engineering and Technology

Analysis of M20 Grade Concrete using Silico Manganese Slag as a Partial Replacement of Coarse Aggregate

B. Udayasree and T. Raja Ramanna

Abstract: Global warming and Environmental degradation have become one of the major issues in recent years. The scarcity of raw materials required for construction is increasing day by day to globalization. The main challenge for the researches and engineers is to preventing the exhaustion of natural resources and increasing the usage of industrial wastage. The rapid rate of growth in population in India as forced the construction industry to use the building materials at rapid rate and resulting in depletion of natural resources and also has a severe impact on the environment causing many hazards either directly or indirectly such as depletion of river due to sand mining being done at alarming rate etc. On the other hand industrialization, rapid growth of industries in India gave birth to numerous kinds of waste products. In the present study Silico Manganese slag which is a byproduct from Ferro Alloys Industries is used as partial replacement of coarse aggregate. The slag will generate during chemical reaction of manganese ore, quartz, dolomite and coal. Main product obtained is Silico Manganese. Ferro Alloys are used as inputs in the manufacture of iron and steel for removal of oxygen and imparting specific properties. These are alloys of iron and elements like manganese, silicon, chromium, etc. The project aims to study experimentally the effect of replacement of coarse aggregate by silico manganese slag on its properties of concrete. The mix design considered in this study is M_{20} Grade of concrete. In this study natural coarse aggregate has been replaced by Silico Manganese slag by 0%, 5%, 10%, 15%, and 20%.

Key Words: Silico Manganese Slag, Industrial byproducts

I. INTRODUCTION

A. Introduction to Concrete:

Concrete is widely used structural material consisting essentially of a binder and mineral filler. It has the unique distinction of being the only construction material actually manufactured on the site, whereas other materials are merely shaped to use at the worksite. Good or bad concrete is made from the same discrete materials like grains of sand, gravel or pieces of crushed rock and the innumerable fine particles of cement powder mixed with water.

Concrete is a composite material composed mainly of water, aggregate, and cement. Often, additives and reinforcements are included in the mixture to achieve the desired physical properties of the finished material. When these ingredients are mixed together, they form a fluid mass that is easily molded into shape. Over time, the cement forms a hard matrix which binds the rest of the ingredients together into a durable stone-like material with many uses.

The steady increase in demands due to population growth as also resulted in increase in production and as the production rate increases to match the consumption rate the waste produced by the process during production also increases proportionality. But the waste products generated by these industries is causing environmental hazards as their disposal being a major problem, due to this over the period of time waste management has become one of the most complex and challenging problems in India.

Fortunately a waste product can be added to concrete to significantly improve its environmental characteristics. The greatest challenge before the construction industry is of two folds. One is to serve the infrastructure requirements of growing population and the other protection of environment by saving natural resources.

Introduction to SiMn Slag:

At the end of original processing of silico Manganese ore to remove as much metallic manganese as possible, one is left what is referred to as a slag, comprising granules of silico manganese denuded ore.

The slag is then further processed by crushing and washing to remove as much of the remaining metal as possible until further processing is no longer economically viable. The remaining ore is then screened and sold for use in cement manufacture as an ingredient, and concrete production as a cementitious, reactive aggregate.

Si Mn Slag in Cement:

After the process described above the material that remains is made up of around 40% silica, 20% lime, 16% aluminum oxide and 10-14% manganese oxides. The iron oxide content generally comes in at around 2%.

Over 70% of this material is glass and has no crystalline structure. As the slag is formed at a lower temperature than that found in the hottest part of the cement kiln one can assume that it will add to the liquid phase of the material moving through the rotary kiln.

The normal liquid phase is made up of calcium oxide, iron oxide and aluminium oxide and the slag contains very little iron oxide.

Manganese sits next to iron in the periodic table and shares many of its properties. In cement clinker a certain amount of iron oxide can be replaced with manganese oxide which means this material is suitable as a raw material, although there will be a limit as to how much manganese can be present in a cement clinker.

Advantages:

Raw Material Cost Saving:

Depending on the delivered cost of the raw materials to the point of production, silico manganese slag can offer a direct raw material saving.

Fuel Saving:

Silico manganese slag is pre calcined. Approximately 65% of the fuel used in cement production is used in the calcination phase, so if a decent proportion of the feed is already calcined then there are savings to be made.

Emissions Reduction:

There are two parts to this.
- One source of CO_2 emissions in the production of cement is from the burning of fuel. If silico manganese slag is used less fuel is required to be burned resulting in reduced emissions and a saving in carbon taxes.
- The other is the CO_2 removed from limestone. As part of the CO_2 producing limestone has been replaced with pre calcined Silico Manganese less CO_2 is produced here as well offering a further reduction in Carbon emissions.

Advantages of using SiMn Slag:
SiMn slag has a series of advantages over natural rock in the field of road construction.

Greater Hardness

Slag has a greater resistance to wear. This is the result of its mineral composition. The consequences: less wear and longer road lifetimes. Roads constructed using SiMn slag demonstrates reduced rutting.

Better Adhesion:

SiMn slag has micro pores and therefore, it retains its adhesiveness with wear. In contrast, natural rock becomes smooth with wear—its surface becomes polished and slippery. As a result, tires can grip better on surfaces constructed using SiMn slag, and this is particularly important on highways and in curves.

Greater Stability and Reduced Wear:

SiMn slag is harder and internally bound. Natural gravel does not have the same stability and load bearing capacity. As Steel slag is harder and more compact than natural rock, roads last longer. And as there is less wear, particulate pollution is reduced.

A disadvantage of SiMn slag is its greater weight compared to natural rock, and this has an impact on logistics and transport costs.

SiMn Slag used in the present investigation was collected from NAVABARATH Steel Plant Palvancha at kothagudam District .The tests on SiMn Slag were carried out as per IS: 383-1970.

An experimental investigation was carried out to evaluate the effect of replacing coarse aggregate by Si-Mn slag on flexural strength and compressive strength of concrete. Coarse aggregate was replaced with four percentages (0%, 5%, and 10%, 15%, 20%) of Si-Mn slag by volume in M_{20} grade of concrete with water cement ratio 0.5.

II. MIX DESIGN OF M20 GRADE CONCRETE

Grade designation	M_{20}
Type of cement	OPC 53 grade
Maximum nominal aggregate	20mm
Minimum water content	186 Kg/m^3
Maximum water cement ratio	0.55
Workability- Slump Compacting factor	 40 mm 0.9
Exposure conditions	Moderate
Type of aggregate	Crushed angular
Type of admixture	Super plasticizer
Test Data for Materials:	
Cement used	JP CEMENT OPC
Specific gravity of cement	3.07
Specific gravity of water	1.00
Chemical admixture	Roof plast
Specific gravity of aggregate	2.61
Specific gravity of sand	2.63

Target Strength for Mix Proportioning	
Target mean strength: $f_{ck}' = f_{ck} + t*s$ $=20+1.65*6$	25.94N/mm^2
Characteristic Strength at 28 days	20 N/mm^2
Maximum water cement ratio	0.502
Adopted water cement ratio	0.55
Maximum water content	186 lit
Estimated water content for 50-75 mm	185.4 lit
Admixture (Conplast WL) used	20 ml per bag of 50 Kgs cement
Calculation of cement content	
Water cement ratio	0.502
Cement content	290 kg/m^3

III. MATERIALS REQUIREMENT FOR M_{20} GRADE

Mix proportions for one cum of concrete	
Mass of Cement in kg/m3	370.51 Kg/m^3
Mass of Water in kg/m3	186 lit
Mass of Fine Aggregate in kg/m3	619.82Kg/m^3
Mass of Coarse Aggregate in kg/m3	1229 Kg/m^3
Water Cement Ratio	0.55

Mix M30	Cement	Fine aggregate	Coarse aggregate	Water
Weight	370.51	619.82	1229.87	186
Ratio	1	1.67	3.31	0.502

Table 1: Batching Proportions for M20 Grade Concrete per m^3 in Flexure

S.No	% of SiMn Slag	Cement Kg.	Fine Aggregate Kg.	Coarse Aggregate Kg.	Water Litres	SiMn Slag Kg.	Roofplast WL ml.
1	0%	11.115	18.56	36.89	5.58	-	4.44
2	5%	11.115	18.56	35.046	5.58	1.844	4.44
3	10%	11.115	18.56	32.901	5.58	3.989	4.44
4	15%	11.115	18.56	31.35	5.58	5.535	4.44
5	20%	11.115	18.56	29.512	5.58	7.378	4.44

Table 2: Batching Proportions for M20 Grade Concrete per m^3 in Compression

S. No	% of LD slag	Cement Kg.	Fine Aggregate Kg.	Coarse Aggregate Kg.	Water Lt	SiMn slag Kg.	Roofplax WL(adm) ml.
1	0%	3.334	5.568	11.035	1.674	-	1.32
2	5%	3.334	5.568	10.485	1.674	0.55	1.32
3	10%	3.334	5.568	9.932	1.674	1.103	1.32
4	15%	3.334	5.568	9.380	1.674	1.655	1.32
5	20%	3.334	5.568	8.828	1.674	2.207	1.32

Observations of Flexural Strength:

Table 3: Flexural Strength of M20 Grade Concrete for 7 Days

S.No	Specimen Size (100*100*500)	% of SiMn Slag	Span Cm	Distance of Fracture	Load KN	Avg. Load KN	Avg. Strength N/mm²
1	1	0	50	22	13	11.3	5.65
	2		50	22	10		
	3		50	20.5	11		
2	1	5%	50	16	15	15.6	7.58
	2		50	18	16.5		
	3		50	17.3	14		
3	1	10%	50	17.6	11.5	15.83	7.91
	2		50	18.5	20		
	3		50	19	16		
4	1	15%	50	21.5	17	16.5	8.25
	2		50	23.3	16		
	3		50	22	16.5		
5	1	20%	50	18.6	15.5	16.66	8.33
	2		50	16	18.5		
	3		50	17	16		

Table 4: Flexural Strength of M20 Grade Concrete for 14 Days

S.No	Specimen size (150x150x700)	% of SiMn Slag	Span Cm	Distance of Fracture	Load KN	Avg. Load KN	Avg. Strength N/mm²
1	1	0	50	18	13	14	7
	2		50	21	14.5		
	3		50	19	14		
2	1	5%	50	21	16	15.6	7.58
	2		50	14.4	14		
	3		50	18	15		
3	1	10%	50	17.5	14	16.33	8.16
	2		50	16	17		
	3		50	18	18		
4	1	15%	50	19.5	14	16.66	8.33
	2		50	18	12		
	3		50	20	24		
5	1	20%	50	18	19	19.5	9.75
	2		50	22.5	19.5		
	3		50	21	20		

Table 5: Flexural Strength of M20 Grade Concrete for 28 Days

S.No	Specimen Size (150x150x700)	% of SiMn Slag	Span Cm	Distance of Fracture	Load KN	Avg. Load KN	Avg. Strength N/mm² (Pl/bd^2)
1	1	0	50	17	16	15.66	7.833
	2		50	23	13		
	3		50	20.2	18		
2	1	5%	50	21	16	17	8.5
	2		50	23.3	18		
	3		50	22.2	17		

3	1	10%	50	18.5	21	18.3	9.16
	2		50	20.5	16		
	3		50	20	18		
4	1	15%	50	22	21.5	19.16	9.583
	2		50	20.5	16		
	3		50	21	20		
5	1	20%	50	18	24	22.33	11.16
	2		50	18.2	21		
	3		50	17	22		

Table 6: % Increase of Flexural Strength in N/mm^2 of Concrete with SiMn Slag with Respect to Conventional Concrete

S. No	% of SiMn Slag	Flexural Strength N/mm^2			% Decrease			% Increase		
		7 days	14 days	28 days	7 days	14 days	28 days	7 days	14 days	28 days
1	0	5.65	7	7.83	-	-	-	-	-	-
2	5%	7.58	7.58	8.5	-	-	-	34.15	8.2	14.31
3	10%	7.91	8.16	9.16	-	-	-	40	16.57	16.98
4	15%	8.25	8.33	9.583	-	-	-	46.01	17.85	17.93
5	20%	8.33	9.75	11.16				47.43	39.28	42.52

Observation of Compressive Strength:

Table 7: Compressive Strength of M20 Grade Concrete for 7 Days

S.No	Specimen Size100*100*100	% of SiMn slag	Load KN	Avg. load KN	Compressive Strength N/mm^2
1	1 2 3	0%	320 170 320	270	27
2	1 2 3	5%	240 280 220	246.6	24.66
3	1 2 3	10%	290 225 300	281.6	27
4	1 2 3	15%	320 290 200	281.6	28.1
5	1 2 3	20%	320 290 370	326.6	32.6

Table 8: Compressive Strength of M20 Grade Concrete for 14 Days

S.No	Specimen Size 100*100*100	% of SiMn slag	Load KN	Avg. load KN	Compressive Strength N/mm^2
1	1 2 3	0%	360 170 340	290	29
2	1 2 3	5%	280 200 320	253.3	25.33
3	1 2 3	10%	300 270 320	296.86	29.6

300

4	1 2 3	15%	370 420 220	336.7	33.6
5	1 2 3	20%	390 380 380	383.3	38.3

Table 9: Compressive Strength of M20Grade Concrete for 28 Days

S.No	Specimen Size100*100*100	% ofSiMn Slag	Load KN	Avg. load KN	Compressive Strength N/mm2
I	123	0%	370 430 310	370	37
2	1 2 3	5%	360 230 380	323.3	32.33
3	1 2 3	10%	350 390 380	373.3	37.33
4	1 2 3	15%	390 385 370	381.67	38.16
5	1 2 3	20%	400 420 400	420	42

Table 10: % Increase of Compressive Strength in N/mm^2 of Concrete with SiMn Slag with Respect to Conventional Concrete

S.No	% of SiMn Slag	Compressive Strength N/mm2			% of Increase/Decrease		
		7 days	14 days	28 days	7 days	14 days	28 days
1	0	27	29	37	-	-	-
2	5%	24.66	25.33	32.3	-8.66	-14.4	-11.62
3	10%	27	29.68	37.3	0	2.34	0.81
4	15%	28.1	33.6	38.1	4.07	15.8	2.97
5	20%	32.6	38.3	42	20.7	32.06	13.51

Outcome of the Proposed Work:

- The specific gravity of SiMn is more as compared to the coarse aggregate.
- 5%, 10%, 15%, 20% of coarse aggregate was replaced by SiMn resulted that theflexural strength is increased when compared with the conventional concrete.
- The flexural strength of concrete was found to be increasing with replacement of SiMn slag at all percentages.
- The flexural strength at 7, 14&28 days for 20% SiMn slag replacement was observed to be very high.
- The compressive strength at 28 days for 20% SiMn slag replacement indicated increase in strength compared to conventional concrete.
- The maximum flexural strength was achieved at20% replacement of slag at 7, 14 and 28 days.
- The maximum flexural strength was achieved at20% at 28 days.
- The maximum compressive strength was achieved at 20% replacement of slag at 28 days.
- The compressive strength for 5% replacement of SiMn slag is decreased when compared to conventional concrete i.e., 0% replacement of SiMn slag.
- Whereas the compressive strength value of 0% and 10% replacement of SiMn slag is comparatively same.
- The concrete which is prepared by using SiMn slag can be used for construction of road pavements, footpaths, low traffic village roads etc.,

Scope for further study:

- The present study can be further carried out on other grades of concrete.
- The effect of fresh properties of concrete due to usage of different proportions may be studied.
- In present investigation the replacement of coarse aggregate was only up to 20%. Further investigation can be carried out at different higher percentages.
- The investigation can also be done by replacing SiMn slag with other materials of concrete i.e., cement, fine aggregate.
- The study can be extended to assess the durability aspects of the concrete with varying replacement proportions.

IV. REFERENCES:

[1] Mechanical Properties of Concrete Using SiMn Slag AggregatJ.Saravanan and N.Suganya International Journal of Engineering Inventionse-ISSN: 2278-7461, p-ISSN: 2319-6491 Volume 4, Issue 9 [May 2015] PP: 07-16.

[2] Usage of SiMn slag in concrete as fine/coarse aggregate Indian journal of Engineering and Material Sciences Vol. 22, June 2015, pp.339-344.

[3] Steel Slag as A Road Construction Material.Department of Geotechnics and Transportation, Faculty of Civil Engineering, University Technology Malaysia, 81310 UTM Johor Bahru, Johor Malaysia Article· January 2015.

[4] Mechanical Properties of Concrete Using SiMn Slag AggregatJ.Saravanan and N.Suganya International Journal of Engineering Inventions e-ISSN: 2278-7461, p-ISSN: 2319-6491 Volume 4, Issue 9 [May 2015] PP: 07-16.

[5] Usage of SiMn slag in concrete as fine/coarse aggregate Indian journal of Engineering and Material Sciences Vol. 22, June 2015, pp.339-344.

[6] Processing, characterization and erosion wear response of Linz-Donawitz(LD) slag filled polypropylene composites Journal of Thermoplastic Composite Materials December 10, 2014PravatRanjanPati, AlokSatapathy.

[7] Experimental study on agricultural recycling of LD slag N. Balcazar, M. Pinto, G. Besga, M. Rodriguez, R. A. Lopez Fertilizers and Environment

[8]Developments in Plant and Soil Sciences Volume 66, 1996, pp 309-316.

[9] IS 456-2000, Indian standard plain and reinforced concrete-code of practice

[10] Concrete technology by M.S.Shetty.

[11] Design of concrete mixes by Krishna Raju N.

[12] IS 10262-2009, recommended guidelines for concrete mix design.

AUTHORS PROFILE

1. B. Udayasree Assistant Professor, Matrusri Engineering College, Hyd
E mail : udayaregalla@gmail.com

2. T. Raja Ramanna, Assistant Professor, Matrusri Engineering College , Hyd

Fig 1: Flexural strength of M20 grade concrete for 7, 14, 28 days

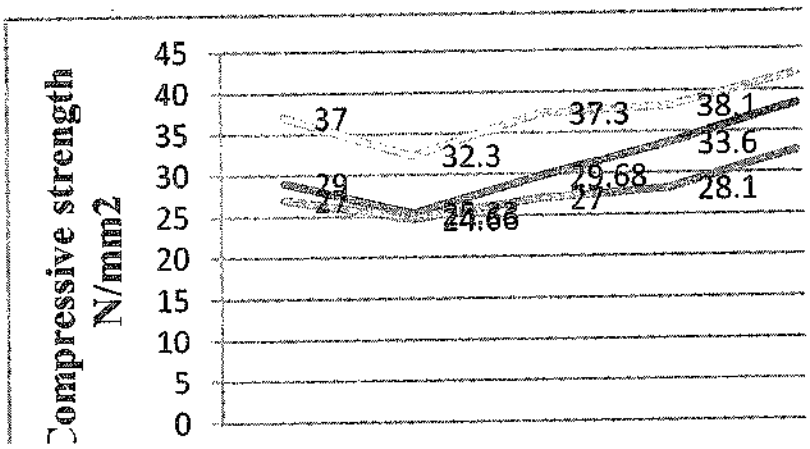

Fig 2: Compressive strength of M20 grade concrete for 7, 14, 28 days

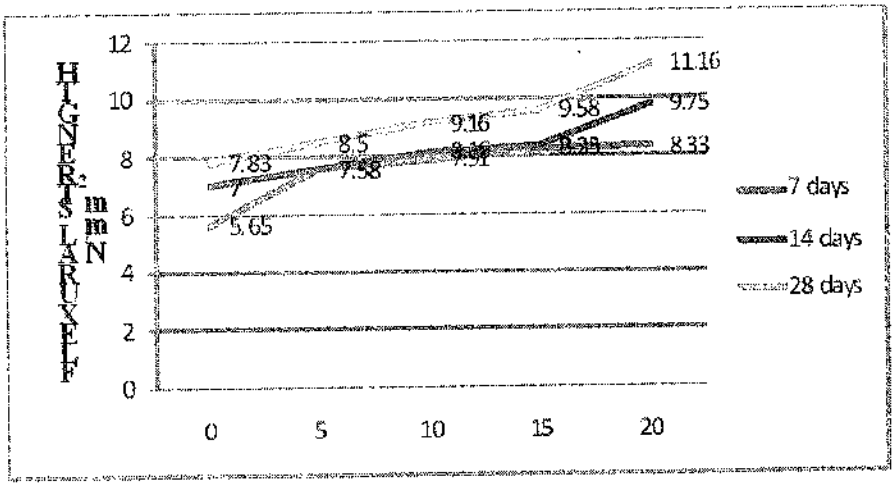

ABOUT THE INSTITUTE

Muffakham Jah College of Engineering and Technology (MJCET) was established in the year 1980 by Sultan-Ul-Uloom Education Society (SUES), which was formed by a group of visionaries and intellectuals from various walks of life. Over the past three decades, it has emerged as a premier institute, offering BE courses of four years duration in eight disciplines (Civil, ECE, CSE, IT, EEE, EIE, Mechanical & Production) and five ME courses (CAD/CAM, Structural Engineering., Digital Systems, Computers & Power Electronics) of two years duration. The current intake of all BE Courses is 780, in addition to 102 students in ME Programmes. Research Centers were started in Civil, Mechanical, EEE, CSE and ECE Departments for Doctoral Studies. The college is affiliated to Osmania University, Hyderabad and approved by AICTE, New Delhi. As per the survey of The Outlook magazine, MJCET was ranked 62nd among top 100 Engineering Colleges in India. MJCET has been ranked 47th in India among the top private institutes in Engineering by Times Engineering Institute ranking survey 2019. MJCET ranked 28th out of top 200 Engineering Colleges by India Today magazine. As per The Week Magazine, MJCET ranked 26th among the top Private Engineering Colleges in South India and 42nd among All India Private Engineering Colleges.

OVERVIEW OF THE CONFERENCE

Civil Engineering Infrastructure is the most significant factor in accelerating the pace of economic development of any country. The recent innovation and advances in the field of Civil Engineering has made a drastic impact in the Construction Industry. As the world's population increases, environmental concerns mount and Civil Engineers are entrusted by the society to achieve a sustainable world and raise the quality of life globally. The balancing of economic, social and environmental objectives now and in the future has become known as Sustainable Development and is increasingly a key driver at a range of organizational and spatial scales.

The Conference on Recent Advances in Civil Engineering Infrastructure – (RACEI-2019) aims at exploring the new horizon of innovation from distinguished researchers, eminent professionals from academia and Industry. The Conference also focuses for the achievement of relevant Sustainable Development Goals as described by United Nation Development Program. This event will be a platform to showcase and deliberate research work, studies and contributions for developing novel concepts in Civil Engineering Infrastructure. The Conference consists of keynote lectures on related themes by eminent personalities and stake holders.

BSP BS Publications
A Unit of BSP Books Pvt. Ltd.
4-4-316/309, Giriraj Lane, Sultan Bazar, Hyderabad - 500 095. (A.P.)
Ph: 040-23445688 / 605. Fax: +91-40-23445611.
e-mail: info@bspbooks.net, marketing@bspbooks.net
Website: www.bspbooks.net

ISBN : 978-93-89354-86-7

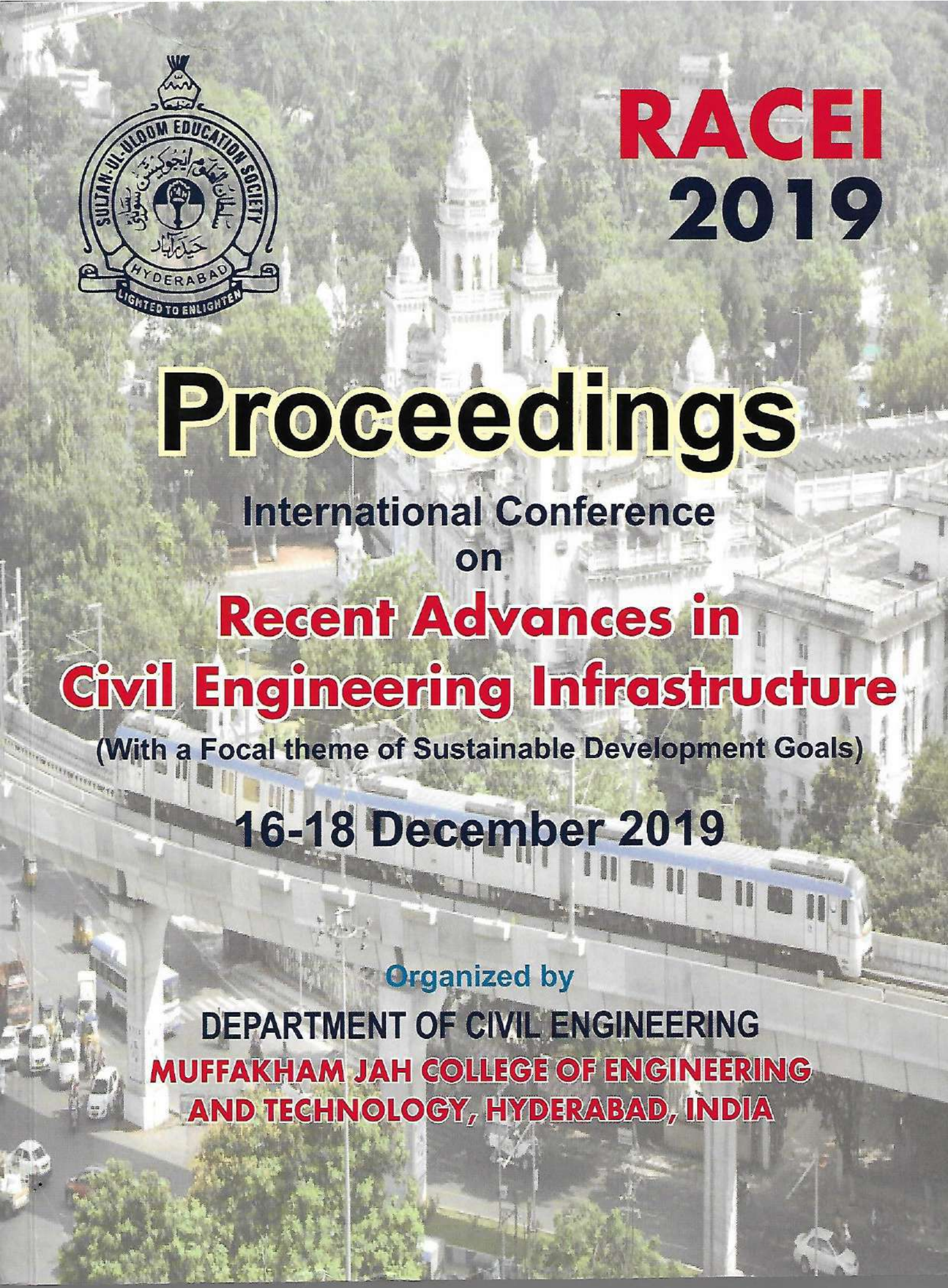

RACEI 2019

Proceedings

International Conference on

Recent Advances in Civil Engineering Infrastructure

(With a Focal theme of Sustainable Development Goals)

16-18 December 2019

Organized by

DEPARTMENT OF CIVIL ENGINEERING

MUFFAKHAM JAH COLLEGE OF ENGINEERING AND TECHNOLOGY, HYDERABAD, INDIA

International Conference on Recent Advances in Civil Engineering Infrastructure (RACEI-2019)
Department of Civil Engineering, Muffakham Jah College of Engineering and Technology

Analysis of M20 Grade Concrete using Silico Manganese Slag as a Partial Replacement of Coarse Aggregate

B. Udayasree and T. Raja Ramanna

Abstract: Global warming and Environmental degradation have become one of the major issues in recent years. The scarcity of raw materials required for construction is increasing day by day to globalization. The main challenge for the researches and engineers is to preventing the exhaustion of natural resources and increasing the usage of industrial wastage. The rapid rate of growth in population in India as forced the construction industry to use the building materials at rapid rate and resulting in depletion of natural resources and also has a severe impact on the environment causing many hazards either directly or indirectly such as depletion of river due to sand mining being done at alarming rate etc. On the other hand industrialization, rapid growth of industries in India gave birth to numerous kinds of waste products. In the present study Silico Manganese slag which is a byproduct from Ferro Alloys Industries is used as partial replacement of coarse aggregate. The slag will generate during chemical reaction of manganese ore, quartz, dolomite and coal. Main product obtained is Silico Manganese. Ferro Alloys are used as inputs in the manufacture of iron and steel for removal of oxygen and imparting specific properties. These are alloys of iron and elements like manganese, silicon, chromium, etc. The project aims to study experimentally the effect of replacement of coarse aggregate by silico manganese slag on its properties of concrete. The mix design considered in this study is M_{20} Grade of concrete. In this study natural coarse aggregate has been replaced by Silico Manganese slag by 0%, 5%, 10%, 15%, and 20%.

Key Words: Silico Manganese Slag, Industrial byproducts

I. INTRODUCTION

A. Introduction to Concrete:

Concrete is widely used structural material consisting essentially of a binder and mineral filler. It has the unique distinction of being the only construction material actually manufactured on the site, whereas other materials are merely shaped to use at the worksite. Good or bad concrete is made from the same discrete materials like grains of sand, gravel or pieces of crushed rock and the innumerable fine particles of cement powder mixed with water.

Concrete is a composite material composed mainly of water, aggregate, and cement. Often, additives and reinforcements are included in the mixture to achieve the desired physical properties of the finished material. When these ingredients are mixed together, they form a fluid mass that is easily molded into shape. Over time, the cement forms a hard matrix which binds the rest of the ingredients together into a durable stone-like material with many uses.

The steady increase in demands due to population growth as also resulted in increase in production and as the production rate increases to match the consumption rate the waste produced by the process during production also increases proportionality. But the waste products generated by these industries is causing environmental hazards as their disposal being a major problem, due to this over the period of time waste management has become one of the most complex and challenging problems in India.

Fortunately a waste product can be added to concrete to significantly improve its environmental characteristics. The greatest challenge before the construction industry is of two folds. One is to serve the infrastructure requirements of growing population and the other protection of environment by saving natural resources.

Introduction to SiMn Slag:

At the end of original processing of silico Manganese ore to remove as much metallic manganese as possible, one is left what is referred to as a slag, comprising granules of silico manganese denuded ore.

The slag is then further processed by crushing and washing to remove as much of the remaining metal as possible until further processing is no longer economically viable. The remaining ore is then screened and sold for use in cement manufacture as an ingredient, and concrete production as a cementitious, reactive aggregate.

Si Mn Slag in Cement:

After the process described above the material that remains is made up of around 40% silica, 20% lime, 16% aluminum oxide and 10-14% manganese oxides. The iron oxide content generally comes in at around 2%.

Over 70% of this material is glass and has no crystalline structure. As the slag is formed at a lower temperature than that found in the hottest part of the cement kiln one can assume that it will add to the liquid phase of the material moving through the rotary kiln.

The normal liquid phase is made up of calcium oxide, iron oxide and aluminium oxide and the slag contains very little iron oxide.

Manganese sits next to iron in the periodic table and shares many of its properties. In cement clinker a certain amount of iron oxide can be replaced with manganese oxide which means this material is suitable as a raw material, although there will be a limit as to how much manganese can be present in a cement clinker.

Advantages:

Raw Material Cost Saving:

Depending on the delivered cost of the raw materials to the point of production, silico manganese slag can offer a direct raw material saving.

Fuel Saving:

Silico manganese slag is pre calcined. Approximately 65% of the fuel used in cement production is used in the calcination phase, so if a decent proportion of the feed is already calcined then there are savings to be made.

Emissions Reduction:

There are two parts to this.
- One source of CO_2 emissions in the production of cement is from the burning of fuel. If silico manganese slag is used less fuel is required to be burned resulting in reduced emissions and a saving in carbon taxes.
- The other is the CO_2 removed from limestone. As part of the CO_2 producing limestone has been replaced with pre calcined Silico Manganese less CO_2 is produced here as well offering a further reduction in Carbon emissions.

Advantages of using SiMn Slag:
SiMn slag has a series of advantages over natural rock in the field of road construction.

Greater Hardness

Slag has a greater resistance to wear. This is the result of its mineral composition. The consequences: less wear and longer road lifetimes. Roads constructed using SiMn slag demonstrates reduced rutting.

Better Adhesion:

SiMn slag has micro pores and therefore, it retains its adhesiveness with wear. In contrast, natural rock becomes smooth with wear—its surface becomes polished and slippery. As a result, tires can grip better on surfaces constructed using SiMn slag, and this is particularly important on highways and in curves.

Greater Stability and Reduced Wear:

SiMn slag is harder and internally bound. Natural gravel does not have the same stability and load bearing capacity. As Steel slag is harder and more compact than natural rock, roads last longer. And as there is less wear, particulate pollution is reduced.

A disadvantage of SiMn slag is its greater weight compared to natural rock, and this has an impact on logistics and transport costs.

SiMn Slag used in the present investigation was collected from NAVABARATH Steel Plant Palvancha at kothagudam District .The tests on SiMn Slag were carried out as per IS: 383-1970.

An experimental investigation was carried out to evaluate the effect of replacing coarse aggregate by Si-Mn slag on flexural strength and compressive strength of concrete. Coarse aggregate was replaced with four percentages (0%, 5%, and 10%, 15%, 20%) of Si-Mn slag by volume in M_{20} grade of concrete with water cement ratio 0.5.

II. MIX DESIGN OF M20 GRADE CONCRETE

Grade designation	M_{20}
Type of cement	OPC 53 grade
Maximum nominal aggregate	20mm
Minimum water content	186 Kg/m^3
Maximum water cement ratio	0.55
Workability- Slump Compacting factor	 40 mm 0.9
Exposure conditions	Moderate
Type of aggregate	Crushed angular
Type of admixture	Super plasticizer
Test Data for Materials:	
Cement used	JP CEMENT OPC
Specific gravity of cement	3.07
Specific gravity of water	1.00
Chemical admixture	Roof plast
Specific gravity of aggregate	2.61
Specific gravity of sand	2.63

Target Strength for Mix Proportioning	
Target mean strength: $f_{ck}' = f_{ck} + t*s$ $=20+1.65*6$	25.94N/mm^2
Characteristic Strength at 28 days	20 N/mm^2
Maximum water cement ratio	0.502
Adopted water cement ratio	0.55
Maximum water content	186 lit
Estimated water content for 50-75 mm	185.4 lit
Admixture (Conplast WL) used	20 ml per bag of 50 Kgs cement
Calculation of cement content	
Water cement ratio	0.502
Cement content	290 kg/m^3

III. MATERIALS REQUIREMENT FOR M_{20} GRADE

Mix proportions for one cum of concrete	
Mass of Cement in kg/m3	370.51 Kg/m^3
Mass of Water in kg/m3	186 lit
Mass of Fine Aggregate in kg/m3	619.82Kg/m^3
Mass of Coarse Aggregate in kg/m3	1229 Kg/m^3
Water Cement Ratio	0.55

Mix M30	Cement	Fine aggregate	Coarse aggregate	Water
Weight	370.51	619.82	1229.87	186
Ratio	1	1.67	3.31	0.502

Table 1: Batching Proportions for M20 Grade Concrete per m^3 in Flexure

S.No	% of SiMn Slag	Cement Kg.	Fine Aggregate Kg.	Coarse Aggregate Kg.	Water Litres	SiMn Slag Kg.	Roofplast WL ml.
1	0%	11.115	18.56	36.89	5.58	-	4.44
2	5%	11.115	18.56	35.046	5.58	1.844	4.44
3	10%	11.115	18.56	32.901	5.58	3.989	4.44
4	15%	11.115	18.56	31.35	5.58	5.535	4.44
5	20%	11.115	18.56	29.512	5.58	7.378	4.44

Table 2: Batching Proportions for M20 Grade Concrete per m^3 in Compression

S. No	% of LD slag	Cement Kg.	Fine Aggregate Kg.	Coarse Aggregate Kg.	Water Lt	SiMn slag Kg.	Roofplax WL(adm) ml.
1	0%	3.334	5.568	11.035	1.674	-	1.32
2	5%	3.334	5.568	10.485	1.674	0.55	1.32
3	10%	3.334	5.568	9.932	1.674	1.103	1.32
4	15%	3.334	5.568	9.380	1.674	1.655	1.32
5	20%	3.334	5.568	8.828	1.674	2.207	1.32

Observations of Flexural Strength:

Table 3: Flexural Strength of M20 Grade Concrete for 7 Days

S.No	Specimen Size (100*100*500)	% of SiMn Slag	Span Cm	Distance of Fracture	Load KN	Avg. Load KN	Avg. Strength N/mm^2
1	1	0	50	22	13	11.3	5.65
	2		50	22	10		
	3		50	20.5	11		
2	1	5%	50	16	15	15.6	7.58
	2		50	18	16.5		
	3		50	17.3	14		
3	1	10%	50	17.6	11.5	15.83	7.91
	2		50	18.5	20		
	3		50	19	16		
4	1	15%	50	21.5	17	16.5	8.25
	2		50	23.3	16		
	3		50	22	16.5		
5	1	20%	50	18.6	15.5	16.66	8.33
	2		50	16	18.5		
	3		50	17	16		

Table 4: Flexural Strength of M20 Grade Concrete for 14 Days

S.No	Specimen size (150x150x700)	% of SiMn Slag	Span Cm	Distance of Fracture	Load KN	Avg. Load KN	Avg. Strength N/mm^2
1	1	0	50	18	13	14	7
	2		50	21	14.5		
	3		50	19	14		
2	1	5%	50	21	16	15.6	7.58
	2		50	14.4	14		
	3		50	18	15		
3	1	10%	50	17.5	14	16.33	8.16
	2		50	16	17		
	3		50	18	18		
4	1	15%	50	19.5	14	16.66	8.33
	2		50	18	12		
	3		50	20	24		
5	1	20%	50	18	19	19.5	9.75
	2		50	22.5	19.5		
	3		50	21	20		

Table 5: Flexural Strength of M20 Grade Concrete for 28 Days

S.No	Specimen Size (150x150x700)	% of SiMn Slag	Span Cm	Distance of Fracture	Load KN	Avg. Load KN	Avg. Strength N/mm^2 (Pl/bd^2)
1	1	0	50	17	16	15.66	7.833
	2		50	23	13		
	3		50	20.2	18		
2	1	5%	50	21	16	17	8.5
	2		50	23.3	18		
	3		50	22.2	17		

3	1	10%	50	18.5	21	18.3	9.16
	2		50	20.5	16		
	3		50	20	18		
4	1	15%	50	22	21.5	19.16	9.583
	2		50	20.5	16		
	3		50	21	20		
5	1	20%	50	18	24	22.33	11.16
	2		50	18.2	21		
	3		50	17	22		

Table 6: % Increase of Flexural Strength in N/mm^2 of Concrete with SiMn Slag with Respect to Conventional Concrete

S. No	% of SiMn Slag	Flexural Strength N/mm^2			% Decrease			% Increase		
		7 days	14 days	28 days	7 days	14 days	28 days	7 days	14 days	28 days
1	0	5.65	7	7.83	-	-	-	-	-	-
2	5%	7.58	7.58	8.5	-	-	-	34.15	8.2	14.31
3	10%	7.91	8.16	9.16	-	-	-	40	16.57	16.98
4	15%	8.25	8.33	9.583	-	-	-	46.01	17.85	17.93
5	20%	8.33	9.75	11.16				47.43	39.28	42.52

Observation of Compressive Strength:

Table 7: Compressive Strength of M20 Grade Concrete for 7 Days

S.No	Specimen Size100*100*100	% of SiMn slag	Load KN	Avg. load KN	Compressive Strength N/mm^2
1	1 2 3	0%	320 170 320	270	27
2	1 2 3	5%	240 280 220	246.6	24.66
3	1 2 3	10%	290 225 300	281.6	27
4	1 2 3	15%	320 290 200	281.6	28.1
5	1 2 3	20%	320 290 370	326.6	32.6

Table 8: Compressive Strength of M20 Grade Concrete for 14 Days

S.No	Specimen Size 100*100*100	% of SiMn slag	Load KN	Avg. load KN	Compressive Strength N/mm^2
1	1 2 3	0%	360 170 340	290	29
2	1 2 3	5%	280 200 320	253.3	25.33
3	1 2 3	10%	300 270 320	296.86	29.6

300

4	1 2 3	15%	370 420 220	336.7	33.6
5	1 2 3	20%	390 380 380	383.3	38.3

Table 9: Compressive Strength of M20Grade Concrete for 28 Days

S.No	Specimen Size100*100*100	% ofSiMn Slag	Load KN	Avg. load KN	Compressive Strength N/mm2
I	123	0%	370 430 310	370	37
2	1 2 3	5%	360 230 380	323.3	32.33
3	1 2 3	10%	350 390 380	373.3	37.33
4	1 2 3	15%	390 385 370	381.67	38.16
5	1 2 3	20%	400 420 400	420	42

Table 10: % Increase of Compressive Strength in N/mm^2 of Concrete with SiMn Slag with Respect to Conventional Concrete

S.No	% of SiMn Slag	Compressive Strength N/mm2			% of Increase/Decrease		
		7 days	14 days	28 days	7 days	14 days	28 days
1	0	27	29	37	-	-	-
2	5%	24.66	25.33	32.3	-8.66	-14.4	-11.62
3	10%	27	29.68	37.3	0	2.34	0.81
4	15%	28.1	33.6	38.1	4.07	15.8	2.97
5	20%	32.6	38.3	42	20.7	32.06	13.51

Outcome of the Proposed Work:

- The specific gravity of SiMn is more as compared to the coarse aggregate.
- 5%, 10%, 15%, 20% of coarse aggregate was replaced by SiMn resulted that theflexural strength is increased when compared with the conventional concrete.
- The flexural strength of concrete was found to be increasing with replacement of SiMn slag at all percentages.
- The flexural strength at 7, 14&28 days for 20% SiMn slag replacement was observed to be very high.
- The compressive strength at 28 days for 20% SiMn slag replacement indicated increase in strength compared to conventional concrete.
- The maximum flexural strength was achieved at20% replacement of slag at 7, 14 and 28 days.
- The maximum flexural strength was achieved at20% at 28 days.
- The maximum compressive strength was achieved at 20% replacement of slag at 28 days.
- The compressive strength for 5% replacement of SiMn slag is decreased when compared to conventional concrete i.e., 0% replacement of SiMn slag.
- Whereas the compressive strength value of 0% and 10% replacement of SiMn slag is comparatively same.
- The concrete which is prepared by using SiMn slag can be used for construction of road pavements, footpaths, low traffic village roads etc.,

Scope for further study:

- The present study can be further carried out on other grades of concrete.
- The effect of fresh properties of concrete due to usage of different proportions may be studied.
- In present investigation the replacement of coarse aggregate was only up to 20%. Further investigation can be carried out at different higher percentages.
- The investigation can also be done by replacing SiMn slag with other materials of concrete i.e., cement, fine aggregate.
- The study can be extended to assess the durability aspects of the concrete with varying replacement proportions.

IV. REFERENCES:

[1] Mechanical Properties of Concrete Using SiMn Slag AggregatJ.Saravanan and N.Suganya International Journal of Engineering Inventionse-ISSN: 2278-7461, p-ISSN: 2319-6491 Volume 4, Issue 9 [May 2015] PP: 07-16.

[2] Usage of SiMn slag in concrete as fine/coarse aggregate Indian journal of Engineering and Material Sciences Vol. 22, June 2015, pp.339-344.

[3] Steel Slag as A Road Construction Material.Department of Geotechnics and Transportation, Faculty of Civil Engineering, University Technology Malaysia, 81310 UTM Johor Bahru, Johor Malaysia Article· January 2015.

[4] Mechanical Properties of Concrete Using SiMn Slag AggregatJ.Saravanan and N.Suganya International Journal of Engineering Inventions e-ISSN: 2278-7461, p-ISSN: 2319-6491 Volume 4, Issue 9 [May 2015] PP: 07-16.

[5] Usage of SiMn slag in concrete as fine/coarse aggregate Indian journal of Engineering and Material Sciences Vol. 22, June 2015, pp.339-344.

[6] Processing, characterization and erosion wear response of Linz-Donawitz(LD) slag filled polypropylene composites Journal of Thermoplastic Composite Materials December 10, 2014PravatRanjanPati, AlokSatapathy.

[7] Experimental study on agricultural recycling of LD slag N. Balcazar, M. Pinto, G. Besga, M. Rodriguez, R. A. Lopez Fertilizers and Environment

[8]Developments in Plant and Soil Sciences Volume 66, 1996, pp 309-316.

[9] IS 456-2000, Indian standard plain and reinforced concrete-code of practice

[10] Concrete technology by M.S.Shetty.

[11] Design of concrete mixes by Krishna Raju N.

[12] IS 10262-2009, recommended guidelines for concrete mix design.

AUTHORS PROFILE

1. B. Udayasree Assistant Professor, Matrusri Engineering College, Hyd
E mail : udayaregalla@gmail.com

2. T. Raja Ramanna, Assistant Professor, Matrusri Engineering College , Hyd

Fig 1: Flexural strength of M20 grade concrete for 7, 14, 28 days

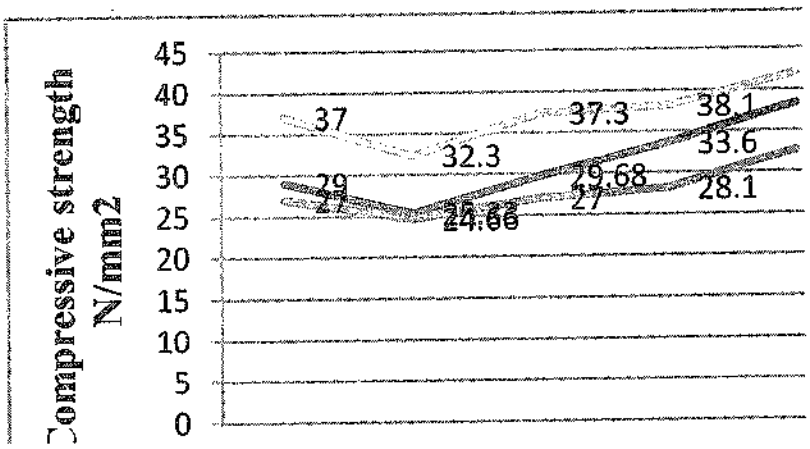

Fig 2: Compressive strength of M20 grade concrete for 7, 14, 28 days

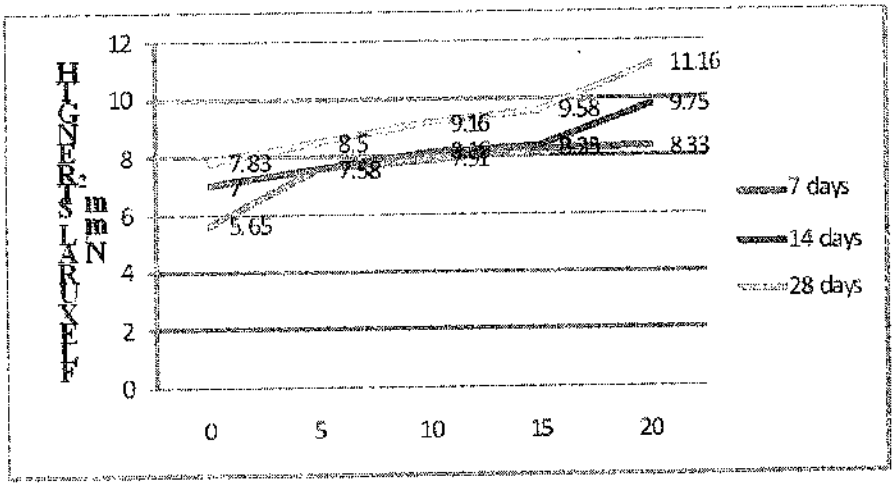

ABOUT THE INSTITUTE

Muffakham Jah College of Engineering and Technology (MJCET) was established in the year 1980 by Sultan-Ul-Uloom Education Society (SUES), which was formed by a group of visionaries and intellectuals from various walks of life. Over the past three decades, it has emerged as a premier institute, offering BE courses of four years duration in eight disciplines (Civil, ECE, CSE, IT, EEE, EIE, Mechanical & Production) and five ME courses (CAD/CAM, Structural Engineering., Digital Systems, Computers & Power Electronics) of two years duration. The current intake of all BE Courses is 780, in addition to 102 students in ME Programmes. Research Centers were started in Civil, Mechanical, EEE, CSE and ECE Departments for Doctoral Studies. The college is affiliated to Osmania University, Hyderabad and approved by AICTE, New Delhi. As per the survey of The Outlook magazine, MJCET was ranked 62nd among top 100 Engineering Colleges in India. MJCET has been ranked 47th in India among the top private institutes in Engineering by Times Engineering Institute ranking survey 2019. MJCET ranked 28th out of top 200 Engineering Colleges by India Today magazine. As per The Week Magazine, MJCET ranked 26th among the top Private Engineering Colleges in South India and 42nd among All India Private Engineering Colleges.

OVERVIEW OF THE CONFERENCE

Civil Engineering Infrastructure is the most significant factor in accelerating the pace of economic development of any country. The recent innovation and advances in the field of Civil Engineering has made a drastic impact in the Construction Industry. As the world's population increases, environmental concerns mount and Civil Engineers are entrusted by the society to achieve a sustainable world and raise the quality of life globally. The balancing of economic, social and environmental objectives now and in the future has become known as Sustainable Development and is increasingly a key driver at a range of organizational and spatial scales.

The Conference on Recent Advances in Civil Engineering Infrastructure – (RACEI-2019) aims at exploring the new horizon of innovation from distinguished researchers, eminent professionals from academia and Industry. The Conference also focuses for the achievement of relevant Sustainable Development Goals as described by United Nation Development Program. This event will be a platform to showcase and deliberate research work, studies and contributions for developing novel concepts in Civil Engineering Infrastructure. The Conference consists of keynote lectures on related themes by eminent personalities and stake holders.

BSP BS Publications
A Unit of BSP Books Pvt. Ltd.
4-4-316/309, Giriraj Lane, Sultan Bazar, Hyderabad - 500 095. (A.P.)
Ph: 040-23445688 / 605. Fax: +91-40-23445611.
e-mail: info@bspbooks.net, marketing@bspbooks.net
Website: www.bspbooks.net

ISBN : 978-93-89354-86-7

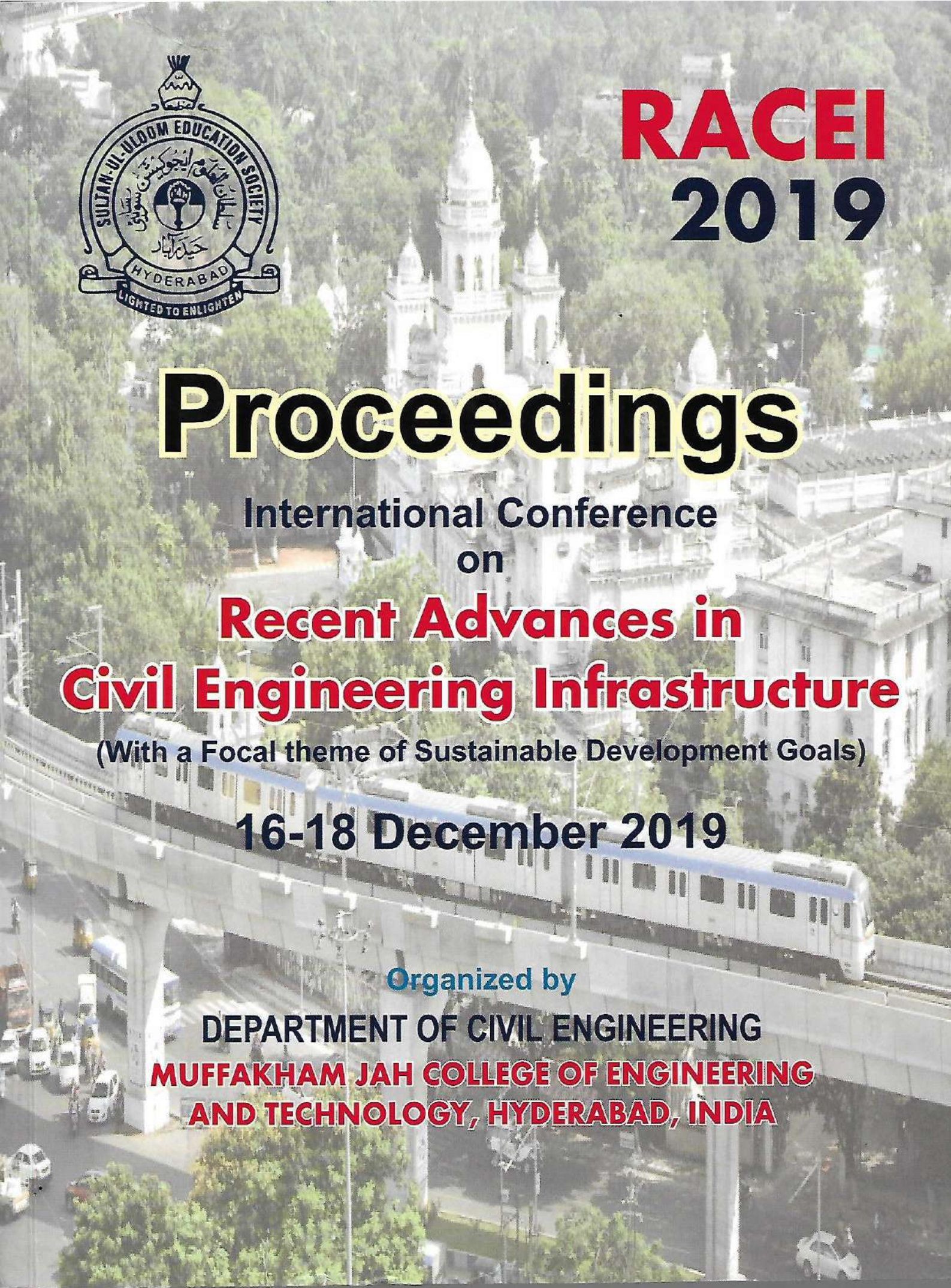

RACEI 2019

Proceedings

International Conference on

Recent Advances in Civil Engineering Infrastructure

(With a Focal theme of Sustainable Development Goals)

16-18 December 2019

Organized by

DEPARTMENT OF CIVIL ENGINEERING

MUFFAKHAM JAH COLLEGE OF ENGINEERING AND TECHNOLOGY, HYDERABAD, INDIA

Evaluation of Capacity of Roundabout at Necklace Road using Gap Acceptance Method

K. Smitha, K. Vamshi Krishna and *B. Hari Priya*

Abstract- Road network connecting the various parts of the country defines the economy of the nation.This lead to vast development of road infrastructure. Intersections form a major unit of the road network. It is of utmost importance to design these intersections safely as they are the areas where maximum conflict points exist, which could otherwise lead to fatal. One such implication can be introducing roundabouts at intersections, which reduces the conflict points, thus providing greater safety and efficient traffic flow. The drivers' behavior is one of the prime factors which influence the performance of these roundabouts. No such procedure of analysis is available in Indian context to identify the performance of roundabouts. To develop such a model, initially, the parameter defining driver behavior, i.e. Gap acceptance parameters had been estimated for heterogeneity in traffic. The capacity of an entry flow is found to vary considerably with the vary in geometrics of the roundabout. A study was conducted to collect the data from roundabout in Hyderabad with different geometry and traffic characteristics. . The developed model validated with the site data. A comparative study with some existing empirical models indicated that the capacities of roundabouts are underestimated or overestimated for Indian heterogeneous traffic condition.

Keywords: Roundabouts; Capacity;
empirical analysis; heterogeneous flow; modeling.

I.INTRODUCTION

Roundabout is the type of unsignalised intersection was the minor traffic from different lanes merges with the major traffic circulating around the central island. The central island is usually circular in shape. Channelization is done by thorough geometric design which enables tangential merging of traffic with the circulating flow at desirable speed. Unsignalised intersection play a vital role in road network to divert the traffic to respective lanes .Roundabouts when compared with other intersection applications including traffic signals and all way stop control can accomplish sustainability goals by eliminating power needs and making more efficient traffic flow .Moreover, roundabouts prove to be eco-friendly as it causes less pollution since vehicles on average spend less time at roundabouts than at signalized intersections.

The propose of this paper is to estimate the capacity of roundabouts using empirical analysis .Using data ,roundabout calculation is evaluated to quantify the impact of minimum acceptable gap and related parameters on roundabout capacity. Since roundabouts are unsignalised with only yield conditions, capacity is dependent on gap seeking logic. The influence of various geometric parameters on the capacity of roundabouts is also observed through the application of proposed model.

II.LITERATURE REVIEW

The progress of being a modern roundabout from the ancient rotaries has seen considerable changes through ages. Timely researches had been carried out to change its shape and size. The modern
Round about was first introduced in UK and then in USA. For the adequate movement of traffic, to determine its performance many models were developed in different parts of world.
UK TRRL model

The first model for estimating the capacity of roundabout by Kimber (1980) for roundabouts is based on empirical analysis. UK had many roundabouts which operated at capacity flow at that time. The effect of various geometric parameters on the entry capacity was determined and six geometrics were selected to form a model. Linear relationship was found between the entry capacity and the circulating flow. Software based on this model were also developed and improvized. RODEL and ARCADY are the software packages based on this method.
French model

Three parallel modeling efforts was going on in France to develop the equation for capacity. The model developed by Louah (1992) is an exponential regression- based model that takes into account the influence of exiting flow and a number of geometric parameters. This model considers both entry and the exit flow and also considers two different conflicting flows. The model also considers driver behavior along with geometrics by taking the follow-up time.
US Federal Highway Administration model

Robinson and Rodegerdts (2000) wrote a synopsis of Federal Highway Administration (FHWA) guide on capacity and performance of roundabouts which included single-lane roundabouts, double- lane roundabouts, and the capacity curves for urban compact roundabouts, as it has been used to estimate capacity in USA till HCM 2000 was formed.

III.METHODOLOGY

In India since the traffic flow is heterogenous to calculate the capacity the following are calculated i.e. critical gap and follow- up time. So to calculate the capacity we use INAFOGA method.

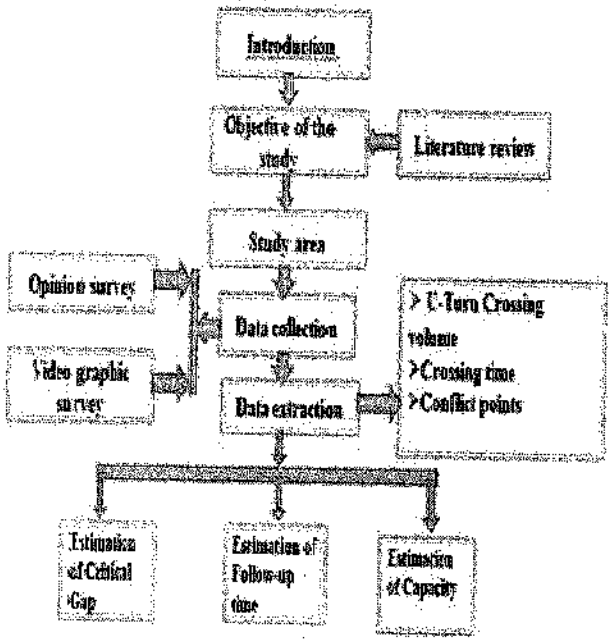

FLOW CHART OF METHODOLOGY

INAFOGA METHOD

Highly heterogeneous traffic flow on urban Indian roads with no proper lane discipline form median openings a complex location for researchers to come up with a concrete idea on gap acceptance behavior of drivers. Although the informatory signs are provided prior to median openings, the U-turn vehicles move to some distance inside the influence area beyond the desirable. So, the reference point for a U-turn vehicle taking a gap in the through traffic must be explained here. Generally the gaps in the through traffic stream are measured at the single arrow line gives the headway distributions when through traffic stream is not obstructed.

IV. STUDYAREA

To develop a model, it is being essential to have a proper and sufficient data-set. Some principles which lay down for selection of site for data collection for purpose of model development are stated below:

1. Location of site in city. 2. Geometry of roundabout 3. Traffic composition

To satisfy the requirements of site selections, many roundabouts were studied and the following roundabouts were selected:

We have choosen the roundabout at Necklace road

Details of geometry of roundabout at Necklace road

Site	Leg	ER(m)	EW(m)	WW(m)	WL(m)	D(m)
Necklace Road	N	29.32	8.6	8.48	57.44	62.2
	E	39.67	8.5	8.46	56.93	62.2
	S	29.17	8.0	8.58	38.12	62.2
	W	17.67	8.1	8.52	46.66	62.2

I. Estimation of Critical Gap

For the purpose of estimating the critical gap, gaps accepted and rejected by driver at the entry of roundabout are to be extracted from the video. To obtain these, two imaginary lines are to be considered, one at the entry of lane of roundabout (L1) and another at the line of conflict (L2) Fig (i). To estimate a gap, two time stamps are considered. The time when front bumper of a vehicle in minor stream & major stream touches L1& L2 is considered as the first time stamp T1, Fig(iv)& the second time stamp T2, Fig (v). The gap is then calculated, as the difference between theses time stamps T2 and T1 and for every gap calculated, it's checked whether the gap was accepted or rejected.

II. Estimation of follow-up time

When back bumper of the first vehicle crosses the line L1 is noted using the first time stamp Ft1 and the time at which the front bumper of the following vehicle touches the line is noted by Ft2. The condition at which each time stamp is noted is clearly described in Fig (ii) and (iii). The follow up time is the difference between these two time stamps. The average value of all the readings is the follow-up time which is considered for further analysis.

A. *1.L1&L2*

2.Ft1

3.Ft2

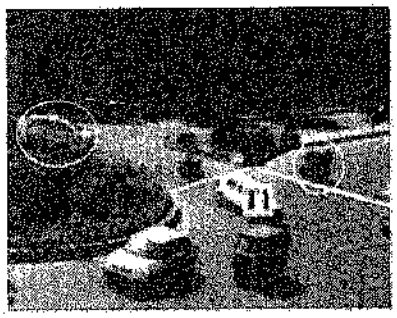

4.Estimation of T1

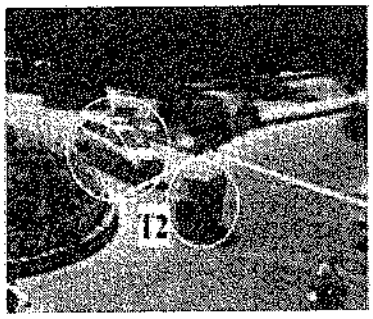

5.Estimation of T2

By extraction of the video graph according to the rejected and accepted gaps we get critical gap. Again from the extraction of the video we get the follow-up time. By substituting in the formulae we get the capacity of round about.

These critical gap graph for the above roundabout it, the parameters like pedestrian behavior and sidewalks could be studied along with it.

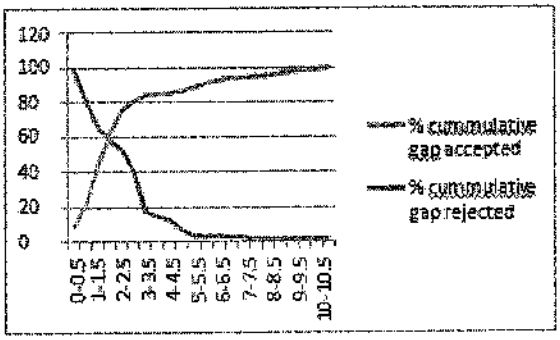

x-axis: gap length y-axis: cumulative %

1) Estimation of Capacity:

$C = 3600/tf * e^{-t} * t / 360\rho_c$

B. *where C = capacity*

t_c = critical gap

tf = follow up time

By substituting the values t_c =1.73sec tf =1.24sec Capacity C=2398 pcu/hr

V. CONCLUSION

The data have been collected during the respective peak hours of the site. The data comprised entry and circulating flow and the geometric variables. The required values of entry and circulating flow for one-minute interval were extracted. The plot between entry and circulating flow depicted exponential relationship for the data so extracted. Regarding the various geometric variables, diameter of Central Island, entry width, weaving width, and the weaving length were found to have significant impact on capacity. These geometrics when plotted against the logarithm value of entry flow showed linear relationship in case of Central island diameter and weaving width both; whereas, the rest of the geometrics showed logarithmic variations. The model for entry capacity was then developed using these geometric parameters and circulating flow.

The relationship between the entry and the circulating flow was found to be exponential for the best fit .Due to the roundabout there is a lot of safe in time and the occurance of accidents are less. There will be free flow of the traffic. The

conflict points are reduced in roundabouts when compared with signalized intersection. The study was conducted only for the unsignalized roundabout intersections,

Thus, a study could be done for the capacity evaluation for the signalized roundabouts for various cities in India. Along with

VI. REFERENCES

[1] Akcelik, R (2011), "Evaluating Roundabout Capacity, Level of Service and Performance". Ramu Arroju et.al (2015),

[2] "Comparative evaluation of roundabout capacities under heterogeneous traffic conditions", IRC 65: Recommended Practice for Traffic Rotaries, 1976, Indian Road Congress,

[3] Lenters, M and C. Rudy (2010), "HCM Roundabout Capacity Methods and Alternative Capacity Models". NCHRP 672: Roundabouts: An informational Guide, Second Edition, TRB, 2010.

AUTHORS PROFILE

1. *K. Smitha*, Matrusri Engineering College, Hyd E mail smithasathuri@gmail.com
2. *K. Vamshi Krishna*, Matrusri Engineering College, Hyd
3. *B. Hari Priya*, Matrusri Engineering College, Hyd

ABOUT THE INSTITUTE

Muffakham Jah College of Engineering and Technology (MJCET) was established in the year 1980 by Sultan-Ul-Uloom Education Society (SUES), which was formed by a group of visionaries and intellectuals from various walks of life. Over the past three decades, it has emerged as a premier institute, offering BE courses of four years duration in eight disciplines (Civil, ECE, CSE, IT, EEE, EIE, Mechanical & Production) and five ME courses (CAD/CAM, Structural Engineering., Digital Systems, Computers & Power Electronics) of two years duration. The current intake of all BE Courses is 780, in addition to 102 students in ME Programmes. Research Centers were started in Civil, Mechanical, EEE, CSE and ECE Departments for Doctoral Studies. The college is affiliated to Osmania University, Hyderabad and approved by AICTE, New Delhi. As per the survey of The Outlook magazine, MJCET was ranked 62nd among top 100 Engineering Colleges in India. MJCET has been ranked 47th in India among the top private institutes in Engineering by Times Engineering Institute ranking survey 2019. MJCET ranked 28th out of top 200 Engineering Colleges by India Today magazine. As per The Week Magazine, MJCET ranked 26th among the top Private Engineering Colleges in South India and 42nd among All India Private Engineering Colleges.

OVERVIEW OF THE CONFERENCE

Civil Engineering Infrastructure is the most significant factor in accelerating the pace of economic development of any country. The recent innovation and advances in the field of Civil Engineering has made a drastic impact in the Construction Industry. As the world's population increases, environmental concerns mount and Civil Engineers are entrusted by the society to achieve a sustainable world and raise the quality of life globally. The balancing of economic, social and environmental objectives now and in the future has become known as Sustainable Development and is increasingly a key driver at a range of organizational and spatial scales.

The Conference on Recent Advances in Civil Engineering Infrastructure – (RACEI-2019) aims at exploring the new horizon of innovation from distinguished researchers, eminent professionals from academia and Industry. The Conference also focuses for the achievement of relevant Sustainable Development Goals as described by United Nation Development Program. This event will be a platform to showcase and deliberate research work, studies and contributions for developing novel concepts in Civil Engineering Infrastructure. The Conference consists of keynote lectures on related themes by eminent personalities and stake holders.

BSP BS Publications
A Unit of BSP Books Pvt. Ltd.
4-4-316/309, Giriraj Lane, Sultan Bazar, Hyderabad - 500 095. (A.P.)
Ph: 040-23445688 / 605. Fax: +91-40-23445611.
e-mail: info@bspbooks.net, marketing@bspbooks.net
Website: www.bspbooks.net

ISBN : 978-93-89354-86-7

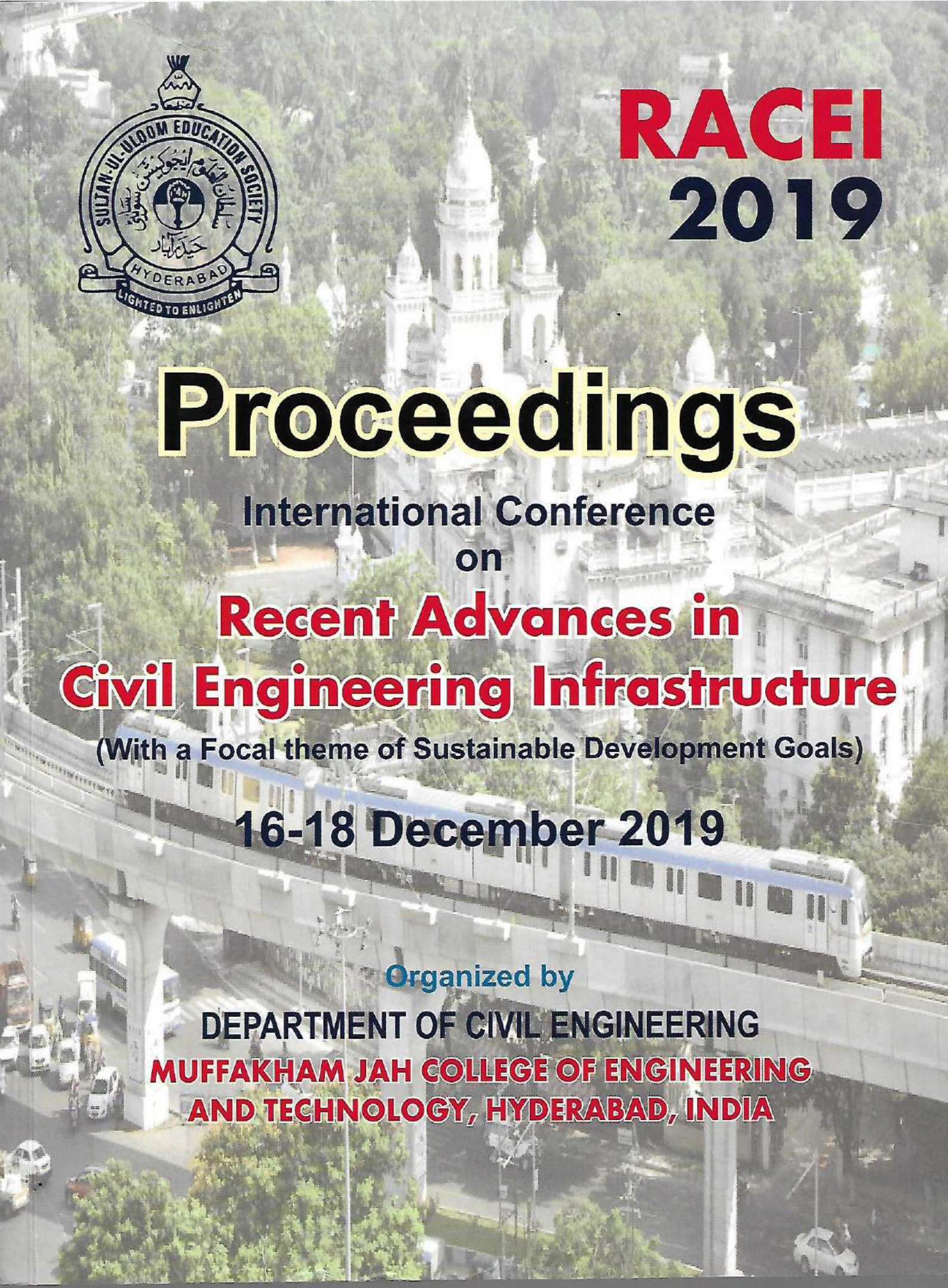

RACEI 2019

Proceedings

International Conference on

Recent Advances in Civil Engineering Infrastructure

(With a Focal theme of Sustainable Development Goals)

16-18 December 2019

Organized by

DEPARTMENT OF CIVIL ENGINEERING

MUFFAKHAM JAH COLLEGE OF ENGINEERING AND TECHNOLOGY, HYDERABAD, INDIA

A Design of Concrete Bridge

NavyaSoni, P Dhanmma and T Raja Ramanna

Abstract: ***In this project, an attempt is being made to design a concrete girder bridge with T beam slab, piers and abutments. The design is initially to be done manually executed in CAD as the same with detailed diagrams and cross sectional views.***
In general there are many types of bridges as follows: ***Post-Tensioned and pre stressed: Post Tensioned Concrete Slab Haunched, Post Tensioned Concrete Box Girder Continuous, Pre stressed Deck Girder Continuous bridges. Steel types: Steel Welded Girder Simple, Steel Riveted Girder Continuous, Weathering Steel Welded Plate Girder Continuous, Steel Welded Girder Haunched bridges. Concrete types: RC Slab Haunched, RC through Arch Fixed, RC Deck Girder Simple, RC Open Spandrel Arch Fixed bridges. Among these we are designing concrete girder bridge. An RCC bridge usually consists of T beams supporting continuous slab. The beams are supported on intermediate piers and abutments in India bridges for roads are designed as per the recommendations of the Indian Road Congress Road. In India all road bridges designed according to IRC loading. This code classifies bridges and culverts into the following categories:***

i) IRC class AA loading
ii) IRC class A loading
iii) IRC class B loading
Among these we are using IRC class AA loading for bridge design. In IRC class AA loading brides subjected to very heavy loading on certain specified areas and highways come under this category. Bridges designed for class AA loading should be checked for class A loading.

I. INTRODUCTION

The aim of this project is to design a T-beam girder concrete bridge of 16m spam and 7.5m width. The loads which are considered are dead loads, live loads such as wind loads, water currents and vehicular loads.

A bridge is a man-made structure built to avoid physical obstacles without closing the way underneath such as a body of water, valley, or road. It is constructed for the purpose of providing passage over the obstacle. The first bridges made by humans were probably spans of cut wooden logs or planks and eventually stones, using a simple support and crossbeam arrangement. The Romans built arch bridges and aqueducts. The Romans also used cement, which reduced the variation of strength found in natural stone.

A. Types of bridges:

The most common types of bridges are described below.

1. *Beam Bridge*
2. *Arch*

Types of arch bridges:

1. Hinge less arch bridge.
2. Two hinged arch bridge.
3. Three hinged arch bridge.
4. Tied hinged arch bridge.

3. *Cantilever bridge.*
4. *Suspension bridge*
5. *Cable stayed bridge* towers is much greater than the suspension bridge.
6. *Truss bridge* wider area.

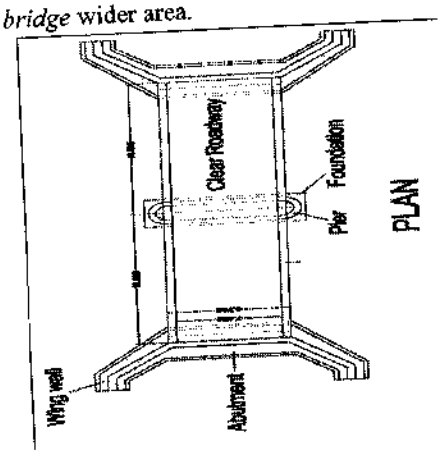

PROPOSED PLAN
MANUAL DESIGN

II. DESIGN OF DECK SLAB

Clear width of loading =7.5m
Live load = class AA & class A
Average thickness of wearing coat = 8cm
Clear span centre to centre of bearing = 16m

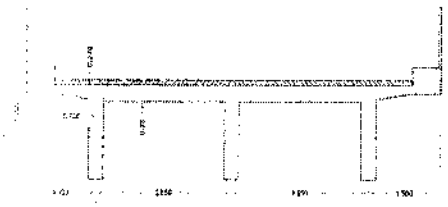

Fig 1

Three girders are provided at c/c distance of =2.85m Kerbs 0.6m wide are provided including railings.

Web widths of 30cm are proposed for longitudinal girder & of cross girder.

Thickness of slab is assumed as 25cm for interior panel.

Thickness of cantilever slab is assumed as 25cm at junction with slab and 20cm at junction with kerb.

Weight of railing is assumed as 70kg/m

Cantilever will be designed by effective width method & interior panels by Pigeaud's theory.

Dimensions of interior panel are 2.85mX4m

Concrete mix M20 is used for deck slab & girders

Impact factors for design of slab:

Class AA loading =25%

For class A loading, maximum impact factor = 50.0%

III. DESIGN OF CANTILEVER PORTION

Item	Load/m-run. (Kg)	Distance of C.G. from edge cantilever (m)	Moment (N-m)
Parapet	700	1.275	892.5
Kerb	0.44X0.6X1X25000=6600	1.05	6930
Wearing coat	0.08X0.75X23000=1880	0.375	517.5
Slab triangular	½X0.75X0.1X25000=937.5	0.25	234.37
Slab rectangular	0.15x0.75x25000=2812.5	0.375	1054.69

Total load =12.430kN

Total D.L BM = 9.63kN-m

Live load B.M:

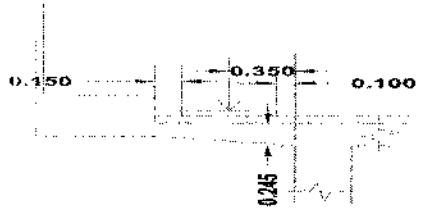

Fig 2

Class AA loading: Minimum clearance of class AA loading from kerb is 1.2m. Hence this loading will not come in cantilever portion class A loading.

Distance of C.G. of load from edge of cantilever=X=0.375m

Effective width of slab =1.2x +bw

= 1.2X0.375+(0.25+2x0.08) = 0.86m

Load per meter width of slab = $\frac{11.43}{0.86}$ = 68.7kN

Dispersion width along span of cantilever = 0.5 + 2(0.08+0.20) = 1.06m

Some portions of dispersion width goes beyond edge of cantilever dispersion width in cantilever portion = 0.54/2 +0.5 +0.1 = 0.87m

Portion of load in cantilever = $\frac{68.7X0.87}{1.06}$ = 56.39kN

B.M = 56.39X0.87/2=24.53 kN-m

B.M = including impact = 1.5X 24.53 =36.79kN-m

Total B.M = 36.79+9.63 = 46.42kN-m

Effective depth = $\sqrt{\frac{46.42X10^6}{0.138X20}}$ = 23cm

Provide an overall depth of 25cm with effective depth of 23cm

Area of steel required = $\frac{46.42X10^6}{0.87X415X220}$ = 971.77mm^2

$\frac{\pi X8^2}{971.77}X1000$= 115.61mm

Provide 12mmØ bars at 10cm c/c

Distribution steel: distribution reinforcement is to be provided for 0.3 times L.L B.M & 0.2 Times D.L B.M

M=0.3X36.79+0.2X9.63 = 12.96 kN-m

Effective depth = 23-0.6-0.4=22cm=220mm

A_t=$\frac{12.96X10^6}{0.87X415X220}$=271.31mm^2

Half reinforcement has to be provided at top &half at bottom.

$\frac{\pi X8^2}{135.65}X1000$=175.46mm

Provide 8mmØ bars at 15mm c/c.

Shear:

Live load shear including impact=56.39X1.50=84.58kN

Dead load shear = 12.43kN

Total shear = 84.58+12.43=97.01

Shear stress=$\frac{97.01X10^3}{1000X220}$=4.88kN/m^2

Design of interior panel:

Dead weight of slab for per m^2=1X1X0.2X25000N=50kN

Dead weight of wearing coat=1X1X0.0823000=1840N=1.84kN

Total D.L =6.84kN/m^2

IV. LIVE LOAD

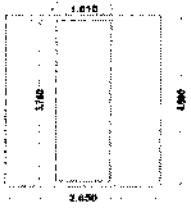

Fig 3

Class AA tracked vehicle: one wheel is placed in the centre of the panel

Thickness of wearing coat =80mm

Dispersion of wheel loads: $\mu=b+2h$ & $v=a+2h$

$\mu=0.85+2(0.08)=1.01$m & $v=3.6+2(0.08)=3.76$m

$\frac{\mu}{B}=\frac{1.01}{2.85}=0.35$ & $\frac{v}{L}=\frac{3.76}{4}=0.94$

$\frac{L}{B}=\frac{4}{2.85}=1.403$

referring to Pigeaud's curves

$M_1=9.0\text{x}10^{-2}$ & $M_2=3.5\text{X}10^{-2}$

Moment along $M_B=W(M_1+0.15M_2)$

$=700/2(9.0\text{X}10^{-2}+0.15\text{X}3.5\text{X}10^{-2})$ = 33.34kN-m

As the slab is continuous, B.M taken for design will be 0.8 times M_B B.M including impact and continuity factor

$M_B=1.25\text{x}33.34\text{X}0.8=33.34$kN-m

$M_L=W(0.15M_1+M_2)$

$=700/2\text{X}(0.15\text{X}9.0\text{X}10^{-2}+3.5\text{X}10^{-2})=16.975$kN-m

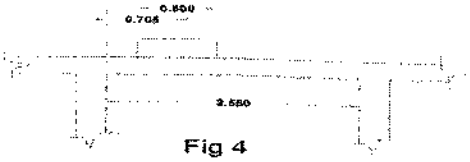

Fig 4

B.M including impact is continuity factor

$M_L=1.25\text{X}16.97\text{X}0.8=16.97$kN-m

V. SHEAR

Dispersion in the direction of the span =0.85+2(0.08+0.2) =1.41m

For maximum shear load is kept such that whole dispersion is in the span load is kept at 1.41/2=0.705m

From edge of beam

Effective width of slab $=kx(1-\frac{x}{l})+b_w$

Breadth of cross girder=30cm

Clear length of span = 4-0.3=3.7

Clear breadth of span = 2.85 – 0.3= 2.55m

$\frac{L}{B}=\frac{3.7}{2.55}=1.45$

K for continuous slab=2.48 (from table)

Effective width of slab=$2.80\text{X}0.705(1-\frac{0.705}{3.7})+3.76=5.18$m

Load per meter width $=\frac{70.000}{1.000}=70$kN

Shear force $=70(2.55-\frac{0.705}{2})=50.65$kN

Shear force including impact=1.25X50.65=63.31kN

Class AA wheeled vehicle: There are 2 possibilities which should be investigated for finding the maximum B.M in the panel.

First possibility is when two loads of 37.5KN each and 2 loads of 62.5kN each are symmetrically placed about the centre line as shown in figure 5a.

Second position is when 2 loads of 37.5kN and 4 loads of 62.5kN each are placed in the panel with central 2 loads of 62.5kN placed at the centre.

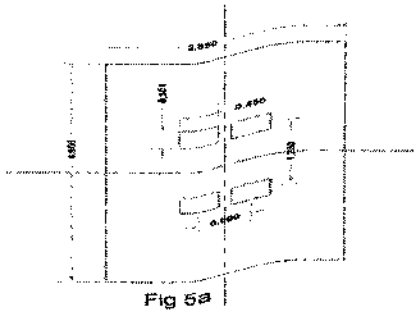

Fig 5a

$\mu_1=0.3+2(0.08)=0.46$m

$v_1=0.15+2(0.08)=0.31$m

The analysis for this case is done as below for each load M_1 & M_2 is found for

i. $\mu=2(\mu_1+x)$ & $v=2(v_1+y)$ and multiply by $(u_1+x)\text{X}(v_1+y)$

ii. $\mu=2x$ & $v=2y$ and multiply by xy

iii. $\mu=2(\mu_1+x)$ & $v=2y$ and multiply by $y(\mu_1+x)$

iv. $\mu=2x$ and $v=2(v_1+y)$ & multiply by $x(v_1+y)$

For design B.M subtract (iii + iv) from (i + ii) & multiply by $\frac{W}{u_1v_1}$

i. $\mu=2(\mu_1+x)=2(0.46+0.07)=1.06$m

$v=2(v_1+y)=2(0.31+0.445)=1.51$m

$\frac{\mu}{B}=\frac{1.06}{2.85}=0.37$ & $\frac{v}{L}=\frac{1.51}{4}=0.38$ & $\frac{L}{B}=k=\frac{4}{2.85}=1.403$

From Pigeaud's curves: $M_1=13.5\text{X}10^{-2}$ & $M_2=8.0\text{X}10^{-2}$

$\mu_1+x=0.46+0.07=0.53$ & $v_1+y=0.31+0.445=0.755$

Modified $M_1=13.5\text{X}10^{-2}\text{X}0.53\text{X}0.755=5.4\text{X}10^{-2}$

Modified $M_2=8.0\text{X}10^{-2}\text{X}0.53\text{X}0.755=3.20\text{X}10^{-2}$

ii. $\mu=2x=2\text{X}0.07=0.14$ & $v=2y=2\text{X}0.455=0.89$

$\frac{\mu}{B}=\frac{0.14}{2.85}=0.049$ & $\frac{v}{L}=\frac{0.89}{4}=0.22$ & $k=1.403$

From Pigeaud's curves $M_1=24\text{X}10^{-2}$ & $M_2=12.5\text{X}10^{-2}$

Modified $M_1=24\text{X}10^{-2}\text{X}0.07\text{X}0.455=0.75\text{X}10^{-2}$

Modified $M_2=12.5\text{X}10^{-2}\text{X}0.07\text{X}0.445=0.39\text{X}10^{-2}$

iii. $\mu=2(\mu+x)=2(0.46+0.07)=1.06$ & $v=2y=2\text{X}$ $=0.89$

$\frac{\mu}{B}=\frac{1.06}{2.85}=0.37$ & $\frac{v}{L}=\frac{0.89}{4}=0.22$ & $k=1.403$

From Pigeaud's curves: $M_1=15.0\text{X}10^{-2}$ & $M_2=11.0\text{X}10^{-2}$

$y(\mu+x)=0.455(0.46+0.07)=0.24$

Modified $M_1=15.0\text{X}10^{-2}\text{X}0.445(0.46+0.07)=3.54\text{X}10^{-2}$

Modified $M_2=11.0\text{X}10^{-2}\text{X}0.445(0.46+0.07)=2.59\text{X}10^{-2}$

iv. $\mu=2x=2\text{X}0.07=0.14$ & $v=2(v_1+y)$ $=2(0.31+0.0445)=1.51$

[illegible] 0.14 [illegible]=0.38 k =1.403

From Pigeaud's curves: M_1 =17.0X10^{-2} M_2 =8.5X10^{-2}

[illegible] =0.07(0.31+0.445)

Modified M_1 =17.0X10^{-2}X0.07X0.755 =0.90X10^{-2}

Modified M_2 =8.5X10^{-2}X.07X0.755 =0.45X10^{-2}

Design values of M_1& M_2 are: (i+ii) – (iii+iv)

M_1 =9.4X10^{-2}+0.75X10^{-2}-3.54X10^{-2}-0.90X10^{-2} =1.71X10^{-2}

M_2 =1.90X10^{-2}+0.39X10^{-2}-2.59X10^{-2}-0.45X10^{-2} =0.55X10^{-2}

B.M due to load is [illegible] *(M_1+0.15M_2)*

Total M_0 due to 4 loads

[illegible](1.71X10^{-2}+(0.15X0.55X10^{-2})) +[illegible]

(1.71X10^{-2}+(0.15X0.55X10^{-2}))

25.14kN-m

B.M including impact and continuity factor

1.25X25.14X0.8 =25.14kN-m

Total M_1 due to 4 loads

[illegible]((0.15X0.55X10^{-2})+0.55X10^{-2}) + [illegible]

((0.15X1.71X10^{-2})+0.55X10^{-2})

11.31kN-m

B.M including impact and continuity factor

1.25X11.31X0.8 =11.31kN-m

Shear due to class AA wheeled vehicle:

Dispersion width in direction of span =0.3+2(0.25+0.08) =0.96m

Loads are placed such that outermost load is at a distance of 0.86/2 0.43m from edge of the beam.

Effective width of 1st wheel= $kx(1-\frac{x}{2})+b_w$

=2.80X0.48(1–[illegible])+0.30+2(0.08) =1.55m

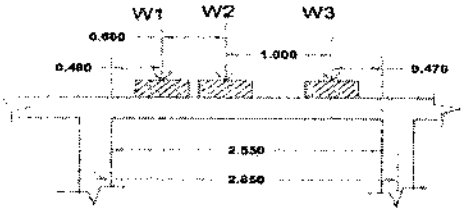

Fig 5b

Dist centre to centre distance of 2 wheels is 1.2m &thus effective width will overlap

Average effective width for 1st wheel =1.2+1.55/2 =1.375m

Load per meter width of slab= 37.5/1.375 =27.27kN

Effective width for 2nd wheel= 2.8x1.08(1–[illegible])+0.48 2.20m

But centre to centre distance of 2 wheels is 1.2m and thus effective widths overlap

Average effective width for 2nd wheel= 1.2+2.2/2 =1.59m

Load per meter width of slab= 62.5/1.7=36.76kN

Effective width for 3rd wheel= 2.8X0.47(1 – [illegible])+0.8 =1.53m

Average= (1.53+1.2)/2 =1.36m

Load per meter width= 62.5=45.95kN

Portion of W_3 in span =45.95/1.36X0.93=31.42kN

Shear force at edge

= 27.27X[illegible] +36.76X[illegible] + 31.42X[illegible] = 43.43

Shear force including impact =1.25X43.43 =54.29kN.

Class A Loading: For maximum B.M., first wheel of 5.7 tonnes should be placed at centre of span and other at 1.2m from it as shown in figure 6.

Imaginary load W_3 = W_2 is placed on other side of W_1 to make loading symmetrical. B.M at centre of panel will be that due to W_1 plus half due to load W_2& W_3

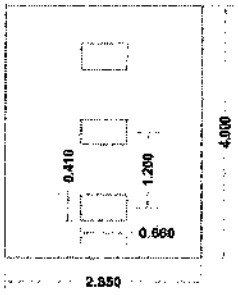

Fig 6

B.M due to load W_1:

μ = 0.5+2(0.08) =0.66m & v =0.25+2(0.08) =0.41m

[illegible]=0.23 [illegible]=0.10

From Pigeaud's curves k =1.403

M_1 =19x10^{-2} M_2 =16.5X10^{-2}

M^1_B = W(M_1+0.15XM_2) =57(0.15X19X10^{-2}+16.5X10^{-2}) =12.24kN-m

M^1_L= W(0.15XM_1+M_2) =57(0.15X19X10^{-2}+16.5X10^{-2}) =11.03kN-m

B.M due to W_2

μ =0.5+2(0.08) =0.66m V_1=0.25+2(0.08) =0.41m

i. μ =μ & v =2(v_1+y)

μ =0.66 v =2(0.995X0.41) =2.81

[illegible]=0.23 [illegible]=0.50

From Pigeaud's curves M_1 =11.5x10^{-2}& M_2 =5X10^{-2}

These are to be multiplied by 1.405

M_1 =11.5X10^{-2} =16.16X10^{-2} M_2 =5X10^{-2}X1.405 =7.03X10^{-2}

ii. μ =μ & v =2y

μ =0.66 & v =1.99

$\frac{y}{x} = \frac{0.56}{2.55} = 0.23$ & $\frac{y}{L} = \frac{1.50}{4} = 0.50$

From Pigeaud's curves: $M_1 = 14.5X10^{-2}$ & $M_2 = 6.8X10^{-2}$

These are to be multiplied by y

$M_1 = 14.5X10^{-2}X0.995 = 14.43X10^{-2}$ & $M_2 = 6.8X10^{-2}X0.995 = 6.77X10^{-2}$

Design values of M_1 & M_2 are I – ii

$M_1 = 16.16X10^{-2} - 14.43X10^{-2} = 1.73X10^{-2}$

$M_2 = 7.03X10^{-2} - 6.77X10^{-2} = 0.6X10^{-2}$

$M^{11}_B = W/V\ (M_1 + 0.5M_2) = \frac{57}{0.41}(1.73X10^{-2} + 0.15X0.26X10^{-2})$ $= 2.46$kN-m

$M^{11}_L = W/V(0.15M_1 + M_2) = \frac{57}{0.41}(0.15X1.73X10^{-2} + 0.26X10^{-2})$ $= 0.72$kN-m

Total B.M due to two loads will be $M_B - M^1_B + M^{11}_B$ & $M^1_L + M^{11}_L - M_2$

$M_B = 12.24 = 14.7$kN-m & $M_L = 11.03 + 0.72 = 11.75$kN-m

B.M including impact and continuity

$M_B = 1.5X14.7X0.8 = 17.64$kN-m

$M_L = 1.5X11.75X0.8 = 14.1$kN-m

Shear due to class A loading:

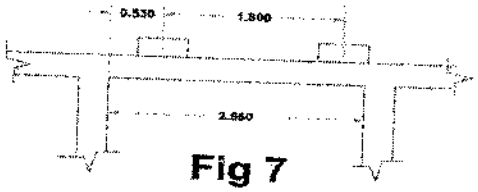

Fig 7

Dispersion width in the direction of span $= 0.5 + 2(0.08 + 0.2) = 1.06$m

For maximum shear the load should be placed at a distance of $1.06/2 = 0.53$m from edge.

Effective width $= kx(1 - \frac{x}{l}) + b_w$ $= 2.48x0.53(1 - 0.53/2.55) + 0.25 + 0.08x2 = 1.45$m

Distance between 2 wheels is 1.2m and hence effective widths overlap

Average effective width per wheel $= 1.45 + 1.2/2 = 1.33$m

Load per meter width of the beam $= 5.7/1.33 = 4.29$kN

Shear force $= 4.29(\frac{2.55 - 0.53}{2.55}) = 3.40$kN

S.F including impact $= 1.5x3.40 = 3.40 = 5.1$kN

Design live load B.M & S.F:

$M_B = 33.34$kN-m (class AA tracked) & $M_L = 16.97$kN-m (class AA tracked)

S.F $= 63.31$kN (class AA tracked)

VI. DEAD LOAD

Dead load per square meter $= 6.84$kN/m^2

Dead load B.M will be found by Pigeaud's method

Total load on panel $= 4X2.85X6.84 = 77.98$kN

$\mu/B = 1$ $V/L = 1$ as panel is loaded with U.D.L

$M_1 = 4.8X10^{-2}$ & $M_2 = 2.1X10^{-2}$

$M_B = 6.84(4.8X10^{-2} + 0.15X2.1X10^{-2}) = 0.35$kN-m

Taking actual B.M 0.8 times value to account for continuity

$M_B = 0.8X0.5 = 0.28$kN-m

$M_L = 6.84(0.15X4.8X10^{-2} + 2.1X10^{-2}) = 0.19$kN-m

Considering effect of continuity for B.M

$M_L = 0.8X0.19 = 0.15$kN-m

Dead load S.F is assumed as $6.84x2.55/2 = 8.72$n

Total M_B due to D.L & L.L $= 33.34 + 0.28 = 33.62$kN-m

Total $M_L = 16.97 + 0.19 = 17.16$kN-m

Total S.F. $= 63.31 + 8972 = 72.0$-3kN

A. Design of section:

Effective depth required $= \sqrt{\frac{[illegible]}{[illegible]}} = 19.54$cm

Provided overall depth of 28cm with effective depth of 25cm

A_t for $M_B = \frac{[illegible]}{[illegible]} = 703.81$mm^2

Provide 12mm Ø bars 15cm c/c

Shear resistance $= 3.5X100X23 = 8050$ kg-cm

As the provided shear resistance is more than the required no additional shear reinforcement is required.

Nominal shear reinforcement: Provide 10mmØ bars at 14mm c/c

Check for shear:

Shear stress $= 7167.0/100X0.903X25 = 3.17$kg/cm^2

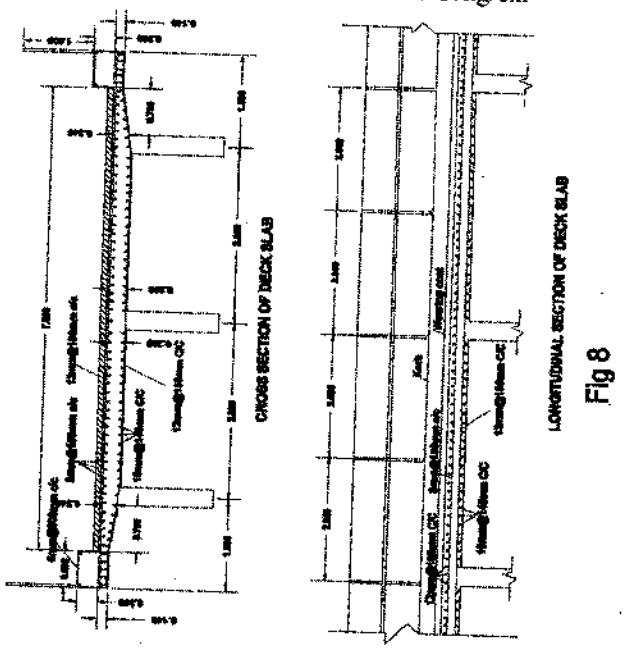

Fig 8

B. Design of longitudinal girders:

Distribution of live loads on longitudinal beams for B.M

Class A loading: Reactions on the girders will be maximum when the eccentricity is maximum eccentricity will be

maximum when the loads are very near to kerb. Position of loads for maximum eccentricity is shown in fig 9a

All the girders are assumed to have same moment of inertia

reaction factor for outer girder

$R_A = \frac{4W_1}{3}(1 + \frac{W}{2 \times 2.85} \times 2.85 \times 0.49)$

$= \frac{4W_1}{3}(1 + \frac{3 \times 0.49}{2 \times 2.85})$

$= 1.68\ W_1$

$R_B = \frac{4W_1}{3}(1+0) = 4W_1/3$

If W is axle load wheel load $W_1 = W/2$

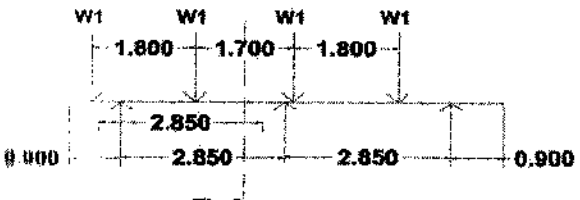

Fig 9a

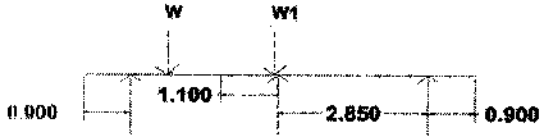

Fig 9b

C.G. of load = 0.9+0.18+1.7/2 =3.05m

Kerb to centre of girder =0.75+0.15+2.85 =3.75m

Eccentricity e = 0.7m

Reaction factor for outer girder = $R_A = \frac{4W_1}{3}(1+\frac{W}{2 \times 2.85^2} \times 2.85 \times 0.7) = 1.82W_1$

Reaction factor for inner girder = (e =0) $R_B = 4/3W_1$

Class AA loading:

C.G. 1.625+2.05/2 =2.65m e =3.75-2.65 =1.1m

Reaction on outer girder $= R_A = \frac{2W_1}{3}(1+\frac{W \times 2.85}{W \times 2.85^2} \times 1.1) = 1.05W_1$

Reaction on inner girder $= R_b = 2W_2/3$

If W is axle load, wheel load $w_2 = w/2$

Reaction on outer girder $= 1.05/2W_1 = 0.53W_1$

Reaction on inner girder $= 2W_3/3 \times 1/2 = W/3$

Dead load from slab per girder:

Total dead load of deck =2x12.43+6.84x6 =65.9kN

It is assumed that dead loads shared equally by all girders.

Dead load per girder =65.9/3 =2.97kN

Live load: impact factor:

Span = 16m impact factor for class AA loading =10%

Impact factor for class A loading $= \frac{4.5}{6+L} = \frac{4.5}{6+16} = 0.2$

Live load including moments and shear force at different sections will be found for class AA tracked vehicle & class A loading. Class AA wheeled vehicle is not considered as it does not produce worst effect.

Live load bending moment:

Centre of span

Class AA loading: Position of loads is shown in figure 10.

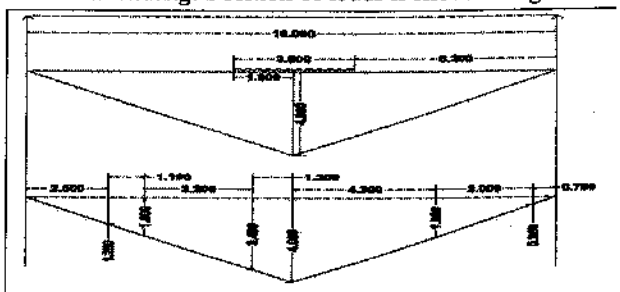

Fig 10

B.M= $(\frac{3+5.1}{2})70$ =248.5cm =2485kN-m

B.M including impact and reaction factor for outer girder

=2485X1.1X0.4833 =1321.10kN-m

B.M including impact and reaction factor for inner girder

= 2485x1.1x1/3 =911.17kN-m

Class A loading: Position of loads for maximum B.M at centre of span is shown in fig 10

B.M

=11.4X4X11.4X3.4+2.7X1.25+2.7X1.8+6.8X0.35+6.8X1.8

=107.195tm =1017.17kN-m

B.M including impact factor & reaction factor for outer girder

=1071.95X0.8625X.204 =1113.17kN-m

B.M including impact factor & reaction factor for inner girder

=1071.95X0.6667X1.204 =860.48kN-m

It is seen that maximum B.M for inner & outer girders is given by class AA tracked vehicle

Maximum live load moment for outer girder =1321.10kN-m

Maximum live load moment for inner girder =911.17kN-m

Quarter span: Class AA loading

Position of load for maximum B.M is shown in figure 11.

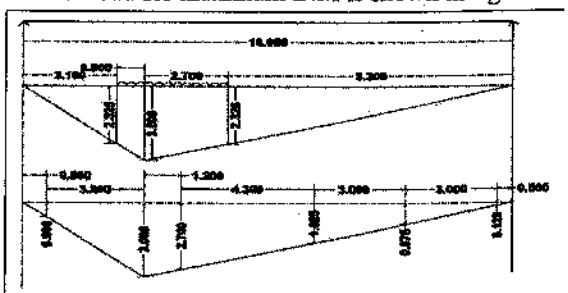

Fig 11

B.M = $(\frac{3+5.1}{2})$x700 =1863.75kN-m

B.M including impact factor for outer girder =1863.75X1.1X0.4833 =990.82 kN-m

B.M including impact factor for inner girder =1863.75X1.1X1/3 =683.37kN-m

Class A loading: Position of loads for max B.M is shown figure11.

M =114X3+114X2.7+6.8X1.625+6.8X0.875+6.8X0.125+2.7X0.6 =844.5kN-m

B.M including impact factor for outer girder =844.5X0.8625X1.204 =877kN-m

B.M including impact factor for inner girder =844.5x0.6667x1.204 =677.8kN-m

Maximum live load for outer girder = 990.82kN-m

Maximum live load for inner girder = 683.37kN-m

Live load shear: Maximum shear at all sections is given by class AA tracked vehicle. For maximum shear at support load should be as near to support as possible. The length of the load is 3.6m whole of load will lie between support and 1st cross girder live load shear at support is found by method described earlier. For intermediate section shear will be found by drawing influences lines the reaction factor found by Courbon's theory will be used for finding shear at intermediate sections.

The position of centre line of load for maximum shear force is shown in figure12a. Let P_A, P_B & P_C be loads coming on the longitudinals considering the slab as simple supported.

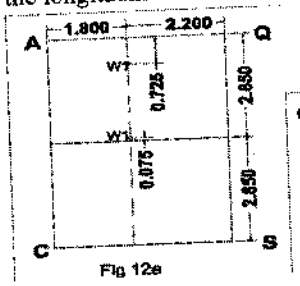

Fig 12a

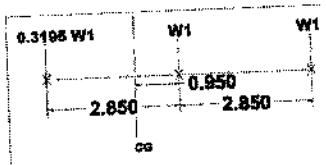

Fig 12b

$P_A = W_1X2.125/2.85 + W_1(0.075)/2.85 = 0.77W_1$

$P_B = W_1X0.725/2.85 + W_1 2.775/2.85 = 1.23W_1$

Due to P_A, shear force at A $= R^1_A = 0.77W1X2.2/4 = 0.385W_1$

$R_Q = 1.23W_1X1.8/4 = 0.315W_1$

Due to P_B shear force at B $= R^1_B = 1.23W_1X2.2/4 = 0.68W_1$

$R_R = 1.8/4X1.23W_1 = 0.55W_1$

The load on the cross girder i.e. R_Q, R_R & R_S are to be distributed by normal Courbon's theory

$\sum W = 0.385W_1 + 0.55W_1 = 0.935W_1$

Let $\bar{x}$ be the distance of C.G. of loads from Q

$\bar{x} = \frac{0.385W_1 \times 2.2}{0.935W_1} = 1.47m$

Inner girder:

Eccentricity e =2.85-1.47=1.38m

$\sum W = \frac{0.935W_1}{3}\left(1+\frac{6X1.38}{2X2.85}\right) = 0.55W_1$

$F_R = 0.935W_1/3(1+0) = 0.31W_1$

Outer girder: $0.55W_1X12/16 = 0.41W_1$

Inner girder: $0.31W_1X12/16 = 0.23W_1$

Total reaction on outer girder $= 0.385W_1 + 0.41W_1 = 0.795W_1$

Total reaction on inner girder $= 0.68W_1 + 0.23W_1 = 0.91W_1$

Max. S.F. on outer girder with impact =0.795X700/2X1.1 =306.07kN

Max. S.F. on inner girder with impact = 0.91X700/2X1.1 =350.35kN

Shear at centre of span:

Position of load for maximum shear is shown in influence line diagram in fig 13

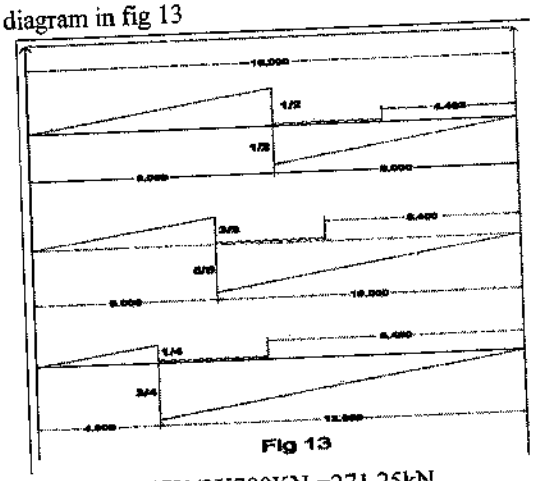
Fig 13

S.F = (1/2+0.275)X1/2X700KN =271.25kN

S.F including impact for outer girder =1.1X0.4833X271.25=144.20kN

S.F including impact for inner girder =1.1X1/3X271.25=99.45kN

Shear at 3/8th span: S.F = (5/8+0.4)x1/2x700 =358.75kN

S.F including impact for outer girder =358.75X1.1X0.4833 =190.72kN

S.F including impact for inner girder =358.75X1.1X1/3 =131.54kN

Shear at quarter span:

S.F = (3/4+0.525)X1/2X700=446.25kN

S.F including impact for outer girder =446.25X1.1X0.4833=237.24kN

S.F including impact for inner girder =446.25X1.1X1/3 =163.63kN

Dead load B.M and S.F:

Assume depth of rib as 1.4m

Weight of rib per meter run =1X0.3X1.4X24000=1008kN

Cross girders are provided at centre quarters points and at the supports width of each cross girder is 30cm & depth 1.4m.

Weight of each cross girder =1X0.3X1.4X24000 =10.08kN
Reaction from deck slab on each cross girder =20.97kN
Total load per meter run of girder =10.08+20.97 =31.05kN

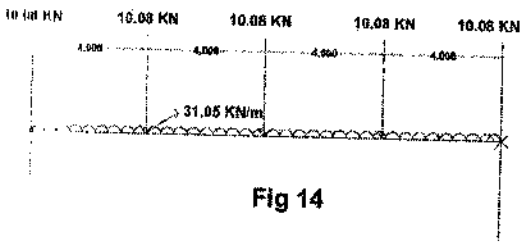

Fig 14

B.M at centre of span =31.05X16X16/8+10008X4+1008/2X8 =1074.24kN-m
B.M at quarters span =31.05X8X4X2+10.08X4+100811/2X4 =805.68kN-m
Dead load shear at support =31.05X8+10.08+10.08/2=263.52kN
Dead load shear at quarter span =263.52-31.05x4 =139.32kN
Dead load shear at 3/8th span= 263.52–31.05X6–10.08= 67.14kN

Design bending moments and shear forces:

Outer girder:

Total B.M. at centre of span= 1321.10+1074.24= 2395.34kNm
Total B.M. at quarter span= 990.82 – 805.68= 1796.5kNm
Total S.F. at support= 263.52+306.07=569.59kN
Total S.F. at 3/8th span=67.14+190.72= 257.86kN
Total S.F. at centre of span = 5.04+144.20=149.24kN
Total S.F. at quarter span= 139.32+237.24=376.56kN

Inner girder:

Total B.M. at centre of span= 683.37+1074.24=1757.61kNm
Total B.M. at quarter span= 677.88+805.68=1483.56kNm
Total S.F. at support =263.52+350.35=613.87kN
Total S.F. at quarter span=139.32+163.63=302.95kN
Total S.F. at 3/8th span=67.14+131.54=198.68kN
Total S.F. at centre of span= 5.04+99.45=104.49kN

Design of Girder:

Outer girder:

Max. B.M.= 2395.34kNm
The beam is designed as T-beam. Assume effective depth as 145cm.
Assume lever arm=0.9X145=130.5cm=1.3m
$A_t = \frac{239.534X100}{2320X130.5} = 8011.17mm^2$
Provide 12 bars of 32mmØ

A_t provided= 80.43cm^2.

Check for stresses:

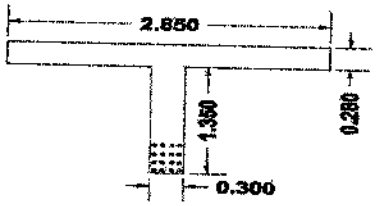

Fig 15

Flange width will be least of:
i. $12d_s+b_r$=12X28+30=366cm
ii. c/c= 2.85m=285cm
iii. span/3=1600/3=5.33m
Hence B=285cm.
For checking stresses, average thickness of flange is assumed as 28cm.
The concrete mix for slab and girders is M_{20}.
As the whole compression is assumed to be taken by the flange, value of m is assumed as 13.
Assuming N.A. to lie in web.
2.85X28(n–10)= 145–n
Solving the above equation we get n=25.64cm
Lever arm $a=d-d_s/2+\frac{d_s^2}{6(2n-d_s)}$= 145– 28/2+ $\frac{28^2}{6(2X25.64-28)}$ = 136.61cm
$B.M. = Bd_sC_a(1+\frac{n-d_s}{n})Xa$ (To find C_a)
=>239.534X100= 280X28XCa(1+$\frac{25.64X100}{25.64}$)X136.61
Solving the equation we get c_a= $\frac{239.534X100}{280X28X136.61X0.897}$ = 24.66kg/cm^2 = 246.6kN/m^2
Area of steel required at quarter span= $\frac{179.65}{2320X0.900X145}$ = 59.65cm^2
Provide 8 bars of 32mmØ.

Check for shear and bond: Max. shear at support= 569.59kN
Assume effective depth as 145cm at support and lever arm as 0.9d.
∑O required for bond= $\frac{569.59}{12X0.9X145}$= 43.65cm
Number of 32mmØ bars required= $\frac{43.65}{\pi X0.8}$=4.34
At least 6 bars are to be taken straight.
Shear stress at support= $\frac{569.59}{28X0.9X145}$= 14.55kg/cm^2
Shear reinforcement is required.
Shear stress at centre of span= $\frac{149.24}{28X0.9X145}$=3.81kg/cm^2
No shear reinforcement is required.

Shear stress at 3/8th span= $\frac{\text{[illegible]}}{\text{[illegible]}}$=6.59kg/cm^2

Bars are bent in sets with 2 bars in each set at every 0.95m. Five sets of bent up bars are provided. Bent up bars will be effective upto 5X0.95=4.75m from support. At every section, 2 sets of bars i.e. 4 bars are effective as bars are bent at spacing of 0.707a. Shear is taken by 4 bent up 32mmØ bars.

= 4X8.04X2300X0.707= 52.29 kg= 522.95kN

Net S.F. at support for which shear reinforcement is to be provided

= 56959–52295= 4664kg=4.66kN

Using 10mmØ 2 legged stirrups

Spacing=$\frac{\text{[illegible]}}{\text{[illegible]}}$ = 101.04cm

Provide 10mmØ 2 legged stirrups at 50cm c/c upto 3.8m from support. After 3.8m from support, only 2 bars are effective.

Shear taken by 2 bars= 26.15kN = 26147kg

Net shear at quarter point for which stirrups are required

= 376.56 – 26.15= 350.41kN

10mmØ stirrups at 50cm c/c are provided between 3.8m and 4.7m from support. Beyond 4.7m from support, no bar is effective.

Providing 12mmØ 2 legged stirrups at quarter span

Spacing = $\frac{\text{[illegible]}}{\text{[illegible]}}$ = 18.01cm

Provide 12mm Ø 2 legged stirrups at 15cm c/c upto 6m from support.

Shear force at 3/8th of span= 25786kg = 25.79kN

Using 12mmØ 2 legged stirrups

Spacing= $\frac{\text{[illegible]}}{\text{[illegible]}}$ =26.31cm

Provide 12mm Ø stirrups at 25cm c/c upto 7.5m from support. In the remaining portion provide 12mmØ stirrups at 50cm c/c.

Inner girder: Max. B.M. at centre= 1757.61kNm

Area of steel provided at centre= $\frac{\text{[illegible]}}{\text{[illegible]}}$= 58.56cm^2

Provide 14 bars of 32mmØ.

Area of steel required at quarter span = $\frac{\text{[illegible]}}{\text{[illegible]}}$ = 49.43cm^2

Provide 12 bars of 32mmØ.

Check for shear and bond: Maximum shear at support= 613.87kN

Assume effective depth as 145cm at support.

$\sum O$ required for bond= $\frac{\text{[illegible]}}{\text{[illegible]}}$= 47.04cm

Number of 32mmØ bars required= $\frac{\text{[illegible]}}{\text{[illegible]}}$=4.68

6 bars of 32mmØ are taken straight.

Shear stress at support= $\frac{\text{[illegible]}}{\text{[illegible]}}$= 15.68kg/cm^2

Shear stress at centre of span=$\frac{\text{[illegible]}}{\text{[illegible]}}$= 2.67kg/cm^2

Shear stress at 3/8th of span= $\frac{\text{[illegible]}}{\text{[illegible]}}$= 5.07kg/cm^2

No shear reinforcement is required between mid span and 3/8th span. Bars are bent in sets at every 0.95m with 2 bars in each set. Four sets of bent up bars are provided. Bent up bars will be effective upto 4X0.95= 3.8m from support. At every section, 2 sets of bars i.e. 4 bars are effective as the bars are bent at spacing of 0.707a.

Shear taken up by 4 bent up bars= 52.29kN

Net shear for which shear reinforcement is to be provided at supports

= 613.87–522.95= 90.92kN

Provide 12mmØ 2 legged stirrups

Spacing= $\frac{\text{[illegible]}}{\text{[illegible]}}$=74.61cm

Provide 12mmØ 2 legged stirrups at 50cm c/c. This spacing is provided upto 3.8m from support. After 2.85m from support, only 2 bars are effective but S.F. is less than that at support.

Shear force at quarter span= 613.87kN

Provide 12mmØ 2 legged stirrups

Spacing= $\frac{\text{[illegible]}}{\text{[illegible]}}$= 11.05cm

Provide 12mmØ stirrups at 10cm c/c between 3.8m from support and 5.0m from support. Provide 12mmØ 2 legged stirrups at 20cm between 5.0m and 6.0m from support.

Maximum web reinforcement= 0.15% of area of web in plan

= $\frac{\text{[illegible]}}{\text{[illegible]}}$X30X100 = 4.5cm^2

Providing 10mmØ stirrups

Spacing = $\frac{\text{[illegible]}}{\text{[illegible]}}$= 34.8cm

Provide 10mmØ stirrups at 25cm c/c.

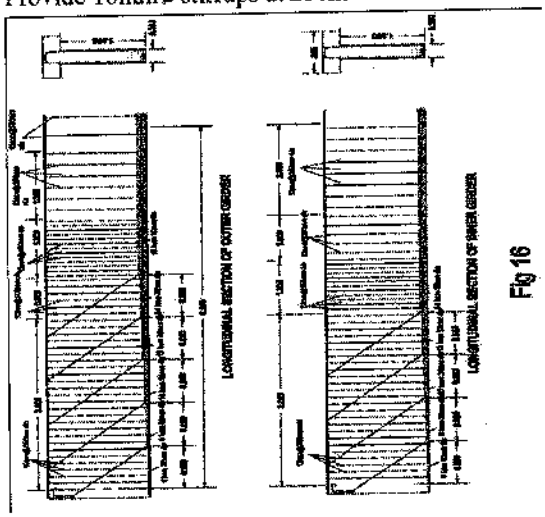

Fig 16

C. **Design of cross girder:** Self weight of cross girder= 10.08kN

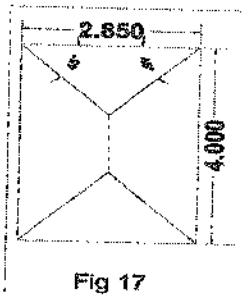

Fig 17

Dead load from slab= 2X1/2X2.85X1.425X6.84 = 27.78kN
This load will be assumed as uniformly distributed load per meter run.

= 9.75kN/m

Total dead load per meter run= 10.08+9.75= 19.83kN
Girder is assumed to be rigid.
Reaction on each girder= 19.83X5/3= 33.05kN
Live load: Max. B.M. and S.F. occurs due to class AA tracked vehicle. For max. B.M. and S.F. in the cross girder, load should be on the cross girder. The position of load for maximum B.M. in the cross girder is shown in fig 18.
Slab is assumed to be simply supported between 2 cross girders.

= 700X = 542.5kN

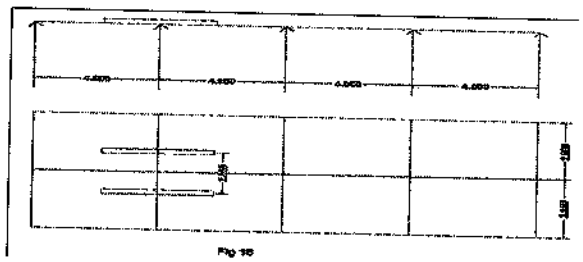

Cross girder is assumed to be rigid.

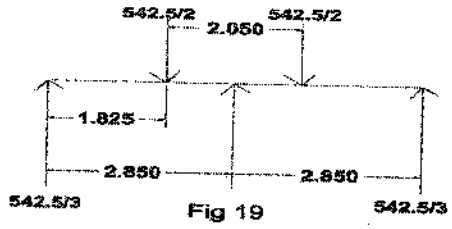

Fig 19

Reaction on each longitudinal girder= 542.5/3= 180.83kN
Maximum B.M. occurs under the load.
Max. L.L.B.M. = 542.5/3X1.825= 330.02kNm
B.M. including impact= 1.1X330.02= 363.02kNm
D.L.B.M. at 1.825m from support= 33.05X1.825–19.83X1.825/2= 42.22kNm
Total B.M. = 42.22+363.02=405.24kNm
Live Load shear including impact= 542.5/3X1.1= 198.92kN
Total shear force= 198.92+33.05= 231.97kN
The cross girder is designed as T-beam. Assuming effective depth as 145cm,

A_t= =13.5cm^2

Provide 3 bars of 25mmØ.

Shear stress= = 5.92kg/cm^2

Using 12mmØ 2 legged stirrups

Spacing= = 29.24cm

Provide 12mmØ 2 legged stirrups at 25cm c/c.

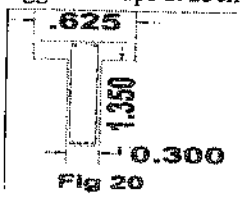

Fig 20

D. Pier design:

Dimensions: Minimum pier length
2X2.85+0.3=6m
6+1.8= 7.8m
Take the length of pier as 8m.
Minimum width = 1.6m
Top area of pier = 1.8X8+πX1.8^2/4 = 16.94m^2
Bottom area of pier = 2.8X8+πX2.8^2/4 = 28.56m^2
Weight of the pier= X8X2.3 = 418.6 tons = 4186kN

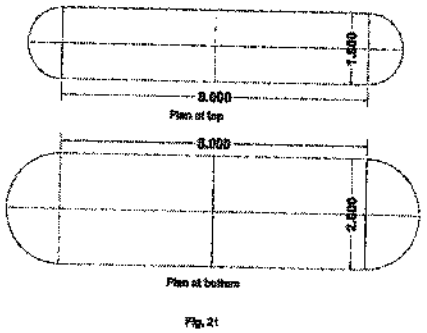

Fig.21

Moments of Inertia:

I_{xx}= + = 17.65m^4

I_{yy}= +2X1/2X + 2X1/2XπX2.8^{2}X4^2/4 = 221.0m^4

Dead loads of superstructure:

Cantilever	=2X12.43X16	= 39.77 tons
Slab	= 6X0.28X16X2.5	= 67.2 tons
Wearing coat= 0.08X2.3X7.5X16		= 22.08 tons
Main girders = 3X0.3X1.35X16X2.5		= 48.6 tons
Cross girders= 10X2.55X0.3X1.35X2.5= 25.82 tons		

Resultant= 202.7 tons

Total dead load including pier= 202.7+418.6= 621.3 tons

Stress due to dead load= $\frac{621.3}{28.86}$= 217.5kN/m^2

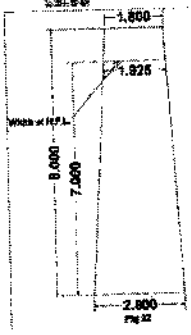

Taking 1m free board.

Volume of submerged portion

Area (H.F.L.)= 8X1.925 + 2X1/2XπX1.925^2/4 = 18.31m^2

Volume = $(\frac{18.31+28.86}{2})$X7 = 164.04m^3

Weight in loss= 164.01X1= 164.04 tons (as unit weight of water= 1 ton/m^3)

Stress at base= $\frac{164.04}{28.86}$ = –57.4kN/m^2

Live load stresses:

Eccentricity of girders=1/2 = 0.5m

Total live load = 70X1.1= 77 tons= 770kN

Moment = 770X0.5 = 385kNm

Stress = $\frac{770}{28.86} \pm \frac{385}{17.32}$X1.4

= 27.0$\pm$ 30.5

Maximum stress= 27.0+30.5 = 57.5kN/m^2

Minimum stress= 27.0–30.5 = –3.5kN/m^2

Longitudinal force= 0.25X770= 192.5kN

Moment at bottom= 192.5X8= 1540kNm

Stress= $\pm \frac{1540X1.4}{17.32}$ = 122.8kN/m^2

Wind Loads:

Exposed area: Girder= 1.35m

Slab = 0.28m

Kerb = 0.3m

Railing=1m

Resultant= 2.93m

2.93X16= 46.88m^2

Assuming wind pressure= 90kg

Total force= 46.88X0.09 = 4.22 tons = 42.2kN

But as per code minimum wind load should not be less than 450kg/m^3.

16mX0.45= 7.2 tons = 72kN

And 240kg for unloaded portion

46.88X0.24 = 251 tons = 2510kN

Moment = 11.25X8 + 2.93/2 = 11.25X8 + 2.93/2 = 106.48 tons-m = 1064.8kNm

Stress = $\frac{M}{I_{yy}} = \frac{1064.8}{132.9}$X4 = 19.3kN/m^2

At edge = $\frac{1064.8}{132.9}$(4+1.4) = 26.0kN/m^2

Stresses due to water currents:

Area of wetted surface = $\frac{(1.925+3.85)}{2}$X7 = 16.54m^2

$P = \frac{1.5KAV^2}{2g}$

Assuming velocity of water = 3m/s

Pressure = $1.5X\frac{1X16.54X3^2}{2X9.81}$ = 11.38 tons = 113.8 kN

This pressure acts at a height of 2/3h from bottom.

Moment= 113.8X2/3X7 = 531.1kNm

Stresses at junction = $\frac{531.1}{132.9}$X4 = 9.6kN/m^2

Stresses at edge = $\frac{531.1}{132.9}$X5.4 = 13.0kN/m^2

Stresses due to longitudinal force:

Maximum longitudinal force will occur due to class AA loading.

Longitudinal force due to class AA loading = 0.2X70 = 14 tons

Moment at base of pier due to this force = 140X8 = 1120kNm

Stresses at base = $\pm \frac{M}{I_{yy}}$Xy = $\frac{1120X1.4}{17.32}$ = 88.84kN/m^2

Total Stresses:

Under dry conditions:

Total stress = dead load + live load (eccentric + longitudinal force + frictional resistance) + wind load

At the end of straight portion (point A or E) maximum

=217.5+57.5+88.84+57.4+19.3+26.0= 466.54kN/m^2

At the end of straight portion (point A or C) minimum

=217.5–3.5–88.84–57.4–19.3–26.0= 22.46kN/m^2

At the end of pier (F or C) maximum

=217.5+26.0= 243.5kN/m^2

At the end of pier (F or C) minimum

=217.5–26.0= 191.5kN/m^2

Under wet conditions:

Total stress = dead load + buoyancy + live load + wind load + wind currents

At the end of straight portion (point A or E) maximum

=217.5–57.4+57.5+88.84+57.4+19.3+96.0= 392.74kN/m^2

At the end of straight portion (point A or E) minimum

=217.5–57.4–3.5–88.84–57.4–19.3–96.0= 18.54kN/m^2

At the end of pier (F or C) maximum

=217.5–57.4+26.0+13.0= 199kN/m^2

At the end of pier (F or C) minimum

=217.5–57.4–26.0–13.0= 121.1kN/m^2

Allowable compressive stress in 1:3:6 concrete is 20N/mm^2 in compression.

E. FOUNDATION:

Total dead load= 6213kN

Taking moorum soil with S.B.C. 350kN/m^2.

Taking 10% load of footing = 621.3kN

Area $= \frac{6213+621.3}{350} = 19.52$ m^2

Proposed dimensions = 11.4X3.4m

Area 38.76 m^2

Provide P.C.C. bed of 11.4mX3.4mX0.2m dimensions

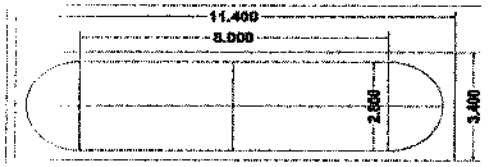

Fig 23

F. ABUTMENTS:

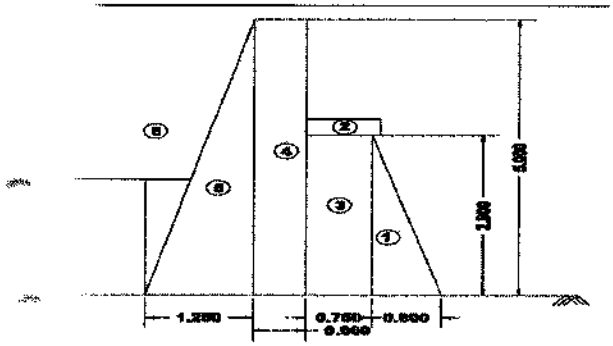

Fig 24

Dead load from superstructure= $\frac{912.15}{9}$ = 101.35 tons = 1013.5kN

Dead load per meter width = 101.35/9 = 11.26 tons = 112.6kN

Live Load max. S.F.= 70X14.2/16 = 62.125 tons = 621.25kN

Live Load with Impact = 621.25X1.1 = 683.38 kN

Live load per meter width = 683.35/9 = 75.93 kN

Resultant = 112.6+75.93 = 188.53kN

Eductive effort = 14/9 = 1.56 tons = 15.6kN

Load from superstructure = 0.15X18.852= 2.835 tons = 28.35kN

Total = 15.6+28.35= 44.3kN

Earth pressure = $\tan\theta$ = 1.25/5 = 0.25

$\theta = \tan^{-1}(0.25) = 14.036°$

$\cos\theta$ = cos(14.036)= 0.97 & sin(14.036)= 0.24

Earth pressure = $\frac{1-\sin\theta}{1+\sin\theta} = \frac{1-0.25}{1+0.25} = 1/3$

Total active earth pressure P = $k_a X \frac{wh^2}{2}$ = 1.8X21^2/2 = 3.969 tons = 39.69 kN

Horizontal force = 39.69X0.97 = 38.5 kN

Vertical force = 39.69X0.24 = 9.5kN

Sl. No.	Description	Weight	Lever Arm	Moment
1.	Reaction	18.853	1.125	21.209
2.	Item 1-1/2X0.8X2.9X2.3	2.668	0.533	1.422
3.	Item 2- 0.85X0.3X2.4	0.612	1.125	0.688
4.	Item 3- 0.75X2.9X2.3	5.003	1.175	5.878
5.	Item 4- 0.6X5.0X2.3	6.900	1.85	12.765
6.	Item 5-1/2X1.25X5.0X2.3	7.188	2.567	18.452
7.	Item 6-1/2X1.25X5.0X1.8	5.625	2.98	16.763
8.	Earth pressure (vertical) 0.95	0.95	2.875	2.731
9.	Earth pressure (horizontal) 3.85		-2.10	-8.085
10.	4.42		-2.90	-12.818

$\sum$= 47.799 tons $\sum$= 59.005ton-m

Point of application of R= $\frac{59.005}{47.799}$ = 1.234m

Eccentricity e= 3.4/2 – 1.234 = 0.466m

P= $\frac{47.799}{3.4}\left(1 \pm \frac{6\times47.799\times0.466}{3.4^2}\right)$ = 17.354(1$\pm$0.822)

Maximum shear stress= 316.19kN/m^2

Minimum shear stress= 30.89kN/m^2

There is no occurrence of tension hence safe.

Taking moorum foundation on site with S.B.C. 350kN/m^2.

G. WING WALLS:

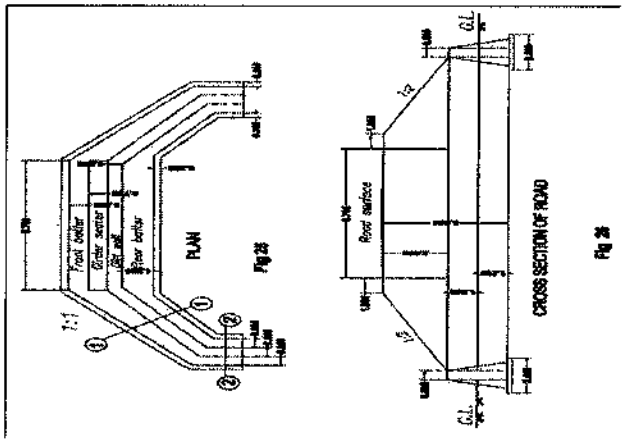

P_a= 1/2X0.54X1.8X2.6^2 = 3.28 tons

$P_a \cos\theta$ = 3.28X0.97 = 3.18 tons

$P_a \sin\theta$ = 3.28X0.24 = 0.79 tons

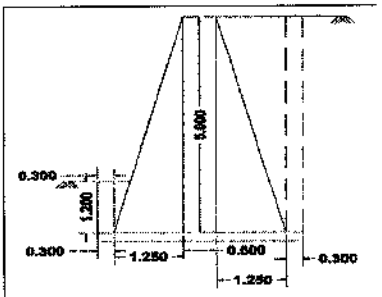

CROSS SECTION "1-1"

Fig. 27

Section 1-1

Sl. No.	Description	Weight	Lever arm	Moment
1.	1/2X0.6X2.4X2.3	1.656	0.7	1.16
2.	0.6X2.4X2.3	3.312	1.2	3.97
3.	1/2X0.6X2.4X2.3	1.656	1.7	2.81
4.	2.4X0.2X2.3	1.104	1.2	1.33
5.	1/2X0.6X1.2X1.8	0.648	0.5	0.32
6.	0.3X1.2X1.8	0.648	0.15	0.10
7.	1/2X0.6X2.4X1.8	1.296	1.80	2.33
8.	0.3X2.4X1.8	1.296	2.25	2.92
9.	Active P_v 3.18		1.09	–3.47
10.	P_H	0.79	1.84	1.45
11.	Passive 5.29		0.87	4.60

$\sum$=12.406 tons $\sum$=1.53 tons-m

Point of application of R= $\frac{1.53}{12.406}$ = 1.41m

e = b/2 – R = 1.2–1.41= –0.21m

P=$\frac{12.406}{2.4}(1 \pm \frac{6\times0.21}{2.4})$ = 5.17(1$\pm$0.525)

Maximum stress = 7.88 tons/m^2 = 78.8kN/m^2

Minimum stress = 2.46 tons/m^2 = 24.6kN/m^2

There is no occurrence of tension hence safe.

Section 2-2

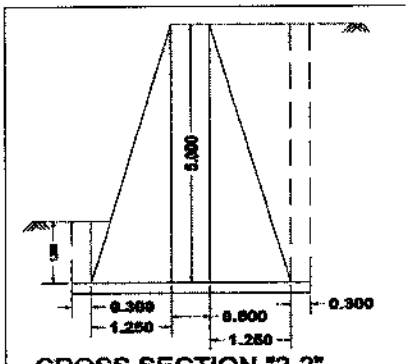

CROSS SECTION "2-2"

Fig. 28

Sl. No.	Description	Weight	Lever Arm	Moment
1.	1/2X1.25X5X2.3	7.19	2.57	18.48
2.	0.6X5X2.3	6.9	1.85	12.76
3.	1/2X1.25X5X2.3	7.19	1.13	8.12
4.	1/2X0.3X1.2X1.8	0.324	0.3	0.09
5.	0.3X1.2X1.8	0.648	0.15	0.09
6.	1/2X1.25X5X1.8	5.625	2.98	16.76
7.	Active P_H 7.86		–2.18	–17.13
8.	P_V 1.94		2.83	5.49
9.	Passive P		0.87	4.6

$\sum$=27.88 tons $\sum$=49.25 tons-m

Point of application of R=$\frac{49.25}{27.88}$ = 1.76m

e= b/2–R= 1.55–1.76 = –0.21m

P=$\frac{27.88}{5.5}(1 \pm \frac{6\times0.21}{5.5})$ = 7.53(1$\pm$0.34)

Maximum stress = 10.09 tons/m^2 = 100.9kN/m^2

Minimum stress = 4.97 tons/m^2 = 49.7kN/m^2

There is no occurrence of tension hence safe.

VII. CONCLUSION

Thus, a concrete girder bridge is designed with length as 32m, width of road as 7.5m, and 8.5m above the bed level. It has been designed on the assumptions that the soil is moorum soil with S.B.C. as 350kN/m^2. Piers and foundation have been designed keeping high flood level as 7m for pier of 8m with due consideration to water pressure and force of buoyancy.

The bridge has been provided with abutments and wing walls on both sides. Abutments, wing walls and piers have been designed as mass concrete works.

The loading conditions have been taken as worst loading conditions i.e. class AA tracked vehicle and class A for the cantilever portion of the bridge.

The design is based on Working Stress Method of design with references from IRC 6:2000 – Standard Specifications and Code of Practice for Road Bridges- Section II Loads and Stresses and IRC 21:2000 – Standard Specifications and Code of Practice for Road Bridges (Plain and Reinforced). The slab for the bridge is designed using Pigeaud's curves.

VIII. REFERENCES

1. G. O. Young, "Synthetic structure of industrial plastics (Book style with paper title and editor)," in *Plastics*, 2nd ed. vol. 3, J. Peters, Ed. New York: McGraw-Hill, 1964, pp. 15–64.
2. W.-K. Chen, *Linear Networks and Systems* (Book style). Belmont, CA: Wadsworth, 1993, pp. 123–135.
3. H. Poor, *An Introduction to Signal Detection and Estimation*. New York: Springer-Verlag, 1985, ch. 4.
4. B. Smith, "An approach to graphs of linear forms (Unpublished work style)," unpublished.
5. E. H. Miller, "A note on reflector arrays (Periodical style—Accepted for publication)," *IEEE Trans. Antennas Propagat.*, to be published.
6. J. Wang, "Fundamentals of erbium-doped fiber amplifiers arrays (Periodical style—Submitted for publication)," *IEEE J. Quantum Electron.*, submitted for publication.
7. C. J. Kaufman, Rocky Mountain Research Lab., Boulder, CO, private communication, May 1995.

8. Y. Yorozu, M. Hirano, K. Oka, and Y. Tagawa, "Electron spectroscopy studies on magneto-optical media and plastic substrate interfaces (Translation Journals style)," *IEEE Transl. J. Magn. Jpn.*, vol. 2, Aug. 1987, pp. 740–741 [*Dig. 9th Annu. Conf. Magnetics* Japan, 1982, p. 301].
9. M. Young, *The Techincal Writers Handbook.* Mill Valley, CA: University Science, 1989.
10. (Basic Book/Monograph Online Sources) J. K. Author. (year, month, day). *Title* (edition) [Type of medium]. Volume (issue). Available: http://www.(URL)
11. J. Jones. (1991, May 10). Networks (2nd ed.) [Online]. Available: http://www.atm.com
12. (Journal Online Sources style) K. Author. (year, month). Title. *Journal* [Type of medium]. Volume (issue), paging if given. Available: http://www.(URL)
13. R. J. Vidmar. (1992, August). On the use of atmospheric plasmas as electromagnetic reflectors. *IEEE Trans. Plasma Sci.* [Online]. *21(3).* pp. 876—880. Available: http://www.halcyon.com/pub/journals/21ps03-vidmar

AUTHORS PROFILE

1. NavyaSoni, Matrusri Engineering College
2. P Dhanmma, Assistant Professor, Matrusri Engineering College
   E mail id : dhanateju@gmail.com
3. T Raja Ramanna, Assistant Professor, Matrusri Engineering College

ABOUT THE INSTITUTE

Muffakham Jah College of Engineering and Technology (MJCET) was established in the year 1980 by Sultan-Ul-Uloom Education Society (SUES), which was formed by a group of visionaries and intellectuals from various walks of life. Over the past three decades, it has emerged as a premier institute, offering BE courses of four years duration in eight disciplines (Civil, ECE, CSE, IT, EEE, EIE, Mechanical & Production) and five ME courses (CAD/CAM, Structural Engineering., Digital Systems, Computers & Power Electronics) of two years duration. The current intake of all BE Courses is 780, in addition to 102 students in ME Programmes. Research Centers were started in Civil, Mechanical, EEE, CSE and ECE Departments for Doctoral Studies. The college is affiliated to Osmania University, Hyderabad and approved by AICTE, New Delhi. As per the survey of The Outlook magazine, MJCET was ranked 62nd among top 100 Engineering Colleges in India. MJCET has been ranked 47th in India among the top private institutes in Engineering by Times Engineering Institute ranking survey 2019. MJCET ranked 28th out of top 200 Engineering Colleges by India Today magazine. As per The Week Magazine, MJCET ranked 26th among the top Private Engineering Colleges in South India and 42nd among All India Private Engineering Colleges.

OVERVIEW OF THE CONFERENCE

Civil Engineering Infrastructure is the most significant factor in accelerating the pace of economic development of any country. The recent innovation and advances in the field of Civil Engineering has made a drastic impact in the Construction Industry. As the world's population increases, environmental concerns mount and Civil Engineers are entrusted by the society to achieve a sustainable world and raise the quality of life globally. The balancing of economic, social and environmental objectives now and in the future has become known as Sustainable Development and is increasingly a key driver at a range of organizational and spatial scales.

The Conference on Recent Advances in Civil Engineering Infrastructure – (RACEI-2019) aims at exploring the new horizon of innovation from distinguished researchers, eminent professionals from academia and Industry. The Conference also focuses for the achievement of relevant Sustainable Development Goals as described by United Nation Development Program. This event will be a platform to showcase and deliberate research work, studies and contributions for developing novel concepts in Civil Engineering Infrastructure. The Conference consists of keynote lectures on related themes by eminent personalities and stake holders.

BSP BS Publications
A Unit of BSP Books Pvt. Ltd.
4-4-316/309, Giriraj Lane, Sultan Bazar, Hyderabad - 500 095. (A.P.)
Ph: 040-23445688 / 605. Fax: +91-40-23445611.
e-mail: info@bspbooks.net, marketing@bspbooks.net
Website: www.bspbooks.net

ISBN : 978-93-89354-86-7

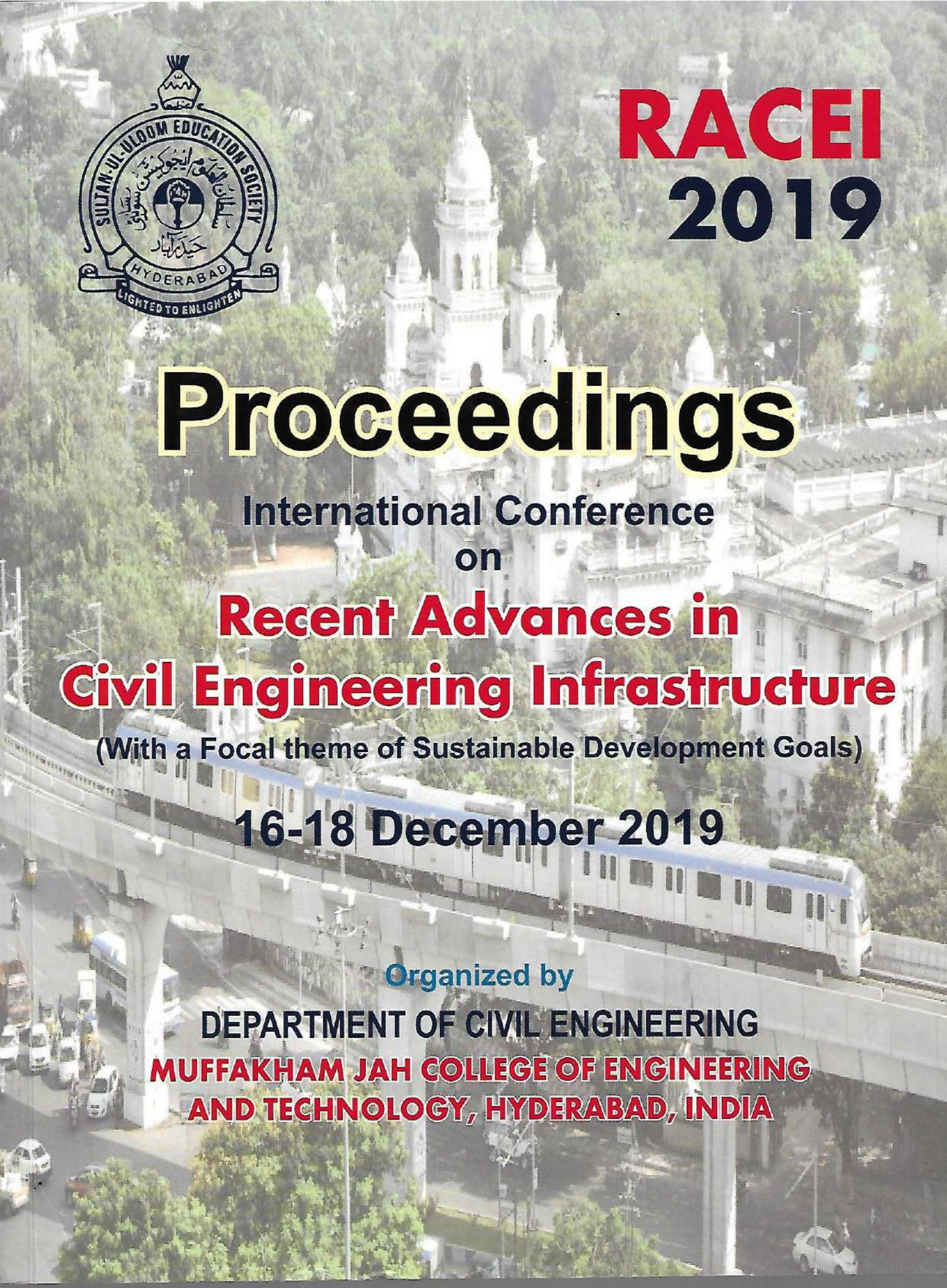

RACEI 2019

Proceedings

International Conference on

Recent Advances in Civil Engineering Infrastructure

(With a Focal theme of Sustainable Development Goals)

16-18 December 2019

Organized by

DEPARTMENT OF CIVIL ENGINEERING

MUFFAKHAM JAH COLLEGE OF ENGINEERING AND TECHNOLOGY, HYDERABAD, INDIA

A Design of Concrete Bridge

NavyaSoni, P Dhanmma and T Raja Ramanna

Abstract: ***In this project, an attempt is being made to design a concrete girder bridge with T beam slab, piers and abutments. The design is initially to be done manually executed in CAD as the same with detailed diagrams and cross sectional views.***
In general there are many types of bridges as follows: ***Post-Tensioned and pre stressed: Post Tensioned Concrete Slab Haunched, Post Tensioned Concrete Box Girder Continuous, Pre stressed Deck Girder Continuous bridges. Steel types: Steel Welded Girder Simple, Steel Riveted Girder Continuous, Weathering Steel Welded Plate Girder Continuous, Steel Welded Girder Haunched bridges. Concrete types: RC Slab Haunched, RC through Arch Fixed, RC Deck Girder Simple, RC Open Spandrel Arch Fixed bridges. Among these we are designing concrete girder bridge. An RCC bridge usually consists of T beams supporting continuous slab. The beams are supported on intermediate piers and abutments in India bridges for roads are designed as per the recommendations of the Indian Road Congress Road. In India all road bridges designed according to IRC loading. This code classifies bridges and culverts into the following categories:***

i) IRC class AA loading
ii) IRC class A loading
iii) IRC class B loading
Among these we are using IRC class AA loading for bridge design. In IRC class AA loading brides subjected to very heavy loading on certain specified areas and highways come under this category. Bridges designed for class AA loading should be checked for class A loading.

I. INTRODUCTION

The aim of this project is to design a T-beam girder concrete bridge of 16m spam and 7.5m width. The loads which are considered are dead loads, live loads such as wind loads, water currents and vehicular loads.

A bridge is a man-made structure built to avoid physical obstacles without closing the way underneath such as a body of water, valley, or road. It is constructed for the purpose of providing passage over the obstacle. The first bridges made by humans were probably spans of cut wooden logs or planks and eventually stones, using a simple support and crossbeam arrangement. The Romans built arch bridges and aqueducts. The Romans also used cement, which reduced the variation of strength found in natural stone.

A. Types of bridges:

The most common types of bridges are described below.

1. *Beam Bridge*
2. *Arch*

Types of arch bridges:

1. Hinge less arch bridge.
2. Two hinged arch bridge.
3. Three hinged arch bridge.
4. Tied hinged arch bridge.

3. *Cantilever bridge.*
4. *Suspension bridge*
5. *Cable stayed bridge* towers is much greater than the suspension bridge.
6. *Truss bridge* wider area.

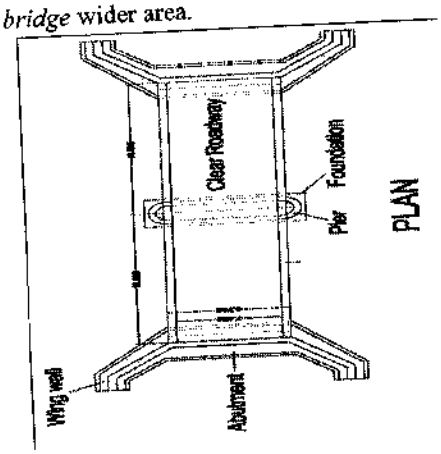

PROPOSED PLAN
MANUAL DESIGN

II. DESIGN OF DECK SLAB

Clear width of loading =7.5m
Live load = class AA & class A
Average thickness of wearing coat = 8cm
Clear span centre to centre of bearing = 16m

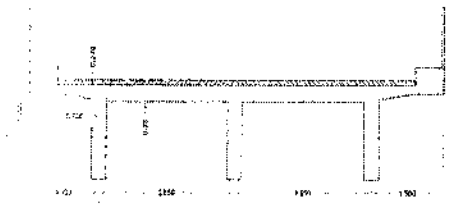

Fig 1

Three girders are provided at c/c distance of =2.85m Kerbs 0.6m wide are provided including railings.

Web widths of 30cm are proposed for longitudinal girder & of cross girder.

Thickness of slab is assumed as 25cm for interior panel.

Thickness of cantilever slab is assumed as 25cm at junction with slab and 20cm at junction with kerb.

Weight of railing is assumed as 70kg/m

Cantilever will be designed by effective width method & interior panels by Pigeaud's theory.

Dimensions of interior panel are 2.85mX4m

Concrete mix M20 is used for deck slab & girders

Impact factors for design of slab:

Class AA loading =25%

For class A loading, maximum impact factor = 50.0%

III. DESIGN OF CANTILEVER PORTION

Item	Load/m-run. (Kg)	Distance of C.G. from edge cantilever (m)	Moment (N-m)
Parapet	700	1.275	892.5
Kerb	0.44X0.6X1X25000=6600	1.05	6930
Wearing coat	0.08X0.75X23000=1880	0.375	517.5
Slab triangular	½X0.75X0.1X25000=937.5	0.25	234.37
Slab rectangular	0.15x0.75x25000=2812.5	0.375	1054.69

Total load =12.430kN

Total D.L BM = 9.63kN-m

Live load B.M:

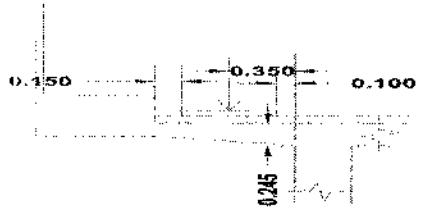

Fig 2

Class AA **loading:** Minimum clearance of class AA loading from kerb is 1.2m. Hence this loading will not come in cantilever portion class A loading.

Distance of C.G. of load from edge of cantilever=X=0.375m

Effective width of slab =1.2x +bw

= 1.2X0.375+(0.25+2x0.08) = 0.86m

Load per meter width of slab = $\frac{11.43}{0.86}$ = 68.7kN

Dispersion width along span of cantilever = 0.5 + 2(0.08+0.20) = 1.06m

Some portions of dispersion width goes beyond edge of cantilever dispersion width in cantilever portion = 0.54/2 +0.5 +0.1 = 0.87m

Portion of load in cantilever = $\frac{68.7X0.87}{1.06}$ = 56.39kN

B.M = 56.39X0.87/2=24.53 kN-m

B.M = including impact = 1.5X 24.53 =36.79kN-m

Total B.M = 36.79+9.63 = 46.42kN-m

Effective depth = $\sqrt{\frac{46.42X10^6}{0.138X20}}$ = 23cm

Provide an overall depth of 25cm with effective depth of 23cm

Area of steel required = $\frac{46.42X10^6}{0.87X415X0.9X220}$ = 971.77mm^2

$\frac{\pi X8^2}{971.77}X1000$= 115.61mm

Provide 12mmØ bars at 10cm c/c

Distribution steel: distribution reinforcement is to be provided for 0.3 times L.L B.M & 0.2 Times D.L B.M

M=0.3X36.79+0.2X9.63 = 12.96 kN-m

Effective depth = 23-0.6-0.4=22cm=220mm

A_t=$\frac{12.96X10^6}{0.87X415X0.9X220}$=271.31mm^2

Half reinforcement has to be provided at top &half at bottom.

$\frac{\pi X8^2}{271.31}X1000$=175.46mm

Provide 8mmØ bars at 15mm c/c.

Shear:

Live load shear including impact=56.39X1.50=84.58kN

Dead load shear = 12.43kN

Total shear = 84.58+12.43=97.01

Shear stress=$\frac{97.01X10^3}{1000X220}$=4.88kN/m^2

Design of interior panel:

Dead weight of slab for per m^2=1X1X0.2X25000N=50kN

Dead weight of wearing coat=1X1X0.0823000=1840N=1.84kN

Total D.L =6.84kN/m^2

IV. LIVE LOAD

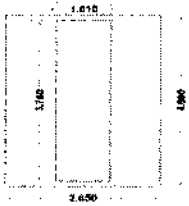

Fig 3

Class AA tracked vehicle: one wheel is placed in the centre of the panel

Thickness of wearing coat =80mm

Dispersion of wheel loads: $\mu=b+2h$ & $v=a+2h$

$\mu=0.85+2(0.08)=1.01$m & $v=3.6+2(0.08)=3.76$m

$\frac{\mu}{B}=\frac{1.01}{2.85}=0.35$ & $\frac{v}{L}=\frac{3.76}{4}=0.94$

$\frac{L}{B}=\frac{4}{2.85}=1.403$

referring to Pigeaud's curves

$M_1=9.0\text{x}10^{-2}$ & $M_2=3.5\text{X}10^{-2}$

Moment along $M_B=W(M_1+0.15M_2)$

$=700/2(9.0\text{X}10^{-2}+0.15\text{X}3.5\text{X}10^{-2})$ = 33.34kN-m

As the slab is continuous, B.M taken for design will be 0.8 times M_B B.M including impact and continuity factor

$M_B=1.25\text{x}33.34\text{X}0.8=33.34$kN-m

$M_L=W(0.15M_1+M_2)$

$=700/2\text{X}(0.15\text{X}9.0\text{X}10^{-2}+3.5\text{X}10^{-2})=16.975$kN-m

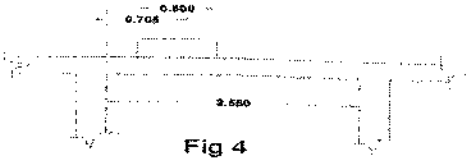

Fig 4

B.M including impact is continuity factor

$M_L=1.25\text{X}16.97\text{X}0.8=16.97$kN-m

V. SHEAR

Dispersion in the direction of the span =0.85+2(0.08+0.2) =1.41m

For maximum shear load is kept such that whole dispersion is in the span load is kept at 1.41/2=0.705m

From edge of beam

Effective width of slab $=kx(1-\frac{x}{l})+b_w$

Breadth of cross girder=30cm

Clear length of span = 4-0.3=3.7

Clear breadth of span = 2.85 – 0.3= 2.55m

$\frac{L}{B}=\frac{3.7}{2.55}=1.45$

K for continuous slab=2.48 (from table)

Effective width of slab=$2.80\text{X}0.705(1-\frac{0.705}{3.7})+3.76=5.18$m

Load per meter width $=\frac{70.000}{1.000}=70$kN

Shear force $=70(2.55-\frac{0.705}{2})=50.65$kN

Shear force including impact=1.25X50.65=63.31kN

Class AA wheeled vehicle: There are 2 possibilities which should be investigated for finding the maximum B.M in the panel.

First possibility is when two loads of 37.5KN each and 2 loads of 62.5kN each are symmetrically placed about the centre line as shown in figure 5a.

Second position is when 2 loads of 37.5kN and 4 loads of 62.5kN each are placed in the panel with central 2 loads of 62.5kN placed at the centre.

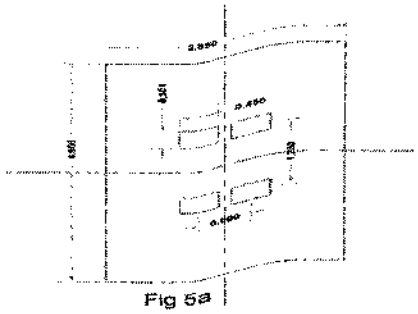

Fig 5a

$\mu_1=0.3+2(0.08)=0.46$m

$v_1=0.15+2(0.08)=0.31$m

The analysis for this case is done as below for each load M_1 & M_2 is found for

i. $\mu=2(\mu_1+x)$ & $v=2(v_1+y)$ and multiply by $(u_1+x)\text{X}(v_1+y)$

ii. $\mu=2x$ & $v=2y$ and multiply by xy

iii. $\mu=2(\mu_1+x)$ & $v=2y$ and multiply by $y(\mu_1+x)$

iv. $\mu=2x$ and $v=2(v_1+y)$ & multiply by $x(v_1+y)$

For design B.M subtract (iii + iv) from (i + ii) & multiply by $\frac{W}{u_1v_1}$

i. $\mu=2(\mu_1+x)=2(0.46+0.07)=1.06$m

$v=2(v_1+y)=2(0.31+0.445)=1.51$m

$\frac{\mu}{B}=\frac{1.06}{2.85}=0.37$ & $\frac{v}{L}=\frac{1.51}{4}=0.38$ & $\frac{L}{B}=k=\frac{4}{2.85}=1.403$

From Pigeaud's curves: $M_1=13.5\text{X}10^{-2}$ & $M_2=8.0\text{X}10^{-2}$

$\mu_1+x=0.46+0.07=0.53$ & $v_1+y=0.31+0.445=0.755$

Modified $M_1=13.5\text{X}10^{-2}\text{X}0.53\text{X}0.755=5.4\text{X}10^{-2}$

Modified $M_2=8.0\text{X}10^{-2}\text{X}0.53\text{X}0.755=3.20\text{X}10^{-2}$

ii. $\mu=2x=2\text{X}0.07=0.14$ & $v=2y=2\text{X}0.455=0.89$

$\frac{\mu}{B}=\frac{0.14}{2.85}=0.049$ & $\frac{v}{L}=\frac{0.89}{4}=0.22$ & $k=1.403$

From Pigeaud's curves $M_1=24\text{X}10^{-2}$ & $M_2=12.5\text{X}10^{-2}$

Modified $M_1=24\text{X}10^{-2}\text{X}0.07\text{X}0.455=0.75\text{X}10^{-2}$

Modified $M_2=12.5\text{X}10^{-2}\text{X}0.07\text{X}0.445=0.39\text{X}10^{-2}$

iii. $\mu=2(\mu+x)=2(0.46+0.07)=1.06$ & $v=2y=2\text{X}$ $=0.89$

$\frac{\mu}{B}=\frac{1.06}{2.85}=0.37$ & $\frac{v}{L}=\frac{0.89}{4}=0.22$ & $k=1.403$

From Pigeaud's curves: $M_1=15.0\text{X}10^{-2}$ & $M_2=11.0\text{X}10^{-2}$

$y(\mu+x)=0.455(0.46+0.07)=0.24$

Modified $M_1=15.0\text{X}10^{-2}\text{X}0.445(0.46+0.07)=3.54\text{X}10^{-2}$

Modified $M_2=11.0\text{X}10^{-2}\text{X}0.445(0.46+0.07)=2.59\text{X}10^{-2}$

iv. $\mu=2x=2\text{X}0.07=0.14$ & $v=2(v_1+y)$ $=2(0.31+0.0445)=1.51$

$\mu = \frac{B.M}{0.14}$ 0.14 $\frac{v}{2} = \frac{0.31}{4}$=0.38 k =1.403

From Pigeaud's curves: M_1 =17.0X10^{-2} M_2 =8.5X10^{-2}

$2(v_1+y)$ =0.07(0.31+0.445)

Modified M_1 =17.0X10^{-2}X0.07X0.755 =0.90X10^{-2}

Modified M_2 =8.5X10^{-2}X.07X0.755 =0.45X10^{-2}

Design values of M_1& M_2 are: (i+ii) – (iii+iv)

M_1 =5.4X10^{-2}+0.75X10^{-2}-3.54X10^{-2}-0.90X10^{-2} =1.71X10^{-2}

M_2 =1.20X10^{-2}+0.39X10^{-2}-2.59X10^{-2}-0.45X10^{-2} =0.55X10^{-2}

B.M due to load is $\frac{W}{u_1 X v_1}(M_1+0.15M_2)$

Total M_B due to 4 loads

$\frac{2X62.5}{0.31X0.48}$(1.71X10^{-2}+(0.15X0.55X10^{-2})) + $\frac{2X37.5}{0.31X0.48}$ (1.71X10^{-2}+(0.15X0.55X10^{-2}))

25.14kN-m

B.M including impact and continuity factor

1.25X25.14X0.8 =25.14kN-m

Total M_L due to 4 loads

$\frac{2X62.5}{0.31X0.48}$((0.15X0.55X10^{-2})+0.55X10^{-2}) + $\frac{2X37.5}{0.31X0.48}$ ((0.15X1.71X10^{-2})+0.55X10^{-2})

11.31kN-m

B.M including impact and continuity factor

1.25X11.31X0.8 =11.31kN-m

Shear due to class AA wheeled vehicle:

Dispersion width in direction of span =0.3+2(0.25+0.08) =0.96m

Loads are placed such that outermost load is at a distance of 0.86/2 = 0.43m from edge of the beam.

Effective width of 1st wheel= $kx(1-\frac{x}{l})+b_w$

=2.80X0.48(1– $\frac{0.48}{0.86}$)+0.30+2(0.08) =1.55m

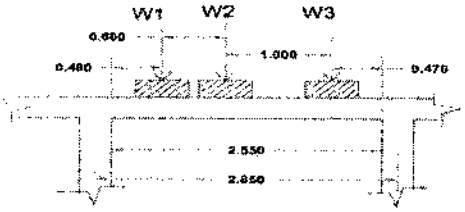

Fig 5b

But centre to centre distance of 2 wheels is 1.2m &thus effective width will overlap

Average effective width for 1st wheel =1.2+1.55/2 =1.375m

Load per meter width of slab= 37.5/1.375 =27.27kN

Effective width for 2nd wheel= 2.8x1.08(1– $\frac{1.08}{0.86}$)+0.48 =2.20m

But centre to centre distance of 2 wheels is 1.2m and thus effective widths overlap

Average effective width for 2nd wheel= 1.2+2.2/2 =1.59m

Load per meter width of slab= 62.5/1.7=36.76kN

Effective width for 3rd wheel= 2.8X0.47(1 – $\frac{0.47}{0.86}$)+0.8 =1.53m

Average= (1.53+1.2)/2 =1.36m

Load per meter width= 62.5=45.95kN

Portion of W_3 in span =45.95/1.36X0.93=31.42kN

Shear force at edge

= 27.27X$\frac{1.55-0.48}{2.55}$ +36.76X$\frac{1.55-1.47}{2.55}$ + 31.42X$\frac{0.93}{2X2.55}$ = 43.43

Shear force including impact =1.25X43.43 =54.29kN.

Class A Loading: For maximum B.M., first wheel of 5.7 tonnes should be placed at centre of span and other at 1.2m from it as shown in figure 6.

Imaginary load W_3 = W_2 is placed on other side of W_1 to make loading symmetrical. B.M at centre of panel will be that due to W_1 plus half due to load W_2& W_3

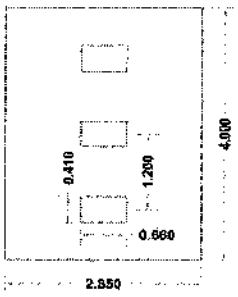

Fig 6

B.M due to load W_1:

μ = 0.5+2(0.08) =0.66m & v =0.25+2(0.08) =0.41m

$\frac{v}{2} = \frac{0.41}{2.81}$=0.23 $\frac{v}{2} = \frac{0.41}{4}$=0.10

From Pigeaud's curves k =1.403

M_1 =19x10^{-2} M_2 =16.5X10^{-2}

M^1_B = W(M_1+0.15XM_2) =57(0.15X19X10^{-2}+16.5X10^{-2}) =12.24kN-m

M^1_L= W(0.15XM_1+M_2) =57(0.15X19X10^{-2}+16.5X10^{-2}) =11.03kN-m

B.M due to W_2

μ =0.5+2(0.08) =0.66m V_1=0.25+2(0.08) =0.41m

i. μ =μ & v =2(v_1+y)

μ =0.66 v =2(0.995X0.41) =2.81

$\frac{v}{2} = \frac{0.41}{2.81}$=0.23 $\frac{v}{2} = \frac{1.97}{4}$=0.50

From Pigeaud's curves M_1 =11.5x10^{-2}& M_2 =5X10^{-2}

These are to be multiplied by 1.405

M_1 =11.5X10^{-2} =16.16X10^{-2} M_2 =5X10^{-2}X1.405 =7.03X10^{-2}

ii. μ =μ & v =2y

μ =0.66 & v =1.99

$\frac{\mu}{B} = \frac{0.58}{2.55} = 0.23$ & $\frac{V}{L} = \frac{1.00}{4} = 0.50$

From Pigeaud's curves: $M_1 = 14.5X10^{-2}$ & $M_2 = 6.8X10^{-2}$

These are to be multiplied by y

$M_1 = 14.5X10^{-2}X0.995 = 14.43X10^{-2}$ & $M_2 = 6.8X10^{-2}X0.995 = 6.77X10^{-2}$

Design values of M_1 & M_2 are I – ii

$M_1 = 16.16X10^{-2} - 14.43X10^{-2} = 1.73X10^{-2}$

$M_2 = 7.03X10^{-2} - 6.77X10^{-2} = 0.6X10^{-2}$

$M^{11}_B = W/V\ (M_1 + 0.5M_2) = \frac{57}{0.41}(1.73X10^{-2} + 0.15X0.26X10^{-2})$ $= 2.46$kN-m

$M^{11}_L = W/V(0.15M_1 + M_2) = \frac{57}{0.41}(0.15X1.73X10^{-2} + 0.26X10^{-2})$ $= 0.72$kN-m

Total B.M due to two loads will be $M_B - M^1_B + M^{11}_B$ & $M^1_L + M^{11}_L - M_2$

$M_B = 12.24 = 14.7$kN-m & $M_L = 11.03 + 0.72 = 11.75$kN-m

B.M including impact and continuity

$M_B = 1.5X14.7X0.8 = 17.64$kN-m

$M_L = 1.5X11.75X0.8 = 14.1$kN-m

Shear due to class A loading:

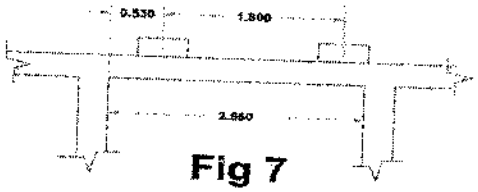

Fig 7

Dispersion width in the direction of span $= 0.5 + 2(0.08 + 0.2) = 1.06$m

For maximum shear the load should be placed at a distance of $1.06/2 = 0.53$m from edge.

Effective width $= kx(1 - \frac{x}{l}) + b_w$ $= 2.48x0.53(1 - 0.53/2.55) + 0.25 + 0.08x2 = 1.45$m

Distance between 2 wheels is 1.2m and hence effective widths overlap

Average effective width per wheel $= 1.45 + 1.2/2 = 1.33$m

Load per meter width of the beam $= 5.7/1.33 = 4.29$kN

Shear force $= 4.29(\frac{2.55 - 0.53}{2.55}) = 3.40$kN

S.F including impact $= 1.5x3.40 = 3.40 = 5.1$kN

Design live load B.M & S.F:

$M_B = 33.34$kN-m (class AA tracked) & $M_L = 16.97$kN-m (class AA tracked)

S.F $= 63.31$kN (class AA tracked)

VI. DEAD LOAD

Dead load per square meter $= 6.84$kN/m^2

Dead load B.M will be found by Pigeaud's method

Total load on panel $= 4X2.85X6.84 = 77.98$kN

$\mu/B = 1$ $V/L = 1$ as panel is loaded with U.D.L

$M_1 = 4.8X10^{-2}$ & $M_2 = 2.1X10^{-2}$

$M_B = 6.84(4.8X10^{-2} + 0.15X2.1X10^{-2}) = 0.35$kN-m

Taking actual B.M 0.8 times value to account for continuity

$M_B = 0.8X0.5 = 0.28$kN-m

$M_L = 6.84(0.15X4.8X10^{-2} + 2.1X10^{-2}) = 0.19$kN-m

Considering effect of continuity for B.M

$M_L = 0.8X0.19 = 0.15$kN-m

Dead load S.F is assumed as $6.84x2.55/2 = 8.72$n

Total M_B due to D.L & L.L $= 33.34 + 0.28 = 33.62$kN-m

Total $M_L = 16.97 + 0.19 = 17.16$kN-m

Total S.F. $= 63.31 + 8972 = 72.0$-3kN

A. Design of section:

Effective depth required $= \sqrt{\frac{[illegible]}{[illegible]}} = 19.54$cm

Provided overall depth of 28cm with effective depth of 25cm

A_t for $M_B = \frac{[illegible]}{[illegible]} = 703.81$mm^2

Provide 12mm Ø bars 15cm c/c

Shear resistance $= 3.5X100X23 = 8050$ kg-cm

As the provided shear resistance is more than the required no additional shear reinforcement is required.

Nominal shear reinforcement: Provide 10mmØ bars at 14mm c/c

Check for shear:

Shear stress $= 7167.0/100X0.903X25 = 3.17$kg/cm^2

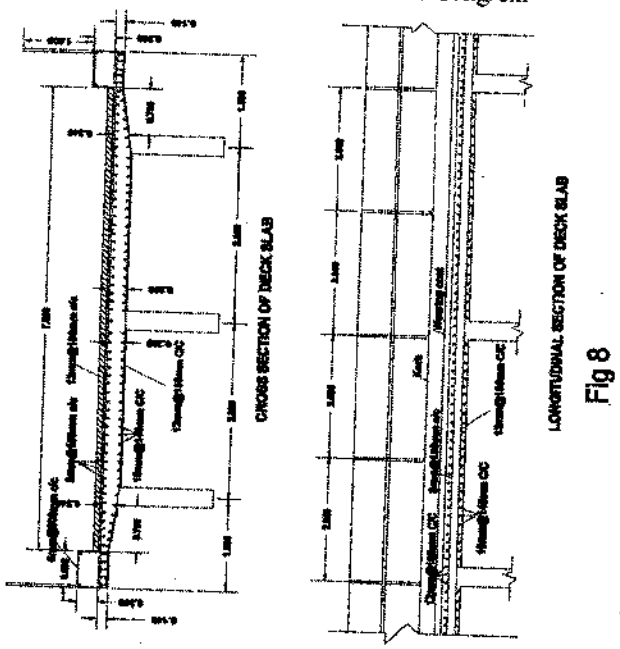

Fig 8

B. Design of longitudinal girders:

Distribution of live loads on longitudinal beams for B.M

Class A loading: Reactions on the girders will be maximum when the eccentricity is maximum eccentricity will be

maximum when the loads are very near to kerb. Position of loads for maximum eccentricity is shown in fig 9a

All the girders are assumed to have same moment of inertia

reaction factor for outer girder

$R_A = \frac{4W_1}{3}(1 + \frac{2e}{2\times2.85}\times2.85\times0.49)$

$= \frac{4W_1}{3}(1 + \frac{2\times0.49}{2\times2.85})$

$= 1.68\ W_1$

$R_B = \frac{4W_1}{3}(1+0) = 4W_1/3$

If W is axle load wheel load $W_1 = W/2$

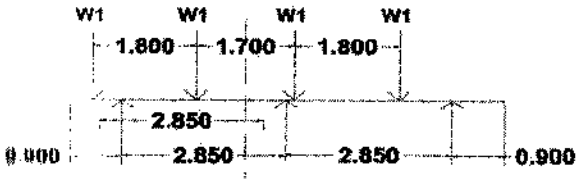

Fig 9a

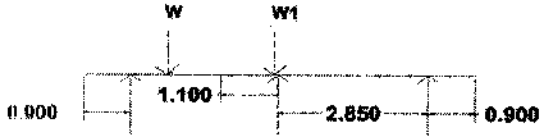

Fig 9b

C.G. of load = 0.9+0.18+1.7/2 =3.05m

Kerb to centre of girder =0.75+0.15+2.85 =3.75m

Eccentricity e = 0.7m

Reaction factor for outer girder = $R_A = \frac{4W_1}{3}(1+\frac{2e}{2\times2.85}\times2.85\times0.7) = 1.82W_1$

Reaction factor for inner girder = (e =0) $R_B = 4/3W_1$

Class AA loading:

C.G. 1.625+2.05/2 =2.65m e =3.75-2.65 =1.1m

Reaction on outer girder $= R_A = \frac{2W_1}{3}(1+\frac{2\times2.85}{2\times2.85}\times1.1) = 1.05W_1$

Reaction on inner girder $= R_b = 2W_2/3$

If W is axle load, wheel load $w_2 = w/2$

Reaction on outer girder $= 1.05/2W_1 = 0.53W_1$

Reaction on inner girder $= 2W_3/3X1/2 = W/3$

Dead load from slab per girder:

Total dead load of deck =2x12.43+6.84x6 =65.9kN

It is assumed that dead loads shared equally by all girders.

Dead load per girder =65.9/3 =2.97kN

Live load: impact factor:

Span = 16m impact factor for class AA loading =10%

Impact factor for class A loading $= \frac{4.5}{6+L} = \frac{4.5}{6+16} = 0.2$

Live load including moments and shear force at different sections will be found for class AA tracked vehicle & class A loading. Class AA wheeled vehicle is not considered as it does not produce worst effect.

Live load bending moment:

Centre of span

Class AA loading: Position of loads is shown in figure 10.

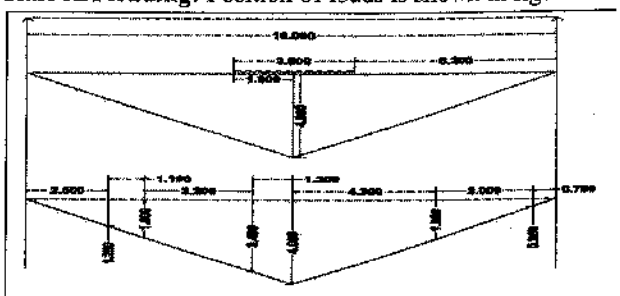

Fig 10

B.M= $(\frac{3+5.1}{2})70$ =248.5cm =2485kN-m

B.M including impact and reaction factor for outer girder

=2485X1.1X0.4833 =1321.10kN-m

B.M including impact and reaction factor for inner girder

= 2485x1.1x1/3 =911.17kN-m

Class A loading: Position of loads for maximum B.M at centre of span is shown in fig 10

B.M

=11.4X4X11.4X3.4+2.7X1.25+2.7X1.8+6.8X0.35+6.8X1.8

=107.195tm =1017.17kN-m

B.M including impact factor & reaction factor for outer girder

=1071.95X0.8625X.204 =1113.17kN-m

B.M including impact factor & reaction factor for inner girder

=1071.95X0.6667X1.204 =860.48kN-m

It is seen that maximum B.M for inner & outer girders is given by class AA tracked vehicle

Maximum live load moment for outer girder =1321.10kN-m

Maximum live load moment for inner girder =911.17kN-m

Quarter span: Class AA loading

Position of load for maximum B.M is shown in figure 11.

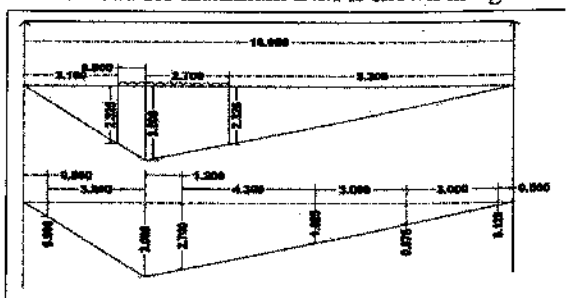

Fig 11

B.M = $(\frac{3+5.125}{2})$x700 =1863.75kN-m

B.M including impact factor for outer girder =1863.75X1.1X0.4833 =990.82 kN-m

B.M including impact factor for inner girder =1863.75X1.1X1/3 =683.37kN-m

Class A loading: Position of loads for max B.M is shown figure11.

M =114X3+114X2.7+6.8X1.625+6.8X0.875+6.8X0.125+2.7X0.6 =844.5kN-m

B.M including impact factor for outer girder =844.5X0.8625X1.204 =877kN-m

B.M including impact factor for inner girder =844.5x0.6667x1.204 =677.8kN-m

Maximum live load for outer girder = 990.82kN-m

Maximum live load for inner girder = 683.37kN-m

Live load shear: Maximum shear at all sections is given by class AA tracked vehicle. For maximum shear at support load should be as near to support as possible. The length of the load is 3.6m whole of load will lie between support and 1st cross girder live load shear at support is found by method described earlier. For intermediate section shear will be found by drawing influences lines the reaction factor found by Courbon's theory will be used for finding shear at intermediate sections.

The position of centre line of load for maximum shear force is shown in figure12a. Let P_A, P_B & P_C be loads coming on the longitudinals considering the slab as simple supported.

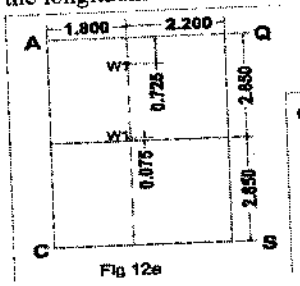

Fig 12a

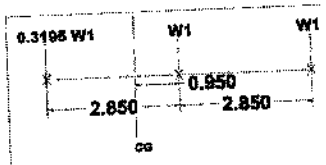

Fig 12b

$P_A = W_1X2.125/2.85 + W_1(0.075)/2.85 = 0.77W_1$

$P_B = W_1X0.725/2.85 + W_1 2.775/2.85 = 1.23W_1$

Due to P_A, shear force at A $= R^1_A = 0.77W1X2.2/4 = 0.385W_1$

$R_Q = 1.23W_1X1.8/4 = 0.315W_1$

Due to P_B shear force at B $= R^1_B = 1.23W_1X2.2/4 = 0.68W_1$

$R_R = 1.8/4X1.23W_1 = 0.55W_1$

The load on the cross girder i.e. R_Q, R_R & R_S are to be distributed by normal Courbon's theory

$\sum W = 0.385W_1 + 0.55W_1 = 0.935W_1$

Let $\bar{x}$ be the distance of C.G. of loads from Q

$\bar{x} = \frac{0.385W_1 \times 2.2}{0.935W_1} = 1.47m$

Inner girder:

Eccentricity e =2.85-1.47=1.38m

$\sum W = \frac{0.935W_1}{3}\left(1+\frac{6X1.38}{2X2.85}\right) = 0.55W_1$

$F_R = 0.935W_1/3(1+0) = 0.31W_1$

Outer girder: $0.55W_1X12/16 = 0.41W_1$

Inner girder: $0.31W_1X12/16 = 0.23W_1$

Total reaction on outer girder $= 0.385W_1 + 0.41W_1 = 0.795W_1$

Total reaction on inner girder $= 0.68W_1 + 0.23W_1 = 0.91W_1$

Max. S.F. on outer girder with impact =0.795X700/2X1.1 =306.07kN

Max. S.F. on inner girder with impact = 0.91X700/2X1.1 =350.35kN

Shear at centre of span:

Position of load for maximum shear is shown in influence line diagram in fig 13

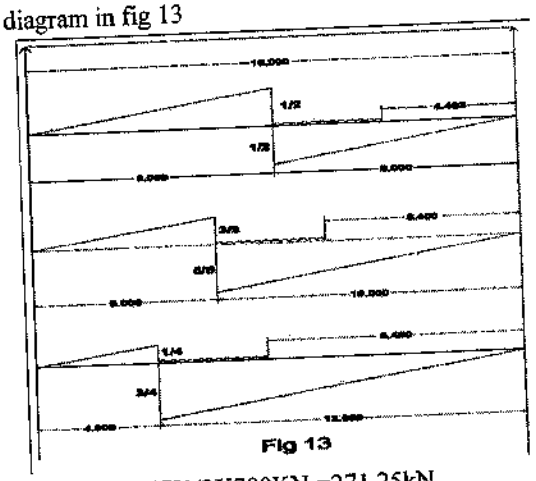
Fig 13

S.F = (1/2+0.275)X1/2X700KN =271.25kN

S.F including impact for outer girder =1.1X0.4833X271.25=144.20kN

S.F including impact for inner girder =1.1X1/3X271.25=99.45kN

Shear at 3/8th span: S.F = (5/8+0.4)x1/2x700 =358.75kN

S.F including impact for outer girder =358.75X1.1X0.4833 =190.72kN

S.F including impact for inner girder =358.75X1.1X1/3 =131.54kN

Shear at quarter span:

S.F = (3/4+0.525)X1/2X700=446.25kN

S.F including impact for outer girder =446.25X1.1X0.4833=237.24kN

S.F including impact for inner girder =446.25X1.1X1/3 =163.63kN

Dead load B.M and S.F:

Assume depth of rib as 1.4m

Weight of rib per meter run =1X0.3X1.4X24000=1008kN

Cross girders are provided at centre quarters points and at the supports width of each cross girder is 30cm & depth 1.4m.

Weight of each cross girder =1X0.3X1.4X24000 =10.08kN
Reaction from deck slab on each cross girder =20.97kN
Total load per meter run of girder =10.08+20.97 =31.05kN

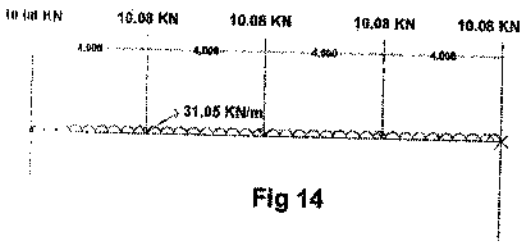

Fig 14

B.M at centre of span =31.05X16X16/8+10008X4+1008/2X8 =1074.24kN-m
B.M at quarters span =31.05X8X4X2+10.08X4+100811/2X4 =805.68kN-m
Dead load shear at support =31.05X8+10.08+10.08/2=263.52kN
Dead load shear at quarter span =263.52-31.05x4 =139.32kN
Dead load shear at 3/8th span= 263.52–31.05X6–10.08= 67.14kN

Design bending moments and shear forces:

Outer girder:

Total B.M. at centre of span= 1321.10+1074.24= 2395.34kNm
Total B.M. at quarter span= 990.82 – 805.68= 1796.5kNm
Total S.F. at support= 263.52+306.07=569.59kN
Total S.F. at 3/8th span=67.14+190.72= 257.86kN
Total S.F. at centre of span = 5.04+144.20=149.24kN
Total S.F. at quarter span= 139.32+237.24=376.56kN

Inner girder:

Total B.M. at centre of span= 683.37+1074.24=1757.61kNm
Total B.M. at quarter span= 677.88+805.68=1483.56kNm
Total S.F. at support =263.52+350.35=613.87kN
Total S.F. at quarter span=139.32+163.63=302.95kN
Total S.F. at 3/8th span=67.14+131.54=198.68kN
Total S.F. at centre of span= 5.04+99.45=104.49kN

Design of Girder:

Outer girder:

Max. B.M.= 2395.34kNm
The beam is designed as T-beam. Assume effective depth as 145cm.
Assume lever arm=0.9X145=130.5cm=1.3m
$A_t = \frac{239.534X100}{2320X130.5} = 8011.17mm^2$
Provide 12 bars of 32mmØ

A_t provided= 80.43cm^2.

Check for stresses:

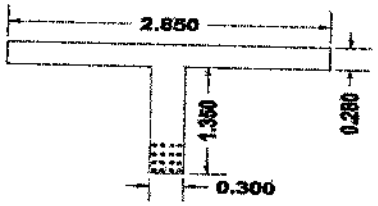

Fig 15

Flange width will be least of:
i. $12d_s+b_r$=12X28+30=366cm
ii. c/c= 2.85m=285cm
iii. span/3=1600/3=5.33m
Hence B=285cm.
For checking stresses, average thickness of flange is assumed as 28cm.
The concrete mix for slab and girders is M_{20}.
As the whole compression is assumed to be taken by the flange, value of m is assumed as 13.
Assuming N.A. to lie in web.
2.85X28(n–10)= 145–n
Solving the above equation we get n=25.64cm
Lever arm $a=d-d_s/2+\frac{d_s^2}{6(2n-d_s)}$= 145– 28/2+ $\frac{28^2}{6(2X25.64-28)}$ = 136.61cm
$B.M. = Bd_sC_a(1+\frac{n-d_s}{n})Xa$ (To find C_a)
=>239.534X100= 280X28XCa(1+$\frac{25.64X100}{25.64}$)X136.61
Solving the equation we get c_a= $\frac{239.534X100}{280X28X136.61X0.897}$ = 24.66kg/cm^2 = 246.6kN/m^2
Area of steel required at quarter span= $\frac{179.65}{2320X0.900X145}$ = 59.65cm^2
Provide 8 bars of 32mmØ.

Check for shear and bond: Max. shear at support= 569.59kN
Assume effective depth as 145cm at support and lever arm as 0.9d.
∑O required for bond= $\frac{569.59}{10X0.9X145}$= 43.65cm
Number of 32mmØ bars required= $\frac{43.65}{\pi X0.8}$=4.34
At least 6 bars are to be taken straight.
Shear stress at support= $\frac{569.59}{28X0.9X145}$= 14.55kg/cm^2
Shear reinforcement is required.
Shear stress at centre of span= $\frac{149.24}{28X0.9X145}$=3.81kg/cm^2
No shear reinforcement is required.

Shear stress at 3/8th span= [illegible]=6.59kg/cm^2

Bars are bent in sets with 2 bars in each set at every 0.95m. Five sets of bent up bars are provided. Bent up bars will be effective upto 5X0.95=4.75m from support. At every section, 2 sets of bars i.e. 4 bars are effective as bars are bent at spacing of 0.707a. Shear is taken by 4 bent up 32mmØ bars.

= 4X8.04X2300X0.707= 52.29 kg= 522.95kN

Net S.F. at support for which shear reinforcement is to be provided

= 56959–52295= 4664kg=4.66kN

Using 10mmØ 2 legged stirrups

Spacing=[illegible] = 101.04cm

Provide 10mmØ 2 legged stirrups at 50cm c/c upto 3.8m from support. After 3.8m from support, only 2 bars are effective.

Shear taken by 2 bars= 26.15kN = 26147kg

Net shear at quarter point for which stirrups are required

= 376.56 – 26.15= 350.41kN

10mmØ stirrups at 50cm c/c are provided between 3.8m and 4.7m from support. Beyond 4.7m from support, no bar is effective.

Providing 12mmØ 2 legged stirrups at quarter span

Spacing = [illegible] = 18.01cm

Provide 12mm Ø 2 legged stirrups at 15cm c/c upto 6m from support.

Shear force at 3/8th of span= 25786kg = 25.79kN

Using 12mmØ 2 legged stirrups

Spacing= [illegible] =26.31cm

Provide 12mm Ø stirrups at 25cm c/c upto 7.5m from support. In the remaining portion provide 12mmØ stirrups at 50cm c/c.

Inner girder: Max. B.M. at centre= 1757.61kNm

Area of steel provided at centre= [illegible]= 58.56cm^2

Provide 14 bars of 32mmØ.

Area of steel required at quarter span = [illegible] = 49.43cm^2

Provide 12 bars of 32mmØ.

Check for shear and bond: Maximum shear at support= 613.87kN

Assume effective depth as 145cm at support.

$\sum O$ required for bond= [illegible]= 47.04cm

Number of 32mmØ bars required= [illegible]=4.68

6 bars of 32mmØ are taken straight.

Shear stress at support= [illegible]= 15.68kg/cm^2

Shear stress at centre of span=[illegible]= 2.67kg/cm^2

Shear stress at 3/8th of span= [illegible]= 5.07kg/cm^2

No shear reinforcement is required between mid span and 3/8th span. Bars are bent in sets at every 0.95m with 2 bars in each set. Four sets of bent up bars are provided. Bent up bars will be effective upto 4X0.95= 3.8m from support. At every section, 2 sets of bars i.e. 4 bars are effective as the bars are bent at spacing of 0.707a.

Shear taken up by 4 bent up bars= 52.29kN

Net shear for which shear reinforcement is to be provided at supports

= 613.87–522.95= 90.92kN

Provide 12mmØ 2 legged stirrups

Spacing= [illegible]=74.61cm

Provide 12mmØ 2 legged stirrups at 50cm c/c. This spacing is provided upto 3.8m from support. After 2.85m from support, only 2 bars are effective but S.F. is less than that at support.

Shear force at quarter span= 613.87kN

Provide 12mmØ 2 legged stirrups

Spacing= [illegible]= 11.05cm

Provide 12mmØ stirrups at 10cm c/c between 3.8m from support and 5.0m from support. Provide 12mmØ 2 legged stirrups at 20cm between 5.0m and 6.0m from support.

Maximum web reinforcement= 0.15% of area of web in plan

= [illegible]X30X100 = 4.5cm^2

Providing 10mmØ stirrups

Spacing = [illegible]= 34.8cm

Provide 10mmØ stirrups at 25cm c/c.

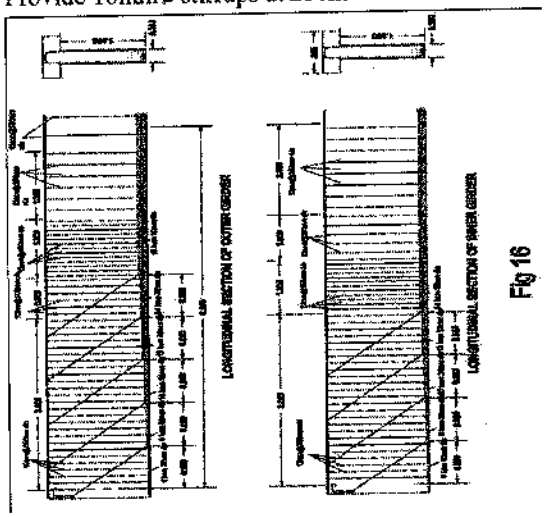

Fig 16

C. **Design of cross girder:** Self weight of cross girder= 10.08kN

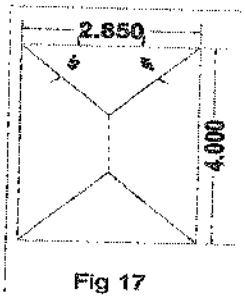

Fig 17

Dead load from slab= 2X1/2X2.85X1.425X6.84 = 27.78kN
This load will be assumed as uniformly distributed load per meter run.

= 9.75kN/m

Total dead load per meter run= 10.08+9.75= 19.83kN
Girder is assumed to be rigid.
Reaction on each girder= 19.83X5/3= 33.05kN
Live load: Max. B.M. and S.F. occurs due to class AA tracked vehicle. For max. B.M. and S.F. in the cross girder, load should be on the cross girder. The position of load for maximum B.M. in the cross girder is shown in fig 18.
Slab is assumed to be simply supported between 2 cross girders.

= 700X = 542.5kN

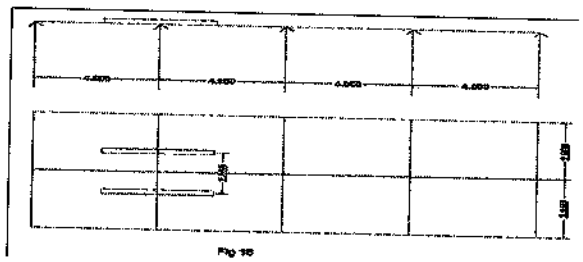

Cross girder is assumed to be rigid.

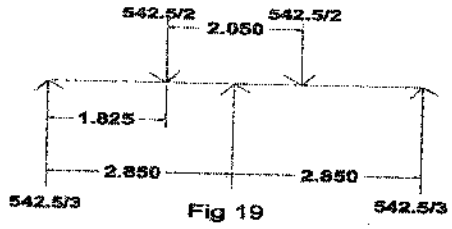

Fig 19

Reaction on each longitudinal girder= 542.5/3= 180.83kN
Maximum B.M. occurs under the load.
Max. L.L.B.M. = 542.5/3X1.825= 330.02kNm
B.M. including impact= 1.1X330.02= 363.02kNm
D.L.B.M. at 1.825m from support= 33.05X1.825–19.83X1.825/2= 42.22kNm
Total B.M. = 42.22+363.02=405.24kNm
Live Load shear including impact= 542.5/3X1.1= 198.92kN
Total shear force= 198.92+33.05= 231.97kN
The cross girder is designed as T-beam. Assuming effective depth as 145cm,

A_t= =13.5cm^2

Provide 3 bars of 25mmØ.

Shear stress= = 5.92kg/cm^2

Using 12mmØ 2 legged stirrups

Spacing= = 29.24cm

Provide 12mmØ 2 legged stirrups at 25cm c/c.

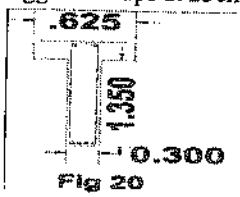

Fig 20

D. Pier design:

Dimensions: Minimum pier length
2X2.85+0.3=6m
6+1.8= 7.8m
Take the length of pier as 8m.
Minimum width = 1.6m
Top area of pier = 1.8X8+πX1.8^2/4 = 16.94m^2
Bottom area of pier = 2.8X8+πX2.8^2/4 = 28.56m^2
Weight of the pier= X8X2.3 = 418.6 tons = 4186kN

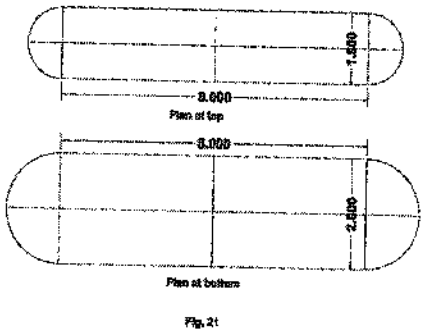

Fig.21

Moments of Inertia:

I_{xx}= + = 17.65m^4

I_{yy}= +2X1/2X + 2X1/2XπX2.8^{2}X4^2/4 = 221.0m^4

Dead loads of superstructure:

Cantilever	=2X12.43X16	= 39.77 tons
Slab	= 6X0.28X16X2.5	= 67.2 tons
Wearing coat= 0.08X2.3X7.5X16		= 22.08 tons
Main girders = 3X0.3X1.35X16X2.5		= 48.6 tons
Cross girders= 10X2.55X0.3X1.35X2.5=		25.82 tons

Resultant= 202.7 tons

Total dead load including pier= 202.7+418.6= 621.3 tons

Stress due to dead load= $\frac{621.3}{28.86}$= 217.5kN/m^2

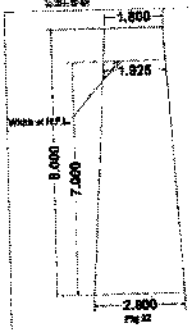

Taking 1m free board.

Volume of submerged portion

Area (H.F.L.)= 8X1.925 + 2X1/2XπX1.925^2/4 = 18.31m^2

Volume = $(\frac{18.31+28.86}{2})$X7 = 164.04m^3

Weight in loss= 164.01X1= 164.04 tons (as unit weight of water= 1 ton/m^3)

Stress at base= $\frac{164.04}{28.86}$ = –57.4kN/m^2

Live load stresses:

Eccentricity of girders=1/2 = 0.5m

Total live load = 70X1.1= 77 tons= 770kN

Moment = 770X0.5 = 385kNm

Stress = $\frac{770}{28.86} \pm \frac{385}{17.32}$X1.4

= 27.0$\pm$ 30.5

Maximum stress= 27.0+30.5 = 57.5kN/m^2

Minimum stress= 27.0–30.5 = –3.5kN/m^2

Longitudinal force= 0.25X770= 192.5kN

Moment at bottom= 192.5X8= 1540kNm

Stress= $\pm \frac{1540X1.4}{17.32}$ = 122.8kN/m^2

Wind Loads:

Exposed area: Girder= 1.35m

Slab = 0.28m

Kerb = 0.3m

Railing=1m

Resultant= 2.93m

2.93X16= 46.88m^2

Assuming wind pressure= 90kg

Total force= 46.88X0.09 = 4.22 tons = 42.2kN

But as per code minimum wind load should not be less than 450kg/m^3.

16mX0.45= 7.2 tons = 72kN

And 240kg for unloaded portion

46.88X0.24 = 251 tons = 2510kN

Moment = 11.25X8 + 2.93/2 = 11.25X8 + 2.93/2 = 106.48 tons-m = 1064.8kNm

Stress = $\frac{M}{I_{yy}} = \frac{1064.8}{132.9}$X4 = 19.3kN/m^2

At edge = $\frac{1064.8}{132.9}$(4+1.4) = 26.0kN/m^2

Stresses due to water currents:

Area of wetted surface = $\frac{(1.925+3.85)}{2}$X7 = 16.54m^2

$P = \frac{1.5KAV^2}{2g}$

Assuming velocity of water = 3m/s

Pressure = $1.5X\frac{1X16.54X3^2}{2X9.81}$ = 11.38 tons = 113.8 kN

This pressure acts at a height of 2/3h from bottom.

Moment= 113.8X2/3X7 = 531.1kNm

Stresses at junction = $\frac{531.1}{132.9}$X4 = 9.6kN/m^2

Stresses at edge = $\frac{531.1}{132.9}$X5.4 = 13.0kN/m^2

Stresses due to longitudinal force:

Maximum longitudinal force will occur due to class AA loading.

Longitudinal force due to class AA loading = 0.2X70 = 14 tons

Moment at base of pier due to this force = 140X8 = 1120kNm

Stresses at base = $\pm \frac{M}{I_{yy}}$Xy = $\frac{1120X1.4}{17.32}$ = 88.84kN/m^2

Total Stresses:

Under dry conditions:

Total stress = dead load + live load (eccentric + longitudinal force + frictional resistance) + wind load

At the end of straight portion (point A or E) maximum

=217.5+57.5+88.84+57.4+19.3+26.0= 466.54kN/m^2

At the end of straight portion (point A or C) minimum

=217.5–3.5–88.84–57.4–19.3–26.0= 22.46kN/m^2

At the end of pier (F or C) maximum

=217.5+26.0= 243.5kN/m^2

At the end of pier (F or C) minimum

=217.5–26.0= 191.5kN/m^2

Under wet conditions:

Total stress = dead load + buoyancy + live load + wind load + wind currents

At the end of straight portion (point A or E) maximum

=217.5–57.4+57.5+88.84+57.4+19.3+96.0= 392.74kN/m^2

At the end of straight portion (point A or E) minimum

=217.5–57.4–3.5–88.84–57.4–19.3–96.0= 18.54kN/m^2

At the end of pier (F or C) maximum

=217.5–57.4+26.0+13.0= 199kN/m^2

At the end of pier (F or C) minimum

=217.5–57.4–26.0–13.0= 121.1kN/m^2

Allowable compressive stress in 1:3:6 concrete is 20N/mm^2 in compression.

E. FOUNDATION:

Total dead load= 6213kN

Taking moorum soil with S.B.C. 350kN/m^2.

Taking 10% load of footing = 621.3kN

Area $= \frac{6213+621.3}{350} = 19.52$ m^2

Proposed dimensions = 11.4X3.4m

Area 38.76 m^2

Provide P.C.C. bed of 11.4mX3.4mX0.2m dimensions

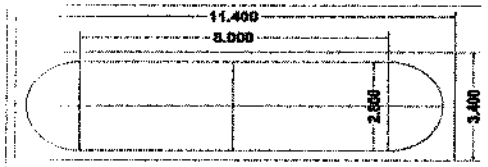

Fig 23

F. ABUTMENTS:

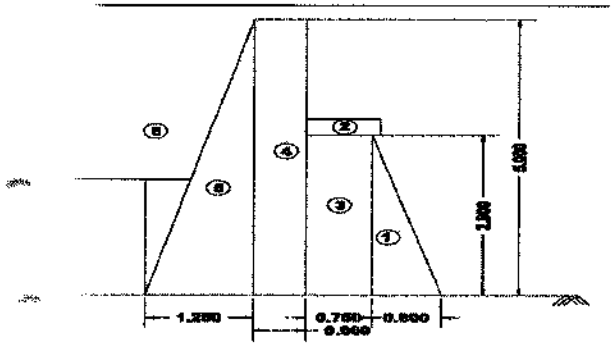

Fig 24

Dead load from superstructure= $\frac{912.15}{9}$ = 101.35 tons = 1013.5kN

Dead load per meter width = 101.35/9 = 11.26 tons = 112.6kN

Live Load max. S.F.= 70X14.2/16 = 62.125 tons = 621.25kN

Live Load with Impact = 621.25X1.1 = 683.38 kN

Live load per meter width = 683.35/9 = 75.93 kN

Resultant = 112.6+75.93 = 188.53kN

Eductive effort = 14/9 = 1.56 tons = 15.6kN

Load from superstructure = 0.15X18.852= 2.835 tons = 28.35kN

Total = 15.6+28.35= 44.3kN

Earth pressure = $\tan\theta$ = 1.25/5 = 0.25

$\theta = \tan^{-1}(0.25) = 14.036°$

$\cos\theta$ = cos(14.036)= 0.97 & sin(14.036)= 0.24

Earth pressure = $\frac{1-\sin\theta}{1+\sin\theta} = \frac{1-0.25}{1+0.25} = 1/3$

Total active earth pressure P = $k_a X \frac{wh^2}{2}$ = 1.8X21^2/2 = 3.969 tons = 39.69 kN

Horizontal force = 39.69X0.97 = 38.5 kN

Vertical force = 39.69X0.24 = 9.5kN

Sl. No.	Description	Weight	Lever Arm	Moment
1.	Reaction	18.853	1.125	21.209
2.	Item 1-1/2X0.8X2.9X2.3	2.668	0.533	1.422
3.	Item 2- 0.85X0.3X2.4	0.612	1.125	0.688
4.	Item 3- 0.75X2.9X2.3	5.003	1.175	5.878
5.	Item 4- 0.6X5.0X2.3	6.900	1.85	12.765
6.	Item 5-1/2X1.25X5.0X2.3	7.188	2.567	18.452
7.	Item 6-1/2X1.25X5.0X1.8	5.625	2.98	16.763
8.	Earth pressure (vertical) 0.95	0.95	2.875	2.731
9.	Earth pressure (horizontal) 3.85		-2.10	-8.085
10.	4.42		-2.90	-12.818

$\sum$= 47.799 tons $\sum$= 59.005ton-m

Point of application of R= $\frac{59.005}{47.799}$ = 1.234m

Eccentricity e= 3.4/2 – 1.234 = 0.466m

P= $\frac{47.799}{3.4}\left(1 \pm \frac{6\times47.799\times0.466}{3.4^2}\right)$ = 17.354(1$\pm$0.822)

Maximum shear stress= 316.19kN/m^2

Minimum shear stress= 30.89kN/m^2

There is no occurrence of tension hence safe.

Taking moorum foundation on site with S.B.C. 350kN/m^2.

G. WING WALLS:

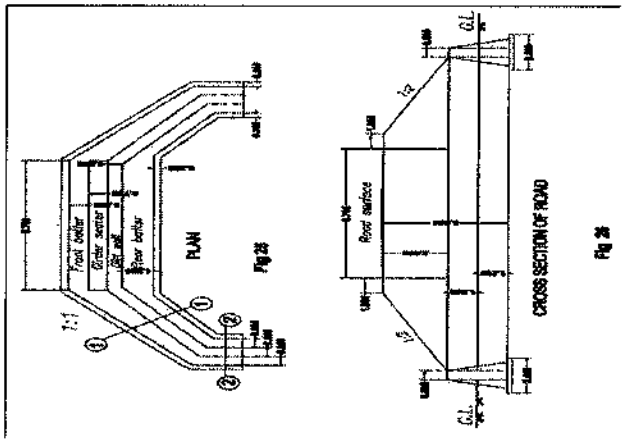

P_a= 1/2X0.54X1.8X2.6^2 = 3.28 tons

$P_a\cos\theta$ = 3.28X0.97 = 3.18 tons

$P_a\sin\theta$ = 3.28X0.24 = 0.79 tons

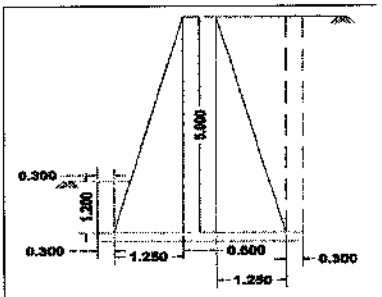

CROSS SECTION "1-1"

Fig. 27

Section 1-1

Sl. No.	Description	Weight	Lever arm	Moment
1.	1/2X0.6X2.4X2.3	1.656	0.7	1.16
2.	0.6X2.4X2.3	3.312	1.2	3.97
3.	1/2X0.6X2.4X2.3	1.656	1.7	2.81
4.	2.4X0.2X2.3	1.104	1.2	1.33
5.	1/2X0.6X1.2X1.8	0.648	0.5	0.32
6.	0.3X1.2X1.8	0.648	0.15	0.10
7.	1/2X0.6X2.4X1.8	1.296	1.80	2.33
8.	0.3X2.4X1.8	1.296	2.25	2.92
9.	Active P_v 3.18		1.09	–3.47
10.	P_H	0.79	1.84	1.45
11.	Passive 5.29		0.87	4.60

$\sum$=12.406 tons $\sum$=1.53 tons-m

Point of application of R= $\frac{1.53}{12.406}$ = 1.41m

e = b/2 – R = 1.2–1.41= –0.21m

P=$\frac{12.406}{2.4}(1 \pm \frac{6\times0.21}{2.4})$ = 5.17(1$\pm$0.525)

Maximum stress = 7.88 tons/m^2 = 78.8kN/m^2

Minimum stress = 2.46 tons/m^2 = 24.6kN/m^2

There is no occurrence of tension hence safe.

Section 2-2

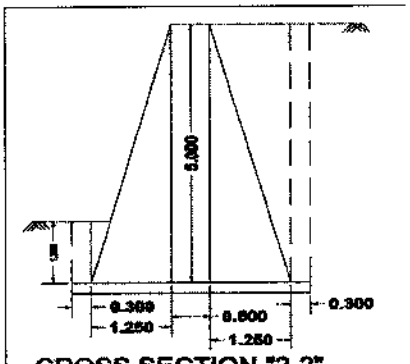

CROSS SECTION "2-2"

Fig. 28

Sl. No.	Description	Weight	Lever Arm	Moment
1.	1/2X1.25X5X2.3	7.19	2.57	18.48
2.	0.6X5X2.3	6.9	1.85	12.76
3.	1/2X1.25X5X2.3	7.19	1.13	8.12
4.	1/2X0.3X1.2X1.8	0.324	0.3	0.09
5.	0.3X1.2X1.8	0.648	0.15	0.09
6.	1/2X1.25X5X1.8	5.625	2.98	16.76
7.	Active P_H 7.86		–2.18	–17.13
8.	P_V 1.94		2.83	5.49
9.	Passive P		0.87	4.6

$\sum$=27.88 tons $\sum$=49.25 tons-m

Point of application of R=$\frac{49.25}{27.88}$ = 1.76m

e= b/2–R= 1.55–1.76 = –0.21m

P=$\frac{27.88}{5.5}(1 \pm \frac{6\times0.21}{5.5})$ = 7.53(1$\pm$0.34)

Maximum stress = 10.09 tons/m^2 = 100.9kN/m^2

Minimum stress = 4.97 tons/m^2 = 49.7kN/m^2

There is no occurrence of tension hence safe.

VII. CONCLUSION

Thus, a concrete girder bridge is designed with length as 32m, width of road as 7.5m, and 8.5m above the bed level. It has been designed on the assumptions that the soil is moorum soil with S.B.C. as 350kN/m^2. Piers and foundation have been designed keeping high flood level as 7m for pier of 8m with due consideration to water pressure and force of buoyancy.

The bridge has been provided with abutments and wing walls on both sides. Abutments, wing walls and piers have been designed as mass concrete works.

The loading conditions have been taken as worst loading conditions i.e. class AA tracked vehicle and class A for the cantilever portion of the bridge.

The design is based on Working Stress Method of design with references from IRC 6:2000 – Standard Specifications and Code of Practice for Road Bridges- Section II Loads and Stresses and IRC 21:2000 – Standard Specifications and Code of Practice for Road Bridges (Plain and Reinforced). The slab for the bridge is designed using Pigeaud's curves.

VIII. REFERENCES

1. G. O. Young, "Synthetic structure of industrial plastics (Book style with paper title and editor)," in *Plastics*, 2nd ed. vol. 3, J. Peters, Ed. New York: McGraw-Hill, 1964, pp. 15–64.
2. W.-K. Chen, *Linear Networks and Systems* (Book style). Belmont, CA: Wadsworth, 1993, pp. 123–135.
3. H. Poor, *An Introduction to Signal Detection and Estimation*. New York: Springer-Verlag, 1985, ch. 4.
4. B. Smith, "An approach to graphs of linear forms (Unpublished work style)," unpublished.
5. E. H. Miller, "A note on reflector arrays (Periodical style—Accepted for publication)," *IEEE Trans. Antennas Propagat.*, to be published.
6. J. Wang, "Fundamentals of erbium-doped fiber amplifiers arrays (Periodical style—Submitted for publication)," *IEEE J. Quantum Electron.*, submitted for publication.
7. C. J. Kaufman, Rocky Mountain Research Lab., Boulder, CO, private communication, May 1995.

8. Y. Yorozu, M. Hirano, K. Oka, and Y. Tagawa, "Electron spectroscopy studies on magneto-optical media and plastic substrate interfaces (Translation Journals style)," *IEEE Transl. J. Magn. Jpn.*, vol. 2, Aug. 1987, pp. 740–741 [*Dig. 9th Annu. Conf. Magnetics* Japan, 1982, p. 301].
9. M. Young, *The Techincal Writers Handbook.* Mill Valley, CA: University Science, 1989.
10. (Basic Book/Monograph Online Sources) J. K. Author. (year, month, day). *Title* (edition) [Type of medium]. Volume (issue). Available: http://www.(URL)
11. J. Jones. (1991, May 10). Networks (2nd ed.) [Online]. Available: http://www.atm.com
12. (Journal Online Sources style) K. Author. (year, month). Title. *Journal* [Type of medium]. Volume (issue), paging if given. Available: http://www.(URL)
13. R. J. Vidmar. (1992, August). On the use of atmospheric plasmas as electromagnetic reflectors. *IEEE Trans. Plasma Sci.* [Online]. *21(3).* pp. 876—880. Available: http://www.halcyon.com/pub/journals/21ps03-vidmar

AUTHORS PROFILE

1. NavyaSoni, Matrusri Engineering College
2. P Dhanmma, Assistant Professor, Matrusri Engineering College
   E mail id : dhanateju@gmail.com
3. T Raja Ramanna, Assistant Professor, Matrusri Engineering College

ABOUT THE INSTITUTE

Muffakham Jah College of Engineering and Technology (MJCET) was established in the year 1980 by Sultan-Ul-Uloom Education Society (SUES), which was formed by a group of visionaries and intellectuals from various walks of life. Over the past three decades, it has emerged as a premier institute, offering BE courses of four years duration in eight disciplines (Civil, ECE, CSE, IT, EEE, EIE, Mechanical & Production) and five ME courses (CAD/CAM, Structural Engineering., Digital Systems, Computers & Power Electronics) of two years duration. The current intake of all BE Courses is 780, in addition to 102 students in ME Programmes. Research Centers were started in Civil, Mechanical, EEE, CSE and ECE Departments for Doctoral Studies. The college is affiliated to Osmania University, Hyderabad and approved by AICTE, New Delhi. As per the survey of The Outlook magazine, MJCET was ranked 62nd among top 100 Engineering Colleges in India. MJCET has been ranked 47th in India among the top private institutes in Engineering by Times Engineering Institute ranking survey 2019. MJCET ranked 28th out of top 200 Engineering Colleges by India Today magazine. As per The Week Magazine, MJCET ranked 26th among the top Private Engineering Colleges in South India and 42nd among All India Private Engineering Colleges.

OVERVIEW OF THE CONFERENCE

Civil Engineering Infrastructure is the most significant factor in accelerating the pace of economic development of any country. The recent innovation and advances in the field of Civil Engineering has made a drastic impact in the Construction Industry. As the world's population increases, environmental concerns mount and Civil Engineers are entrusted by the society to achieve a sustainable world and raise the quality of life globally. The balancing of economic, social and environmental objectives now and in the future has become known as Sustainable Development and is increasingly a key driver at a range of organizational and spatial scales.

The Conference on Recent Advances in Civil Engineering Infrastructure – (RACEI-2019) aims at exploring the new horizon of innovation from distinguished researchers, eminent professionals from academia and Industry. The Conference also focuses for the achievement of relevant Sustainable Development Goals as described by United Nation Development Program. This event will be a platform to showcase and deliberate research work, studies and contributions for developing novel concepts in Civil Engineering Infrastructure. The Conference consists of keynote lectures on related themes by eminent personalities and stake holders.

BSP BS Publications
A Unit of BSP Books Pvt. Ltd.
4-4-316/309, Giriraj Lane, Sultan Bazar, Hyderabad - 500 095. (A.P.)
Ph: 040-23445688 / 605. Fax: +91-40-23445611.
e-mail: info@bspbooks.net, marketing@bspbooks.net
Website: www.bspbooks.net

ISBN : 978-93-89354-86-7

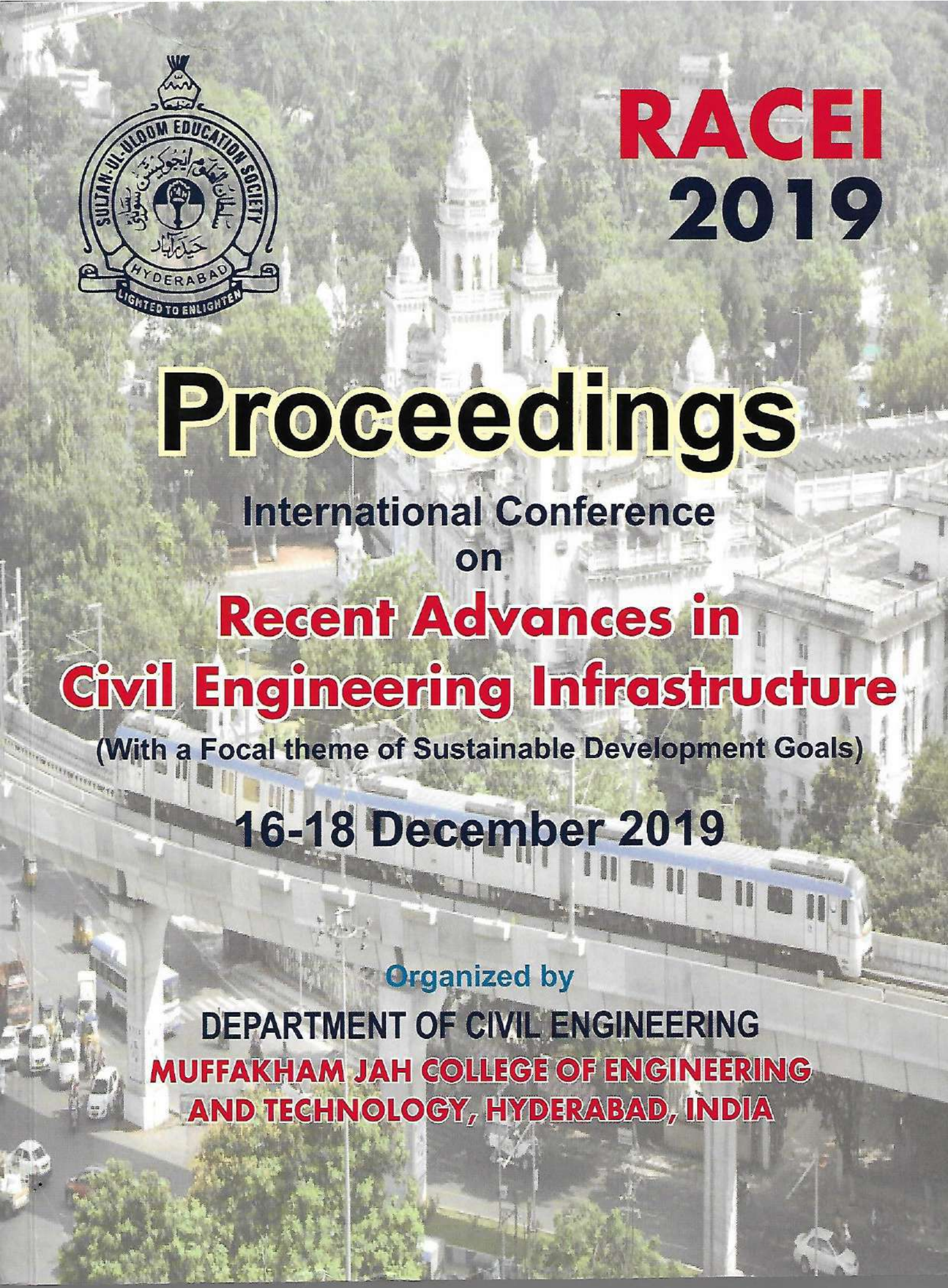

RACEI 2019

Proceedings

International Conference on

Recent Advances in Civil Engineering Infrastructure

(With a Focal theme of Sustainable Development Goals)

16-18 December 2019

Organized by

DEPARTMENT OF CIVIL ENGINEERING

MUFFAKHAM JAH COLLEGE OF ENGINEERING AND TECHNOLOGY, HYDERABAD, INDIA

International Conference on Recent Advances in Civil Engineering Infrastructure (RACEI-2019)
Department of Civil Engineering, Muffakham Jah College of Engineering and Technology

Influence of Velocity on Major Lift Irrigation Projects

M.Pratibha, S. Lokeswari and Arn Sharma

Abstract: ***Lift Irrigation Projects are drawing more attention in changed scenario owing to the non-feasibility of Dams and Barrages; Lift Irrigation Projects gained momentum. In the days to come ;Lift irrigation projects are going to play vital role in irrigation sector to fill the gap ayacut created due to non provision of conventional irrigation structure. There are many regions located far away from water source high elevation requiring water immediately and providing lift irrigation projects has become inevitable. With thrust and lift irrigation projects, many projects are being taken up with lifting huge quantity of water from rivers and high heads with lengthy pipes; which was not dealt before with those magnitudes. Discharge and pumping head are the parameters; which g0 oven the planning of the project. To achieve economy, better control over them is required. Major Lift irrigation Project needs optimization in planning while fixing the pumping head and pump capacity along with length and diameter of pressure mains. For optimization, discharge if pumps can be fixed with effective usage of tanks enroute the alignment and deriving advantage of lesser demand crop during non-peak period. Pumping head can be reduced considerable by selecting the duty point of pumps with respect to water levels in the source where maximum operation period is expected. Function and efficiency of the Lift Irrigation Projects mainly depend on the performance of pumps and pressure mains of pumps act as heart of Lift Irrigation Project and pressure mains act as nerves of Lift Irrigation Project.***

In this study an attempt has been made to analyze influence of velocity on project cost referring a case study of Alisagar Lift Irrigation Project apart from Pumps, Pumping head, Pump Capacity, advantages of minimum number of rows, precautions taken in laying and design of pressure mains, selection of pipe materials, number of pumps for better production at lower costs and explore means to optimize the efficiency of planning design, construction, operation and maintenance of Major Lift Irrigation Project.

Keywords: Lift Irrigation Project, Planning and Design, Velocity, Pumping Head and Discharge, Pump Capacity and Project Cost

I. INTRODUCTION

Alisagar Lift Irrigation Project- A Case Study

the objective of the alisagar lift irrigation project is to irrigate 21,778 ha (53,793 acres) of nizamsagar project command area situated in nizamabad district. the project envisages lifting of 20.39 cumecs (720 c/s) of water from el +321.50 m on river godavari on right bank near kosli village from the foreshore of sriram sagar project. the project was executed on epc basis at the cost of rs.163.98 cr. alisagar lift irrigation project is one among the major lift irrigation projects under taken on epc basis by the irrigation department of govt of telangana.

II. ANALYSIS

Influence of Velocity in Pressure Mains on Pump and Project Cost. For every 0.50 m/s rise in Velocity of pipe, frictional loss rises by 75% to 100% with reduction of diameter by 11% to 13% only. Smaller diameter is economical during initial stage of construction but power consumption will be high. Higher diameter needs less power but with high initial cost. Hence, it is desirable to allow higher velocities in shorter length of pipes and lower velocities in lengthy pipes (particularly when the length of pipe is in KM) owing to the recurring power consumption annually

III. FORMULAE

The following formulae are used in calculating discharge in each pipe and pump, different heads, head loss due to friction, hydraulic radius of pipe, velocity, pump capacities and quantity of steels etc.

Discharge in pipe (Q_e)	=	Q/N
Discharge in pump (Q_p)	=	Q/n
Max Static Head (H_{smx})	=	(Max water level of tank) – (Min water level of tank)
Normal Static Head (H_{sn})	=	(Min water level of tank) – (Min water level in river)
Velocity In pipe (V)	=	$Q_e/\pi/4D^2$
Hydraulic Radius of pipe	=	D/4
Frictional loss per KM (h_f)	=	h_f L / 1000
Frictional loss per KM (h_f)	=	$L(1.1778\ V\ /\ C\ R\ 0.63^{0.63})^{1.853}$ By (William Hazen Formula)
Frictional loss in pipe (H_f)	=	h_f L / 1000
TOTAL BEND LOSSES (HB)	=	N K V^2 /2G
MAX PUMPING	=	$H_{SMX}+H_F+H_E+H_B$

HEAD (H_{MAX})

NORMAL PUMPING HEAD (H_{NRML}) = $H_S+H_F+H_E+H_B$

MIN PUMPING HEAD(H_{MIN}) = $H_{SMN}+H_F+H_E+H_B$

PUMP CAPACITY IN KW = 9.81 Q H / H

PUMP CAPACITY IN (HP) = 9.81 Q H / 0.746 H

QUANTITY OF STEEL IN MTONS = ΠDLTP/1000

different analysis for calculating various parameters as mentioned above have been made using simple mathematical relations in **computer (excel) program** by substituting the input parameters of alisagar lift irrigation project case study . but as far as this paper is concerned only velocity results have been tabulated which shows as velocity increases frictional losses and power requirement also increases hence project cost also increases. it is inferred that smaller diameter is economical during initial stage of construction but power consumption is very high. higher diameter needs less power but with high initial cost.

TABLE NO.1

S.NO	PARTICULARS	VARIOUS VELOCITIES IN PIPE (M/S)		
		1.5	2	2.5
	DISCHARGE IN CUMECS	12.88	12.88	12.88
	DIA OF PIPE IN M	2.339	2.035	1.811
	LENGTH OF PIPE IN KM	1.53	1.53	1.53
	THICKNESS OF PIPE IN MM	14	12	10
	HAZEN WILLIAM COEFFICIENT	140	140	140
	FRICTION LOSSES H_F IN M	0.872	1.76	3.029
	QUANTITY OF STEEL IN MTONS	247	183.4	136.7
	TOTAL KW FOR 4 PUMPS FOR NORMAL HEAD	3392	3516	3696
	PROJECT COST IN MILLIONS	1959.836	1954.732	1990.992

as the velocity increases frictional losses, power consumption increases hence the project cost also increases

IV. RESULTS AND CONCLUSIONS

It can be noticed that increase in the velocity reduces the pressure main diameter thereby reduces capital cost, but at the same time increases power requirement as the analysis shows for 1.5 m/s project cost is 1959.836 millions where as 2.5 m/s it is 1990.292 millions, and power requirement is from 3392 KW to 3696 KW.

V. FUTURE WORK

As the pressure mains act as nerves of Lift Irrigation Project, care shall be taken for pipes when they are to be laid in BC soils, water logged area and at crossing of drains. Low velocity in the pipe would be economical for the projects with very lengthy pressure mains, however higher velocity may be permitted for the projects with shorter length. Larger diameter with less number of rows may be economical with respect to installation cost as well running cost. Adequate clearance shall be maintained between pipes for stability as well as maintenance purpose.

VI. REFERENCES

[1] Dracup, John.A (1996): "*The optimal use of a ground water and surface water system; A parametric linear programming approach*", Water Resources Center
[2] Contribution, No.107, University of California, Berkely, USA.
Dudley. N.J, (1971): "*Optimal intra seasonal Irrigation Water Allocation*", Water Resources Research; Vol.7,No. 4,Pp770-788
[3] Hall. W.A.(1964):"*Optimum Design of a multiple-purpose reservoir; Journal of hydraulics division*", ASCE;Vol.90;No. HY4,Pp 141-149..
[4] Hall, Warren. A and William Butcher (1968):"*Optimal Timing of Irrigation*", Journal of the Irrigation and Drainage Division, Proceedings of the ASCE, Vol.95, No.IRI Proc. Paper 6428, Pp 254-257.

[5] ModiP.N(2008): *Irrigation Water Resources and Water Power Engineering*, Standard book house, India. Pp220

Roark.R.J (1974): *Formulas for Stress and Strain* McGraw Hill, New York, Pp851

[6] Raju I S N (2008):" *Lift Irrigation Scheme a Solution to Tail end Ayacut Case Study of Alisagar and Guthpa L I Schemes"* A National Seminar on lift irrigation organized by Institution of Engineers (India), Hyderabad

[7] Sharma. A.R.N (2008):"*Planning, Design and Optimization of major Lift Irrigation Schemes"* A National Seminar on lift irrigation organized by Institution of Engineers (India), Hyderabad

Spangler. M.G. (1956):"*Stresses in Pressure Pipelines and Protective Casing Pipes*", Proceedings of ASCE, Vol.82 Pp 1054

Subramanya K(1997) *Engineering Hydrology* McGraw Hill, New York,pp452.

[8] Watkins. R.K., and Spangler M.G. (1958): "*Some characteristic of the Modulus of Passive Resistance of Soil –A Study in Similitude,* "Proc.37 of the Highway Research Board, HRB, Washington D C, Pp576.

[9] "*Irrigation in India through ages*", Central Board of Irrigation and Power, New Delhi (1971).

[10] "*A Guide for Estimation Irrigation Water requirements"*(1971): Issued by the Water Management Division, Ministry of Agriculture (Dept. of Agriculture), New Delhi-1

Andhra Pradesh State Irrigation Development Corporation, Hyderabad.

AUTHORS PROFILE

1. M. Pratibha, Matrusri Engineering College, Hyd
   E mailpratibhagundepally@gmail.com.
2. S. Lokeswari, Matrusri Engineering College, Hyd
3. Arn Sharma, Matrusri Engineering College, Hyd

ABOUT THE INSTITUTE

Muffakham Jah College of Engineering and Technology (MJCET) was established in the year 1980 by Sultan-Ul-Uloom Education Society (SUES), which was formed by a group of visionaries and intellectuals from various walks of life. Over the past three decades, it has emerged as a premier institute, offering BE courses of four years duration in eight disciplines (Civil, ECE, CSE, IT, EEE, EIE, Mechanical & Production) and five ME courses (CAD/CAM, Structural Engineering., Digital Systems, Computers & Power Electronics) of two years duration. The current intake of all BE Courses is 780, in addition to 102 students in ME Programmes. Research Centers were started in Civil, Mechanical, EEE, CSE and ECE Departments for Doctoral Studies. The college is affiliated to Osmania University, Hyderabad and approved by AICTE, New Delhi. As per the survey of The Outlook magazine, MJCET was ranked 62nd among top 100 Engineering Colleges in India. MJCET has been ranked 47th in India among the top private institutes in Engineering by Times Engineering Institute ranking survey 2019. MJCET ranked 28th out of top 200 Engineering Colleges by India Today magazine. As per The Week Magazine, MJCET ranked 26th among the top Private Engineering Colleges in South India and 42nd among All India Private Engineering Colleges.

OVERVIEW OF THE CONFERENCE

Civil Engineering Infrastructure is the most significant factor in accelerating the pace of economic development of any country. The recent innovation and advances in the field of Civil Engineering has made a drastic impact in the Construction Industry. As the world's population increases, environmental concerns mount and Civil Engineers are entrusted by the society to achieve a sustainable world and raise the quality of life globally. The balancing of economic, social and environmental objectives now and in the future has become known as Sustainable Development and is increasingly a key driver at a range of organizational and spatial scales.

The Conference on Recent Advances in Civil Engineering Infrastructure – (RACEI-2019) aims at exploring the new horizon of innovation from distinguished researchers, eminent professionals from academia and Industry. The Conference also focuses for the achievement of relevant Sustainable Development Goals as described by United Nation Development Program. This event will be a platform to showcase and deliberate research work, studies and contributions for developing novel concepts in Civil Engineering Infrastructure. The Conference consists of keynote lectures on related themes by eminent personalities and stake holders.

BSP BS Publications
A Unit of BSP Books Pvt. Ltd.
4-4-316/309, Giriraj Lane, Sultan Bazar, Hyderabad - 500 095. (A.P.)
Ph: 040-23445688 / 605. Fax: +91-40-23445611.
e-mail: info@bspbooks.net, marketing@bspbooks.net
Website: www.bspbooks.net

ISBN : 978-93-89354-86-7

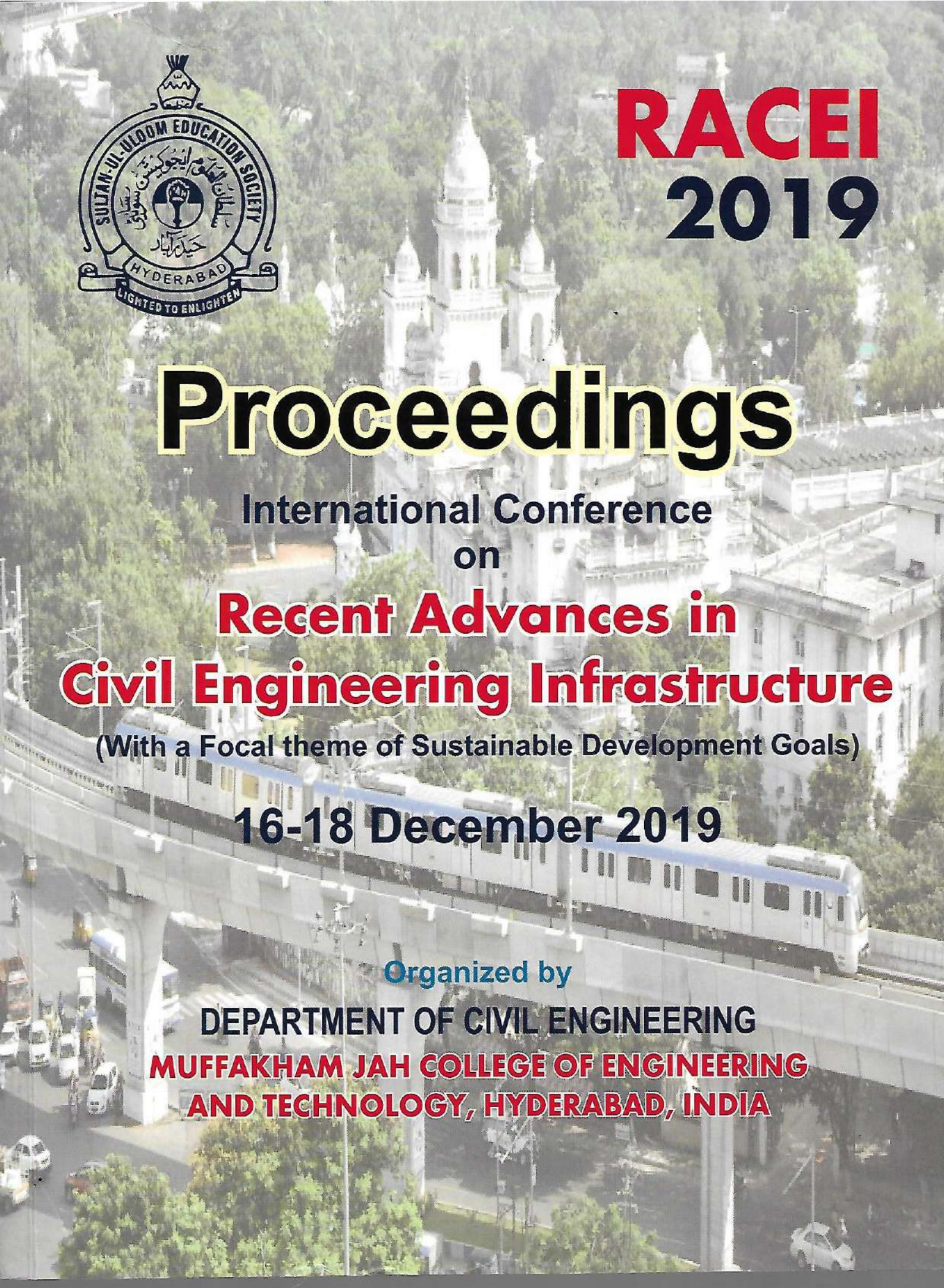

RACEI 2019

Proceedings

International Conference on

Recent Advances in Civil Engineering Infrastructure

(With a Focal theme of Sustainable Development Goals)

16-18 December 2019

Organized by

DEPARTMENT OF CIVIL ENGINEERING

MUFFAKHAM JAH COLLEGE OF ENGINEERING AND TECHNOLOGY, HYDERABAD, INDIA

International Conference on Recent Advances in Civil Engineering Infrastructure (RACEI-2019)
Department of Civil Engineering, Muffakham Jah College of Engineering and Technology

Influence of Velocity on Major Lift Irrigation Projects

M.Pratibha, S. Lokeswari and Arn Sharma

Abstract: ***Lift Irrigation Projects are drawing more attention in changed scenario owing to the non-feasibility of Dams and Barrages; Lift Irrigation Projects gained momentum. In the days to come ;Lift irrigation projects are going to play vital role in irrigation sector to fill the gap ayacut created due to non provision of conventional irrigation structure. There are many regions located far away from water source high elevation requiring water immediately and providing lift irrigation projects has become inevitable. With thrust and lift irrigation projects, many projects are being taken up with lifting huge quantity of water from rivers and high heads with lengthy pipes; which was not dealt before with those magnitudes. Discharge and pumping head are the parameters; which g0 oven the planning of the project. To achieve economy, better control over them is required. Major Lift irrigation Project needs optimization in planning while fixing the pumping head and pump capacity along with length and diameter of pressure mains. For optimization, discharge if pumps can be fixed with effective usage of tanks enroute the alignment and deriving advantage of lesser demand crop during non-peak period. Pumping head can be reduced considerable by selecting the duty point of pumps with respect to water levels in the source where maximum operation period is expected. Function and efficiency of the Lift Irrigation Projects mainly depend on the performance of pumps and pressure mains of pumps act as heart of Lift Irrigation Project and pressure mains act as nerves of Lift Irrigation Project.***

In this study an attempt has been made to analyze influence of velocity on project cost referring a case study of Alisagar Lift Irrigation Project apart from Pumps, Pumping head, Pump Capacity, advantages of minimum number of rows, precautions taken in laying and design of pressure mains, selection of pipe materials, number of pumps for better production at lower costs and explore means to optimize the efficiency of planning design, construction, operation and maintenance of Major Lift Irrigation Project.

Keywords: Lift Irrigation Project, Planning and Design, Velocity, Pumping Head and Discharge, Pump Capacity and Project Cost

I. INTRODUCTION

Alisagar Lift Irrigation Project- A Case Study

the objective of the alisagar lift irrigation project is to irrigate 21,778 ha (53,793 acres) of nizamsagar project command area situated in nizamabad district. the project envisages lifting of 20.39 cumecs (720 c/s) of water from el +321.50 m on river godavari on right bank near kosli village from the foreshore of sriram sagar project. the project was executed on epc basis at the cost of rs.163.98 cr. alisagar lift irrigation project is one among the major lift irrigation projects under taken on epc basis by the irrigation department of govt of telangana.

II. ANALYSIS

Influence of Velocity in Pressure Mains on Pump and Project Cost. For every 0.50 m/s rise in Velocity of pipe, frictional loss rises by 75% to 100% with reduction of diameter by 11% to 13% only. Smaller diameter is economical during initial stage of construction but power consumption will be high. Higher diameter needs less power but with high initial cost. Hence, it is desirable to allow higher velocities in shorter length of pipes and lower velocities in lengthy pipes (particularly when the length of pipe is in KM) owing to the recurring power consumption annually

III. FORMULAE

The following formulae are used in calculating discharge in each pipe and pump, different heads, head loss due to friction, hydraulic radius of pipe, velocity, pump capacities and quantity of steels etc.

Discharge in pipe (Q_e)	=	Q/N
Discharge in pump (Q_p)	=	Q/n
Max Static Head (H_{smx})	=	(Max water level of tank) – (Min water level of tank)
Normal Static Head (H_{sn})	=	(Min water level of tank) – (Min water level in river)
Velocity In pipe (V)	=	$Q_e/\pi/4D^2$
Hydraulic Radius of pipe	=	D/4
Frictional loss per KM (h_f)	=	h_f L / 1000
Frictional loss per KM (h_f)	=	$L(1.1778\ V\ /\ C\ R\ 0.63^{0.63})^{1.853}$ By (William Hazen Formula)
Frictional loss in pipe (H_f)	=	h_f L / 1000
TOTAL BEND LOSSES (HB)	=	$N\ K\ V^2\ /2G$
MAX PUMPING	=	$H_{SMX}+H_F+H_E+H_B$

HEAD (H_{MAX})

NORMAL PUMPING HEAD (H_{NRML}) = $H_S+H_F+H_E+H_B$

MIN PUMPING HEAD(H_{MIN}) = $H_{SMN}+H_F+H_E+H_B$

PUMP CAPACITY IN KW = 9.81 Q H / H

PUMP CAPACITY IN (HP) = 9.81 Q H / 0.746 H

QUANTITY OF STEEL IN MTONS = ΠDLTP/1000

different analysis for calculating various parameters as mentioned above have been made using simple mathematical relations in **computer (excel) program** by substituting the input parameters of alisagar lift irrigation project case study . but as far as this paper is concerned only velocity results have been tabulated which shows as velocity increases frictional losses and power requirement also increases hence project cost also increases. it is inferred that smaller diameter is economical during initial stage of construction but power consumption is very high. higher diameter needs less power but with high initial cost.

TABLE NO.1

S.NO	PARTICULARS	VARIOUS VELOCITIES IN PIPE (M/S)		
		1.5	2	2.5
	DISCHARGE IN CUMECS	12.88	12.88	12.88
	DIA OF PIPE IN M	2.339	2.035	1.811
	LENGTH OF PIPE IN KM	1.53	1.53	1.53
	THICKNESS OF PIPE IN MM	14	12	10
	HAZEN WILLIAM COEFFICIENT	140	140	140
	FRICTION LOSSES H_F IN M	0.872	1.76	3.029
	QUANTITY OF STEEL IN MTONS	247	183.4	136.7
	TOTAL KW FOR 4 PUMPS FOR NORMAL HEAD	3392	3516	3696
	PROJECT COST IN MILLIONS	1959.836	1954.732	1990.992

as the velocity increases frictional losses, power consumption increases hence the project cost also increases

IV. RESULTS AND CONCLUSIONS

It can be noticed that increase in the velocity reduces the pressure main diameter thereby reduces capital cost, but at the same time increases power requirement as the analysis shows for 1.5 m/s project cost is 1959.836 millions where as 2.5 m/s it is 1990.292 millions, and power requirement is from 3392 KW to 3696 KW.

V. FUTURE WORK

As the pressure mains act as nerves of Lift Irrigation Project, care shall be taken for pipes when they are to be laid in BC soils, water logged area and at crossing of drains. Low velocity in the pipe would be economical for the projects with very lengthy pressure mains, however higher velocity may be permitted for the projects with shorter length. Larger diameter with less number of rows may be economical with respect to installation cost as well running cost. Adequate clearance shall be maintained between pipes for stability as well as maintenance purpose.

VI. REFERENCES

[1] Dracup, John.A (1996): "*The optimal use of a ground water and surface water system; A parametric linear programming approach*", Water Resources Center
[2] Contribution, No.107, University of California, Berkely, USA.
Dudley. N.J, (1971): "*Optimal intra seasonal Irrigation Water Allocation*", Water Resources Research; Vol.7,No. 4,Pp770-788
[3] Hall. W.A.(1964):"*Optimum Design of a multiple-purpose reservoir; Journal of hydraulics division*", ASCE;Vol.90;No. HY4,Pp 141-149..
[4] Hall, Warren. A and William Butcher (1968):"*Optimal Timing of Irrigation*", Journal of the Irrigation and Drainage Division, Proceedings of the ASCE, Vol.95, No.IRI Proc. Paper 6428, Pp 254-257.

[5] ModiP.N(2008): *Irrigation Water Resources and Water Power Engineering*, Standard book house, India. Pp220

Roark.R.J (1974): *Formulas for Stress and Strain* McGraw Hill, New York, Pp851

[6] Raju I S N (2008):" *Lift Irrigation Scheme a Solution to Tail end Ayacut Case Study of Alisagar and Guthpa L I Schemes"* A National Seminar on lift irrigation organized by Institution of Engineers (India), Hyderabad

[7] Sharma. A.R.N (2008):"*Planning, Design and Optimization of major Lift Irrigation Schemes"* A National Seminar on lift irrigation organized by Institution of Engineers (India), Hyderabad

Spangler. M.G. (1956):"*Stresses in Pressure Pipelines and Protective Casing Pipes*", Proceedings of ASCE, Vol.82 Pp 1054

Subramanya K(1997) *Engineering Hydrology* McGraw Hill, New York,pp452.

[8] Watkins. R.K., and Spangler M.G. (1958): "*Some characteristic of the Modulus of Passive Resistance of Soil –A Study in Similitude,* "Proc.37 of the Highway Research Board, HRB, Washington D C, Pp576.

[9] "*Irrigation in India through ages*", Central Board of Irrigation and Power, New Delhi (1971).

[10] "*A Guide for Estimation Irrigation Water requirements"*(1971): Issued by the Water Management Division, Ministry of Agriculture (Dept. of Agriculture), New Delhi-1

Andhra Pradesh State Irrigation Development Corporation, Hyderabad.

AUTHORS PROFILE

1. M. Pratibha, Matrusri Engineering College, Hyd
   E mailpratibhagundepally@gmail.com.
2. S. Lokeswari, Matrusri Engineering College, Hyd
3. Arn Sharma, Matrusri Engineering College, Hyd

ABOUT THE INSTITUTE

Muffakham Jah College of Engineering and Technology (MJCET) was established in the year 1980 by Sultan-Ul-Uloom Education Society (SUES), which was formed by a group of visionaries and intellectuals from various walks of life. Over the past three decades, it has emerged as a premier institute, offering BE courses of four years duration in eight disciplines (Civil, ECE, CSE, IT, EEE, EIE, Mechanical & Production) and five ME courses (CAD/CAM, Structural Engineering., Digital Systems, Computers & Power Electronics) of two years duration. The current intake of all BE Courses is 780, in addition to 102 students in ME Programmes. Research Centers were started in Civil, Mechanical, EEE, CSE and ECE Departments for Doctoral Studies. The college is affiliated to Osmania University, Hyderabad and approved by AICTE, New Delhi. As per the survey of The Outlook magazine, MJCET was ranked 62nd among top 100 Engineering Colleges in India. MJCET has been ranked 47th in India among the top private institutes in Engineering by Times Engineering Institute ranking survey 2019. MJCET ranked 28th out of top 200 Engineering Colleges by India Today magazine. As per The Week Magazine, MJCET ranked 26th among the top Private Engineering Colleges in South India and 42nd among All India Private Engineering Colleges.

OVERVIEW OF THE CONFERENCE

Civil Engineering Infrastructure is the most significant factor in accelerating the pace of economic development of any country. The recent innovation and advances in the field of Civil Engineering has made a drastic impact in the Construction Industry. As the world's population increases, environmental concerns mount and Civil Engineers are entrusted by the society to achieve a sustainable world and raise the quality of life globally. The balancing of economic, social and environmental objectives now and in the future has become known as Sustainable Development and is increasingly a key driver at a range of organizational and spatial scales.

The Conference on Recent Advances in Civil Engineering Infrastructure – (RACEI-2019) aims at exploring the new horizon of innovation from distinguished researchers, eminent professionals from academia and Industry. The Conference also focuses for the achievement of relevant Sustainable Development Goals as described by United Nation Development Program. This event will be a platform to showcase and deliberate research work, studies and contributions for developing novel concepts in Civil Engineering Infrastructure. The Conference consists of keynote lectures on related themes by eminent personalities and stake holders.

BSP BS Publications
A Unit of BSP Books Pvt. Ltd.
4-4-316/309, Giriraj Lane, Sultan Bazar, Hyderabad - 500 095. (A.P.)
Ph: 040-23445688 / 605. Fax: +91-40-23445611.
e-mail: info@bspbooks.net, marketing@bspbooks.net
Website: www.bspbooks.net

ISBN : 978-93-89354-86-7

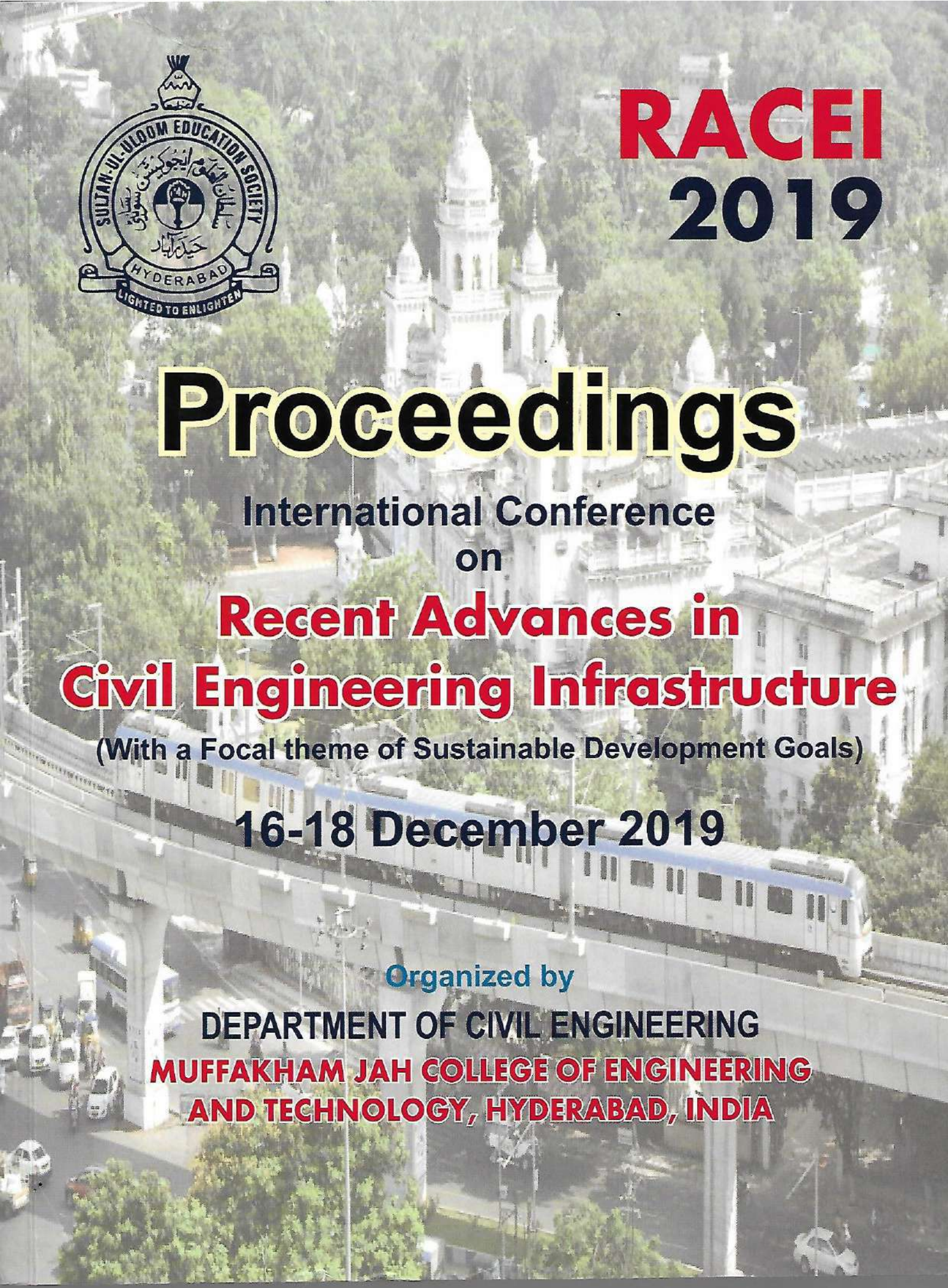

RACEI 2019

Proceedings

International Conference on

Recent Advances in Civil Engineering Infrastructure

(With a Focal theme of Sustainable Development Goals)

16-18 December 2019

Organized by

DEPARTMENT OF CIVIL ENGINEERING

MUFFAKHAM JAH COLLEGE OF ENGINEERING AND TECHNOLOGY, HYDERABAD, INDIA

Analysis of Liquefaction of Soil using SPT Data

K. SaiKiran, M. Sri Vidya and P. Dhanamma

Abstract: ***Soil liquefaction is a phenomenon whereby saturated or partially saturated loose cohesionless soil substantially losses strength and stiffness in response to a applied stress, usually earthquake shaking or other sudden change in stress condition, causing it to behave like liquid. All the structures which are built over the soil which is susceptible to Liquefaction can be damaged during an Earthquake even if they are structurally strong. As one of the most hazardous events is discussed, certain analysis for soil are to be performed to understand the behavior of soil and its stability towards such actions on different sites and determining the liquefaction susceptibility.In this paper we have analysed liquefaction potential of ten sites (2 from Visakhapatnam, 4 from Bangalore and 4 from Delhi region) as per the simplified procedure provided in Annexure-F of IS 1893-Part1(2016). This analysis will help in Liquefaction Mapping of our country (India), which finally help in preliminary understanding of liquefaction susceptibility of the site chosen for construction. Mitigation measures to reduce liquefaction susceptibility of soil such as Deep Dynamic compaction, Vibro-Compaction and Stone columns and suitability of each method are also discussed in this paper. As per our analysis Visakhapatnam is very safe, Bangalore is moderately safe and Delhi region is not safe against liquefaction.***

Keywords: soil, liquefaction

I GENERAL INTRODUCTION

A. Definition

Liquefaction is the phenomena when there is loss of strength in saturated and cohesion-less soils because of increased pore water pressures and hence reduced effective stresses due to dynamic loading. It is a phenomenon in which the strength and stiffness of a soil is reduced by earthquake shaking or other rapid loading.

Liquefaction occurs in saturated soils and saturated soils are the soils in which the space between individual particles is completely filled with water. This water exerts a pressure on the soil particles that.

C. Past records of liquefaction

Earthquakes accompanied with liquefaction have been observed for many years. In fact, written records dating back hundreds and even thousands of years have descriptions of earthquake effects that are now known to be associated with liquefaction. However, liquefaction has been so common in a number of recent earthquakes that it is often considered to be associated with them. Some of those earthquakes are

(1) Niigata, Japan (1964)
(2) Alaska, USA (1964)
(3) Loma Prieta, USA (1989)
(4) Kobe, Japan (1995)
(5) Bhuj Earthquake, India (2001)

The water pressure is however relatively low before the occurrence of earthquake. But earthquake shaking can cause the water pressure to increase to the point at which the soil particles can readily move with respect to one another.

Although earthquakes often triggers this increase in water pressure, but activities such as blasting can also cause an increase in water pressure. When liquefaction occurs, the strength of the soil decreases and the ability of a soil deposit to support the construction above it.

Soil liquefaction can also exert higher pressure on retaining walls, which can cause them to slide or tilt. This movement can cause destruction of structures on the ground surface and settlement of the retained soil.

B. Cause behind liquefaction

It is required to recognize the conditions that exist in a soil deposit before an earthquake in order to identify liquefaction. Soil is basically an assemblage of many soil particles which stay in contact with many neighboring soil. The contact forces produced by the weight of the overlying particles holds individual soil particle in its place and provide strength.

Occurrence of liquefaction is the result of rapid load application and break down of the loose and saturated sand and the loosely-packed individual soil particles tries to move into a denser configuration. However, there is not enough time for the pore-water of the soil to be squeezed out in case of earthquake. Instead, the water is trapped and prevents the soil particles from moving closer together. Thus, there is an increase in water pressure which reduces the contact forces between the individual soil particles causing softening and weakening of soil deposit. In extreme conditions, the soil particles may lose contact with each other due to the increased pore-water pressure. In such cases, the soil will have very little strength, and will behave more like a liquid than a solid - hence, the name "liquefaction".

D. Methods of reducing liquefaction hazards

There are basically three methods of reducing hazards liquefaction hazards:

1) By Avoiding Liquefaction Susceptible Soils
Construction on liquefaction susceptible soils is to be avoided. It is required to characterize the soil at a particular building site according to the various criteria available to determine the liquefaction potential of the soil in a site

2) Build Liquefaction Resistant Structures
The structure constructed should be liquefaction resistant i.e., designing the foundation elements to resist the effects of liquefaction if at all it is necessary to construct the structure on liquefiable soil because of favorable location, space restriction and other reasons.

3) Improve the Soil
This involves mitigation of the liquefaction hazards by improving the strength, density and drainage characteristics of the soil. This can be done using variety of soil improvement techniques.

II SIMPLIFIED PROCEDURE

Step 1- The subsurface data used to assess liquefaction susceptibility should include the location of the water table , either SPT blow count N or tip resistance q_c of a CPT cone or shear wave velocity V_s, unit weight and fines content of the soil (percent by weight passing the IS standard sieve no 75μ) .

Step 2- Evaluate total vertical overburden stress σ_{vo} and effective vertical overburden stress σ'_{vo} at different depths for all potentially liquefiable layers within deposit

Step 3- Evaluate stress reduction factor reducing:

r_d= 1-0.00765*Z for 0<Z<9.15m

=1.174-0.0267*Z for 9.15m<Z<23m

Where,

Z = depth in metres

Step 4 - Calculate cyclic stress ratio CSR induced by the earthquake using:

$$\mathbf{CSR = 0.65 \times (a_{max}/g) \times (\sigma_{vo}/\sigma'_{vo}) \times r_d}$$

Where,
a_{max}=peak ground acceleration preferably in terms of g,

G=acceleration due to gravity, and

R_d =stress reduction factor

If value of PGA is not available the ratioa_{max}/gmay be taken equal to seismic zone factor, Z

Siesmic Zone Factor, Z				
Zone	II	III	IV	V
Z	0.10	0.16	0.24	36

Step 5- Obtain cyclic resistance ratio CRR by correcting standard cyclic resistance $CRR_{7.5}$ for earthquake magnitude, high overburden stress level and high initial static shear strength using:

$$\mathbf{CRR=CRR_{7.5}*(MSF)*K\sigma*K\alpha}$$

Where,$CRR_{7.5}$=standard cyclic resistance ratio for 7.5 magnitude earthquake obtained using values of SPT
MSF= magnitude scaling factor given by following equation

$$\mathbf{MSF = 10^{2.24}/m_w^{2.56}}$$

This factor is required when the magnitude is different than 7.5 the correction for high overburden pressure is high and can be found using following equation

$$\mathbf{K\alpha=(\sigma'_{vo}/P_a)^{(f-1)}}$$

Where σ'_{vo} effective overburden pressure P_a atmospheric pressure are measured in the same units and f is an exponent and its value depends on the relative density D_r for D_r=40 percent ~60 percent, f=0.8~0.7 and for D_r =60 PERCENT ~80 PERCENT, f=0.7~0.6. The correction for static shear stresses Kα is required only for sloping ground and is not required in routine engineering practice. Therefore, in the scope of this standard, value of Kα shall be assumed unity.

STEP 6- Obtain cyclic resistance ratio CRR7.5

Evaluate the SPT blow count N_{60} , for a hammer efficiency of 60 percent .

$$\mathbf{(N_1)_{60} = C_N N_{60},}$$

Where,

$$\mathbf{C_N = \sqrt{(P_a / \sigma'_{vo})} \leq 1.7,}$$

The cyclic resistance ratio $CRR_{7.5}$ is estimated from fig 4.1, using $(N_1)_{60}$ and finding $(N_1)_{60cs}$ as follows :
$\mathbf{(N_1)_{60cs} = \alpha + \beta (N_1)_{60},}$

Where,
α=0 β = 1 For FC ≤5%

β= 0.99+ $FC^{1.5}$/ 1000 for 5%

and

1.2 for FC ≥ 35 %

$$\frac{1}{(N_1)_{60CS}} + \frac{(N_1)_{60CS}}{135} + \frac{50}{10\cdot(N_1)_{60CS}+45)^2} - \frac{1}{200}$$

Step 7 - Calculate the factor of safety FS against

FOS = CRR/CSR

Where CSR is as estimated in step 4 and CRR in step 5.When the design ground motion is conservative, earthquake related permanent ground deformation is generally small , if FS≥1.2.

Step 8 - if FS<1, then the soil is said to be liquef

CALCULATIONS

Dilshad Garden, Delhi.

S.No.	Depth(m)	σ(kN/m²)	σ'(kN/m²)	r_d	CSR	N_{60}	FC (%)	$(N_1)_{60CS}$	$CRR_{7.5}$	MSF	CRR	FOS	Comments
1.	2.0	37.2	37.2	0.984	0.1532	15	60.2	30.2	0.482	1.0	0.482	3.15	SAFE
2.	4.0	75.2	75.5	0.969	0.1514	28	27.5	55.5	0.359	1.0	0.359	2.37	SAFE
3.	6.0	114	114	0.954	0.1481	38	22.0	56.6	0.370	1.0	0.370	2.50	SAFE
4.	8.0	152	132	0.938	0.1686	41	56.9	43.5	0.213	1.0	0.213	1.26	SAFE
5.	10.0	189.2	149.2	0.907	0.1795	45	56.9	44.9	0.236	1.0	0.236	1.31	SAFE
6.	12.0	228.4	168.4	0.853	0.1803	59	22.0	71.3	0.496	1.0	0.496	2.75	SAFE
7.	14.0	267.6	187.6	0.800	0.1787	61	15.0	56.8	0.372	1.0	0.372	2.08	SAFE

Rohini, Delhi.

S.No.	Depth(m)	σ(kN/m²)	σ'(kN/m²)	r_d	CSR	N_{60}	FC (%)	$(N_1)_{60CS}$	$CRR_{7.5}$	MSF	CRR	FOS	Comments
1.	2.0	39.40	39.40	0.984	0.1531	16	70.2	31.2	0.594	1.0	0.594	3.88	SAFE
2.	4.0	77.71	77.71	0.969	0.1514	26	37.0	36.1	0.555	1.0	0.555	3.67	SAFE
3.	6.0	114.96	114.96	0.954	0.1487	32	18.0	35.2	0.556	1.0	0.556	3.74	SAFE
4.	8.0	153.22	153.22	0.938	0.1464	39	60.0	38.5	0.059	1.0	0.059	0.40	UNSAFE
5.	10.0	193.24	153.46	0.907	0.1570	44	56.0	40.8	0.152	1.0	0.152	0.97	UNSAFE
6.	12.0	223.00	193.00	0.853	0.1602	54	52.0	47.4	0.271	1.0	0.271	1.69	SAFE
7.	14.0	253.08	173.08	0.800	0.1822	65	12.0	52.8	0.330	1.0	0.330	1.81	SAFE

Noida Sector-1, Delhi.

S.No.	Depth(m)	σ(kN/m²)	σ'(kN/m²)	r_d	CSR	N_{60}	FC (%)	$(N_1)_{60CS}$	$CRR_{7.5}$	MSF	CRR	FOS	Comments
1.	1.5	27.1	27.1	0.9885	0.1542	10	60.2	20.9	0.227	1.0	0.227	1.47	SAFE
2.	3.0	55.0	55.0	0.9771	0.1524	18	56.9	29.9	0.461	1.0	0.461	3.02	SAFE
3.	4.5	83.3	83.3	0.9656	0.1506	19	27.5	28.2	0.377	1.0	0.377	2.50	SAFE
4.	6.0	112.4	112.4	0.9541	0.1488	14	22.0	18.4	0.196	1.0	0.196	1.32	SAFE
5.	7.5	141.5	141.5	0.9426	0.1470	20	15.0	20.3	0.219	1.0	0.219	1.49	SAFE
6.	9.0	170.8	165.8	0.9321	0.1498	28	16.5	25.9	0.311	1.0	0.311	2.08	SAFE
7.	10.5	200.5	180.5	0.8937	0.1549	32	13.6	27.1	0.341	1.0	0.341	2.20	SAFE
8.	12.0	230.2	195.2	0.8536	0.1570	47	12.2	36.5	0.134	1.0	0.134	0.85	UNSAFE
9.	13.5	260.4	210.4	0.8136	0.1571	56	12.0	41.4	0.167	1.0	0.167	1.06	SAFE
10.	15.0	290.5	225.5	0.7735	0.1554	62	12.0	44.4	0.228	1.0	0.228	1.47	SAFE

Noida Sector-6, Delhi.

S.No.	Depth(m)	σ(kN/m²)	σ'(kN/m²)	r_d	CSR	N_{60}	FC (%)	$(N_1)_{60CS}$	$CRR_{7.5}$	MSF	CRR	FOS	Comments
1.	1.5	26.3	26.1	0.9885	0.1542	6	60.5	12.7	0.138	1.0	0.138	0.89	UNSAFE
2.	3.0	54.2	54.2	0.9770	0.1524	8	60.0	13.5	0.145	1.0	0.145	0.95	UNSAFE
3.	4.5	82.1	82.1	0.9655	0.1506	7	55.5	9.8	0.111	1.0	0.111	0.74	UNSAFE
4.	6.0	110.8	110.8	0.9541	0.1488	8	40.0	9.6	0.109	1.0	0.109	0.73	UNSAFE
5.	7.5	139.9	139.9	0.9426	0.1470	12	38.0	12.7	0.138	1.0	0.138	0.94	UNSAFE
6.	9.0	169	169	0.9311	0.1498	20	35.0	18.9	0.203	1.0	0.203	1.36	SAFE
7.	10.5	198.7	183.7	0.8936	0.1507	16	32.0	18.0	0.192	1.0	0.192	1.27	SAFE
8.	12.0	228.7	198.4	0.8536	0.1532	15	20.0	14.2	0.152	1.0	0.152	0.99	UNSAFE
9.	13.5	258.1	213.1	0.8135	0.1537	17	14.0	13.1	0.142	1.0	0.142	0.92	UNSAFE
10.	15.0	288.1	228.1	0.7735	0.1524	20	12.0	13.7	0.147	1.0	0.147	0.96	UNSAFE

E. Shanthi Nagar, Bangalore.

S.No.	Depth(m)	σ(kN/m^2)	σ'(kN/m^2)	r_d	CSR	N_{60}	FC (%)	$(N_1)_{60CS}$	$CRR_{7.5}$	MSF	CRR	FOS	Comments
1	1.5	28.95	28.95	0.9885	0.0642	9	24.8	21.3	0.232	1.442	0.335	5.21	SAFE
2	3	57.45	47.45	0.9770	0.0768	5	65.9	7.4	0.091	1.442	0.131	1.71	SAFE
3	4.5	86.7	61.7	0.9655	0.0881	9	27.5	12.9	0.139	1.442	0.200	2.28	SAFE
4	6	115.5	75.5	0.9541	0.0948	7	5.0	4.5	0.068	1.442	0.098	1.03	SAFE
5	7.5	144.6	89.6	0.9426	0.0988	5	3.0	2.6	0.056	1.442	0.081	0.82	UNSAFE
6	9	173.7	103.7	0.9311	0.1013	16	2.0	7.0	0.087	1.442	0.125	1.24	SAFE

F. RK Hegde Nagar, Bangalore.

S.No.	Depth(m)	σ(kN/m^2)	σ'(kN/m^2)	r_d	CSR	N_{60}	FC (%)	$(N_1)_{60CS}$	$CRR_{7.5}$	MSF	CRR	FOS	Comments
1.	1.5	28.95	28.95	0.9885	0.0643	7	31.41	18.7	0.201	1.442	0.290	4.51	SAFE
2.	3	87.45	77.45	0.9771	0.0717	9	22.02	15.1	0.160	1.442	0.231	3.22	SAFE
3.	4.5	165.45	145.45	0.9656	0.0714	10	17	11.8	0.132	1.442	0.190	2.67	SAFE
4.	6	286.65	246.65	0.9546	0.0721	13	11	9.7	0.113	1.442	0.163	2.26	SAFE
5.	7.5	442.65	392.15	0.9426	0.0692	8	15	6.7	0.092	1.442	0.133	1.92	SAFE
6.	9	629.85	559.85	0.9321	0.0682	9	4	3.7	0.060	1.442	0.087	1.27	SAFE

G. Halasuru, Bangalore.

S.No.	Depth(m)	σ(kN/m^2)	σ''(kN/m^2)	r_d	CSR	N_{60}	FC (%)	$(N_1)_{60CS}$	$CRR_{7.5}$	MSF	CRR	FOS	Comments
1	1.5	28.95	28.95	0.9885	0.0642	9	65.4	36.4	0.150	1.442	0.216	3.37	SAFE
2	3.0	58.2	48.2	0.9770	0.0766	5	24.5	23.5	0.266	1.442	0.384	5.01	SAFE
3	4.5	87	62	0.9655	0.0880	9	4.9	17.8	0.190	1.442	0.274	3.11	SAFE
4	6.0	115.8	75.8	0.9541	0.0947	7	3.2	15.0	0.160	1.442	0.231	2.44	SAFE
5	7.5	144.6	89.6	0.9426	0.0988	5	4.6	39.3	0.100	1.442	0.144	1.46	SAFE
6	9.0	173.4	103.4	0.9311	0.1014	16	1.5	44.5	0.230	1.442	0.332	3.27	SAFE

H. Hesaragatta, Bangalore.

S.No.	Depth(m)	σ(kN/m^2)	σ'(kN/m^2)	r_d	CSR	N_{60}	FC (%)	$(N_1)_{60CS}$	$CRR_{7.5}$	MSF	CRR	FOS	Comments
1.	1.50	30	30	0.9885	0.0643	19	48	39.3	0.098	1.442	0.141	2.20	SAFE
2.	3.50	70	57	0.9732	0.0777	28	43	45.1	0.239	1.442	0.345	4.44	SAFE
3.	4.50	90	67	0.9656	0.0843	26	60	38.9	0.079	1.442	0.114	1.35	SAFE
4.	6.00	120	82	0.9541	0.0908	41	48	55.1	0.356	1.442	0.513	5.65	SAFE
5.	7.50	150	97	0.9426	0.0947	55	37	67.8	0.468	1.442	0.675	7.13	SAFE
6.	9.00	180	112	0.9312	0.0973	100	28	109.1	0.790	1.442	1.139	11.71	SAFE
7.	10.50	210	127	0.8937	0.0961	100	28	102.5	0.740	1.442	1.067	11.10	SAFE
8.	12.50	250	147	0.8403	0.0929	100	28	95.9	0.690	1.442	0.995	10.71	SAFE

I. Med. Tech. Zone, Visakhapatnam.

S.No.	Depth(m)	σ(kN/m^2)	σ'(kN/m^2)	r_d	CSR	N_{60}	FC (%)	$(N_1)_{60CS}$	$CRR_{7.5}$	MSF	CRR	FOS	Comments
1	2	39.5	39.5	0.9847	0.0640	26	43.4	50.4	0.308	1.442	0.444	6.94	SAFE
2	4	79.5	65.6	0.9694	0.0760	42	38.5	62.9	0.427	1.442	0.616	8.10	SAFE
3	5	99.6	75.6	0.9617	0.0820	48	38.6	66.7	0.459	1.442	0.662	8.07	SAFE
4	6.5	130.35	91.3	0.9502	0.0880	55	64.7	69.8	0.484	1.442	0.698	7.93	SAFE
5	8	161.1	107.1	0.9388	0.0910	62	59.5	72.6	0.507	1.442	0.731	8.03	SAFE
6	9	181.3	117.3	0.9311	0.0930	78	3.63	71.7	0.500	1.442	0.721	7.75	SAFE

J. SBI Colony, Visakhapatnam.

S.No.	Depth(m)	σ(kN/m^2)	σ'(kN/m^2)	r_d	CSR	N_{60}	FC (%)	$(N_1)_{60CS}$	$CRR_{7.5}$	MSF	CRR	FOS	Comments
1.	2.0	38.10	38.10	0.9847	0.0640	35	39	68.9	0.477	1.442	0.688	10.75	SAFE
2.	4.0	76.98	58.48	0.9694	0.0829	> 100	4.7	----	----	1.442	----	----	VERY SAFE
3.	6.5	125.56	82.06	0.9503	0.0945	63	45.9	84.4	0.600	1.442	0.865	9.16	SAFE
4.	8.0	154.13	95.53	0.9388	0.0985	71	48.7	88.2	0.631	1.442	0.910	9.24	SAFE
5.	9.0	173.66	105.16	0.9321	0.1001	78	4.6	76.4	0.538	1.442	0.776	7.75	SAFE
6.	10.0	193.66	115.16	0.9070	0.0991	> 100	4.2	----	----	1.442	----	----	VERY SAFE

Comments
SAFE
SAFE
SAFE
SAFE
UNSAFE
SAFE

Comments
SAFE
SAFE
SAFE
SAFE
SAFE
SAFE

Comments
SAFE
SAFE
SAFE
SAFE
SAFE
SAFE

Comments
SAFE
SAFE
SAFE
SAFE
SAFE
SAFE
SAFE
SAFE

Comments
SAFE
SAFE
SAFE
SAFE
SAFE
SAFE

Comments
SAFE
VERY SAFE
SAFE
SAFE
SAFE
VERY SAFE

IV. CONCLUSION

Thus it can be concluded that Visakhapatnam is very safe, Bangalore is moderately safe and Delhi region is not safe against liquefaction. Hence, from the limited studies done in this paper we may state the above but for more accurate results more bore hole log reports should beanalyzed.

Liquefaction Susceptiblesites

- Rohini, Delhi
- Sector-1Noida
- Sector-6Noida
- Shanthinagar,Bangalore

Moderately Safe sites

- Hyderpur, Delhi
- Halasuru, Bangalore
- Hesaraghatta, Bangalore
- R.K Hegdenagar, Bangalore

Very Safesites

- Med .Tech zone,Visakhapatnam
- SBI Colony,Visakhapatnam

Deep dynamic compaction should be the first option for increasing liquefaction resistance of soil if the soils fail up to 10 m deep during analysis, as it is very cheap and also it will increases the bearing capacity, reduces the settlement and reduces the substructure cost. Vibro-Compaction is preferred in pure sands. Vibro-Stone columns are suggested when there is low drainage due to presence of silts and clays in sand.

REFERENCES

1. IS 1893:Part-1(2016), Criteria for Earthquake Resistance Design of Structures.
2. IS 2131 (1981): Method for standard penetration test for soils [CED 43: Soil and Foundation Engineering]
3. "Geotechnical investigation report", Andhra Pradesh Med. Tech Zone, Visakhapatnam, Andhra Pradesh. By IDAX CONSULTING & RESEARCH PVT. LTD.
4. "Geotechnical investigation report", SBI Colony, Visakhapatnam, Andhra Pradesh. By IDAX CONSULTING & RESEARCH PVT. LTD.
5. "Geotechnical investigation report", Halasuru, Banglore. By PATIL ENGINEERS & CONTRACTORS.
6. "Geotechnical investigation report", Hesaraghatta, Banglore. By PATIL ENGINEERS & CONTRACTORS.
7. "Geotechnical investigation report", R.K. Hegde Nagar, Banglore. By PATIL ENGINEERS & CONTRACTORS.
8. "Geotechnical investigation report", Shanthi Nagar, Banglore. By PATIL ENGINEERS & CONTRACTORS.
9. "Liquefaction Hazard Assessment Using SPT and V_S for Two Cities in India", By K S RAO, Dr D NeelimaSatyam , IIT Hyderabad.
10. Sladen, J. A., D□Hollander, R. D., and Krahn, J. _1985_. „„The liquefaction of sands, a collapse surface approach.□□ Can. Geotech. J., 22, 564– 578.
11. Finn, W. L., Ledbetter, R. H., and Wu, G.: Liquefaction in silty soils: design and analysis, Ground failures under seismic conditions, Geotechnical Special Publication No 44, ASCE, Reston, 51–79, 1994
12. Castro, G., (1975) Liquefaction and cyclic mobility of saturated sands. Journal of the Geotechnical Engineering Division, ASCE, 101 (GT6), 551-569.
13. Seed, H. B. 1979. "Soil Liquefaction and Cyclic Mobility Evaluation for Level Ground During Earthquake," Journal of Geotechnical Engineering Division, ASCE, Vol 105, No. GT2, pp 201-225.
14. Selig, E.T., and Chang C.S.(1981), "soil failure modes in undrained cyclic loading" J. Geotech. Engg. Div.,ASCE, Vol.107, No.GT5, May, pp 539-551
15. Robertson, P.K.1994, "suggested terminology for liquefaction":An Internal CANLEX Report
16. Robertson, P.K.and Fear, C.E. (1996), "Soil liquefaction and its evaluation based on SPT and CPT", Liquefaction Workshop, January 1996
17. National Research Council□s Committee on Earthquake Engineering (1985) Krinitzky et al.1993
18. M. Idriss and R. W. Boulanger, "Semi-empirical Procedures for Evaluating Liquefaction Potential During Earthquakes", Proceedings of the 11th ICSDEE & 3rd ICEGE, pp 32 – 56, January 7 – 9, 2004.
19. Jin-Hung Hwangand Chin-Wen Yang, "A Practical Reliability-Based Method for Assessing Soil Liquefaction Potential", Department of Civil Engineering, National Central University.
20. Adel M. Hanna, Derin Ural and GokhanSaygili, "Evaluation of liquefaction potential of soil deposits using artificial neural networks".
21. Poulos, S.J., Castro, G., and France, W., 1985. Liquefaction evaluation procedure, J. Geotechnical Engineering Div., ASCE, Vol. 111, No.6, pp. 772-792.
22. Ishihara, K., "Liquefaction and Flow Failure during earthquakes (Rankine Lecture)". Geotechnique, 43 (3): 351-415, 1993
23. Koester, J.P. (1994) "The Influence Of Fine Type And Content On Cyclic Strength" Ground Failures Under Seismic Conditions, Geotechnical Special Publication No. 44, ASCE, pp. 17-33.
24. Robertson, P.K., Woeller, D.J. & Finn, W.D.L. 1992. Seismic cone penetration test for evaluating liquefaction potential under cyclic loading. Canadian Geotech. Jnl, 29, 686695.

AUTHORS PROFILE

1. K. SaiKiran, Matrusri Engineering College, Hyd.
   Email: Saikirankondrathi786@gmail.com
2. M. Sri Vidya, Matrusri Engineering College, Hyd
3. P. Dhanamma, Matrusri Engineering College, Hyd.

ABOUT THE INSTITUTE

Muffakham Jah College of Engineering and Technology (MJCET) was established in the year 1980 by Sultan-Ul-Uloom Education Society (SUES), which was formed by a group of visionaries and intellectuals from various walks of life. Over the past three decades, it has emerged as a premier institute, offering BE courses of four years duration in eight disciplines (Civil, ECE, CSE, IT, EEE, EIE, Mechanical & Production) and five ME courses (CAD/CAM, Structural Engineering., Digital Systems, Computers & Power Electronics) of two years duration. The current intake of all BE Courses is 780, in addition to 102 students in ME Programmes. Research Centers were started in Civil, Mechanical, EEE, CSE and ECE Departments for Doctoral Studies. The college is affiliated to Osmania University, Hyderabad and approved by AICTE, New Delhi. As per the survey of The Outlook magazine, MJCET was ranked 62nd among top 100 Engineering Colleges in India. MJCET has been ranked 47th in India among the top private institutes in Engineering by Times Engineering Institute ranking survey 2019. MJCET ranked 28th out of top 200 Engineering Colleges by India Today magazine. As per The Week Magazine, MJCET ranked 26th among the top Private Engineering Colleges in South India and 42nd among All India Private Engineering Colleges.

OVERVIEW OF THE CONFERENCE

Civil Engineering Infrastructure is the most significant factor in accelerating the pace of economic development of any country. The recent innovation and advances in the field of Civil Engineering has made a drastic impact in the Construction Industry. As the world's population increases, environmental concerns mount and Civil Engineers are entrusted by the society to achieve a sustainable world and raise the quality of life globally. The balancing of economic, social and environmental objectives now and in the future has become known as Sustainable Development and is increasingly a key driver at a range of organizational and spatial scales.

The Conference on Recent Advances in Civil Engineering Infrastructure – (RACEI-2019) aims at exploring the new horizon of innovation from distinguished researchers, eminent professionals from academia and Industry. The Conference also focuses for the achievement of relevant Sustainable Development Goals as described by United Nation Development Program. This event will be a platform to showcase and deliberate research work, studies and contributions for developing novel concepts in Civil Engineering Infrastructure. The Conference consists of keynote lectures on related themes by eminent personalities and stake holders.

BSP BS Publications
A Unit of BSP Books Pvt. Ltd.
4-4-316/309, Giriraj Lane, Sultan Bazar, Hyderabad - 500 095. (A.P.)
Ph: 040-23445688 / 605. Fax: +91-40-23445611.
e-mail: info@bspbooks.net, marketing@bspbooks.net
Website: www.bspbooks.net

ISBN : 978-93-89354-86-7

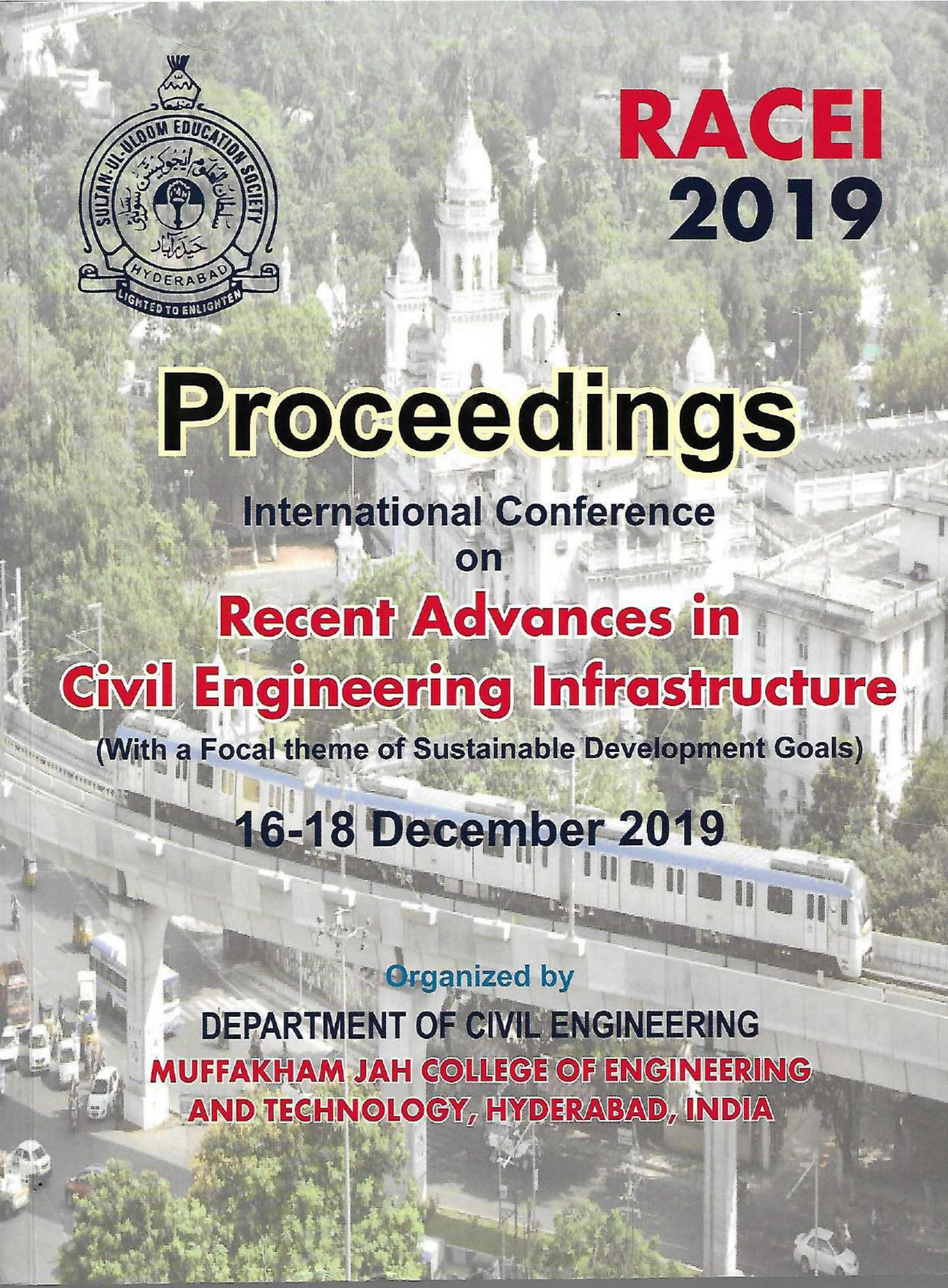

RACEI 2019

Proceedings

International Conference on

Recent Advances in Civil Engineering Infrastructure

(With a Focal theme of Sustainable Development Goals)

16-18 December 2019

Organized by

DEPARTMENT OF CIVIL ENGINEERING

MUFFAKHAM JAH COLLEGE OF ENGINEERING AND TECHNOLOGY, HYDERABAD, INDIA

Analysis of Liquefaction of Soil using SPT Data

K. SaiKiran, M. Sri Vidya and P. Dhanamma

Abstract: ***Soil liquefaction is a phenomenon whereby saturated or partially saturated loose cohesionless soil substantially losses strength and stiffness in response to a applied stress, usually earthquake shaking or other sudden change in stress condition, causing it to behave like liquid. All the structures which are built over the soil which is susceptible to Liquefaction can be damaged during an Earthquake even if they are structurally strong. As one of the most hazardous events is discussed, certain analysis for soil are to be performed to understand the behavior of soil and its stability towards such actions on different sites and determining the liquefaction susceptibility.In this paper we have analysed liquefaction potential of ten sites (2 from Visakhapatnam, 4 from Bangalore and 4 from Delhi region) as per the simplified procedure provided in Annexure-F of IS 1893-Part1(2016). This analysis will help in Liquefaction Mapping of our country (India), which finally help in preliminary understanding of liquefaction susceptibility of the site chosen for construction. Mitigation measures to reduce liquefaction susceptibility of soil such as Deep Dynamic compaction, Vibro-Compaction and Stone columns and suitability of each method are also discussed in this paper. As per our analysis Visakhapatnam is very safe, Bangalore is moderately safe and Delhi region is not safe against liquefaction.***

Keywords: soil, liquefaction

I GENERAL INTRODUCTION

A. Definition

Liquefaction is the phenomena when there is loss of strength in saturated and cohesion-less soils because of increased pore water pressures and hence reduced effective stresses due to dynamic loading. It is a phenomenon in which the strength and stiffness of a soil is reduced by earthquake shaking or other rapid loading.

Liquefaction occurs in saturated soils and saturated soils are the soils in which the space between individual particles is completely filled with water. This water exerts a pressure on the soil particles that.

C. Past records of liquefaction

Earthquakes accompanied with liquefaction have been observed for many years. In fact, written records dating back hundreds and even thousands of years have descriptions of earthquake effects that are now known to be associated with liquefaction. However, liquefaction has been so common in a number of recent earthquakes that it is often considered to be associated with them. Some of those earthquakes are

(1) Niigata, Japan (1964)
(2) Alaska, USA (1964)
(3) Loma Prieta, USA (1989)
(4) Kobe, Japan (1995)
(5) Bhuj Earthquake, India (2001)

The water pressure is however relatively low before the occurrence of earthquake. But earthquake shaking can cause the water pressure to increase to the point at which the soil particles can readily move with respect to one another.

Although earthquakes often triggers this increase in water pressure, but activities such as blasting can also cause an increase in water pressure. When liquefaction occurs, the strength of the soil decreases and the ability of a soil deposit to support the construction above it.

Soil liquefaction can also exert higher pressure on retaining walls, which can cause them to slide or tilt. This movement can cause destruction of structures on the ground surface and settlement of the retained soil.

B. Cause behind liquefaction

It is required to recognize the conditions that exist in a soil deposit before an earthquake in order to identify liquefaction. Soil is basically an assemblage of many soil particles which stay in contact with many neighboring soil. The contact forces produced by the weight of the overlying particles holds individual soil particle in its place and provide strength.

Occurrence of liquefaction is the result of rapid load application and break down of the loose and saturated sand and the loosely-packed individual soil particles tries to move into a denser configuration. However, there is not enough time for the pore-water of the soil to be squeezed out in case of earthquake. Instead, the water is trapped and prevents the soil particles from moving closer together. Thus, there is an increase in water pressure which reduces the contact forces between the individual soil particles causing softening and weakening of soil deposit. In extreme conditions, the soil particles may lose contact with each other due to the increased pore-water pressure. In such cases, the soil will have very little strength, and will behave more like a liquid than a solid - hence, the name "liquefaction".

D. Methods of reducing liquefaction hazards

There are basically three methods of reducing hazards liquefaction hazards:

1) By Avoiding Liquefaction Susceptible Soils
Construction on liquefaction susceptible soils is to be avoided. It is required to characterize the soil at a particular building site according to the various criteria available to determine the liquefaction potential of the soil in a site

2) Build Liquefaction Resistant Structures
The structure constructed should be liquefaction resistant i.e., designing the foundation elements to resist the effects of liquefaction if at all it is necessary to construct the structure on liquefiable soil because of favorable location, space restriction and other reasons.

3) Improve the Soil
This involves mitigation of the liquefaction hazards by improving the strength, density and drainage characteristics of the soil. This can be done using variety of soil improvement techniques.

II SIMPLIFIED PROCEDURE

Step 1- The subsurface data used to assess liquefaction susceptibility should include the location of the water table , either SPT blow count N or tip resistance q_c of a CPT cone or shear wave velocity V_s, unit weight and fines content of the soil (percent by weight passing the IS standard sieve no 75μ) .

Step 2- Evaluate total vertical overburden stress σ_{vo} and effective vertical overburden stress σ'_{vo} at different depths for all potentially liquefiable layers within deposit

Step 3- Evaluate stress reduction factor reducing:

r_d= 1-0.00765*Z for 0<Z<9.15m

=1.174-0.0267*Z for 9.15m<Z<23m

Where,

Z = depth in metres

Step 4 - Calculate cyclic stress ratio CSR induced by the earthquake using:

$$\mathbf{CSR = 0.65 \times (a_{max}/g) \times (\sigma_{vo}/\sigma'_{vo}) \times r_d}$$

Where,
a_{max}=peak ground acceleration preferably in terms of g,

G=acceleration due to gravity, and

R_d =stress reduction factor

If value of PGA is not available the ratioa_{max}/gmay be taken equal to seismic zone factor, Z

Siesmic Zone Factor, Z				
Zone	II	III	IV	V
Z	0.10	0.16	0.24	36

Step 5- Obtain cyclic resistance ratio CRR by correcting standard cyclic resistance $CRR_{7.5}$ for earthquake magnitude, high overburden stress level and high initial static shear strength using:

$$\mathbf{CRR=CRR_{7.5}*(MSF)*K\sigma*K\alpha}$$

Where,$CRR_{7.5}$=standard cyclic resistance ratio for 7.5 magnitude earthquake obtained using values of SPT
MSF= magnitude scaling factor given by following equation

$$\mathbf{MSF = 10^{2.24}/m_w^{2.56}}$$

This factor is required when the magnitude is different than 7.5 the correction for high overburden pressure is high and can be found using following equation

$$\mathbf{K\alpha=(\sigma'_{vo}/P_a)^{(f-1)}}$$

Where σ'_{vo} effective overburden pressure P_a atmospheric pressure are measured in the same units and f is an exponent and its value depends on the relative density D_r for D_r=40 percent ~60 percent, f=0.8~0.7 and for D_r =60 PERCENT ~80 PERCENT, f=0.7~0.6. The correction for static shear stresses Kα is required only for sloping ground and is not required in routine engineering practice. Therefore, in the scope of this standard, value of Kα shall be assumed unity.

STEP 6- Obtain cyclic resistance ratio CRR7.5

Evaluate the SPT blow count N_{60} , for a hammer efficiency of 60 percent .

$$\mathbf{(N_1)_{60} = C_N N_{60},}$$

Where,

$$\mathbf{C_N = \sqrt{(P_a / \sigma'_{vo})} \leq 1.7,}$$

The cyclic resistance ratio $CRR_{7.5}$ is estimated from fig 4.1, using $(N_1)_{60}$ and finding $(N_1)_{60cs}$ as follows :
$\mathbf{(N_1)_{60cs} = \alpha + \beta (N_1)_{60},}$

Where,
α=0 β = 1 For FC ≤5%

[illegible] $\beta = 0.99 + FC^{1.5}/1000$ for 5%

[illegible] and

[illegible] $\beta = 1.2$ for $FC \geq 35$ %

[illegible] $\frac{1}{(N1)_{60CS}} + \frac{(N1)_{60CS}}{135} + \frac{50}{10\cdot(N1)_{60CS}+45)^2} - \frac{1}{200}$

[illegible] calculate the factor of safety FS against

[illegible]

FOS = CRR/CSR

Where CSR is as estimated in step 4 and CRR in step 5.When the design ground motion is conservative, earthquake related permanent ground deformation is generally small , if FS≥1.2.

Step 8 - if FS<1, then the soil is said to be liquef

III CALCULATIONS

A. **Shahdara, Delhi.**

[illegible]	Depth(m)	σ(kN/m^2)	σ'(kN/m^2)	r_d	CSR	N_{60}	FC (%)	$(N_1)_{60CS}$	$CRR_{7.5}$	MSF	CRR	FOS	Comments
[illegible]	[illegible]0	37.2	37.2	0.984	0.1532	15	60.2	30.2	0.482	1.0	0.482	3.15	SAFE
[illegible]	[illegible]0	75.2	75.5	0.969	0.1514	28	27.5	55.5	0.359	1.0	0.359	2.37	SAFE
[illegible]	6.0	114	114	0.954	0.1481	38	22.0	56.6	0.370	1.0	0.370	2.50	SAFE
[illegible]	[illegible]0	152	132	0.938	0.1686	41	56.9	43.5	0.213	1.0	0.213	1.26	SAFE
[illegible]	10.0	189.2	149.2	0.907	0.1795	45	56.9	44.9	0.236	1.0	0.236	1.31	SAFE
[illegible]	12.0	228.4	168.4	0.853	0.1803	59	22.0	71.3	0.496	1.0	0.496	2.75	SAFE
[illegible]	14.0	267.6	187.6	0.800	0.1787	61	15.0	56.8	0.372	1.0	0.372	2.08	SAFE

B. **Rohini, Delhi.**

[illegible] No.	Depth(m)	σ(kN/m^2)	σ'(kN/m^2)	r_d	CSR	N_{60}	FC (%)	$(N_1)_{60CS}$	$CRR_{7.5}$	MSF	CRR	FOS	Comments
[illegible]	2.0	39.40	39.40	0.984	0.1531	16	70.2	31.2	0.594	1.0	0.594	3.88	SAFE
[illegible]	4.0	77.71	77.71	0.969	0.1514	26	37.0	36.1	0.555	1.0	0.555	3.67	SAFE
[illegible]	6.0	114.96	114.96	0.954	0.1487	32	18.0	35.2	0.556	1.0	0.556	3.74	SAFE
[illegible]	8.0	153.22	153.22	0.938	0.1464	39	60.0	38.5	0.059	1.0	0.059	0.40	UNSAFE
[illegible]	10.0	193.24	153.46	0.907	0.1570	44	56.0	40.8	0.152	1.0	0.152	0.97	UNSAFE
[illegible]	12.0	223.00	193.00	0.853	0.1602	54	52.0	47.4	0.271	1.0	0.271	1.69	SAFE
[illegible]	14.0	253.08	173.08	0.800	0.1822	65	12.0	52.8	0.330	1.0	0.330	1.81	SAFE

C. **Noida Sector-1, Delhi.**

[illegible] S.No.	Depth(m)	σ(kN/m^2)	σ'(kN/m^2)	r_d	CSR	N_{60}	FC (%)	$(N_1)_{60CS}$	$CRR_{7.5}$	MSF	CRR	FOS	Comments
[illegible]	1.5	27.1	27.1	0.9885	0.1542	10	60.2	20.9	0.227	1.0	0.227	1.47	SAFE
[illegible]	3.0	55.0	55.0	0.9771	0.1524	18	56.9	29.9	0.461	1.0	0.461	3.02	SAFE
[illegible]	4.5	83.3	83.3	0.9656	0.1506	19	27.5	28.2	0.377	1.0	0.377	2.50	SAFE
[illegible]	6.0	112.4	112.4	0.9541	0.1488	14	22.0	18.4	0.196	1.0	0.196	1.32	SAFE
[illegible]	7.5	141.5	141.5	0.9426	0.1470	20	15.0	20.3	0.219	1.0	0.219	1.49	SAFE
[illegible]	9.0	170.8	165.8	0.9321	0.1498	28	16.5	25.9	0.311	1.0	0.311	2.08	SAFE
[illegible]	10.5	200.5	180.5	0.8937	0.1549	32	13.6	27.1	0.341	1.0	0.341	2.20	SAFE
[illegible]	12.0	230.2	195.2	0.8536	0.1570	47	12.2	36.5	0.134	1.0	0.134	0.85	UNSAFE
[illegible]	13.5	260.4	210.4	0.8136	0.1571	56	12.0	41.4	0.167	1.0	0.167	1.06	SAFE
[illegible]	15.0	290.5	225.5	0.7735	0.1554	62	12.0	44.4	0.228	1.0	0.228	1.47	SAFE

D. **Noida Sector-6, Delhi.**

S.No.	Depth(m)	σ(kN/m^2)	σ'(kN/m^2)	r_d	CSR	N_{60}	FC (%)	$(N_1)_{60CS}$	$CRR_{7.5}$	MSF	CRR	FOS	Comments
1.	1.5	26.3	26.1	0.9885	0.1542	6	60.5	12.7	0.138	1.0	0.138	0.89	UNSAFE
2.	3.0	54.2	54.2	0.9770	0.1524	8	60.0	13.5	0.145	1.0	0.145	0.95	UNSAFE
3.	4.5	82.1	82.1	0.9655	0.1506	7	55.5	9.8	0.111	1.0	0.111	0.74	UNSAFE
4.	6.0	110.8	110.8	0.9541	0.1488	8	40.0	9.6	0.109	1.0	0.109	0.73	UNSAFE
5.	7.5	139.9	139.9	0.9426	0.1470	12	38.0	12.7	0.138	1.0	0.138	0.94	UNSAFE
6.	9.0	169	169	0.9311	0.1498	20	35.0	18.9	0.203	1.0	0.203	1.36	SAFE
7.	10.5	198.7	183.7	0.8936	0.1507	16	32.0	18.0	0.192	1.0	0.192	1.27	SAFE
8.	12.0	228.7	198.4	0.8536	0.1532	15	20.0	14.2	0.152	1.0	0.152	0.99	UNSAFE
9.	13.5	258.1	213.1	0.8135	0.1537	17	14.0	13.1	0.142	1.0	0.142	0.92	UNSAFE
10.	15.0	288.1	228.1	0.7735	0.1524	20	12.0	13.7	0.147	1.0	0.147	0.96	UNSAFE

E. Shanthi Nagar, Bangalore.

S.No.	Depth(m)	σ(kN/m^2)	σ'(kN/m^2)	r_d	CSR	N_{60}	FC (%)	$(N_1)_{60CS}$	$CRR_{7.5}$	MSF	CRR	FOS	Comments
1	1.5	28.95	28.95	0.9885	0.0642	9	24.8	21.3	0.232	1.442	0.335	5.21	SAFE
2	3	57.45	47.45	0.9770	0.0768	5	65.9	7.4	0.091	1.442	0.131	1.71	SAFE
3	4.5	86.7	61.7	0.9655	0.0881	9	27.5	12.9	0.139	1.442	0.200	2.28	SAFE
4	6	115.5	75.5	0.9541	0.0948	7	5.0	4.5	0.068	1.442	0.098	1.03	SAFE
5	7.5	144.6	89.6	0.9426	0.0988	5	3.0	2.6	0.056	1.442	0.081	0.82	UNSAFE
6	9	173.7	103.7	0.9311	0.1013	16	2.0	7.0	0.087	1.442	0.125	1.24	SAFE

F. RK Hegde Nagar, Bangalore.

S.No.	Depth(m)	σ(kN/m^2)	σ'(kN/m^2)	r_d	CSR	N_{60}	FC (%)	$(N_1)_{60CS}$	$CRR_{7.5}$	MSF	CRR	FOS	Comments
1.	1.5	28.95	28.95	0.9885	0.0643	7	31.41	18.7	0.201	1.442	0.290	4.51	SAFE
2.	3	87.45	77.45	0.9771	0.0717	9	22.02	15.1	0.160	1.442	0.231	3.22	SAFE
3.	4.5	165.45	145.45	0.9656	0.0714	10	17	11.8	0.132	1.442	0.190	2.67	SAFE
4.	6	286.65	246.65	0.9546	0.0721	13	11	9.7	0.113	1.442	0.163	2.26	SAFE
5.	7.5	442.65	392.15	0.9426	0.0692	8	15	6.7	0.092	1.442	0.133	1.92	SAFE
6.	9	629.85	559.85	0.9321	0.0682	9	4	3.7	0.060	1.442	0.087	1.27	SAFE

G. Halasuru, Bangalore.

S.No.	Depth(m)	σ(kN/m^2)	σ''(kN/m^2)	r_d	CSR	N_{60}	FC (%)	$(N_1)_{60CS}$	$CRR_{7.5}$	MSF	CRR	FOS	Comments
1	1.5	28.95	28.95	0.9885	0.0642	9	65.4	36.4	0.150	1.442	0.216	3.37	SAFE
2	3.0	58.2	48.2	0.9770	0.0766	5	24.5	23.5	0.266	1.442	0.384	5.01	SAFE
3	4.5	87	62	0.9655	0.0880	9	4.9	17.8	0.190	1.442	0.274	3.11	SAFE
4	6.0	115.8	75.8	0.9541	0.0947	7	3.2	15.0	0.160	1.442	0.231	2.44	SAFE
5	7.5	144.6	89.6	0.9426	0.0988	5	4.6	39.3	0.100	1.442	0.144	1.46	SAFE
6	9.0	173.4	103.4	0.9311	0.1014	16	1.5	44.5	0.230	1.442	0.332	3.27	SAFE

H. Hesaragatta, Bangalore.

S.No.	Depth(m)	σ(kN/m^2)	σ'(kN/m^2)	r_d	CSR	N_{60}	FC (%)	$(N_1)_{60CS}$	$CRR_{7.5}$	MSF	CRR	FOS	Comments
1.	1.50	30	30	0.9885	0.0643	19	48	39.3	0.098	1.442	0.141	2.20	SAFE
2.	3.50	70	57	0.9732	0.0777	28	43	45.1	0.239	1.442	0.345	4.44	SAFE
3.	4.50	90	67	0.9656	0.0843	26	60	38.9	0.079	1.442	0.114	1.35	SAFE
4.	6.00	120	82	0.9541	0.0908	41	48	55.1	0.356	1.442	0.513	5.65	SAFE
5.	7.50	150	97	0.9426	0.0947	55	37	67.8	0.468	1.442	0.675	7.13	SAFE
6.	9.00	180	112	0.9312	0.0973	100	28	109.1	0.790	1.442	1.139	11.71	SAFE
7.	10.50	210	127	0.8937	0.0961	100	28	102.5	0.740	1.442	1.067	11.10	SAFE
8.	12.50	250	147	0.8403	0.0929	100	28	95.9	0.690	1.442	0.995	10.71	SAFE

I. Med. Tech. Zone, Visakhapatnam.

S.No.	Depth(m)	σ(kN/m^2)	σ'(kN/m^2)	r_d	CSR	N_{60}	FC (%)	$(N_1)_{60CS}$	$CRR_{7.5}$	MSF	CRR	FOS	Comments
1	2	39.5	39.5	0.9847	0.0640	26	43.4	50.4	0.308	1.442	0.444	6.94	SAFE
2	4	79.5	65.6	0.9694	0.0760	42	38.5	62.9	0.427	1.442	0.616	8.10	SAFE
3	5	99.6	75.6	0.9617	0.0820	48	38.6	66.7	0.459	1.442	0.662	8.07	SAFE
4	6.5	130.35	91.3	0.9502	0.0880	55	64.7	69.8	0.484	1.442	0.698	7.93	SAFE
5	8	161.1	107.1	0.9388	0.0910	62	59.5	72.6	0.507	1.442	0.731	8.03	SAFE
6	9	181.3	117.3	0.9311	0.0930	78	3.63	71.7	0.500	1.442	0.721	7.75	SAFE

J. SBI Colony, Visakhapatnam.

S.No.	Depth(m)	σ(kN/m^2)	σ'(kN/m^2)	r_d	CSR	N_{60}	FC (%)	$(N_1)_{60CS}$	$CRR_{7.5}$	MSF	CRR	FOS	Comments
1.	2.0	38.10	38.10	0.9847	0.0640	35	39	68.9	0.477	1.442	0.688	10.75	SAFE
2.	4.0	76.98	58.48	0.9694	0.0829	> 100	4.7	----	----	1.442	----	----	VERY SAFE
3.	6.5	125.56	82.06	0.9503	0.0945	63	45.9	84.4	0.600	1.442	0.865	9.16	SAFE
4.	8.0	154.13	95.53	0.9388	0.0985	71	48.7	88.2	0.631	1.442	0.910	9.24	SAFE
5.	9.0	173.66	105.16	0.9321	0.1001	78	4.6	76.4	0.538	1.442	0.776	7.75	SAFE
6.	10.0	193.66	115.16	0.9070	0.0991	> 100	4.2	----	----	1.442	----	----	VERY SAFE

Comments
SAFE
SAFE
SAFE
SAFE
UNSAFE
SAFE

Comments
SAFE
SAFE
SAFE
SAFE
SAFE
SAFE

Comments
SAFE
SAFE
SAFE
SAFE
SAFE
SAFE

Comments
SAFE
SAFE
SAFE
SAFE
SAFE
SAFE
SAFE
SAFE

Comments
SAFE
SAFE
SAFE
SAFE
SAFE
SAFE

Comments
SAFE
VERY SAFE
SAFE
SAFE
SAFE
VERY SAFE

IV. CONCLUSION

Thus it can be concluded that Visakhapatnam is very safe, Bangalore is moderately safe and Delhi region is not safe against liquefaction. Hence, from the limited studies done in this paper we may state the above but for more accurate results more bore hole log reports should beanalyzed.

Liquefaction Susceptiblesites

- Rohini, Delhi
- Sector-1Noida
- Sector-6Noida
- Shanthinagar,Bangalore

Moderately Safe sites

- Hyderpur, Delhi
- Halasuru, Bangalore
- Hesaraghatta, Bangalore
- R.K Hegdenagar, Bangalore

Very Safesites

- Med .Tech zone,Visakhapatnam
- SBI Colony,Visakhapatnam

Deep dynamic compaction should be the first option for increasing liquefaction resistance of soil if the soils fail up to 10 m deep during analysis, as it is very cheap and also it will increases the bearing capacity, reduces the settlement and reduces the substructure cost. Vibro-Compaction is preferred in pure sands. Vibro-Stone columns are suggested when there is low drainage due to presence of silts and clays in sand.

REFERENCES

1. IS 1893:Part-1(2016), Criteria for Earthquake Resistance Design of Structures.
2. IS 2131 (1981): Method for standard penetration test for soils [CED 43: Soil and Foundation Engineering]
3. "Geotechnical investigation report", Andhra Pradesh Med. Tech Zone, Visakhapatnam, Andhra Pradesh. By IDAX CONSULTING & RESEARCH PVT. LTD.
4. "Geotechnical investigation report", SBI Colony, Visakhapatnam, Andhra Pradesh. By IDAX CONSULTING & RESEARCH PVT. LTD.
5. "Geotechnical investigation report", Halasuru, Banglore. By PATIL ENGINEERS & CONTRACTORS.
6. "Geotechnical investigation report", Hesaraghatta, Banglore. By PATIL ENGINEERS & CONTRACTORS.
7. "Geotechnical investigation report", R.K. Hegde Nagar, Banglore. By PATIL ENGINEERS & CONTRACTORS.
8. "Geotechnical investigation report", Shanthi Nagar, Banglore. By PATIL ENGINEERS & CONTRACTORS.
9. "Liquefaction Hazard Assessment Using SPT and V_S for Two Cities in India", By K S RAO, Dr D NeelimaSatyam , IIT Hyderabad.
10. Sladen, J. A., D□Hollander, R. D., and Krahn, J. _1985_. „„The liquefaction of sands, a collapse surface approach.□□ Can. Geotech. J., 22, 564– 578.
11. Finn, W. L., Ledbetter, R. H., and Wu, G.: Liquefaction in silty soils: design and analysis, Ground failures under seismic conditions, Geotechnical Special Publication No 44, ASCE, Reston, 51–79, 1994
12. Castro, G., (1975) Liquefaction and cyclic mobility of saturated sands. Journal of the Geotechnical Engineering Division, ASCE, 101 (GT6), 551-569.
13. Seed, H. B. 1979. "Soil Liquefaction and Cyclic Mobility Evaluation for Level Ground During Earthquake," Journal of Geotechnical Engineering Division, ASCE, Vol 105, No. GT2, pp 201-225.
14. Selig, E.T., and Chang C.S.(1981), "soil failure modes in undrained cyclic loading" J. Geotech. Engg. Div.,ASCE, Vol.107, No.GT5, May, pp 539-551
15. Robertson, P.K.1994, "suggested terminology for liquefaction":An Internal CANLEX Report
16. Robertson, P.K.and Fear, C.E. (1996), "Soil liquefaction and its evaluation based on SPT and CPT", Liquefaction Workshop, January 1996
17. National Research Council□s Committee on Earthquake Engineering (1985) Krinitzky et al.1993
18. M. Idriss and R. W. Boulanger, "Semi-empirical Procedures for Evaluating Liquefaction Potential During Earthquakes", Proceedings of the 11th ICSDEE & 3rd ICEGE, pp 32 – 56, January 7 – 9, 2004.
19. Jin-Hung Hwangand Chin-Wen Yang, "A Practical Reliability-Based Method for Assessing Soil Liquefaction Potential", Department of Civil Engineering, National Central University.
20. Adel M. Hanna, Derin Ural and GokhanSaygili, "Evaluation of liquefaction potential of soil deposits using artificial neural networks".
21. Poulos, S.J., Castro, G., and France, W., 1985. Liquefaction evaluation procedure, J. Geotechnical Engineering Div., ASCE, Vol. 111, No.6, pp. 772-792.
22. Ishihara, K., "Liquefaction and Flow Failure during earthquakes (Rankine Lecture)". Geotechnique, 43 (3): 351-415, 1993
23. Koester, J.P. (1994) "The Influence Of Fine Type And Content On Cyclic Strength" Ground Failures Under Seismic Conditions, Geotechnical Special Publication No. 44, ASCE, pp. 17-33.
24. Robertson, P.K., Woeller, D.J. & Finn, W.D.L. 1992. Seismic cone penetration test for evaluating liquefaction potential under cyclic loading. Canadian Geotech. Jnl, 29, 686695.

AUTHORS PROFILE

1. K. SaiKiran, Matrusri Engineering College, Hyd.
   Email: Saikirankondrathi786@gmail.com
2. M. Sri Vidya, Matrusri Engineering College, Hyd
3. P. Dhanamma, Matrusri Engineering College, Hyd.

ABOUT THE INSTITUTE

Muffakham Jah College of Engineering and Technology (MJCET) was established in the year 1980 by Sultan-Ul-Uloom Education Society (SUES), which was formed by a group of visionaries and intellectuals from various walks of life. Over the past three decades, it has emerged as a premier institute, offering BE courses of four years duration in eight disciplines (Civil, ECE, CSE, IT, EEE, EIE, Mechanical & Production) and five ME courses (CAD/CAM, Structural Engineering., Digital Systems, Computers & Power Electronics) of two years duration. The current intake of all BE Courses is 780, in addition to 102 students in ME Programmes. Research Centers were started in Civil, Mechanical, EEE, CSE and ECE Departments for Doctoral Studies. The college is affiliated to Osmania University, Hyderabad and approved by AICTE, New Delhi. As per the survey of The Outlook magazine, MJCET was ranked 62nd among top 100 Engineering Colleges in India. MJCET has been ranked 47th in India among the top private institutes in Engineering by Times Engineering Institute ranking survey 2019. MJCET ranked 28th out of top 200 Engineering Colleges by India Today magazine. As per The Week Magazine, MJCET ranked 26th among the top Private Engineering Colleges in South India and 42nd among All India Private Engineering Colleges.

OVERVIEW OF THE CONFERENCE

Civil Engineering Infrastructure is the most significant factor in accelerating the pace of economic development of any country. The recent innovation and advances in the field of Civil Engineering has made a drastic impact in the Construction Industry. As the world's population increases, environmental concerns mount and Civil Engineers are entrusted by the society to achieve a sustainable world and raise the quality of life globally. The balancing of economic, social and environmental objectives now and in the future has become known as Sustainable Development and is increasingly a key driver at a range of organizational and spatial scales.

The Conference on Recent Advances in Civil Engineering Infrastructure – (RACEI-2019) aims at exploring the new horizon of innovation from distinguished researchers, eminent professionals from academia and Industry. The Conference also focuses for the achievement of relevant Sustainable Development Goals as described by United Nation Development Program. This event will be a platform to showcase and deliberate research work, studies and contributions for developing novel concepts in Civil Engineering Infrastructure. The Conference consists of keynote lectures on related themes by eminent personalities and stake holders.

BSP BS Publications
A Unit of BSP Books Pvt. Ltd.
4-4-316/309, Giriraj Lane, Sultan Bazar, Hyderabad - 500 095. (A.P.)
Ph: 040-23445688 / 605. Fax: +91-40-23445611.
e-mail: info@bspbooks.net, marketing@bspbooks.net
Website: www.bspbooks.net

ISBN : 978-93-89354-86-7

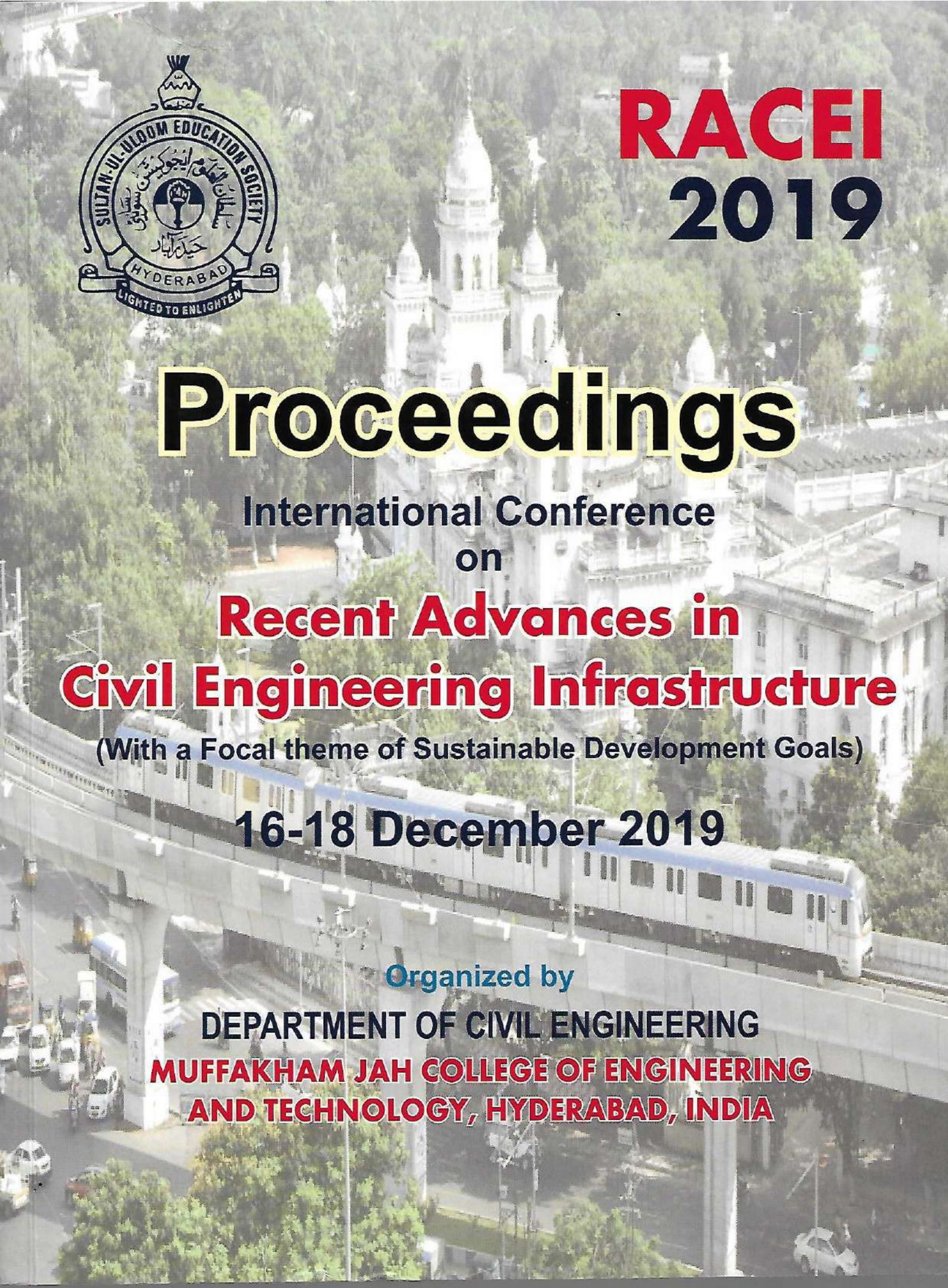

RACEI 2019

Proceedings

International Conference on

Recent Advances in Civil Engineering Infrastructure

(With a Focal theme of Sustainable Development Goals)

16-18 December 2019

Organized by

DEPARTMENT OF CIVIL ENGINEERING

MUFFAKHAM JAH COLLEGE OF ENGINEERING AND TECHNOLOGY, HYDERABAD, INDIA

A Review on Light Weight Vermiculite Concrete

M Preethi, P Ashveen Kumar and Mohd. Hamraj

Abstract: ***Concrete is most using material in the world. In Concrete aggregate occupies nearly 80%. Most of the aggregates of normal weight Concrete are natural stone such as granite, Lime stone and fine aggregate sand. Light weight aggregate capable for concrete may be regular materials such as pumice or scoria, or they may be prepared aggregates such as expanded clays, shale's, slates and slag's. Vermiculite is an aggregate that is created when volcanic rock is heated to intense temperatures. It is being a granular expanded aggregate with numerous air voids, when mixed with suitable binder develops lighter structure and sound insulating properties. In recent years research is going on light weight vermiculite materials as replacement for fine and course aggregate in concrete. In this paper an attempt is made to gather all the studies made on light weight vermiculite concrete in the recent years and put together at one place.***

Keywords: - cement, fine aggregate, coarse aggregate, fly ash, silica fume, vermiculite, GGBFS

I. INTRODUCTION

There is rapid growth in construction all over the world which demands development in concrete with new materials to reduce dead weight of structural elements with light weight aggregates. Light weight concrete is generally obtained by incorporating light weight aggregate like Pumice, expanded clay, Perlite, Dolamite, Vermiculite. The specific weight of aggregate less than 1120kg/m3 are generally considered as light weight; in some cases 90 to 900kg/m^3 are also obtained. The bulk weight weight of vermiculite ranges from 60 to 130kg/m^3. The concrete with weight less than 1800kg/m^3 are
Considered as light weight concrete. The density of vermiculite concretes are from 400 to 900kg/m^3.

As compared to conventional concrete light weight concrete shows good features like low density, thermal insulation, permeability, sound insulation, reduction in dead weight. Due to their lower density, the demand of light weight concrete is increasing, which makes reduction of cross sections of structural elements.
Vermiculite is a natural occurring material and is composed through the disintegration of mica. It is a micaceous mineral that expands many times (nearly 30) when heated to 650-1000° C. The Chemical composition is made with complex compound of hydrated aluminum and magnesium silica. The expanded vermiculite is consists of low bulk density, and thermal conductivity but high refractoriness.

light weight concrete is used with vermiculite as replacement to coarse aggregate and fine aggregate and also usage of mineral ad mixtures like fly ash and silica fume makes the light weight vermiculate concrete best suitable. To gain strength.

II. LIGHT WEIGHT CONCRETE USING VERMICULITE

S. Jyothi Manjula, G. VijayMano, J. Sundar Prabu, M. PrabanjanS.Pradeep(2018)This work presents the experimental testing of light weight self compacting concrete.(LWSCC) for M_{30} grade of concrete using pumice stone, expanded perlite, exfoliated vermiculite test were conducted on hardened concrete for compressive, split tensile, flexural, and impact and also on fresh concrete for Slump test, flow test, vee-bee consistometer, compaction factor tests were done. Further self-compacting concrete for M_{30} the proportion of coarse aggregate is replaced by pumice stone, vermiculate and perlite at vartions of 2.5%, 5%, 7.5%, 10%, 12.5% and 15%it was found that the light weight aggregate replacement for coarse aggregate with percentage like 2.5% to 15%.from 2.5% to 7.5 % replacement given good results. But beyond 7.5% has reduced the mechanical properties when compared with conventional concrete.

M.V.S.S. Sastry, P. Ashveen Kumar, K. Jagannadha Rao (2018) In this experimental study, properties of M_{20} concrete with different percentages from range of 0-100% at an increment of 20% as partly replacement with vermiculite to the total weight of fine aggregate along with mineral additives like Ultra fine Fly ash (UFA) and micro silica (SF) is partially replaced with cement by percentages i.e., from 5-15%, and Micro silica (SF) at 5%, 10% and 15% by weight of cement. The compressive strength at all duration is decreasing due to the replacement of Exfoliated Vermiculite (EV), but an economical design was obtained with 20% replacement to sand.

T. Subramani, M. Meghnathan S. Priyanka (2017) this paper presents investigation on Fiber Reinforced High Strength Concrete, using recycled aggregate for 20% and40% replacement of coarse aggregate for M_{30} grade of concrete with replacement of natural sand with vermiculite mineral with varying percentages. And 1% steel fibers is also used and compared with conventional concrete casted using plastic fibers. all the specimens are tested for 28 days using cubes and cylinders and tested the compressive strength,

split tensile strength and workability. Investigation resulted that strength of vermiculite concrete although decreased but was increased using super plasticizer and usage of vermiculite had given less density proving to be suitable for light weight structures.

A.V.V. Sairam, K. Sailaja (2017)This paper presents Mechanical Properties onM_{35} grade concrete mix for varying percentages with 5%,10%15%20% 25% and 30% replacement with vermiculite to fine aggregate and fly ash to replace cement with varying percentages of10%15% and20%and silica fume as additive to cement with varying percentages of 5%7.5%10% and12.5%with constant w/c ratio of 0.42 and it was found that10% of silica fume and 15% flyash and 5%vermiculite has given optimum increase in compressive strength whereas10%silicafume and 10%flyash with 5%vermiculite has given increase in split tensile strength compare to concrete with no vermiculite.

Ramapradheep. G.S, M. Sivaraja (2017) This paper presents Experimental studies on self compacting self curing concrete using light weight aggregate for M_{40} grade using 5%,10% LECA as and 5%,10% replacement to fine aggregate and test was conducted using cubes and cylinders the workability and properties improved for 10% LECA and 10% vermiculate as a partial replacement of fine aggregate .

Thangam D, Geetha. V (2017) this paper presents Experimental studies on self curing concrete for M_{20} grade using vermiculite and GGBFS 50% of ggbfs as replacement to cement and vermiculite with diff variations of 20%,40%,60% and80% with fine aggregate and it was found that 20% replacement with fine aggregate and 50% ggbfs replacement to cement used for casting of self curing concrete has given good strength. With usage of poly ethylene glycol as self curing agent.

S. Syed Abdul Rahman, Gijo. K. Babu (2016) the paper presents about M_{30} grade of concrete to know variation in density of concrete with and without vermiculite. For constant w/c ratio of 0.40 for different variation 0%, 5% and10% of replacement of natural sand with vermiculite powder and it was found that there is a decrease in strength with the increase in vermiculite but decrease in density from 2486 to 2167 kgs/m^3 with proves that use of vermiculite decrease the self weight of concrete with slight decrease in compressive strength.

M. R. Divya, Prof. M. Rajalingam, Dr. Sunilaa George (2016) This paper presents study of M_{30} grade concrete mechanical properties experimental set up were done by replacing fine aggregate with vermiculite passing through 2.36mm sieve by 40%,50%and60%by weight it was found that concrete mix with replacement with 40% vermiculite has given increase in compressive strength, split tensile strength and flexural strength alternately indicates use of high percentage of vermiculite that is beyond 40% as replacement to fine aggregate reduce the strength.

Chandraseker.G., Hemanth Kumar.Ch., V. Manikantha, Simhachalam, (2016) this paper investigated on comparia of compressive strength and density of concrete betwe light weight concrete and convention concrete using cub for different concrete mix proportions of1:1:1(c:s:v) water cement ratio of 0.6,1 :1:2(c:s:v)for water cement ra of 0.65,1:5(c:v)) for water cement ratio1.6125 for differ variation with replacement of fine aggregate 100%,50%,33%, and cement is replaced with fly a 0%10%20%and30% and tested for 7,14,and28days it w found that 20%replacement of cement with fly ash a 33%replacement of fine aggregate with vermiculite h given optimum increase in compressive strength with lo density comparatively with conventional concrete.

Rashad Alaa M (2016) gave an extensive review of about th Exfoliated vermiculite (EV) which exhibits differe properties like low thermal conductivity, low bulk densit endurance, chemical inertness and comparatively hig melting point. EV has effective use in the field of civi engineering, chemical and agriculture fields. In thi overview, the author summarized the previous studies usin EV as a constructive material in existing cementiciou materials, geopolymers and binders.

Chandra et al. (2016) studied the replacement of the fin aggregate to the material named vermiculite. It belongs t the lightweight aggregates. The exfoliated vermiculite i made for replacement of fine aggregate. This project i mostly related to places whose temperature is very high. The Replacements are done with 5, 10 and 15% of the fin aggregate. The authors concluded that the Vermiculite replaced concrete shows a valuable decrease in density up t 15% as compared to normal concrete. In split tensile test no much variation in split tensile strength was observed i compared to standard concrete.

Yuvraj Chavdaa, Shilpa Kewate (2015) The paper investigated the study of vermiculite as a replacement o nominal aggregate and its use as a light weight concrete. The test was conducted according to BIS codes to determine the suitableness of the vermiculite for structural and non-structural application with fractional replacement of up to 25% of cement. The cement-vermiculite samples could not meet the required strength for structural applications. The strength and other properties framed from Bureau of Indian Standards(BIS) for non-structural materials like wise flooring tiles, solid blocks, pavement blocks, and bricks. Economic feasible study is to be done for further research.

P. Santosh Murugan Dr. M. Devesene Dr. R. Venkatasubramani (2015) The paper presents study to determine the mechanical features of M_{25} light weight concrete with vermiculite. In this experimental study vermiculite was used for both fine aggregate and coarse aggregate in two different concrete mixes. The vermiculite is of low density which minimizes the entire density of the

concrete and hence makes light weight concrete. The strength properties of both the mixes were examined. The concrete binding material was completely replaced with vermiculite. Test samples proved that the Fine aggregate replacement has given better result than coarse aggregate.

Fuat Koksal (2012) the experimental investigation has been done to know the suitability of vermiculite for cement in concrete. The study of effect with replace of vermiculite to cement in order to increase the compressive strength of concrete. Two experimental groups were prepared with the variations' replacement of percentages 0%, 5%, and 10%.The results proved that effect of vermiculite on concrete has a appreciable increase in compressive strength. Which indicates that Light weight concrete is widely suitable to reduce self-weight of element with an increase in strength as compared to conventional concrete?

III. CONCLUSIONS

From this review study for various experimental investigations conducted for different concrete mixes following conclusions are made.

1. Vermiculite is good replacement for fine aggregate rather than coarse aggregate.
2. Vermiculite with replacement up to 20% to fine aggregate gives optimum increase in mechanical properties
3. Vermiculite with replacement to fine aggregate and the mineral additives like silica fume, fly ash, micro silica ggbfs as replacement to cement do resemble properties of self compacting concrete, and self curing concrete with low density which in turn reduce dead weight of structures.
4. Vermiculite as replacement can be used up to M_{30} grade concrete. With addition of super plasticizer.
5. Vermiculite is also suitable for roof and floor insulation

Mrs M.Preethi is working as Asst. Professor in Deccan college of Engineering and Technology, Hyderabad. She is having 11 years of teaching and 2 years of industry experience. Her interest area is High strength concrete, Light weight concrete , Vermiculate concrete
E mail : preethi.sreerang@gmail.com

Mr P.Ashveen Kumar is working as Asst. Professor in Matrusri Engineering college , Hyderabad. He is having 23 years of teaching and 2 years of industry experience. His interest area is Engineering Mechanics,High strength concrete, Light weight concrete , Vermiculate concrete.

Dr. Mohd.Hamraj has been working as Professor and H.O.D., C.E.D, in M.J. college of Engineering and Technology, Hyderabad with 22 years of teaching and 3Years industry experience having more than 33 publications. Presently Supervising 8 research scholars and guided more than 25 M.E. projects succeecfully.

IV. REFERENCES

1.M.V.S.S.Sastri, P. Ashveen Kumar and K. Jagannadha Rao "Experimental Investigation on Strength Properties of Ultrafine Fly ash and Micro Silica as Mineral Admixtures for Vermiculate Mortar ",(2019) under publication in i-manager's Journal on Journal on Material Science (JMS) .
2. A. Azad, S.F. Mousavi, H. Karami, and S. Farzin, "Using Waste Vermiculite and Dolomite as Eco-Friendly Additives for Improving the Performance of Porous Concrete", Eng. J., vol. 22, (2018).
3. S. Jyothi Manjula, G. VijayMano, J. Sundar Prabu, M. Prabanjan S. Pradeep "Structural
And Impact Behaviors Of Light Weight Self-Compacting Concrete." The Asian Review of Civil Engineering ISSN Vol. 7 (2018)
4.T.Subramani, M. Meganathan, S. Priyanka , " Experimental Study On Strength Properties Of Diaphanous Concrete With Vermiculite " , International Journal of Application or Innovation in Engineering & Management , Vol.6.(2017)
5. A.V.V Sairam and K Sailaja " An Experimental Study on Strength Properties of Vermiculite Concrete Using Flyash as Partially Replacement of Cement and Silica Fume as Mineral Admixture" , International Research Journal of Engineering and Technology, Vol. 4(2017)
6. Thangam D., Geetha.V "Effect Of Vermiculite and GGBFS On Concrete By Self Curing Parameter" International Journal of Advances in Engineering Research (IJAER) Vol.13 (2017)
7. Rampradheep G. S., M. Sivaraja "Experimental Investigation on Self-Compacting, Self-Curing Concrete Incorporated with the Light Weight Aggregates" Brazilian. Archives. Biology Technology. ISSN 1678-4324vol.59 (2017)
8. Chandraseker.G., Hemanth Kumar.Ch., V. Manikantha,
M. Simhachalam., "Effect of Flyash on Mechanical Properties of Light Weight Vermiculite Concrete." International Journal of Innovative Research in Science, Engineering and Technology.Vol.5 (2016)
9. Rashad, Alaa M. "Vermiculite as a construction material–A short guide for Civil Engineer." Construction and Building Materials (2016)
10.P.santoshmuruganDr.M.Devesene Dr.R.Venkatasubramani "An Experimental Study On Strength Properties Of The Diaphanous Concrete With Vermiculite." International Journal Of Applied Engineering Research. Vol.10 (2015)
11. Yuvraj Chavdaa, Shilpa Kewate "Use of vermiculite for light weight floating concrete" International Journal of Scientific & Engineering Research, Vol.6, Issue ISSN 2229-5518 (2015)
12. Fuat Koksal "Effect Of High Temperature on Mechanical and Physical Properties of Lightweight Cement Based Refractory Including Expanded Vermiculite", Journal of Materials Research Innovations, Vol. 16, (2012)

ABOUT THE INSTITUTE

Muffakham Jah College of Engineering and Technology (MJCET) was established in the year 1980 by Sultan-Ul-Uloom Education Society (SUES), which was formed by a group of visionaries and intellectuals from various walks of life. Over the past three decades, it has emerged as a premier institute, offering BE courses of four years duration in eight disciplines (Civil, ECE, CSE, IT, EEE, EIE, Mechanical & Production) and five ME courses (CAD/CAM, Structural Engineering., Digital Systems, Computers & Power Electronics) of two years duration. The current intake of all BE Courses is 780, in addition to 102 students in ME Programmes. Research Centers were started in Civil, Mechanical, EEE, CSE and ECE Departments for Doctoral Studies. The college is affiliated to Osmania University, Hyderabad and approved by AICTE, New Delhi. As per the survey of The Outlook magazine, MJCET was ranked 62nd among top 100 Engineering Colleges in India. MJCET has been ranked 47th in India among the top private institutes in Engineering by Times Engineering Institute ranking survey 2019. MJCET ranked 28th out of top 200 Engineering Colleges by India Today magazine. As per The Week Magazine, MJCET ranked 26th among the top Private Engineering Colleges in South India and 42nd among All India Private Engineering Colleges.

OVERVIEW OF THE CONFERENCE

Civil Engineering Infrastructure is the most significant factor in accelerating the pace of economic development of any country. The recent innovation and advances in the field of Civil Engineering has made a drastic impact in the Construction Industry. As the world's population increases, environmental concerns mount and Civil Engineers are entrusted by the society to achieve a sustainable world and raise the quality of life globally. The balancing of economic, social and environmental objectives now and in the future has become known as Sustainable Development and is increasingly a key driver at a range of organizational and spatial scales.

The Conference on Recent Advances in Civil Engineering Infrastructure – (RACEI-2019) aims at exploring the new horizon of innovation from distinguished researchers, eminent professionals from academia and Industry. The Conference also focuses for the achievement of relevant Sustainable Development Goals as described by United Nation Development Program. This event will be a platform to showcase and deliberate research work, studies and contributions for developing novel concepts in Civil Engineering Infrastructure. The Conference consists of keynote lectures on related themes by eminent personalities and stake holders.

BSP BS Publications
A Unit of BSP Books Pvt. Ltd.
4-4-316/309, Giriraj Lane, Sultan Bazar, Hyderabad - 500 095. (A.P.)
Ph: 040-23445688 / 605. Fax: +91-40-23445611.
e-mail: info@bspbooks.net, marketing@bspbooks.net
Website: www.bspbooks.net

ISBN : 978-93-89354-86-7

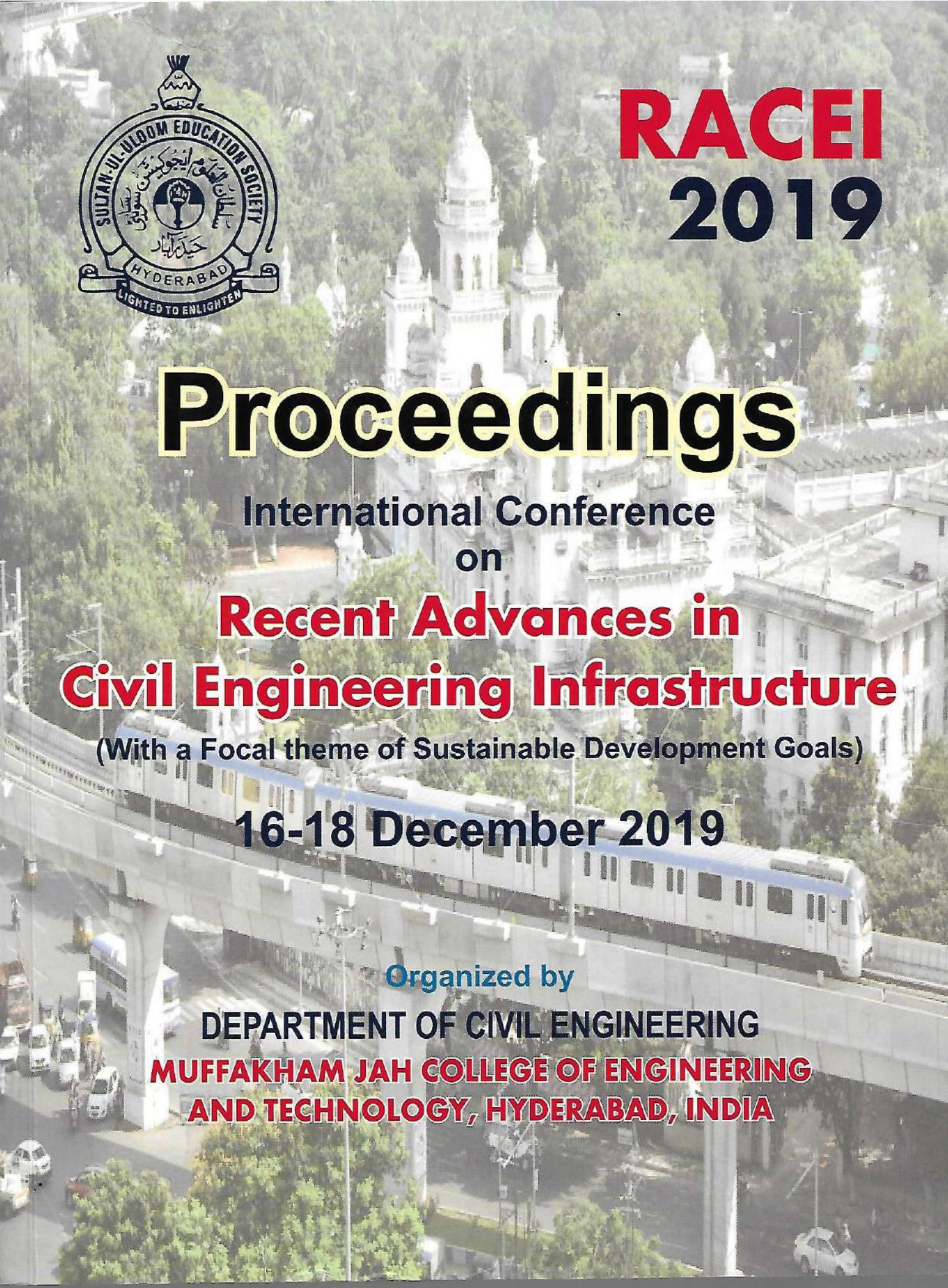

RACEI 2019

Proceedings

International Conference on

Recent Advances in Civil Engineering Infrastructure

(With a Focal theme of Sustainable Development Goals)

16-18 December 2019

Organized by

DEPARTMENT OF CIVIL ENGINEERING

MUFFAKHAM JAH COLLEGE OF ENGINEERING AND TECHNOLOGY, HYDERABAD, INDIA

Evaluation Studies of Existing Aqueduct on Kalwakurthy Main Canal of Mahatma Gandhi Lift Irrigation Scheme in Mahabubnagar District

S. Lokeswari, T Raja Ramanna, M Pratibha and K.V.R. Satya Sai

Abstract: To provide irrigation facility to an extent of 3.65 lakhs acres in drought prone areas of Wanaparthy, Nagarkurnool and Mahabubnagar Districts by lifting 25 TMC from Foreshore of Srisailam Reservoir. The Scheme is intended to provide drinking water to the enroute villages for 1 TMC covering about (336) villages in erstwhile talukas of Kollapur, Nagarkurnool, Achampet, Jadcherla, Wanaparthy and Kalwakurthy constituencies (in 24 mandal). From foreshore of Srisailam Reservoir to Stage-I pumping station, an approach channel of length of 1.60 km is excavated. The water is pumped into Yellur Balancing Reservoir (YBR) of 0.35 TMC for serving canals for an ayacut of 70,000 acres as well as to Singotam Balancing Reservoir (SBR) of 0.55 TMC up to Stage-II. This pumping station, lifts 2.14 TMC of water to Jonnala boguda (JBBR) to serve for an ayacut of 1,80,000 acres and to Stage-III 90,000 acres respectively. This pumping station, lifts water to Gudipalli Gattu Balancing Reservoir (GGBR) of 0.96 TMC.

For the irrigation purpose, this water is utilized for the last 2 to 3 years. The water supply is for one crop only. For efficient irrigation network, it is proposed to identify local ponds for collection and usage of return flow from agriculture fields up to 15 to 20% and there by the irrigation efficiency could be increased by 20%.

Keywords: Balancing Reservoir, Approach Channel, Lift Irrigation, Rainfall.

I. INTRODUCTION

Mahatma Gandhi Kalwakurthy lift irrigation project (KLIP) is a lift irrigation project on River Krishna located in Mahabubnagar district in Telangana, India. The lift canal starts from the back waters of Srisailam Dam near Kollapur. The gravity driven, 100 Km canal provides cultivation for nearly 4,00,000 acres in 300 villages located in constituencies of Kollapur, Wanaparthy, Nagarkurnool, Kalwakurthy, Jadcherla and Achampet.

The Kalwakurthy Lift Irrigation Scheme foundation stone was laid way back in 1984. It was started again in 2005 but delayed again. In August 2014 the work started with a spending of □2100 crores and completed in October 2017. It took a little over three decades to be completed.

The original design for the project was 25 TMC water capacity, but later it was increased to 40 TMC to reach the prescribed target. This project provides water to the most drought prone areas in Mahabubnagar. The water is sourced from Krishna river, by lifting water 300 meters above river level and channeling into the reservoir.

II. NESESSITY OF CROSS DRAINAGE WORKS

A cross drainage work (also called CD work) is a structure built on a canal where it is crosses a natural drainage, such as a stream or a river. Sometimes, a cross-drainage work is required when the canal crosses another canal. The cross-drainage work is required to dispose of the drainage water so that the canal supply remains uninterrupted. A cross-drainage work also called as drainage crossing or the canal at a crossing. However, it is not possible to avoid the CDW in the initial reach of a main canal because it takes off from a diversion head works (or storage works) located on a river which is a valley.

The scheme consists of 4 balancing reservoirs at

1. Yellur
2. Singotam
3. Jonnalaboguda
4. GudiipallyGattu

Table 1: Study Area

Location :	**Foreshore of Srisailam Reservoir at Regumangadda, Yellur (V), Kollapur (M)**		
Source:	Krishna River	Sub Basin:	Upper Krishna
Latitude:	16^0 25' North	Longitude:	78^0 16' East

Table 2: Components

S.No	Description	
1.	Lifts	3 Nos
2.	Proposed Balancing Reservoirs	4 Nos
3.	Approach Channel	1.60 km
4.	Tunnels	10.96 km
5.	Pressure Main	1.60 km
6.	Gravity Canal	29 km

Table 3: Pump House & Tunnel Details (Lift Wise)

S. No	Description	Stage		
		I	II	III
1	Location	YBR	JBBR	GGBR
2	Height of lift	95	86	117
3	No of Pump Houses	5	5	5
4	Capacity of Each Pump	30	30	30
5	Discharge of Each Pump	800	800	650
6	Total Power Required	150	150	150

Table 4: Reservoir Details

	Location	Reguman	Singotam	Jonnalabo guda	Narsaipally
2	Latitude	16^0	$16^0$10' N	$16^0$16' N	$16^0$25' N
3	Longitude	78^0	$78^0$16' E	78^0 16' E	$16^0$25' E
4	Capacity	0.35	0.55	2.14	$78^0$16' E
5	Ayacut	13000		43,300	0.98
6	FRL	+338.00	+338.00	+407.00	+283.800
7	MDDL	+332.00			+492.500
8	TBL	+341.5	+337.68	+410.00	+504.5
9	Capacity in TMC	0.35	0.55	2.14	0.96

Tunnel Details

Table 5: Earth Bund Details

1	Length of Tunnel	0.50km	4.33km	6.15km
2	Dia of Tunnel	7m	6.85m	6.85m
3	Shape of Tunnel	Horse shoe	D-type	D-type

S.No	Earth Bund				
1	Length of Earth Bund at top (R/S)	1.68	1.4	1.7	3.45
2	Top Width	6	6	6	6
3	No. of Berms	1	1	2	2

Table 6: Irrigation Potential (in Acres)

S. No	District	No of Mandals	Ayacut in Acres
1	Nagarkurnool	14	268165
2	Wanaparthy	6	78000
3	Mahabubnagar	2	9015
4	Shamshabad	2	9820
Total		24	365000

Table 7: Land Acquisition / R&R

S. No	Description	Required	Acquired	Balance
1	Forest area in Acres	84	84	-
2	Government land in Acres	591	591	-
3	Private land	1498	1361	135
	Total	2171	2171	135

III. DESIGN OF WELL FOUNDATION – FOR ABUTMENT

Abutment top width = 15 m
Abutment bottom width = 3 m
Outer diameter of well, D = 5 m
Thickness of well staining = 0.75m
Inner diameter of well, d = 3.5m
Diameter of well of well curb = 51m
Depth of top plug, p1 = 0.5 m
Depth of bottom plug, p2 = 0.5m
Height of curb, 2t = 1.5m
Coefficient of active pressure (Rankine's) = 0.275
Bed level = 477.585

Proposing M20 grade concrete & Fe 415 Steel

MFL = 480.960 m
LWL = 477.966 m
HFL = 480.95 m
Scour level = 470.658 m
Proposed grip length = 3.600 m
Proposed well foundation top level = 476.466 m
Proposed well foundation bottom level = 467.068 m
Density of water = 1.000 t/m^3
Density of soil = 1.800 t/m^3
Destiny of RCC concrete = 2.400 t/m^3
Active earth pressure coefficient under normal condition = 0.275 = 2.500 t/m^2
Passive earth pressure coefficient under normal condition = 7.333
Design is carried by trail end correction method
Height of active earth pressure = 10.508 m

Height of passive earth pressure	=	3.600 m
Outer dia. of well	=	5.000 m
Internal dia. of well	=	3.500 m
Thickness of well staining	=	0.750 m

Design of Pier

No of vents for canal	=	2 Nos
Clear width of each vent	=	4.4 m
Thickness of walls	=	3 m
FSD of canal	=	3 m
FB	=	0.6 m
Clear span between the piers	=	15.0 m
Overall width of canal trough	=	10 m
Road width	=	4.25 m
Road level	=	+485.001
Height of kerb	=	0.225 m
Top level of pier above bed level	=	+480.20 m
MFL of drain	=	480.950 m
Bearing capacity of soil	=	50 t/sqm
Ht of side wall to bottom of road slab	=	4.075 m
Thickness of trough bottom slab	=	0.4 m
Thickness of road slab	=	0.45 m
W.C over road slab	=	0.075 m
W.C over trough slab	=	0.075 m
Bottom level of Foundation`	=	+475.466
Thickness of pier	=	1.50 m
Top level of foundation	=	+476.466
thickness of bed block	=	0.45 m
foundation offset in x direction	=	1.75 m
foundation offset in y Direction	=	1.75 m
semi circular cut and ease	=	0.75 m
maximum velocity in river	=	2.92 m/s (as per MFLs)
thickness of railing	=	0.2 m
ht of rail in	=	0.425 m

Design Of U/S & D/S Bridge Abutments

Span in between bearings	=	9.20 m
Dead load transferred from the super structure	=	573.95 KN
Live load + impact	=	236.23 KN
Length of the abutment	=	5 m
Proposed depth of the abutment	=	7.686 m
Impact factor percentage	=	0.5-7.686/3*0.5
Load coming on to the abutment	=	810.18 KN
Load coming on to the abutment per meter length	=	810.18/5.1= 159 KN
Total depth from deck slab top to bearing bottom	=	0.85 m
Horizontal force due to breaking effect	=	20% of LL 364*20% = 72.8 KN
Total horizontal force	=	36 KN
Hence correction to vertical reaction	=	72.8*(0.85+1.2)/9.2 = 16.2 KN
Horizontal load coming on to the abutment	=	36.40 KN
Horizontal load on the abutment per meter length	=	36.4/5.1 = 8 KN
Depth of beam portion	=	0.775 m
Thickness of wearing coat	=	0.775 m
Thickness of approach slab	=	0.15 m
Front batter adopted	=	1 in 100000
Top width	=	1 m
Bottom width	=	5.2 mm
Thickness of expansion joint	=	20 mm
Off-set of foundation	=	0.6 m
Depth of footing	=	0.6 m
Distance of bearing reaction	=	0.49 m/s
Reaction due to beam	=	142.778 KN
Width of dirt wall	=	0.49 m
Depth of bed block	=	225 mm
Angle of internal friction	=	32
Bulk density of soil	=	21 KN/m^3
Bulk density of concrete	=	24 KN/m^3
Hr breaking force	=	8 KN
Live load equivalent surcharge	=	1.2m

IV. CONCLUSION(S)

From the above analysis, the following conclusions are arrived:

In respect of design of trough for a discharge of 38.966 cumecs
By applying head loss theory, it is found to be satisfactory.
Size of the trough = 4.4*3.0 m.
Head loss provided is 0.20 m.
The velocity in this trough is as follows:
Area = 4.4*3.0 = 13.20 sqm
Velocity = 38.966/13.20 = 3 m/sec
Froude number $F_N = V/\sqrt{gd} = 3/\sqrt{10} * 3 = 0.6 < 1$
Hence critical flow and design is ok.
In respect of drain system the maximum discharge provided is Max Q = 2833 cumecs
This could be arrived by one of the following formulae
Catchment = 1108 sqkm

Dicken's formulae
$Q = CA^{3/4}$
For central India
C = 14 to 20

Number of piers	=	22
Abutments	=	2

Number of spans = 23
Deepest B.L = 477.782 m
Max FSL = 481.197 m
Depth of flow = 3.21 m

The flood discharge provided seems to be pk.

The maximum flood occurred in 2009 and the same max flood level was observed.

It is to be noted down that once in a way, there is a scope of occurring the max flood level in 25, 50, 75, 100 years and the discharge through the drains vents will be under pressure flow.

Hence care should be taken during monsoon season since there will be uplift pressure, causing for the canal trough causing break down.

In fact, in other seasons, the flow through the vents of drain are normal and sub critical flow ranging 2 m to 4 m/sec.

Since this system is functioning well for the last 2 to 3 years, the designs parameters provide are up to the mark.

All the foundations are taken up to S D R for piers and abutments. The total Depth taken below bed of stream has shown as below.

Deepest stream bed = 478.835 – 465.645 = 13.09 m. no tension is induced.

Hence safe.

V. REFERENCES

[1]. Central Design Organization (2004); Design Process Manual of Gates. Outlets, Canal Structures and Head Works.:

[2]. IS 3370 PART - 1, PART – 2.

[3]. IRC 5, IRC-6, IRC-21, IRC-78, IRC-83.

[4]. Indian Standard: IS 7331: (200 I). 'Code of Practice for Inspection and Maintenance of Cross Drainage Works'.

[5]. Indian Standard: IS 7784 (Part I) (1993). 'Design of Cross Drainage Works - Code of Practice: Part-I General Features'.

[6]. Indian Standard: IS 7784 (Part 2/Sec I) (1995). 'Design of Cross Drainage Works -Code of Practice: Part-2 Specific Requirements, Section 1: Aqueduct'.

[7]. Indian Standard: IS 800 (2007). 'Code of Practice General Construction in Steel.

[8]. Modi PN (2008). 'Irrigation Water Resources and Water Power Engineering'· Standard Book House, Delhi.

[9]. Public Works Departments' Handbook: Chapter: 18 'Hydraulics' (1983).

[10]. Punmia BC, Panda BBL Ashok KJ, Arun KJ (2009)

AUTHOR PROFILE

S. Lokeswari
Asst. Prof., Dept. of Civil Engineering, Matrusri Engineering College, Hyderabad, Telangana.
sankaralokeswari@gmail.com

T Raja Ramanna
Asst. Prof., Dept. of Civil Engineering, Matrusri Engineering College, Hyderabad, Telangana.
t.rajaramanna@gmail.com,

M Pratibha
Asst. Prof., Dept. of Civil Engineering, Matrusri Engineering College, Hyderabad, Telangana.
pratibhagundepally@gmail.com

K.V.R.Satya Sai
Assoc. Prof., Dept. of Civil Engineering, TKR College of Engineering & Technology, Hyderabad, Telangana
kvr.satya.sai@gmail.com

ABOUT THE INSTITUTE

Muffakham Jah College of Engineering and Technology (MJCET) was established in the year 1980 by Sultan-Ul-Uloom Education Society (SUES), which was formed by a group of visionaries and intellectuals from various walks of life. Over the past three decades, it has emerged as a premier institute, offering BE courses of four years duration in eight disciplines (Civil, ECE, CSE, IT, EEE, EIE, Mechanical & Production) and five ME courses (CAD/CAM, Structural Engineering., Digital Systems, Computers & Power Electronics) of two years duration. The current intake of all BE Courses is 780, in addition to 102 students in ME Programmes. Research Centers were started in Civil, Mechanical, EEE, CSE and ECE Departments for Doctoral Studies. The college is affiliated to Osmania University, Hyderabad and approved by AICTE, New Delhi. As per the survey of The Outlook magazine, MJCET was ranked 62nd among top 100 Engineering Colleges in India. MJCET has been ranked 47th in India among the top private institutes in Engineering by Times Engineering Institute ranking survey 2019. MJCET ranked 28th out of top 200 Engineering Colleges by India Today magazine. As per The Week Magazine, MJCET ranked 26th among the top Private Engineering Colleges in South India and 42nd among All India Private Engineering Colleges.

OVERVIEW OF THE CONFERENCE

Civil Engineering Infrastructure is the most significant factor in accelerating the pace of economic development of any country. The recent innovation and advances in the field of Civil Engineering has made a drastic impact in the Construction Industry. As the world's population increases, environmental concerns mount and Civil Engineers are entrusted by the society to achieve a sustainable world and raise the quality of life globally. The balancing of economic, social and environmental objectives now and in the future has become known as Sustainable Development and is increasingly a key driver at a range of organizational and spatial scales.

The Conference on Recent Advances in Civil Engineering Infrastructure – (RACEI-2019) aims at exploring the new horizon of innovation from distinguished researchers, eminent professionals from academia and Industry. The Conference also focuses for the achievement of relevant Sustainable Development Goals as described by United Nation Development Program. This event will be a platform to showcase and deliberate research work, studies and contributions for developing novel concepts in Civil Engineering Infrastructure. The Conference consists of keynote lectures on related themes by eminent personalities and stake holders.

BSP BS Publications
A Unit of BSP Books Pvt. Ltd.
4-4-316/309, Giriraj Lane, Sultan Bazar, Hyderabad - 500 095. (A.P.)
Ph: 040-23445688 / 605. Fax: +91-40-23445611.
e-mail: info@bspbooks.net, marketing@bspbooks.net
Website: www.bspbooks.net

ISBN : 978-93-89354-86-7

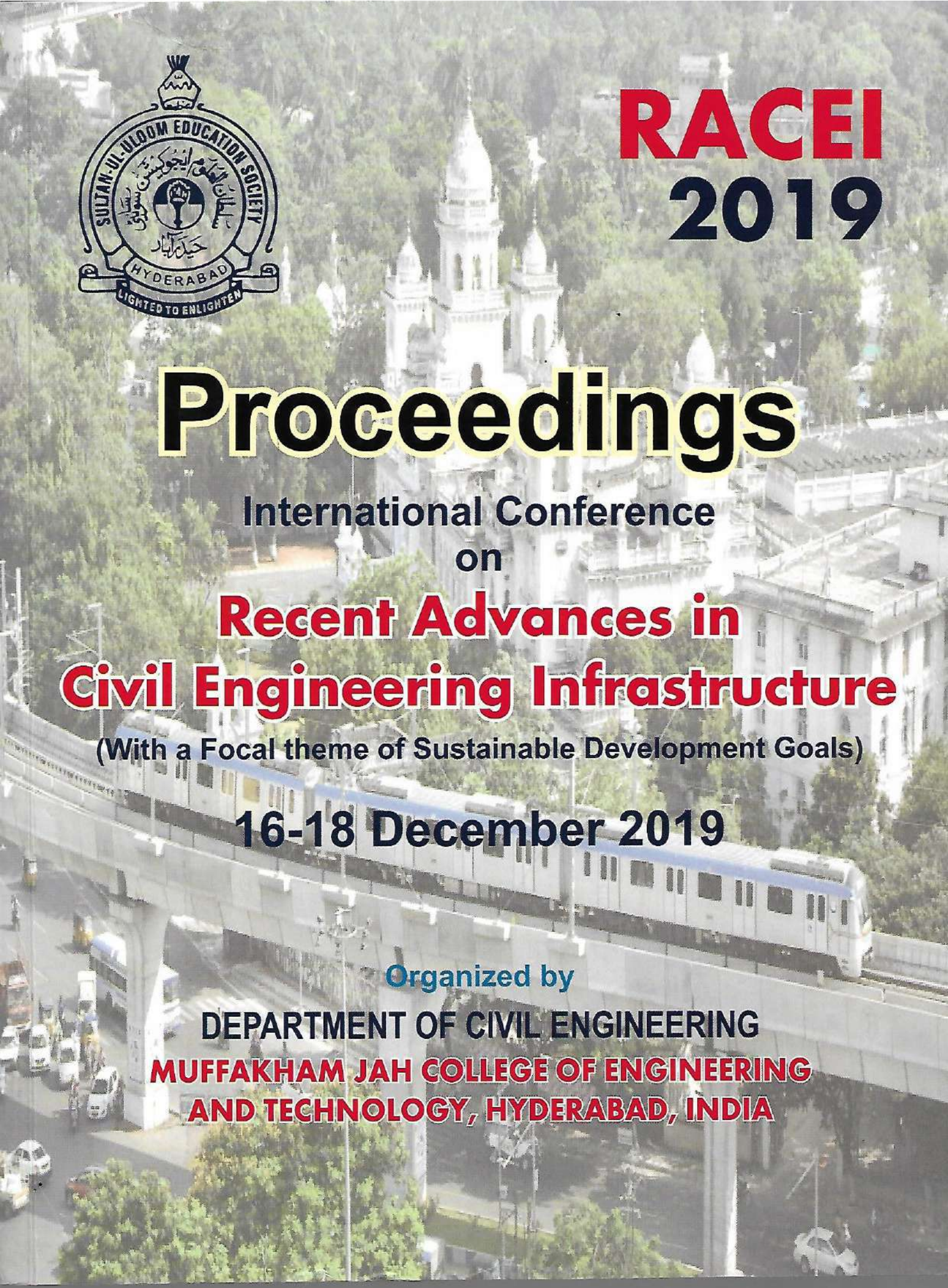

RACEI 2019

Proceedings

International Conference on

Recent Advances in Civil Engineering Infrastructure

(With a Focal theme of Sustainable Development Goals)

16-18 December 2019

Organized by

DEPARTMENT OF CIVIL ENGINEERING

MUFFAKHAM JAH COLLEGE OF ENGINEERING AND TECHNOLOGY, HYDERABAD, INDIA

Evaluation Studies of Existing Aqueduct on Kalwakurthy Main Canal of Mahatma Gandhi Lift Irrigation Scheme in Mahabubnagar District

S. Lokeswari, T Raja Ramanna, M Pratibha and K.V.R. Satya Sai

Abstract: To provide irrigation facility to an extent of 3.65 lakhs acres in drought prone areas of Wanaparthy, Nagarkurnool and Mahabubnagar Districts by lifting 25 TMC from Foreshore of Srisailam Reservoir. The Scheme is intended to provide drinking water to the enroute villages for 1 TMC covering about (336) villages in erstwhile talukas of Kollapur, Nagarkurnool, Achampet, Jadcherla, Wanaparthy and Kalwakurthy constituencies (in 24 mandal). From foreshore of Srisailam Reservoir to Stage-I pumping station, an approach channel of length of 1.60 km is excavated. The water is pumped into Yellur Balancing Reservoir (YBR) of 0.35 TMC for serving canals for an ayacut of 70,000 acres as well as to Singotam Balancing Reservoir (SBR) of 0.55 TMC up to Stage-II. This pumping station, lifts 2.14 TMC of water to Jonnala boguda (JBBR) to serve for an ayacut of 1,80,000 acres and to Stage-III 90,000 acres respectively. This pumping station, lifts water to Gudipalli Gattu Balancing Reservoir (GGBR) of 0.96 TMC.

For the irrigation purpose, this water is utilized for the last 2 to 3 years. The water supply is for one crop only. For efficient irrigation network, it is proposed to identify local ponds for collection and usage of return flow from agriculture fields up to 15 to 20% and there by the irrigation efficiency could be increased by 20%.

Keywords: Balancing Reservoir, Approach Channel, Lift Irrigation, Rainfall.

I. INTRODUCTION

Mahatma Gandhi Kalwakurthy lift irrigation project (KLIP) is a lift irrigation project on River Krishna located in Mahabubnagar district in Telangana, India. The lift canal starts from the back waters of Srisailam Dam near Kollapur. The gravity driven, 100 Km canal provides cultivation for nearly 4,00,000 acres in 300 villages located in constituencies of Kollapur, Wanaparthy, Nagarkurnool, Kalwakurthy, Jadcherla and Achampet.

The Kalwakurthy Lift Irrigation Scheme foundation stone was laid way back in 1984. It was started again in 2005 but delayed again. In August 2014 the work started with a spending of □2100 crores and completed in October 2017. It took a little over three decades to be completed.

The original design for the project was 25 TMC water capacity, but later it was increased to 40 TMC to reach the prescribed target. This project provides water to the most drought prone areas in Mahabubnagar. The water is sourced from Krishna river, by lifting water 300 meters above river level and channeling into the reservoir.

II. NESESSITY OF CROSS DRAINAGE WORKS

A cross drainage work (also called CD work) is a structure built on a canal where it is crosses a natural drainage, such as a stream or a river. Sometimes, a cross-drainage work is required when the canal crosses another canal. The cross-drainage work is required to dispose of the drainage water so that the canal supply remains uninterrupted. A cross-drainage work also called as drainage crossing or the canal at a crossing. However, it is not possible to avoid the CDW in the initial reach of a main canal because it takes off from a diversion head works (or storage works) located on a river which is a valley.

The scheme consists of 4 balancing reservoirs at

1. Yellur
2. Singotam
3. Jonnalaboguda
4. GudiipallyGattu

Table 1: Study Area

Location :	**Foreshore of Srisailam Reservoir at Regumangadda, Yellur (V), Kollapur (M)**		
Source:	Krishna River	Sub Basin:	Upper Krishna
Latitude:	16^0 25' North	Longitude:	78^0 16' East

Table 2: Components

S.No	Description	
1.	Lifts	3 Nos
2.	Proposed Balancing Reservoirs	4 Nos
3.	Approach Channel	1.60 km
4.	Tunnels	10.96 km
5.	Pressure Main	1.60 km
6.	Gravity Canal	29 km

Table 3: Pump House & Tunnel Details (Lift Wise)

S. No	Description	Stage		
		I	II	III
1	Location	YBR	JBBR	GGBR
2	Height of lift	95	86	117
3	No of Pump Houses	5	5	5
4	Capacity of Each Pump	30	30	30
5	Discharge of Each Pump	800	800	650
6	Total Power Required	150	150	150

Table 4: Reservoir Details

	Location	Reguman	Singotam	Jonnalabo guda	Narsaipally
2	Latitude	16^0	$16^0$10' N	$16^0$16' N	$16^0$25' N
3	Longitude	78^0	$78^0$16' E	78^0 16' E	$16^0$25' E
4	Capacity	0.35	0.55	2.14	$78^0$16' E
5	Ayacut	13000		43,300	0.98
6	FRL	+338.00	+338.00	+407.00	+283.800
7	MDDL	+332.00			+492.500
8	TBL	+341.5	+337.68	+410.00	+504.5
9	Capacity in TMC	0.35	0.55	2.14	0.96

Tunnel Details

Table 5: Earth Bund Details

1	Length of Tunnel	0.50km	4.33km	6.15km
2	Dia of Tunnel	7m	6.85m	6.85m
3	Shape of Tunnel	Horse shoe	D-type	D-type

S.No	Earth Bund				
1	Length of Earth Bund at top (R/S)	1.68	1.4	1.7	3.45
2	Top Width	6	6	6	6
3	No. of Berms	1	1	2	2

Table 6: Irrigation Potential (in Acres)

S. No	District	No of Mandals	Ayacut in Acres
1	Nagarkurnool	14	268165
2	Wanaparthy	6	78000
3	Mahabubnagar	2	9015
4	Shamshabad	2	9820
Total		24	365000

Table 7: Land Acquisition / R&R

S. No	Description	Required	Acquired	Balance
1	Forest area in Acres	84	84	-
2	Government land in Acres	591	591	-
3	Private land	1498	1361	135
	Total	2171	2171	135

III. DESIGN OF WELL FOUNDATION – FOR ABUTMENT

Abutment top width = 15 m
Abutment bottom width = 3 m
Outer diameter of well, D = 5 m
Thickness of well staining = 0.75m
Inner diameter of well, d = 3.5m
Diameter of well of well curb = 51m
Depth of top plug, p1 = 0.5 m
Depth of bottom plug, p2 = 0.5m
Height of curb, 2t = 1.5m
Coefficient of active pressure (Rankine's) = 0.275
Bed level = 477.585

Proposing M20 grade concrete & Fe 415 Steel

MFL = 480.960 m
LWL = 477.966 m
HFL = 480.95 m
Scour level = 470.658 m
Proposed grip length = 3.600 m
Proposed well foundation top level = 476.466 m
Proposed well foundation bottom level = 467.068 m
Density of water = 1.000 t/m^3
Density of soil = 1.800 t/m^3
Destiny of RCC concrete = 2.400 t/m^3
Active earth pressure coefficient under normal condition = 0.275 = 2.500 t/m^2
Passive earth pressure coefficient under normal condition = 7.333
Design is carried by trail end correction method
Height of active earth pressure = 10.508 m

Height of passive earth pressure	=	3.600 m
Outer dia. of well	=	5.000 m
Internal dia. of well	=	3.500 m
Thickness of well staining	=	0.750 m

Design of Pier

No of vents for canal	=	2 Nos
Clear width of each vent	=	4.4 m
Thickness of walls	=	3 m
FSD of canal	=	3 m
FB	=	0.6 m
Clear span between the piers	=	15.0 m
Overall width of canal trough	=	10 m
Road width	=	4.25 m
Road level	=	+485.001
Height of kerb	=	0.225 m
Top level of pier above bed level	=	+480.20 m
MFL of drain	=	480.950 m
Bearing capacity of soil	=	50 t/sqm
Ht of side wall to bottom of road slab	=	4.075 m
Thickness of trough bottom slab	=	0.4 m
Thickness of road slab	=	0.45 m
W.C over road slab	=	0.075 m
W.C over trough slab	=	0.075 m
Bottom level of Foundation`	=	+475.466
Thickness of pier	=	1.50 m
Top level of foundation	=	+476.466
thickness of bed block	=	0.45 m
foundation offset in x direction	=	1.75 m
foundation offset in y Direction	=	1.75 m
semi circular cut and ease	=	0.75 m
maximum velocity in river	=	2.92 m/s (as per MFLs)
thickness of railing	=	0.2 m
ht of rail in	=	0.425 m

Design Of U/S & D/S Bridge Abutments

Span in between bearings	=	9.20 m
Dead load transferred from the super structure	=	573.95 KN
Live load + impact	=	236.23 KN
Length of the abutment	=	5 m
Proposed depth of the abutment	=	7.686 m
Impact factor percentage	=	0.5-7.686/3*0.5
Load coming on to the abutment	=	810.18 KN
Load coming on to the abutment per meter length	=	810.18/5.1= 159 KN
Total depth from deck slab top to bearing bottom	=	0.85 m
Horizontal force due to breaking effect	=	20% of LL 364*20% = 72.8 KN
Total horizontal force	=	36 KN
Hence correction to vertical reaction	=	72.8*(0.85+1.2)/9.2 = 16.2 KN
Horizontal load coming on to the abutment	=	36.40 KN
Horizontal load on the abutment per meter length	=	36.4/5.1 = 8 KN
Depth of beam portion	=	0.775 m
Thickness of wearing coat	=	0.775 m
Thickness of approach slab	=	0.15 m
Front batter adopted	=	1 in 100000
Top width	=	1 m
Bottom width	=	5.2 mm
Thickness of expansion joint	=	20 mm
Off-set of foundation	=	0.6 m
Depth of footing	=	0.6 m
Distance of bearing reaction	=	0.49 m/s
Reaction due to beam	=	142.778 KN
Width of dirt wall	=	0.49 m
Depth of bed block	=	225 mm
Angle of internal friction	=	32
Bulk density of soil	=	21 KN/m^3
Bulk density of concrete	=	24 KN/m^3
Hr breaking force	=	8 KN
Live load equivalent surcharge	=	1.2m

IV. CONCLUSION(S)

From the above analysis, the following conclusions are arrived:

In respect of design of trough for a discharge of 38.966 cumecs
By applying head loss theory, it is found to be satisfactory.
Size of the trough = 4.4*3.0 m.
Head loss provided is 0.20 m.
The velocity in this trough is as follows:
Area = 4.4*3.0 = 13.20 sqm
Velocity = 38.966/13.20 = 3 m/sec
Froude number $F_N = V/\sqrt{gd} = 3/\sqrt{10} * 3 = 0.6 < 1$
Hence critical flow and design is ok.
In respect of drain system the maximum discharge provided is Max Q = 2833 cumecs
This could be arrived by one of the following formulae
Catchment = 1108 sqkm

Dicken's formulae
$Q = CA^{3/4}$
For central India
C = 14 to 20
Number of piers = 22
Abutments = 2

Number of spans = 23
Deepest B.L = 477.782 m
Max FSL = 481.197 m
Depth of flow = 3.21 m

The flood discharge provided seems to be pk.

The maximum flood occurred in 2009 and the same max flood level was observed.

It is to be noted down that once in a way, there is a scope of occurring the max flood level in 25, 50, 75, 100 years and the discharge through the drains vents will be under pressure flow.

Hence care should be taken during monsoon season since there will be uplift pressure, causing for the canal trough causing break down.

In fact, in other seasons, the flow through the vents of drain are normal and sub critical flow ranging 2 m to 4 m/sec.

Since this system is functioning well for the last 2 to 3 years, the designs parameters provide are up to the mark.

All the foundations are taken up to S D R for piers and abutments. The total Depth taken below bed of stream has shown as below.

Deepest stream bed = 478.835 – 465.645 = 13.09 m. no tension is induced.

Hence safe.

V. REFERENCES

[1]. Central Design Organization (2004); Design Process Manual of Gates. Outlets, Canal Structures and Head Works.:

[2]. IS 3370 PART - 1, PART – 2.

[3]. IRC 5, IRC-6, IRC-21, IRC-78, IRC-83.

[4]. Indian Standard: IS 7331: (200 I). 'Code of Practice for Inspection and Maintenance of Cross Drainage Works'.

[5]. Indian Standard: IS 7784 (Part I) (1993). 'Design of Cross Drainage Works - Code of Practice: Part-I General Features'.

[6]. Indian Standard: IS 7784 (Part 2/Sec I) (1995). 'Design of Cross Drainage Works -Code of Practice: Part-2 Specific Requirements, Section 1: Aqueduct'.

[7]. Indian Standard: IS 800 (2007). 'Code of Practice General Construction in Steel.

[8]. Modi PN (2008). 'Irrigation Water Resources and Water Power Engineering'· Standard Book House, Delhi.

[9]. Public Works Departments' Handbook: Chapter: 18 'Hydraulics' (1983).

[10]. Punmia BC, Panda BBL Ashok KJ, Arun KJ (2009)

AUTHOR PROFILE

S. Lokeswari
Asst. Prof., Dept. of Civil Engineering, Matrusri Engineering College, Hyderabad, Telangana.
sankaralokeswari@gmail.com

T Raja Ramanna
Asst. Prof., Dept. of Civil Engineering, Matrusri Engineering College, Hyderabad, Telangana.
t.rajaramanna@gmail.com,

M Pratibha
Asst. Prof., Dept. of Civil Engineering, Matrusri Engineering College, Hyderabad, Telangana.
pratibhagundepally@gmail.com

K.V.R.Satya Sai
Assoc. Prof., Dept. of Civil Engineering, TKR College of Engineering & Technology, Hyderabad, Telangana
kvr.satya.sai@gmail.com

ABOUT THE INSTITUTE

Muffakham Jah College of Engineering and Technology (MJCET) was established in the year 1980 by Sultan-Ul-Uloom Education Society (SUES), which was formed by a group of visionaries and intellectuals from various walks of life. Over the past three decades, it has emerged as a premier institute, offering BE courses of four years duration in eight disciplines (Civil, ECE, CSE, IT, EEE, EIE, Mechanical & Production) and five ME courses (CAD/CAM, Structural Engineering., Digital Systems, Computers & Power Electronics) of two years duration. The current intake of all BE Courses is 780, in addition to 102 students in ME Programmes. Research Centers were started in Civil, Mechanical, EEE, CSE and ECE Departments for Doctoral Studies. The college is affiliated to Osmania University, Hyderabad and approved by AICTE, New Delhi. As per the survey of The Outlook magazine, MJCET was ranked 62nd among top 100 Engineering Colleges in India. MJCET has been ranked 47th in India among the top private institutes in Engineering by Times Engineering Institute ranking survey 2019. MJCET ranked 28th out of top 200 Engineering Colleges by India Today magazine. As per The Week Magazine, MJCET ranked 26th among the top Private Engineering Colleges in South India and 42nd among All India Private Engineering Colleges.

OVERVIEW OF THE CONFERENCE

Civil Engineering Infrastructure is the most significant factor in accelerating the pace of economic development of any country. The recent innovation and advances in the field of Civil Engineering has made a drastic impact in the Construction Industry. As the world's population increases, environmental concerns mount and Civil Engineers are entrusted by the society to achieve a sustainable world and raise the quality of life globally. The balancing of economic, social and environmental objectives now and in the future has become known as Sustainable Development and is increasingly a key driver at a range of organizational and spatial scales.

The Conference on Recent Advances in Civil Engineering Infrastructure – (RACEI-2019) aims at exploring the new horizon of innovation from distinguished researchers, eminent professionals from academia and Industry. The Conference also focuses for the achievement of relevant Sustainable Development Goals as described by United Nation Development Program. This event will be a platform to showcase and deliberate research work, studies and contributions for developing novel concepts in Civil Engineering Infrastructure. The Conference consists of keynote lectures on related themes by eminent personalities and stake holders.

BSP BS Publications
A Unit of BSP Books Pvt. Ltd.
4-4-316/309, Giriraj Lane, Sultan Bazar, Hyderabad - 500 095. (A.P.)
Ph: 040-23445688 / 605. Fax: +91-40-23445611.
e-mail: info@bspbooks.net, marketing@bspbooks.net
Website: www.bspbooks.net

ISBN : 978-93-89354-86-7

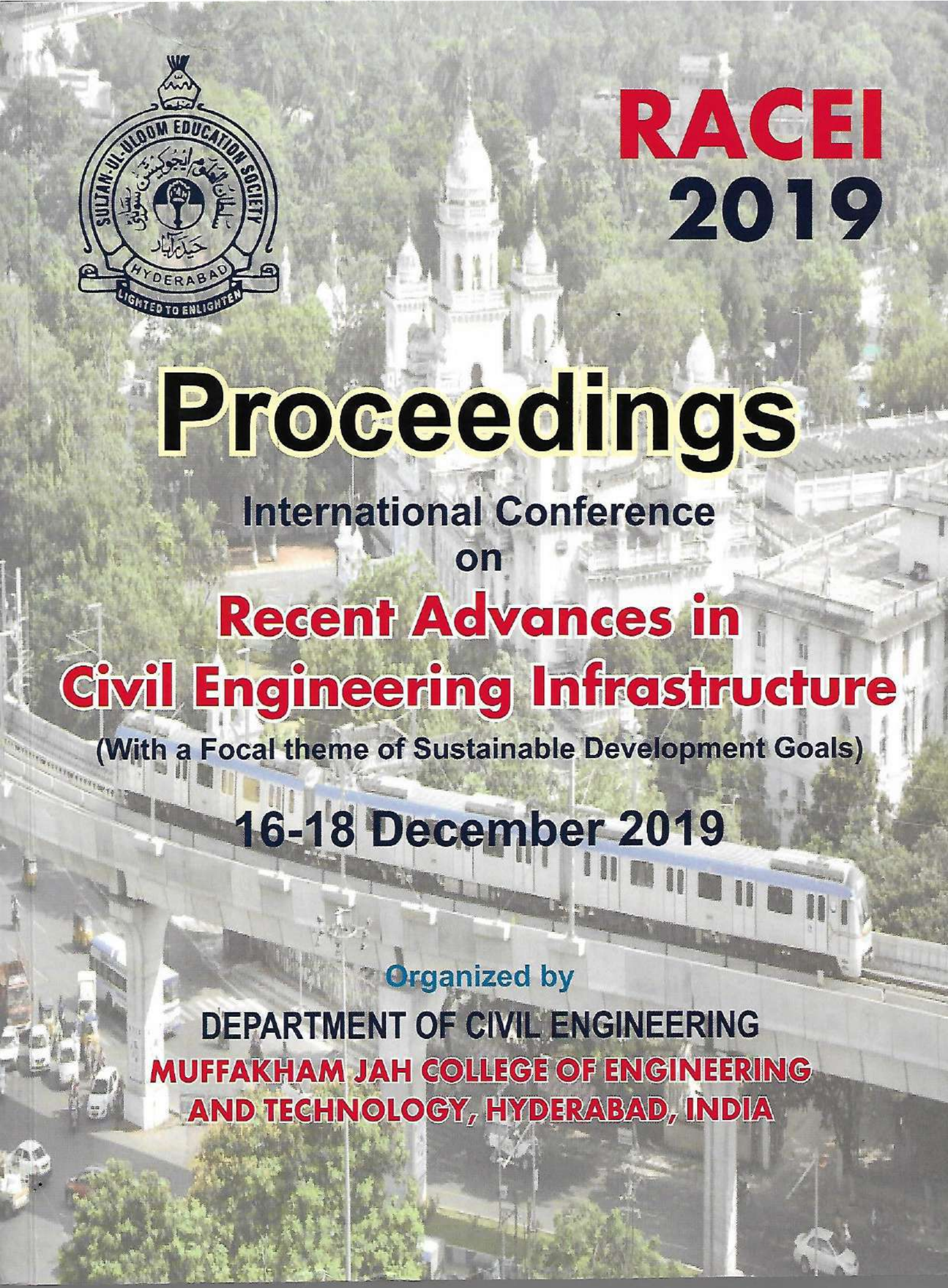

RACEI 2019

Proceedings

International Conference on

Recent Advances in Civil Engineering Infrastructure

(With a Focal theme of Sustainable Development Goals)

16-18 December 2019

Organized by

DEPARTMENT OF CIVIL ENGINEERING

MUFFAKHAM JAH COLLEGE OF ENGINEERING AND TECHNOLOGY, HYDERABAD, INDIA

Evaluation Studies of Existing Aqueduct on Kalwakurthy Main Canal of Mahatma Gandhi Lift Irrigation Scheme in Mahabubnagar District

S. Lokeswari, T Raja Ramanna, M Pratibha and K.V.R. Satya Sai

Abstract: To provide irrigation facility to an extent of 3.65 lakhs acres in drought prone areas of Wanaparthy, Nagarkurnool and Mahabubnagar Districts by lifting 25 TMC from Foreshore of Srisailam Reservoir. The Scheme is intended to provide drinking water to the enroute villages for 1 TMC covering about (336) villages in erstwhile talukas of Kollapur, Nagarkurnool, Achampet, Jadcherla, Wanaparthy and Kalwakurthy constituencies (in 24 mandal). From foreshore of Srisailam Reservoir to Stage-I pumping station, an approach channel of length of 1.60 km is excavated. The water is pumped into Yellur Balancing Reservoir (YBR) of 0.35 TMC for serving canals for an ayacut of 70,000 acres as well as to Singotam Balancing Reservoir (SBR) of 0.55 TMC up to Stage-II. This pumping station, lifts 2.14 TMC of water to Jonnala boguda (JBBR) to serve for an ayacut of 1,80,000 acres and to Stage-III 90,000 acres respectively. This pumping station, lifts water to Gudipalli Gattu Balancing Reservoir (GGBR) of 0.96 TMC.

For the irrigation purpose, this water is utilized for the last 2 to 3 years. The water supply is for one crop only. For efficient irrigation network, it is proposed to identify local ponds for collection and usage of return flow from agriculture fields up to 15 to 20% and there by the irrigation efficiency could be increased by 20%.

Keywords: Balancing Reservoir, Approach Channel, Lift Irrigation, Rainfall.

I. INTRODUCTION

Mahatma Gandhi Kalwakurthy lift irrigation project (KLIP) is a lift irrigation project on River Krishna located in Mahabubnagar district in Telangana, India. The lift canal starts from the back waters of Srisailam Dam near Kollapur. The gravity driven, 100 Km canal provides cultivation for nearly 4,00,000 acres in 300 villages located in constituencies of Kollapur, Wanaparthy, Nagarkurnool, Kalwakurthy, Jadcherla and Achampet.

The Kalwakurthy Lift Irrigation Scheme foundation stone was laid way back in 1984. It was started again in 2005 but delayed again. In August 2014 the work started with a spending of □2100 crores and completed in October 2017. It took a little over three decades to be completed.

The original design for the project was 25 TMC water capacity, but later it was increased to 40 TMC to reach the prescribed target. This project provides water to the most drought prone areas in Mahabubnagar. The water is sourced from Krishna river, by lifting water 300 meters above river level and channeling into the reservoir.

II. NESESSITY OF CROSS DRAINAGE WORKS

A cross drainage work (also called CD work) is a structure built on a canal where it is crosses a natural drainage, such as a stream or a river. Sometimes, a cross-drainage work is required when the canal crosses another canal. The cross-drainage work is required to dispose of the drainage water so that the canal supply remains uninterrupted. A cross-drainage work also called as drainage crossing or the canal at a crossing. However, it is not possible to avoid the CDW in the initial reach of a main canal because it takes off from a diversion head works (or storage works) located on a river which is a valley.

The scheme consists of 4 balancing reservoirs at

1. Yellur
2. Singotam
3. Jonnalaboguda
4. GudiipallyGattu

Table 1: Study Area

Location :	**Foreshore of Srisailam Reservoir at Regumangadda, Yellur (V), Kollapur (M)**		
Source:	Krishna River	Sub Basin:	Upper Krishna
Latitude:	16^0 25' North	Longitude:	78^0 16' East

Table 2: Components

S.No	Description	
1.	Lifts	3 Nos
2.	Proposed Balancing Reservoirs	4 Nos
3.	Approach Channel	1.60 km
4.	Tunnels	10.96 km
5.	Pressure Main	1.60 km
6.	Gravity Canal	29 km

Table 3: Pump House & Tunnel Details (Lift Wise)

S. No	Description	Stage		
		I	II	III
1	Location	YBR	JBBR	GGBR
2	Height of lift	95	86	117
3	No of Pump Houses	5	5	5
4	Capacity of Each Pump	30	30	30
5	Discharge of Each Pump	800	800	650
6	Total Power Required	150	150	150

Table 4: Reservoir Details

	Location	Reguman	Singotam	Jonnalabo guda	Narsaipally
2	Latitude	16^0	$16^0$10' N	$16^0$16' N	$16^0$25' N
3	Longitude	78^0	$78^0$16' E	78^0 16' E	$16^0$25' E
4	Capacity	0.35	0.55	2.14	$78^0$16' E
5	Ayacut	13000		43,300	0.98
6	FRL	+338.00	+338.00	+407.00	+283.800
7	MDDL	+332.00			+492.500
8	TBL	+341.5	+337.68	+410.00	+504.5
9	Capacity in TMC	0.35	0.55	2.14	0.96

Tunnel Details

Table 5: Earth Bund Details

1	Length of Tunnel	0.50km	4.33km	6.15km
2	Dia of Tunnel	7m	6.85m	6.85m
3	Shape of Tunnel	Horse shoe	D-type	D-type

S.No	Earth Bund				
1	Length of Earth Bund at top (R/S)	1.68	1.4	1.7	3.45
2	Top Width	6	6	6	6
3	No. of Berms	1	1	2	2

Table 6: Irrigation Potential (in Acres)

S. No	District	No of Mandals	Ayacut in Acres
1	Nagarkurnool	14	268165
2	Wanaparthy	6	78000
3	Mahabubnagar	2	9015
4	Shamshabad	2	9820
Total		24	365000

Table 7: Land Acquisition / R&R

S. No	Description	Required	Acquired	Balance
1	Forest area in Acres	84	84	-
2	Government land in Acres	591	591	-
3	Private land	1498	1361	135
	Total	2171	2171	135

III. DESIGN OF WELL FOUNDATION – FOR ABUTMENT

Abutment top width = 15 m
Abutment bottom width = 3 m
Outer diameter of well, D = 5 m
Thickness of well staining = 0.75m
Inner diameter of well, d = 3.5m
Diameter of well of well curb = 51m
Depth of top plug, p1 = 0.5 m
Depth of bottom plug, p2 = 0.5m
Height of curb, 2t = 1.5m
Coefficient of active pressure (Rankine's) = 0.275
Bed level = 477.585

Proposing M20 grade concrete & Fe 415 Steel

MFL = 480.960 m
LWL = 477.966 m
HFL = 480.95 m
Scour level = 470.658 m
Proposed grip length = 3.600 m
Proposed well foundation top level = 476.466 m
Proposed well foundation bottom level = 467.068 m
Density of water = 1.000 t/m^3
Density of soil = 1.800 t/m^3
Destiny of RCC concrete = 2.400 t/m^3
Active earth pressure coefficient under normal condition = 0.275 = 2.500 t/m^2
Passive earth pressure coefficient under normal condition = 7.333
Design is carried by trail end correction method
Height of active earth pressure = 10.508 m

Height of passive earth pressure	=	3.600 m
Outer dia. of well	=	5.000 m
Internal dia. of well	=	3.500 m
Thickness of well staining	=	0.750 m

Design of Pier

No of vents for canal	=	2 Nos
Clear width of each vent	=	4.4 m
Thickness of walls	=	3 m
FSD of canal	=	3 m
FB	=	0.6 m
Clear span between the piers	=	15.0 m
Overall width of canal trough	=	10 m
Road width	=	4.25 m
Road level	=	+485.001
Height of kerb	=	0.225 m
Top level of pier above bed level	=	+480.20 m
MFL of drain	=	480.950 m
Bearing capacity of soil	=	50 t/sqm
Ht of side wall to bottom of road slab	=	4.075 m
Thickness of trough bottom slab	=	0.4 m
Thickness of road slab	=	0.45 m
W.C over road slab	=	0.075 m
W.C over trough slab	=	0.075 m
Bottom level of Foundation`	=	+475.466
Thickness of pier	=	1.50 m
Top level of foundation	=	+476.466
thickness of bed block	=	0.45 m
foundation offset in x direction	=	1.75 m
foundation offset in y Direction	=	1.75 m
semi circular cut and ease	=	0.75 m
maximum velocity in river	=	2.92 m/s (as per MFLs)
thickness of railing	=	0.2 m
ht of rail in	=	0.425 m

Design Of U/S & D/S Bridge Abutments

Span in between bearings	=	9.20 m
Dead load transferred from the super structure	=	573.95 KN
Live load + impact	=	236.23 KN
Length of the abutment	=	5 m
Proposed depth of the abutment	=	7.686 m
Impact factor percentage	=	0.5-7.686/3*0.5
Load coming on to the abutment	=	810.18 KN
Load coming on to the abutment per meter length	=	810.18/5.1= 159 KN
Total depth from deck slab top to bearing bottom	=	0.85 m
Horizontal force due to breaking effect	=	20% of LL 364*20% = 72.8 KN
Total horizontal force	=	36 KN
Hence correction to vertical reaction	=	72.8*(0.85+1.2)/9.2 = 16.2 KN
Horizontal load coming on to the abutment	=	36.40 KN
Horizontal load on the abutment per meter length	=	36.4/5.1 = 8 KN
Depth of beam portion	=	0.775 m
Thickness of wearing coat	=	0.775 m
Thickness of approach slab	=	0.15 m
Front batter adopted	=	1 in 100000
Top width	=	1 m
Bottom width	=	5.2 mm
Thickness of expansion joint	=	20 mm
Off-set of foundation	=	0.6 m
Depth of footing	=	0.6 m
Distance of bearing reaction	=	0.49 m/s
Reaction due to beam	=	142.778 KN
Width of dirt wall	=	0.49 m
Depth of bed block	=	225 mm
Angle of internal friction	=	32
Bulk density of soil	=	21 KN/m^3
Bulk density of concrete	=	24 KN/m^3
Hr breaking force	=	8 KN
Live load equivalent surcharge	=	1.2m

IV. CONCLUSION(S)

From the above analysis, the following conclusions are arrived:

In respect of design of trough for a discharge of 38.966 cumecs
By applying head loss theory, it is found to be satisfactory.
Size of the trough = 4.4*3.0 m.
Head loss provided is 0.20 m.
The velocity in this trough is as follows:
Area = 4.4*3.0 = 13.20 sqm
Velocity = 38.966/13.20 = 3 m/sec
Froude number $F_N = V/\sqrt{gd} = 3/\sqrt{10} * 3 = 0.6 < 1$
Hence critical flow and design is ok.
In respect of drain system the maximum discharge provided is Max Q = 2833 cumecs
This could be arrived by one of the following formulae
Catchment = 1108 sqkm

Dicken's formulae
$Q = CA^{3/4}$
For central India
C = 14 to 20

Number of piers	=	22
Abutments	=	2

Number of spans = 23
Deepest B.L = 477.782 m
Max FSL = 481.197 m
Depth of flow = 3.21 m

The flood discharge provided seems to be pk.

The maximum flood occurred in 2009 and the same max flood level was observed.

It is to be noted down that once in a way, there is a scope of occurring the max flood level in 25, 50, 75, 100 years and the discharge through the drains vents will be under pressure flow.

Hence care should be taken during monsoon season since there will be uplift pressure, causing for the canal trough causing break down.

In fact, in other seasons, the flow through the vents of drain are normal and sub critical flow ranging 2 m to 4 m/sec.

Since this system is functioning well for the last 2 to 3 years, the designs parameters provide are up to the mark.

All the foundations are taken up to S D R for piers and abutments. The total Depth taken below bed of stream has shown as below.

Deepest stream bed = 478.835 – 465.645 = 13.09 m. no tension is induced.

Hence safe.

V. REFERENCES

[1]. Central Design Organization (2004); Design Process Manual of Gates. Outlets, Canal Structures and Head Works.:

[2]. IS 3370 PART - 1, PART – 2.

[3]. IRC 5, IRC-6, IRC-21, IRC-78, IRC-83.

[4]. Indian Standard: IS 7331: (200 I). 'Code of Practice for Inspection and Maintenance of Cross Drainage Works'.

[5]. Indian Standard: IS 7784 (Part I) (1993). 'Design of Cross Drainage Works - Code of Practice: Part-I General Features'.

[6]. Indian Standard: IS 7784 (Part 2/Sec I) (1995). 'Design of Cross Drainage Works -Code of Practice: Part-2 Specific Requirements, Section 1: Aqueduct'.

[7]. Indian Standard: IS 800 (2007). 'Code of Practice General Construction in Steel.

[8]. Modi PN (2008). 'Irrigation Water Resources and Water Power Engineering'· Standard Book House, Delhi.

[9]. Public Works Departments' Handbook: Chapter: 18 'Hydraulics' (1983).

[10]. Punmia BC, Panda BBL Ashok KJ, Arun KJ (2009)

AUTHOR PROFILE

S. Lokeswari
Asst. Prof., Dept. of Civil Engineering, Matrusri Engineering College, Hyderabad, Telangana.
sankaralokeswari@gmail.com

T Raja Ramanna
Asst. Prof., Dept. of Civil Engineering, Matrusri Engineering College, Hyderabad, Telangana.
t.rajaramanna@gmail.com,

M Pratibha
Asst. Prof., Dept. of Civil Engineering, Matrusri Engineering College, Hyderabad, Telangana.
pratibhagundepally@gmail.com

K.V.R.Satya Sai
Assoc. Prof., Dept. of Civil Engineering, TKR College of Engineering & Technology, Hyderabad, Telangana
kvr.satya.sai@gmail.com

ABOUT THE INSTITUTE

Muffakham Jah College of Engineering and Technology (MJCET) was established in the year 1980 by Sultan-Ul-Uloom Education Society (SUES), which was formed by a group of visionaries and intellectuals from various walks of life. Over the past three decades, it has emerged as a premier institute, offering BE courses of four years duration in eight disciplines (Civil, ECE, CSE, IT, EEE, EIE, Mechanical & Production) and five ME courses (CAD/CAM, Structural Engineering., Digital Systems, Computers & Power Electronics) of two years duration. The current intake of all BE Courses is 780, in addition to 102 students in ME Programmes. Research Centers were started in Civil, Mechanical, EEE, CSE and ECE Departments for Doctoral Studies. The college is affiliated to Osmania University, Hyderabad and approved by AICTE, New Delhi. As per the survey of The Outlook magazine, MJCET was ranked 62nd among top 100 Engineering Colleges in India. MJCET has been ranked 47th in India among the top private institutes in Engineering by Times Engineering Institute ranking survey 2019. MJCET ranked 28th out of top 200 Engineering Colleges by India Today magazine. As per The Week Magazine, MJCET ranked 26th among the top Private Engineering Colleges in South India and 42nd among All India Private Engineering Colleges.

OVERVIEW OF THE CONFERENCE

Civil Engineering Infrastructure is the most significant factor in accelerating the pace of economic development of any country. The recent innovation and advances in the field of Civil Engineering has made a drastic impact in the Construction Industry. As the world's population increases, environmental concerns mount and Civil Engineers are entrusted by the society to achieve a sustainable world and raise the quality of life globally. The balancing of economic, social and environmental objectives now and in the future has become known as Sustainable Development and is increasingly a key driver at a range of organizational and spatial scales.

The Conference on Recent Advances in Civil Engineering Infrastructure – (RACEI-2019) aims at exploring the new horizon of innovation from distinguished researchers, eminent professionals from academia and Industry. The Conference also focuses for the achievement of relevant Sustainable Development Goals as described by United Nation Development Program. This event will be a platform to showcase and deliberate research work, studies and contributions for developing novel concepts in Civil Engineering Infrastructure. The Conference consists of keynote lectures on related themes by eminent personalities and stake holders.

BSP BS Publications
A Unit of BSP Books Pvt. Ltd.
4-4-316/309, Giriraj Lane, Sultan Bazar, Hyderabad - 500 095. (A.P.)
Ph: 040-23445688 / 605. Fax: +91-40-23445611.
e-mail: info@bspbooks.net, marketing@bspbooks.net
Website: www.bspbooks.net

ISBN : 978-93-89354-86-7

White Bird
9912719385, 9030406700

RECENT ADVANCES IN MATERIALS AND CHEMICAL SCIENCES (RAMCS-2019)

National Seminar on

RECENT ADVANCES IN MATERIALS AND CHEMICAL SCIENCES (RAMCS-2019)

28th March, 2019

Organized by

DEPARTMENT OF CHEMISTRY
SRI VENKATESWARA UNIVERISITY

TIRUPATI-517 502
(Accredited with 'A+' grade by NAAC)

Sponsored by :

UGC-SAP (DRS-II)
New Delhi-110002

ज्ञान-विज्ञान विमुक्तये

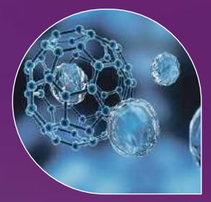

PP-94

APPLICATIONS OF NANOMATERIALS

C.Swathi

Assistant professor in chemistry, Sree vidyanikethan educational institutions.

A.Rangampet, Tirupati. Mobile no-9505364505

E-mail ID-swathinaidu.chem@gmail.com

Abstract

Nanomaterials (NMs) used in plant protection or fertilizer products in many Scientific publications and patents. The United States and Germany have published the highest number of patents, Asian countries released most scientific articles. About 40% of all contributions deal with carbon-based NMs, followed by titanium dioxide, silver, silica, and alumina. Indeed, the review of available literature indicates that some nano materials can enhance plant-growth in certain concentration ranges and could be used as nano fertilizers in agriculture to increase agronomic yields of crops and/or minimize environmental pollution. Application of new types of fertilizers using innovative nanotechnology are one of the potentially effective options of significantly enhancing the global agricultural productions needed to meet the future demands of the growing population

Keywords: Nanofertilizer, Nanomaterial, Plant production product, Agriculture environment

PP-95

GREEN SYNTHESIS AND CHARACTERIZATION OF SILVER NANOPARTICLES BY USING MANGO LEAF EXTRACT

R. Gangadhara[1] ,K.P.Satheesh[2],N.Devanna[3] ,T.Vishnu[4],P.Jalapathi[5]

[1]Research Scholar, Jawaharlal Nehru Technological University Anantapur, Ananthapuramu, Anantapur (DT), A.P., India.

[2]Lecturer in Chemistry , Jawaharlal Nehru Technological University Anantapur, ,Ananthapuramu,A.P.,India.

[3]Director,Oil Technological and Pharmaceutical Research Institute,Ananthapuramu,A.P.,India.

[4]Dept of Sciences and Humanities,Matrusri Engineering College,Saidabad,Hyderabad.

[5]Dept of Chemistry,Osmania University,Hyderabad.

Abstract:

In this study, rapid, simple approach was applied for synthesis of silver nanoparticles by using Mango leaf extract. The plant extract acts as both reducing agent and capping agent. The green synthesized silver nanoparticles were characterized by using physic-chemical techniques viz, UV-Visible spectroscopy, Fourier Transform Infrared Spectrophotometer [FTIR], Particle size Analyser and Scanning Electron Microscopy. UV-Visible spectrophotometer showed absorbance peak in the range of 419nm.The compounds responsible for silver ions and the functional groups present in plant extract were identified and investigated by FTIR technique. The characterization data reveals that the particles were in crystalline in nature with an average size of 68nm. The silver nanoparticles (Ag NPs) were rapidly synthesized using aqueous extract of Mango with $AgNO_3$ solution within 20min at room temperature, without the involvement of any hazardous chemicals.

Keywords: Nano particles, green synthesis, Silver, Mango leaf Extract and reducing agents.

GREEN SYNTHESISANDCHARACTERIZATION OF SILVER NANOPARTICLES BY USING MANGO LEAF EXTRACT

R. Gangadhara[1],K.P.Satheesh[2],N.Devanna[3] ,T.Vishnu[4],P.Jalapathi[5]

1Research Scholar, Jawaharlal Nehru Technological University Anantapur, Ananthapuramu, Anantapur (DT), A.P., India.

2Lecturer in Chemistry , Jawaharlal Nehru Technological University Anantapur, ,Ananthapuramu,A.P.,India.

3Director,Oil Technological and Pharmaceutical Research Institute,Ananthapuramu,A.P.,India.

4Dept of Sciences and Humanities,Matrusri Engineering College,Saidabad,Hyderabad.

5Dept of Chemistry,OsmaniaUniversity,Hyderabad.

Abstract:

In this study, rapid, simple approach was applied for synthesis of silver nanoparticles by using mango aqueous leaf extract. The plant extract acts as both reducing agent and capping agent. The green synthesized silver nanoparticles were characterized by using physic-chemical techniques viz, UV-Visible spectroscopy, Fourier Transform Infrared Spectrophotometer [FTIR], Particle size analyser and Scanning electron microscopy. UV-Visible spectrophotometer showed absorbance peak in the range of 419nm.The compounds responsible for silver ions and the functional groups present in plant extract were identified and investigated by FTIR technique. The characterization data reveals that the particles were in crystalline in nature with an average size of 62nm. The silver nanoparticles (Ag NPs) were rapidly synthesized using aqueous extract of guava leaf with AgNO3 solution within 15min at room temperature, without the involvement of any hazardous chemicals.

Keywords: *Nano particles, green synthesis, Silver, Mango leaf and reducing agents.*

1. INTRODUCTION

Nowadays,nanomaterials area the emerging trends in thefield of nanotechnology1,2.The environment friendly process in chemistry is known as green synthesis method,which is more acceptable in worldwide for the sakeofenvironmental concerns3-7. Among many nanomaterials, silver is one of the most commercialized nanomaterials with five hundred tons of silver nanoparticles per year 8. Nanomaterials are superior because of thei runiquesize- dependent property.Although there are many chemical and physical methods also produce pure,well-defined nanoparticles successfully but their methods were potentially dangerous to the environment and quite expensive.But the use of plant extract could be an alternative to physical and chemical methods for the production of nanoparticles in an eco-friendly pattern. Production of silver nanoparticles is estimated to increase in the next few years because of its profound role in field of catalysis, high sensitivity, bio-molecular detection, medicine and biosensors. It has been acknowledged to have strong inhibitory and bactericidal effects. The Noble silver nanoparticles are striving towards the edge-level utilities in every aspect of science and technology including the medical fields, thus cannot be neglected just because of their source of generation. Hence, it is becoming a responsibility to emphasise on an alternate as the synthetic route which is not only cost effective but should be environmental friendly in parallel. Keeping in view of aesthetic sense, the green synthesis are rendering themselves as key procedures and proving their potential at the top. The techniques for obtaining nanoparticles using naturally occurring reagents such as sugars, bio-degradable films, plant extracts, and microorganisms as reductants and capping agents could be considered attractive for nanotechnology 9,10. Very recently plant extract of Gloriosasuperba 11, Ocimumtenuiflorum12, are bringing in literature considering the vast potentiality of plants as a source this work aims to apply a biological green technique for the synthesis of silver nanoparticles as an alternative to the conventional methods. In this regard, leaf extract of Mango species of family myrtaceae was used for bio-conversion of silver ions to nanoparticles. This plant is commonly available in India and the leaves of Psidiumguajava tree have a long history of medicinal uses that are still employed in these days 13. This guava leaves have several chemical constituents such as coumarins, essential oils, triterpenes and ellagitannins 14,15. In this paper, an attempt was made to study the synthesis

of silver nanoparticles from leaves of Mango without using any additional harmful chemical/physical methods. The method applied is simple, cost-effective, easy to perform and sustainable.

2. EXPERIMENTAL:

Typically, a plant extract mediated bio reduction involves mixing the aqueous extract with an aqueous solution of the appropriate metal salt. The synthesis of nanoparticles occurs at room temperature and completes within a few minutes.

Materials:

Psidiumguajava leaves were collected from the trees growing in the Dravidian University fields, Kuppam, Andhra Pradesh, India. Silver nitrate was purchased from SRL chemicals, India. Fully purified Milli-Q water used for synthesis of Ag-NPs.

Preparation of Plant Extract:

Psidium guajava leaf extract was used to prepare silver nanoparticles on the basis of cost effectiveness, ease of availability and its medicinal property. The guava leaves were collected from the trees growing in the fields of Dravidian University campus. It was thoroughly washed in distilled water to remove mud and other dust particles and poached for 20min. in 100ml distilled water taken in a pan and then cooled at room temperature. Once it is cooled, 20ml extract of dark green was filtered to a conical flask using watt man filter paper and kept in refrigerator for further usage.

Green Synthesis of Silver Nanoparticles

Silver nitrate GR used as such (purchased from SRL Chemicals, India).100ml, 1 Mm solution of silver nitrate was prepared in an Erlenmeyer flask. Then 1,2,3,4 and
5ml of plant extract was added separately to 10ml of silver nitrate solution keeping its concentration at 1mM. Silver nanoparticles were also synthesized by varying concentration of silver nitrate. This set up was incubated at in dark chamber to minimize photo-activation of silver nitrate at room temperature. the reduction of Ag+ to Ag was confirmed by the colour change of solution from colourless to brown. Its formation was also confirmed by UV-Visible spectroscopy.

Characterization of Synthesized Silver Nanoparticles:

UV-Vis spectral analysis was done by using Shimadzu UV-Visible spectrophotometer (UV-1800, Japan). The UV-Visible absorption spectrophotometer with a resolution of 1 nm between 200 and 800nm was used. Dynamic light scattering was used to determine the average size of the synthesized nanoparticles. FT-IR spectra were recorded in Perkin Elmer (1750) FTIR Spectrophotometer. The size of synthesized silver nanoparticles was determined by using particle size analyser. SEM analyses were recorded by using LEO 435VP SEM.

3. RESULTS AND DISCUSSION

3.1.ColourChange

The particles exhibit different colour when they are in nanoscale compared to its bulk state.Silver nanoparticles will be either black or brown in colour which is shown in the Figure1.Afte raddition of guava leavesextract,the colour of the solution changed from colourless to brown colour.

UV-VisSpectralAnalysis

The noble silver metal nanoparticle was showed a well- defined absorption peak at 419 nm and confirmed the reduction of silver by the colour change from colourless to yellowish red[10]. UV-Visible spectroscopy analysis was carried out on SYSTRONICS spectrophotometer from range of 200 to 800nm.The double distilled water was used as blank[16].

FTIRAnalysis

The dual role of plant extract as capping and reducing agent and presence of functional groups of silver nanoparticles was confirmed by FTIR analysis. The broad band of spectrum shows vibrational stretches at 3317 cm^{-1} was due to O-H stretch[17], 2125 cm^{-1} was due to -C≡C- stretch, the peak 1635 cm^{-1} due to -C=O-stretching[18] and peak obtained i.e. 579 cm-1 due to C-X stretching[19]. The FTIR results were confirms that the some of organic compounds from plant extract formed as a reducing/capping on the nanoparticles. From the spectrum reveals that carbonyl group (C=O i.e., 1635 cm-1) was involved in the reduction of Ag+ to Ag .

ParticleSizeDetermination:

Particle size determinations of synthesized AgNPs were shown under by intensity the size of silver nanoparticles was synthesized with Psidiumguajava leaf extract was characterised by dynamic light scattering experiment. The average size of the synthesized silver nanoparticles from Mango leaf extract was found to be 62 nm. [20].

Morphology of Copper Nanoparticles:

The scanning electron microscopy (SEM)has been used to identify the size,shape and morphology of nanoparticles synthesized by using P. guava leaf extract. The SEM images of synthesised silver nano particles were shown in the Figure 5. The size and shape of the silver nanoparticles depends on the precursor, reducing agents used to synthesize nanoparticles and shows that silver nanoparticles are crystalline in nature.In the present study, the SEM analysis confirms the formation of silver nanoparticles, which contains the crystalline structure as shown in Figure 5.

4. CONCLUSIONS

In this study, there was presented a simple one-pot green synthesis of stable silver nanoparticles using Mango extract at room temperature was reported. The use of natural extracts, distilled water and non-toxic reagents proves to be an eco-friendly, rapid green approach for synthesis of silver nanoparticles which was a cost effective and an efficient way of synthesis. The size of AgNPswas estimated at 62nm. The SEM analysisshowed that silver nanoparticles were crystalline in nature. The reduction of silver nanoparticles was confirmed by FTIR technique. Benefits of using plant extract for synthesis is that it is cost effective, energy efficient, protecting environment and human health also leading to lesser waste and safer products. This eco-friendly method could be a competitive alternative to the conventional physical/chemical methods were used for the synthesis of silver nanoparticles.

Figure 1: 0.01 M Silver Nitrate is added to 100mL Distilled Water, Vigorously Stirred under 80° C, and 2). Mango leaf Extract being Added Drop Wise

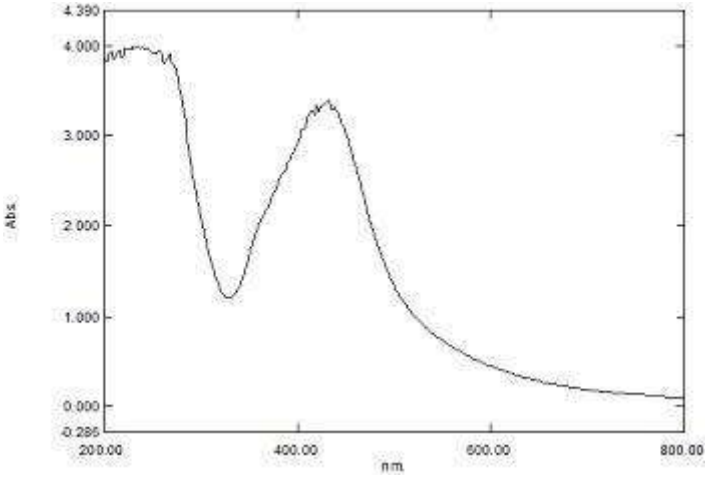

Figure 2: UV–Vis Spectra of Ag Nanoparticles Synthesized by Using Mango leaf Extract

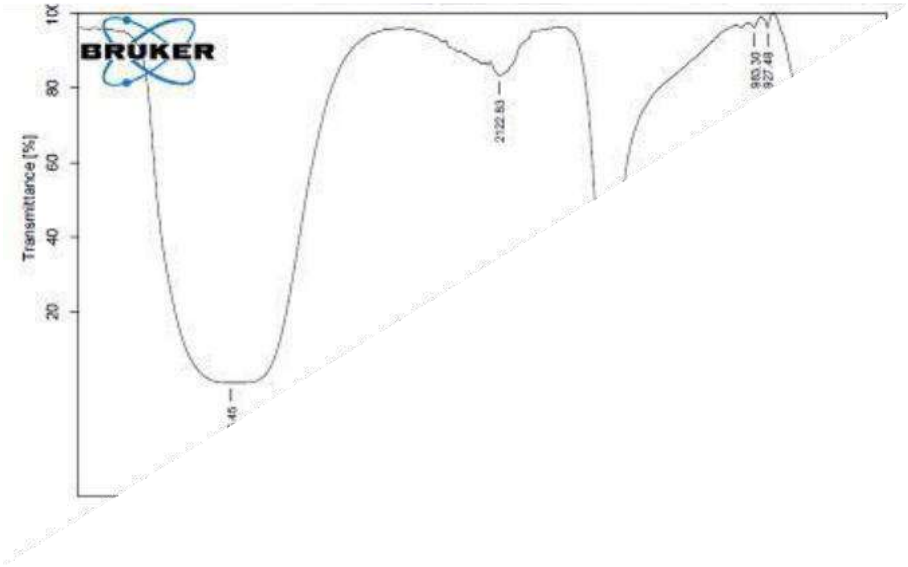

Figure 3: FTIR Spectrum of Silver Nanoparticles

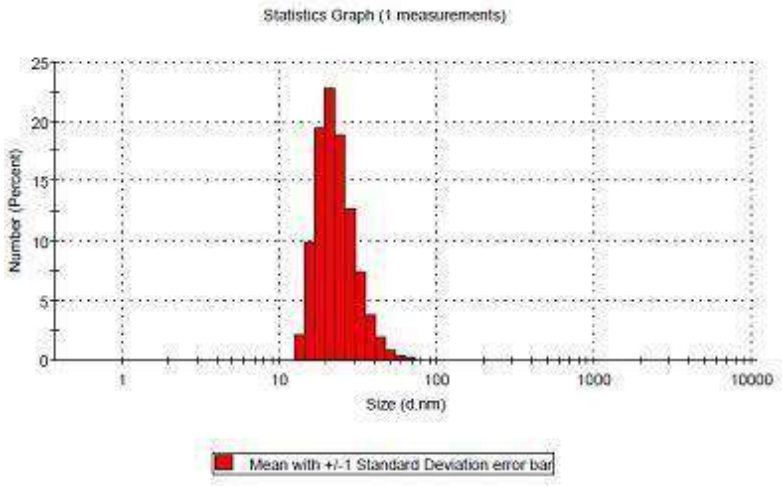

Figure 4: Particle size Distribution Pattern of Ag nano Particle was synthesized by Reducing AgNO3 using Mango leaf Extract

Figure 5: SEM Analysis of Silver Nanoparticles

5. REFERENCES

1. Albrecht M.A, Evans C.W, Raston C.L. Green chemistry and the health implications of nanoparticles. Green Chem.; 2006; 8:417–432.
2. Peter Logeswari, SivagnanamSilambarasan, Jayanthi Abraham. Synthesis of silver nanoparticles using plants extract and analysis of their antimicrobial property. Journal of Saudi Chemical Society; 2015; 19: 311–317.
3. Thuesombat P, Hannongbua S, Akasit S, Chadchawan S. Eco-toxicology and environmental safety effect on rice (Oryzasativa L. CV. KDML 105) seed germination and seedling growth. Eco-toxicology and Environmental Safety; 2014; 104:302-309.
4. Joerger R, Klaus T, Granqvist C.G. Biologically produced silver-carbon composite materials for optically functional thin-film coatings. Adv. Mater.; 2000; 12: 407–409.
5. Chandran S.P, Chaudhary M, Pasricha R, Ahmad A, Sastry M. Synthesis of gold nano triangles and silver nanoparticles using Aloe Vera plant extract. Biotechnol. Prog.; 2006; 22: 577–583.

6. Shankar S.S, Ahmad A, Sastry M. Geranium leaf assisted bio-synthesis of silver nanoparticles. Biotechnol. Prog.; 2003;19:1627–1631.
7. GardeaTorresdey J.L, Gomez E, Peralta-Videa J.R, Parsons J.G, Troiani H, Jose-Yacaman M, Alfalfa sprouts: a natural source for the synthesis of silver nanoparticles. Langmuir; 2003; 19:1357–1361.
8. Larue C, Castillo-Michel H, Sobanska S, Bureau S, Barth V. et al. Foliar exposure of the crop Lactucasativa to silver nanoparticles: evidence for internalization and changes in Ag speciation. Journal of Hazardous Materials; 2014; 264:98-106.
9. Ahmed S, Ahmad M, Ikram S. Chitosan: a natural anti microbial agent e a review. Journal of Applicable Chemistry; 2014; 3(2): 493-503.
10. Shakeel Ahmed, Saifullah, Mudasir Ahmad, Babu Lal Swami, SaiqaIkram. Green synthesis of silver nanoparticles using AzadirachtaIndica aqueous leaf extract. Journal of Radiation Research and Applied Sciences; 2016; 9;1 -7.
11. Ashok kumar S, Ravi S, Velmurugan S. Green synthesis of silver nanoparticles from Gloriosasuperba Leaf extract and their catalytic activity. SpectrochimicaActa Part A: Molecular and Bio molecular Spectroscopy; 2013; 115:388-392.
12. Logeswari P, Silambarasan S, & Abraham J. Synthesis of silver nanoparticles using plants extract and analysis of theirantimicrobial property. Journal of Saudi Chemical Society; 2012; 19(3):311-317.
13. Perez Gutierrez RM, S Mitchell, and RV Solis. "*Psidiumguajava*: A review of its traditional uses, Phyto chemistry and pharmacology. J. Ethnopharmacol; 2008; 117:1027.
14. Mittal J, Batra A, Singh A, & Sharma M. M. Phyto fabrication of nanoparticles through plant as Nano factories. Advances in Natural Sciences: Nano science and Nanotechnology; 2014; 5:1-10.
15. Geetha V. Green synthesis of silver nanoparticles from Psidiumguajava leaves and its antibacterial activity. International Journal of Bioassays; 2017; 6(7):5441-5443

16. Debadin Bose, Someswar Chatterjee Biogenic synthesis of silver nanoparticles using guava (Psidiumguajava) leaf extract and its antibacterial activity against Pseudo monasaeruginosa. Journal of applied nano science; 2016; 6:895-901.
17. Johara N, Ahmad I, Dufresne A. Ind. Crops Prod; 2012; 37:93–99.
18. Maheswari CU, Reddy KO, Muzenda M, Guduri BR, Rajulu AV. Biomass Bio energy; 2012; 46:555-563.
19. Reddy KO, Maheswari UC, Mukul S, Song JI, Rajulu AV. Composites Part B; 2013; 44:433-438.
20. Subba Rao Y, Venkata S. Kota kadi,.et. al., Green synthesis and spectral characterization of silver nanoparticles from Lakshmi tulasi (Osmium sanctum) leaf extract. Journal of molecular and bio molecular spectroscopy; 2013; 103:156-159.

Book Detection Using Deep Learning

Publisher: IEEE

Cite This Cite This PDF

P. Prashanth ; K. Sai Vivek ; D. Ruthvik Reddy ; K. Aruna All Authors

149
Full
Text Views

Export to
Collabratec

Alerts

Manage
Content Alerts

Add to Citation
Alerts

Abstract

Document Sections

I. INTRODUCTION

II. LITERATURE SURVEY

III. PROPOSED SYSTEM

IV. CONCLUSION

Authors

Figures

References

Keywords

Metrics

More Like This

Downl
PDF

Abstract: This paper deals with library automation and book detection using deep learning which comes under field of computer vision [1]. In order to automate a large Library where... **View more**

Metadata

Abstract:
This paper deals with library automation and book detection using deep learning which comes under field of computer vision [1]. In order to automate a large Library where finding a book is a tough task, this paper shows a solution for it. Here we detect the required book with the help of deep learning concept through MATLAB Neural network toolbox which can pick the particular book with the help of a mobile manipulator. Convolutional neural network used is Alex Net which can detect around 1000 classes.Deep learning is a part of machine learning in which a network learns how to classify objects from texts, Images, and sound. The first part in the name Deep Learning i.e. "deep" means number of layers in the network-A network is said to be deeper when it has many layers. Generally neural networks contain 2 or 3 layers, while deeper networks contain hundreds of layers.The device used is a rover with capability of holding a book with its fingers. It also consists of a camera which scans through the books whose output is then analysed by a neural network.

Published in: 2019 3rd International Conference on Computing Methodologies and Communication (ICCMC)

Date of Conference: 27-29 March 2019 **INSPEC Accession Number:** 18958349

More Like This

An Embedded Computer-Vision System for Multi-Object Detection in Traffic Surveillance
IEEE Transactions on Intelligent Transportation Systems
Published: 2019

Object Detection Model Based on Deep Dilated Convolutional Networks by Fusing Transfer Learning
IEEE Access
Published: 2019

Show More

Loading [MathJax]/extensions/MathZoom.js

Date Added to IEEE *Xplore*: 29 August 2019

ISBN Information:

DOI: 10.1109/ICCMC.2019.8819725

Publisher: IEEE

Conference Location: Erode, India, India

Contents

I. INTRODUCTION

Now a days, using computer vision in object detection is the focus of research, and convolution neural networks are providing more accurate results and has made great progress in object detection [1]. Object detection is developed to multi object recognition from the single object recognition. In the field of computer vision Image recognition is the skill of a software to recognise writings, actions, objects, places, and people from images. Computers equipped with a camera and artificial intelligence software can perform image recognition task. In object detection task, deep learning has formed a mainstream in object detection task based on CNN (Convolution Neural Networks) and with these algorithms accuracy in object detection have increased [1].

Sign in to Continue Reading

Authors

Figures

References

Keywords

Metrics

IEEE Personal Account

CHANGE USERNAME/PASSWORD

Purchase Details

PAYMENT OPTIONS

VIEW PURCHASED DOCUMENTS

Profile Information

COMMUNICATIONS PREFERENCES

PROFESSION AND EDUCATION

TECHNICAL INTERESTS

Need Help?

US & CANADA: +1 800 678 4333

WORLDWIDE: +1 732 981 0060

CONTACT & SUPPORT

Follow

About IEEE *Xplore* | Contact Us | Help | Accessibility | Terms of Use | Nondiscrimination Policy | Sitemap | Privacy & Opting Out of Cookies

A not-for-profit organization, IEEE is the world's largest technical professional organization dedicated to advancing technology for the benefit of humanity.

© Copyright 2021 IEEE - All rights reserved. Use of this web site signifies your agreement to the terms and conditions.

IEEE Account

» Change Username/Password

» Update Address

Purchase Details

» Payment Options

» Order History

» View Purchased Documents

Profile Information

» Communications Preferences

» Profession and Education

» Technical Interests

Need Help?

» **US & Canada:** +1 800 678 4333

» **Worldwide:** +1 732 981 0060

» Contact & Support

About IEEE *Xplore* | Contact Us | Help | Accessibility | Terms of Use | Nondiscrimination Policy | Sitemap | Privacy & Opting Out of Cookies

A not-for-profit organization, IEEE is the world's largest technical professional organization dedicated to advancing technology for the benefit of humanity.

© Copyright 2021 IEEE - All rights reserved. Use of this web site signifies your agreement to the terms and conditions.

Loading [MathJax]/extensions/MathZoom.js

Proceedings of the Third International Conference on Computing Methodologies and Communication (ICCMC 2019)
IEEE Xplore Part Number: CFP19K25-ART; ISBN: 978-1-5386-7808-4

BOOK DETECTION USING DEEP LEARNING

P. Prashanth, K. Sai Vivek, D. Ruthvik Reddy
B.E students, Department of ECE
Matrusri Engineering College, Saidabad
Hyderabad, 500059, Telangana state, India
pala.prashanth@yahoo.com

K. Aruna, Assistant Professor
Department of ECE
Matrusri Engineering College, Saidabad
Hyderabad, 500059, Telangana state, India
kokkulaaruna@gmail.com

Abstract: **This paper deals with library automation and book detection using deep learning which comes under field of computer vision [1]. In order to automate a large Library where finding a book is a tough task, this paper shows a solution for it. Here we detect the required book with the help of deep learning concept through MATLAB Neural network toolbox which can pick the particular book with the help of a mobile manipulator. Convolutional neural network used is Alex Net which can detect around 1000 classes.**

Deep learning is a part of machine learning in which a network learns how to classify objects from texts, Images, and sound. The first part in the name Deep Learning i.e. "deep" means number of layers in the network—A network is said to be deeper when it has many layers. Generally neural networks contain 2 or 3 layers, while deeper networks contain hundreds of layers.

The device used is a rover with capability of holding a book with its fingers. It also consists of a camera which scans through the books whose output is then analysed by a neural network.

KEYWORDS: Matlab, Deep learning, Convolutional Neural Network, Alex Net.

I. INTRODUCTION

Object Detection: Now a days, using computer vision in object detection is the focus of research, and convolution neural networks are providing more accurate results and has made great progress in object detection [1]. Object detection is developed to multi object recognition from the single object recognition. In the field of computer vision Image recognition is the skill of a software to recognise writings, actions, objects, places, and people from images. Computers equipped with a camera and artificial intelligence software can perform image recognition task. In object detection task, deep learning has formed a mainstream in object detection task based on CNN (Convolution Neural Networks) and with these algorithms accuracy in object detection have increased [1].

Computer Vision: Computer Vision is a technique of giving information to machines about their physical surroundings with the help of transducers like cameras. In previous days this was a complicated task which requires a specific algorithm to analyse basic unit of image i.e. Pixels. There is no flexibility in these algorithms and are to be used in specific cases. Recent researches and developments in computer vision techniques allowed computer vision to use the ability of Deep learning networks that help to resolve the issues prevailed with past computer vision algorithms.

Robotics: As the name itself says it is about the branch of engineering related to robots, and their design, application. It is a mixed application of Electronics, mechanics and software [9]. Research today is focused on developing robots that perform specified task accurately by taking less time. Some researchers are being done on automation of manufacturing process or a task. If task is bulkier, to perform that task the main constraints are time and human power. The automation is a process to save human efforts in most of the regular and frequently carried works.

The robotic arm is a microprocessor based mechatronic system that detects the book, picks that book from source location. Camera is used for detection of object. Vehicle will be controlled by Matlab which is employed as an interface between computer and vehicle (robot). It is a microprocessor-based control system which works in alliance with Matlab.

Contributions are as follows

1. Retraining a neural network namely AlexNet to detect the books using Matlab.
2. Building a mobile manipulator to pick the detected book.
3. Integrating the trained network with the mobile manipulator designed.

II. LITERATURE SURVEY

Deep Learning:

Deep learning is the subset of machine learning that learns from experience teaches computers the same. These algorithms learn information from data. Deep learning is a machine learning technique that teaches computers to learn by example which is the natural ability of humans. Deep learning is mainly used for image recognition, which gives solution for achieving better facial recognition, motion detection, and many applications such as autonomous driving, lane detection, and pedestrian detection. It have major role in consumer devices like phones, and in devices which include voice control. Deep learning is achieving results that were not possible in the past due to which it is getting lots of attention. It is a concept in which a model is trained to detect and classify different types of objects. It is a part of machine learning. It makes use of an artificial neural network in which an artificial Neuron is the basic building block. The word "Deep" in deep learning refers to number of layers in the network, the more the layers the deeper the network it is.

Deep Neural Network: A neural network is a computing model which consists of a layered structure that is similar to the networked structure of neurons in a human brain [8]. A neural network can learn from data, thus can be trained to recognize patterns, classify data, and forecast future events. Neural networks are powerful technology and require large set of training data [5].

A neural network breaks down the input into layers of abstraction. The behavior of a neural net is defined by the strength, or weights of individual elements that are connected. During the process of training, these weights are automatically adjusted until the neural network performs the required task accurately.

Convolutional Neural Network: The development of deep convolutional networks have advanced computer vision task like object detection [13]. Convolutional Neural Networks (CNN) are widely used tools for implementing the

concept of Deep Learning. CNN's consists of multiple layers. They are:

1.*Convolution layer*: This layer helps in breaking the images into smaller pieces which helps in feature detecting [3].

2.*Batch Normalization Layer*: This layer helps to speed up the CNN's and reduce the sensitivity to network initialization. These layers are used between convolutional layers and non-linearities, such as ReLu layers.

3.*Rectified Linear Unit*: This layer performs threshold operation to each element of the given input and maps negative values to zero.

4.*Pooling Layers*: Pooling layers simplifies the output by performing non-linear down sampling and reduces the number of parameters that the network is going to study.

5.*Dropout Layers*: A dropout layer randomly sets input elements to zero with the given probability.

6. *Fully Connected Layers*: This layer multiplies the input by a weight matrix and then adds a bias vector.

AlexNet in Matlab: AlexNet is trained on more than a million images. It consists of 25 layers. The use of AlexNet makes the process of neural learning easy [3].

First five are convolutional layers and last three are fully connected layers.

- It also consists of intermediate pooling layers.
- The network has an image input size of 227-by-227[8].
- Thousand object categories can be classified using AlexNet, such as mouse, laptop, pencil, keyboard, and many animals.

III. PROPOSED SYSTEM

The proposed system consists of two parts:

The first part deals with retraining an existing convolutional neural network [7] with the data that is collected (images of certain books present in library) for the purpose of detection and the second part is all about integrating the trained network with mobile manipulator which consists of a robotic arm equipped with a gripper.

Fig.1 shows the pictorial representation of the entire proposed system. This is the representation after we have the neural network that detects the target books in the library. The second step is optional i.e. Run GUI. If GUI is created, then this step adds up to the proposed system.

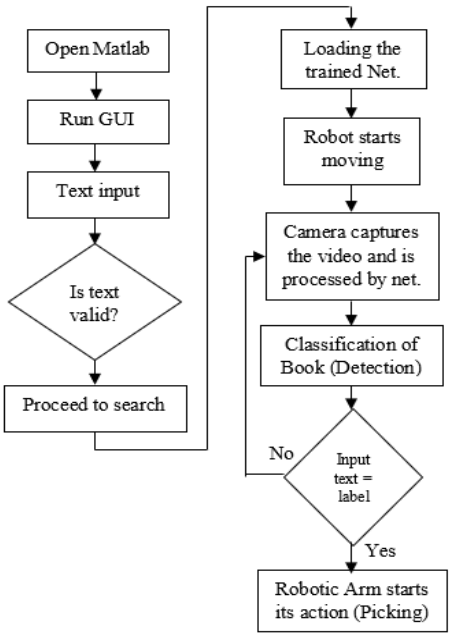

Fig. 1 Flow chart for entire proposed system

Fig.2 shows the flow chart for training the existed neural network provided by neural network toolbox in Matlab, this is called as retraining a neural network or fine tuning a network [2]. In order to retrain it requires around 1000 images of each class (Book, in this case).

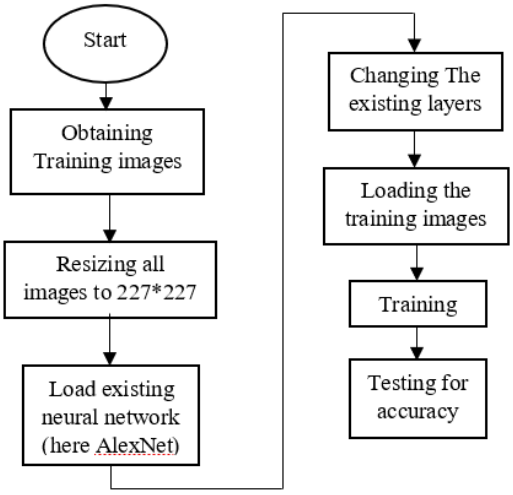

Fig. 2 Flow chart for Retraining AlexNet in Matlab

The above said mobile manipulator can be designed and fabricated in many ways which include preparing a 3d model and 3d printing it or directly proceeding with fabrication by procuring different parts required for fabrication with simple design. The mobile manipulator can have any types of arms i.e. cylindrical arm, axial arms, cartesian arms, spherical arms and Scara robot

Integration of hardware with Matlab: The designed robot can be operated with microprocessor or microcontroller. Matlab also provides hardware support packages which can be used for controlling the hardware with Matlab itself. Hardware support packages in Matlab include support package for Arduino, Support package for Raspberry Pi[8]. In this paper we prefer Raspberry Pi because of its facility that it provides camera support with the board and algorithms can be developed for raspberry pi which works as standalone application.

IV. CONCLUSION

Presently Deep learning is used in many applications like self-driven vehicles, automatic handwriting generation, machine translation, Image caption generation, text to speech conversion, Colourization of Black and white images, breast cancer classification [6], classification of electrocardiogram signals [6] etc. But in this paper, we present method to use deep learning for library automation using Matlab. But it requires a wired connection to the hardware device with the computer in which Matlab is installed, it can be extended to build a standalone device by developing hardware compatible algorithms like python programming for Raspberry Pi. Many algorithms are being developed in python to implement the technique of Deep learning which can be used for recognition and detection of objects.

ACKNOWLEDGEMENT

Furthermore, we would like to appreciate the reviewer(s) for their valuable comments on the proposed work. In addition, we are grateful to K. Aruna for the encouragement and valuable discussions.

REFERENCES

[1] Xinyi Zhou, Wei Gong, WenLong Fu, Fengtong Du. "Application of deep learning in object detection", 2017 IEEE/ACIS 16th International Conference on Computer and Information Science (ICIS), 2017.

[2] Sehla Loussaief, Afef Abdelkrim. "Convolutional Neural Network Hyper-Parameters Optimization based on Genetic Algorithms", International Journal of Advanced Computer Science and Applications, 2018.

[3] Mohamad Hazim Johari, Hasliza Abu Hassan, Ahmad Ihsan Mohd Yassin, Nooritawati Md Tahir et al. "Early Detection of Diabetic Retinopathy by Using Deep Learning Neural Network", International Journal of Engineering & Technology, 2018.

[4] Nils Gessert, Matthias Schlüter, Alexander Schlaefer. "A deep learning approach for pose estimation from volumetric OCT data", Medical Image Analysis, 2018.

[5] Yoshihiro Shima, Yumi Nakashima, Michio Yasuda. "Pattern augmentation for handwritten digit classification based on combination of pre-trained CNN and SVM", 2017 6th International Conference on Informatics, Electronics and Vision & 2017 7th International Symposium in Computational Medical and Health Technology (ICIEV-ISCMHT), 2017.

[6] Ali Abd Almisreb, Nursuriati Jamil, N. Md Din. "Utilizing AlexNet Deep Transfer Learning for Ear Recognition", 2018 Fourth International Conference on Information Retrieval and Knowledge Management (CAMP), 2018.

[7] A.U. Tajane, J. M. Patil, A.S. Shahane, P.A. Dhulekar, S. T. Gandhe, G.M. Phade. "Deep Learning Based Indian Currency Coin Recognition", 2018 International Conference On Advances in Communication and Computing Technology (ICACCT), 2018.

[8] www.mathworks.com

[9] seminarprojects.com

[10] Murphy, K. P. Machine Learning: A Probabilistic Perspective. Cambridge, Massachusetts: The MIT Press, 2012.

[11] Krizhevsky, A., I. Sutskever, and G. E. Hinton. "*ImageNet Classification with Deep Convolutional Neural Networks".* Advances in Neural Information Processing Systems. Vol 25, 2012.

[12] Ioffe, Sergey, and Christian Szegedy. "*Batch normalization: Accelerating deep network training by reducing internal covariate shift."* preprint, arXiv:1502.03167 (2015)

[13] Kien Nguyen ; Clinton Fookes ; Sridha Sridharan,*" Improving deep convolutional neural networks with unsupervised feature learning," Proc.* 2015 IEEE International Conference on Image Processing (ICIP), 27-30 Sept. 2015

[14] Aylin Sevik, Pakize Erdogmus, Erdi Yalein, "*Font and Turkish Letter Recognition in Images with Deep Learning," Big Data Deep Learning and Fighting Cyber Terrorism"* 2018 International Congress on, pp.61-64, 2018.

[15] Deepak Kumar, Ramandeep Singh, *"Deep Learning Approach: A New Trend in Text Detection in Natural Images", Proc. IEEE ,4th International conference on computing sciences,* 30-31 August 2018.

Conferences > 2019 International Conference...

Design and Implementation of Uart Protocol for Avionics Applications

Publisher: IEEE

Cite This Cite This PDF

A. S. Keerthi Nayani ; G. Nikhilesh ; S. Shiva Tej Kumar All Authors

33
Full
Text Views

Export to
Collabratec

Alerts

Manage
Content Alerts

Add to Citation
Alerts

Abstract

Document Sections

1. INTRODUCTION

II. PROPOSED SYSTEM

III. UART OPERATION

IV. TRANSMITTER

» IV.UART RECEIVER

Show Full Outline

Authors

Figures

References

Keywords

Metrics

More Like This

Downl
PDF

Abstract: Revolutionary strides that serial communication has made in the past four decades, importance of serial communication has been realized and in today's world these serial ... **View more**

Metadata

Abstract:
Revolutionary strides that serial communication has made in the past four decades, importance of serial communication has been realized and in today's world these serial communication ports are included in even high-end FPGA's. UART is a serial communication protocol which is used as a transmitter and receiver to transmit and receive data asynchronously via UART ports present in FPGA's. UART converts parallel data to serial for transmitting the data and serial data to parallel for receiving the data. For fast transmission of information UART uses Buffer and can also be up to 2 kilo bytes. It has extra registers to provide information about transmission states and flow of data from ports and to govern the plethora of data when accepting device is not prepared to accept the information. UART can glide the data when it has a huge buffer to hoard the data coming from the transmitter and receiver. The size of the buffer is contingent with the design of the UART. This Universal Asynchronous Receiver Transmitter protocols are implemented in Remote data acquisition units (RDAU) present in missiles as a part of telemetry which is an avionics application.

Published in: 2019 International Conference on Intelligent Computing and Control Systems (ICCS)

More Like This

New communication network protocol for a data acquisition system
IEEE Transactions on Nuclear Science
Published: 2006

FPGA based data acquisition with Modbus protocol
2016 International Conference on Communication and Signal Processing (ICCSP)
Published: 2016

Show More

Date of Conference: 15-17 May 2019 **INSPEC Accession Number:** 19532124

Date Added to IEEE *Xplore*: 16 April 2020 **DOI:** 10.1109/ICCS45141.2019.9065366

ISBN Information: **Publisher:** IEEE

Conference Location: Madurai, India, India

Contents

1. INTRODUCTION

UART is capable of establishing full-duplex communication and this is mostly found in serial links. UART is systematized with a Transmitter which regulates the transmission by accepting a data word in parallel format and supervises the UART to transmit it in a serial manner. Moreover, the receiver in UART should be able to notice the transmission, receive the data in serial way, and accommodate the serial data in a parallel format. The reorganizing of serial to parallel data is handled by UART. Serial communication decreases changes in the amplification or reproduces accurate results [6]. So, data can be exchanged between two systems isolated by a large distance. The module of Universal Asynchronous Receiver Transmitter is segregated into receiver, transmitter and baud rate generator. The internal clocks of receiver and the transmitter are synchronized to a local clock produced by baud rate generator with a frequency after a desired baud rate can be achieved [8].

Sign in to Continue Reading

Authors

Figures

References

Keywords

Metrics

IEEE Personal Account

CHANGE USERNAME/PASSWORD

Purchase Details

PAYMENT OPTIONS

VIEW PURCHASED DOCUMENTS

Profile Information

COMMUNICATIONS PREFERENCES

PROFESSION AND EDUCATION

TECHNICAL INTERESTS

Need Help?

US & CANADA: +1 800 678 4333

WORLDWIDE: +1 732 981 0060

CONTACT & SUPPORT

Follow

About IEEE *Xplore* | Contact Us | Help | Accessibility | Terms of Use | Nondiscrimination Policy | Sitemap | Privacy & Opting Out of Cookies

A not-for-profit organization, IEEE is the world's largest technical professional organization dedicated to advancing technology for the benefit of humanity.

© Copyright 2021 IEEE - All rights reserved. Use of this web site signifies your agreement to the terms and conditions.

IEEE Account

» Change Username/Password

» Update Address

Purchase Details

» Payment Options

» Order History

» View Purchased Documents

Profile Information

» Communications Preferences

» Profession and Education

» Technical Interests

Need Help?

» **US & Canada:** +1 800 678 4333

» **Worldwide:** +1 732 981 0060

» Contact & Support

About IEEE *Xplore* | Contact Us | Help | Accessibility | Terms of Use | Nondiscrimination Policy | Sitemap | Privacy & Opting Out of Cookies

A not-for-profit organization, IEEE is the world's largest technical professional organization dedicated to advancing technology for the benefit of humanity.
© Copyright 2021 IEEE - All rights reserved. Use of this web site signifies your agreement to the terms and conditions.

Proceedings of the International Conference on Intelligent Computing and Control Systems (ICICCS 2019)
IEEE Xplore Part Number: CFP19K34-ART; ISBN: 978-1-5386-8113-8

DESIGN AND IMPLEMENTATION OF UART PROTOCOL FOR AVIONICS APPLICATIONS

A. S. Keerthi Nayani, Assistant Professor
Department of ECE
Matrusri Engineering College, Saidabad
Hyderabad, 500059, Telangana state, India
naskeerthi@gmail.com

G. Nikhilesh, S. Shiva Tej Kumar
B.E students, Department of ECE
Matrusri Engineering College, Saidabad
Hyderabad, 500059, Telangana state, India
nikhileshgandrapu@gmail.com

Abstract: **Revolutionary strides that serial communication has made in the past four decades, importance of serial communication has been realized and in today's world these serial communication ports are included in even high-end FPGA's. UART is a serial communication protocol which is used as a transmitter and receiver to transmit and receive data asynchronously via UART ports present in FPGA's. UART converts parallel data to serial for transmitting the data and serial data to parallel for receiving the data. For fast transmission of information UART uses Buffer and can also be up to 2 kilo bytes. It has extra registers to provide information about transmission states and flow of data from ports and to govern the plethora of data when accepting device is not prepared to accept the information. UART can glide the data when it has a huge buffer to hoard the data coming from the transmitter and receiver. The size of the buffer is contingent with the design of the UART. This Universal Asynchronous Receiver Transmitter protocols are implemented in Remote data acquisition units (RDAU) present in missiles as a part of telemetry which is an avionics application.**
KEYWORDS: RDAU, Transmitter, Receiver, Verilog HDL, Vivado 2018.3, FPGA

1. INTRODUCTION

UART is capable of establishing full-duplex communication and this is mostly found in serial links. UART is systematized with a Transmitter which regulates the transmission by accepting a data word in parallel format and supervises the UART to transmit it in a serial manner. Moreover, the receiver in UART should be able to notice the transmission, receive the data in serial way, and accommodate the serial data in a parallel format. The reorganizing of serial to parallel data is handled by UART. Serial communication decreases changes in the amplification or reproduces accurate results [6]. So, data can be exchanged between two systems isolated by a large distance. The module of Universal Asynchronous Receiver Transmitter is segregated into receiver, transmitter and baud rate generator. The internal clocks of receiver and the transmitter are synchronized to a local clock produced by baud rate generator with a frequency after a desired baud rate can be achieved [8].

II. PROPOSED SYSTEM

FPGA's are equipped with UART ports for serial communication purposes [12]. Missile consists of several signal conditioners which transmit signals that are received by RDAU's connected to them which are placed in various subsystems of a missile. RDAU stands for remote data acquisition unit. There can be multiple RDAU's which gather information from almost more than 200 signal conditioners from various subsystems. The measurement parameters transmitted to RDAU's from signal conditioners can be stress, strain, pressure, temperature etc. based on the requirement. Using these acquisition units simplifies the structure of the wiring in the missile and also in turn reducing the cost of wiring and weight of the missile. These RDAU's play an active role in transmitting data from signal conditioners to Master data acquisition unit acting as a mediator. Master data acquisition unit receives data from various subsystems and this data is properly processed with techniques such as modulation and multiplexing and then transmitted through antenna from inaccessible locations to the ground station. Generally, these Master data acquisition units can be FPGA's and data transmission and reception from RDAU's to MDAU can be achieved through implementing serial communication protocols [4]. Master data acquisition units does many other parallel processes based on the features of FPGA and requirements. One of the process is forming a duplex communication between RDAU's and Master data acquisition unit (FPGA) with the help of UART

Authorized licensed use limited to: Auckland University of Technology. Downloaded on May 26,2020 at 09:35:41 UTC from IEEE Xplore. Restrictions apply.

protocols is shown in figure 1.

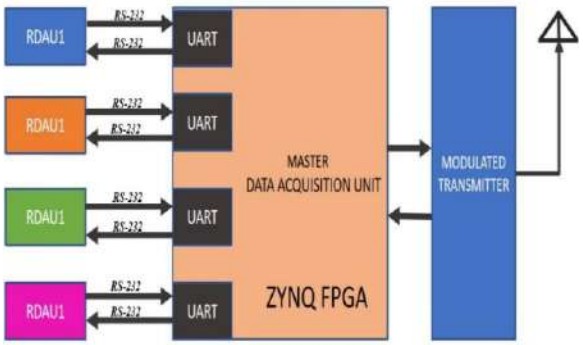

Fig 1 Proposed System

III. UART OPERATION

UART manages the data based on American standard code for information interchange (ASCII) codes where 7-bit encoding done with each character and a parity bit is included which is an added advantage for simple error detection. In UART frame the start-bit is the LSB and the stop bit is the MSB. UART module appends these both bits forming a 10-bit word for transmission which can be seen in the figure 2. Starting with the assertion of start bit for one clock cycle, transmission of 9 bits takes place in a sequential manner synchronizing with modem clock. Multiple clock cycles duration may take place for the assertion of a single stop-bit.

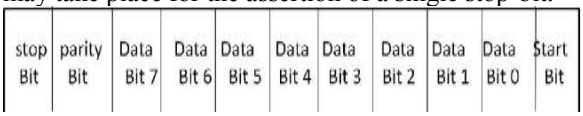

Fig 2: Data format of UART

The transmitter section is an integral part of a broader domain where a host processor governs transmission guiding the UART to arrange the data

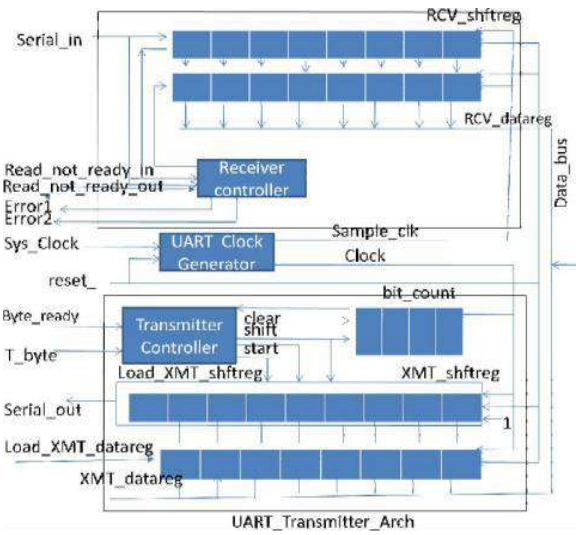

Fig 3 Architecture of UART

in a serial by retrieving the parallel format of a data word and format for transmission. On the other side receiver should be capable of detecting the transmission to obtain serial format data and trim the additional start bits and stop bits and stockpile the data in a parallel format. The receiver's activity is way more complex than as often imagined, because the clock engaged to direct data is not available for large distances [1].The receiver which is placed remotely will have to re-establish the clock at a local level, exploiting the receiver unit clock instead of using transmitting unit clock. The uncluttered architecture of Universal Asynchronous Receiver Transmitter is depicted in figure 3 which indicates the signal employed by the host processor to direct the Universal Asynchronous Receiver Transmitter and shifting of the data from a data bus. Information about the host machine is not demonstrated [3].

IV. TRANSMITTER

The signals used in transmitter section are depicted in the structural block diagram in figure 4. The host processor yields the input signals and the flow of output signals is controlled by UART. The transmitter module architecture is equipped with a controller, status register for counting, a data register, a data shift register [11].

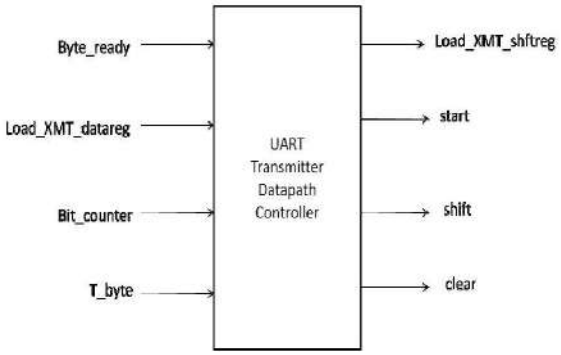

Fig 4 State machine controller schematic of a UART transmitter

State machine controller controls the transmitter and the ASM chart is shown in the figure 5. The machine consists of main three states and they are idle state, waiting state and sending state.The state machine controller enters idle state asynchronously when reset bit is asserted, bit count is activated, 1s is loaded into XMT-shiftreg, load-XMT-shftreg, shift and start are all driven to 0.During idle state, when load_XMT-datareg gets asserted by a host (external) then the contents in XMT-datareg are updated with the contents of the databus if an active edge clock arises which is an independent process and the state of the machine will

Authorized licensed use limited to: Auckland University of Technology. Downloaded on May 26,2020 at 09:35:41 UTC from IEEE Xplore. Restrictions apply.

be in idle state and will change when the start is asserted.

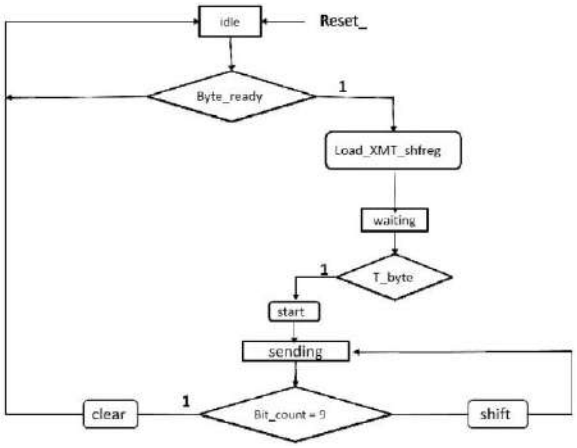

Fig 5 ASM chart of UART transmitter

If the byte-ready and load-XMT-shftreg are asserted due to which waiting state becomes the next-state. To understand that XMT-datareg is filled with data, load-XMT-shftreg is asserted and the transfer of to the internal shift register can be done. Continuing with the load-XMT-shftreg asserted during the next active edge clock three events occur:

(1) Idle state changes to waiting state

(2) XMT-datareg contents are sent to the left most bits of XMT-shftreg of size (word-size +1) – bit shift reg. The LSB indicates the starting and ending of the event and the Least Significant Bit of XMT-shftreg is reloaded with 1. The external processor will change its waiting state if T-byte is asserted.

During the next active edge of clock when T-byte is asserted, the state changes from waiting state to sending state and LSB is loaded with 0 to convey that it is start of the transmission and also the shift is driven to 1 and the next state still remains in the state corresponding to the sending state. During upcoming sequences of active edges of clock, the sending state is continued with the shift asserted and the XMR-shftreg contents are shifted to the Least Significant Bit, simultaneously the bit-count gets incremented after movement of data each time. When the bit-count increments to nine, clear gets asserted implying all the bits in augmented word have got shifted to the serial output. Machine goes again into idle state during next active edge clock [7].

IV.UART RECEIVER

The UART receiver is tasked to receive the bit stream of serial data, trimming the start bit and the data is sent in a parallel format to a storage register connected to the host data bus. There is no guarantee that the data is synchronized with the internal clock at the host of the receiver. A local clock is generated at high frequency to solve the synchronization issue and the receiver data is sampled using clock in a way that preserves the integrity of the message. A 10-bit data sampling is done at a rate determined by Sample _clock generated at the receiver‘s host. The counting of S_clk cycles is done so that the data is sampled at the middle of bit time. As depicted in figure 6 the sampling algorithm should

(i) Check whether the start bit has been fetched.

(ii) Also produce the samples from 8 bits of the data and

(iii) Load the data to the bus.

Even though there was a possibility of using higher sampling frequency, In the example the data was transmitted at S_clk frequency which is 8 times the bit clock frequency. Even if a slight misalignment occurs between the leading edge of a cycle of S_clk and the incoming of the start-bit, this will not disturb the sampling format. It is because when the input data goes low the sample will still be taken into account within the time interval corresponding to value zero. To confirm whether or not there is a valid start-bit that has arrived, the additional three samples will be taken into consideration. So, the sampling will be done to 8 successive bits at the center of their bit times approximately. Even under worst possible condition, A full cycle of S_clk ahead of center of bit time will be chosen as a sample unequivocally, which can be considered as a tolerable skew [5].

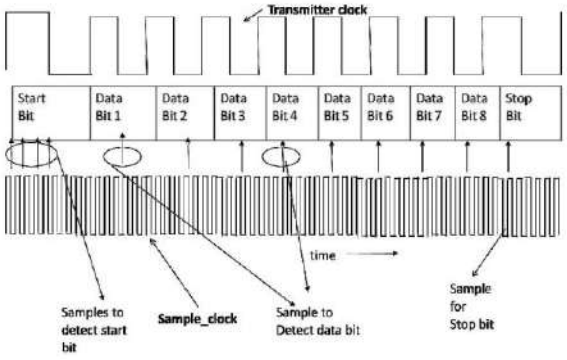

Fig 6 Sampling format of UART receiver for clock regeneration

Figure 7 is the Structural level block diagram of the state machine controller which is directing the receiver’s sample scheme when interfaced with the host processor with input-output signals [10].

The State machine controller of UART Receiver’s ASM chart is depicted in figure 8. This state machine has 3 main states namely idle state, starting state, and receiving state. Sample_clk is used to synchronize the transitions between the states. The

Authorized licensed use limited to: Auckland University of Technology. Downloaded on May 26,2020 at 09:35:41 UTC from IEEE Xplore. Restrictions apply.

machine goes into the idle state if asynchronous active-low reset is asserted. Until Serial_in is low, the machine will be in the same state and then transition takes place to starting state. To confirm whether the

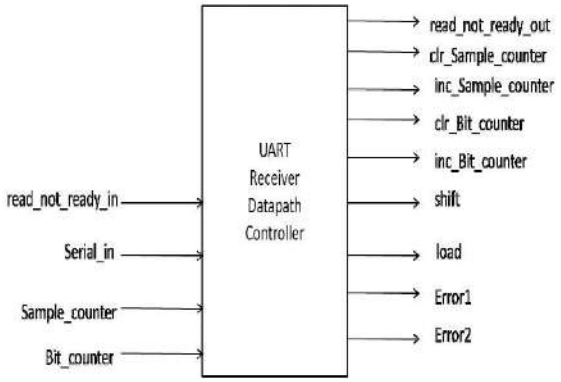

Fig 7 State-machine controller of UART receiver

1st bit is a valid start bit the machine samples Serial_in in the starting state. Based on the values sampled, Assertion of increment or clearing the counter at the next active edge of S_clk is done to the inc_sample and clr_sample. The start bit will be valid if the next three samples of Serial_in are 0 and the machine goes into the next state which is receiving state. When the state is transitioned to receiving state the Sample_counter is cleared. With inc_sample asserted 8 successive samples are considered at an active edge clock for each bit of the byte. This results the Bit_counter to be incremented. Shift and inc_Bit_counter are asserted if there is no parity bit (last bit) as a sampled bit. The sample value will be loaded into the MSB of the RCV_shftreg(receiver shift register) if the assertion of the shift takes place and 7 leftmost bits are shifted towards the LSB from the register.

The bit counter is cleared after the last bit has been sampled, read_out is asserted by the machine which is an out signal to the processor which works as a handshake. The status of the host processor and the data bits integrity are checked during this time. The host processor is not ready to accept the data, if read_in is asserted which is called as Error1. Error2 is the framing error i.e. It occurs if a stop bit is not the next bit and it is detected when Serial_in is zero. The contents in shift register are transferred to Receiver_register which is directly connected to data_bus as parallel word and works as a data register in the host machine. The received data word is $b5_h$=0101_0000$_2$. LSB to the MSB is the reception sequence of the data register and MSB to LSB is the sequence for movement of data in inbound shift register. The start bit gets appended to the data word in the beginning and a stop bit is preceded by the data word. The counters are cleared and the reset value is 0 resulting the state to be the idle state. The state of the controller will enter into starting state to find out whether there is a start bit being received. This happens when the reset condition is de asserted at the first active edge of the clock and if Serial_in value is 0. Similarly, when a total of four samples occur as 0 the state enters receiving state and the Sample_counter is cleared as usually. Shift is asserted after the 8th sample and the 9th sample is shifted into most significant bit of RCV_shftreg at the next active edge clock. RCV_shftreg values is updated to 80_h=1000_0000$_2$. The sampling cycle is repeated again, the sampled value 0 is loaded into RCV_shftreg , the register contents are updated to 0100_0000$_2$=40_h . The sampling cycle of the end of the word received cab be seen in the figure 8. To recognize the stop bit the controller samples one more time after the last data bit is also sampled. The contents of RCV_shftreg are transferred to Receiver_register if there is no error detected.

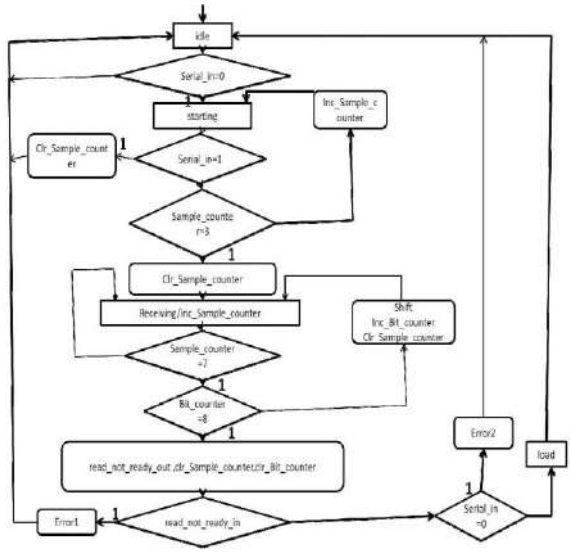

Fig 8 ASM chart of UART Receiver

V. SIMULATION RESULTS

UART Transmitter

When T-byte is asserted during an active edge of a clock the state of the machine is entered into sending state and 0 is loaded into Shift_register_transmitter to give intimation about the start of the transmission and simultaneously shift is driven to 1 and next state will be remaining in the sending state [2]. The contents of Shift_register_transmitter are shifted towards the least significant bit of the serial output, bit count is incremented for each time there is a movement of data. The machine will again return to the idle state in

Authorized licensed use limited to: Auckland University of Technology. Downloaded on May 26,2020 at 09:35:41 UTC from IEEE Xplore. Restrictions apply.

the next active clock edge when bit count reaches 9 stating that the transfer of all the bits have been done.

Fig 9 when T _byte=1, then the transmission of data will occur i.e. Serial _out=LSB of the XMT shift register

UART Receiver

When the reset will be de asserted again, the controller's state goes into starting state to check whether there is a start bit being received when the Serial_in value is 0 at the first active edge of the clock. The Sample_counter is cleared after additional 3 samples are found to be 0 and that is a total four samples with 0 value then the state enters receiving state. Shift is asserted after the eighth sample. The sample is shifted into the most significant bit of the RCV_shftreg at the next active edge of the clock.

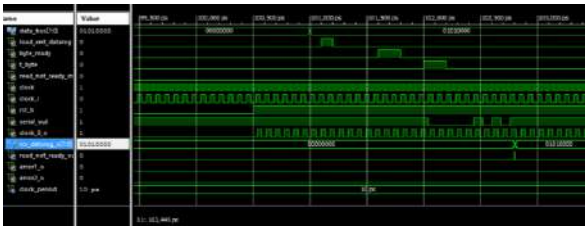

Fig 10 Waveform of Receiver Transmitter

Here the output of transmitter is directly given to the input of the receiver by a creating a top module for Transmitter and Receiver in Verilog HDL for the ease of simulation [9].

VI. APPLICATIONS

(1) UART ports consisting IP cores are used in FPGA's
(2) Modems
(3) Wired communication
(4) Bluetooth modules

VII. CONCLUSION

UART allows the full duplex serial communication in RDAU's and MDAU present in sub modules of a missile. It is an essential equipment to RDAU's and allows them to communicate with sub modules of a missile, where communication can be achieved with other without synchronization with framing error detection. UART ports have receiver and transmitter pins as inputs and outputs used to control data traffic. UART increases the accuracy and reduces noise effects and good speed can be achieved. This UART protocol is widely used as an interface between RS232 and microcontroller. The main aim of designing and implementing UART protocol using Verilog HDL is to establish a simplified communication between sub modules of a missile consisting FPGA's. The simulation is done using Vivado 2018.3 and XILINX ISE 14.6. simulators. The transmitter and receiver simulation results are achieved and depicted in the figure 9 and figure 10 respectively.

ACKNOWLEDGEMENT

Furthermore, we would like to appreciate the reviewer(s) for their valuable comments on the proposed work. In addition, we are grateful to Dr. N Srinivas Rao, Dr. P H Gopal Mani, Dr. Sushanth Babu and K. Ashok kumar and scientist P. Veeranna (RCI) for the encouragement and valuable discussions.

REFERENCES

[1]. Advanced digital design with the verilog HDL, Michael D.Ciletti, TMH,2002.
[2]. Naresh Patel, Vatsalkumar Patel, Vikaskumar Patel," VHDL Implementation of UART with Status Register", 2012 IEEE International Conference on Communication Systems and Network Technologies, 2012.
[3]. Roth CW.Jr, Digital Systems Design Using VHDL., Boston, MA: CL-Engineering, 1998.
[4]. Introduction to Telemetry. Instrument Society of America (1987).
[5]. Parul Shrivastava1, Prof. Sourabh Sharma2, "Design and simulation of 16 Bit UART Serial Communication Module Based on VHDL" International Journal of Emerging Technology and Advanced Engineering Website: www.ijetae.com (ISSN 2250- 2459, ISO 9001:2008 Certified Journal, Volume 4, Issue 4, April 2014.
[6]. Gallo R, Delvai M, Elmenreich W, Steininger A, "Revision and verification of an enhanced UART", 2004, Proceedings, 2004 IEEE International Workshop on Factory Communication Systems, pp. 315- 318, 22-24, Sept. 2004.
[7]. Elmenreich W, Delvai M, "Time-triggered communication with UARTs", 4thIEEE International Workshop on Factory Communication Systems, 2002, pp. 97- 104, 2002.
[8]. Norhuzaimin J, Maimun H.H, "The design of high speed UART", AsiaPacific Conference on Applied Electromagnetics (APACE), pp. 20- 21, Dec. 2005.

Authorized licensed use limited to: Auckland University of Technology. Downloaded on May 26,2020 at 09:35:41 UTC from IEEE Xplore. Restrictions apply.

[9]. Hazim Kamal Ansari, Asad Suhail Farooqi," Design Of High Speed Uart For Programming FPGA"International Journal Of Engineering And Computer Science Volume1 Issue 1 Oct 2012.Strock, O.J.
[10]. R.W.Hamming, "Error detecting and error correcting codes", The Bell System Technical journal Vol. XXIX, April 1950, Vol. 2, American Telephone and Telegraph company.
[11]. A. Raghavendra Reddy, D.Chinna Babu, G.Manikanta Chowdary, S.Mansoor Basha, H.S.Ijaz "A novel approach to design and implement High Speed UART by Using Verilog HDL", International Journal of Advanced Research in Electrical, Electronics and Instrumentation Engineering (IJAREEIE), Vol. 5, Issue 4, April 2016.
[12]. Testworld.com. (2019). [online] Available at: https://testworld.com/wp-content/uploads/Tutorial-Telemetry-Testing-Data-Acquisition.pdf [Accessed 23 Apr. 2019].

Authorized licensed use limited to: Auckland University of Technology. Downloaded on May 26,2020 at 09:35:41 UTC from IEEE Xplore. Restrictions apply.

UGC Sponsored

a Two Day National Seminar

on

EMERGING TRENDS IN CHEMICAL SCIENCES

UGC
University Grants Commission

March 11th and 12th 2019

Souvenir

Organized by
Department of Chemistry
School of Herbal Studies and Naturo Sciences
Dravidian University
Srinivasavanam, Kuppam - 517 426. A.P. India

Department of Chemistry

ETCS - 2019

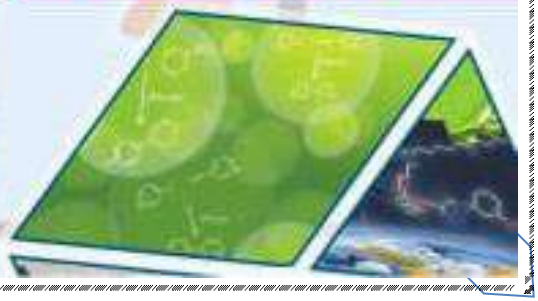

SOUVENIR & ABSTRACTS

Accredited By NAAC With "B" Grade

Dravidian University, Srinivasavanam, Kuppam

Department of Chemistry

A Two Day

National Seminar

on

"EMERGING TRENDS IN CHEMICAL SCIENCES"

(ETCS -2019)

March 11th&12th, 2019

Sponsored By

University Grants Commission (UGC)
New Delhi.

ETCS-2019-26

UV – Visible Spectrophotometric Method for the Determination of Lamivudine

B. Ramachandra[1]*,P. Chandrasekhar[1],K.Siva Rami Reddy[2]&
N. Venkata Subba Naidu[2]*
[1&2]*Department of H&S, Annamacharya Institute of Technology and Sciences, Tirupati-517520.A.P., India.
*[2]Department of Chemistry, S.V.University, Tirupati -517502, A.P., India.

ABSTRACT

A simple, sensitive, selective rapid Spectrophotometric method has been developed for the determination of Lamivudine in pure form, pharmaceutical formulations and blood sample based on the oxidative coupling reaction with MBTH (3-methyl-2-benzothiazolone hydrazone hydrochloride) reagent, at P^H–4.0 which is extractable at 620 nm. Beer's law is obeyed in the concentration ranges 10-60 µg ml^{-1} for formulations and 4-24 µg ml^{-1} for a blood sample. The developed method was applied directly and easily for the analysis of the Pharmaceutical formulations and blood samples. % R.S.D was found to be 0.19148%, 0.19157% and Recovery 99.20% to 99.78% and 99.84 respectively. The method was completely validated and proven to be rugged. The repeatability and the performance of the proved method were established by point and internal hypothesis and through recovery studies.

Keywords: Spectrophotometry, Lamivudine, Blood Sample & MBTH / $FeCl_3$.
E-mail:ramachandrabandi111@gmail.com.

ETCS-2019-27

Synthesis and Characterization of Bio-nanocomposite Films and Their Antimicrobial Studies

R. Gangadhara[1], K. P. Satish[1], N. Devanna[1] and T. Vishnu[2,]

[1]Department of Chemistry, J. N. T.U, Ananthapuramu, Anantapur (DT), A.P., India.

[2]Department of Chemistry & HAS, Matrusri Eng.College, Hyderabad, Telangana state, India.

ABSTRACT

Methylcellulose blended with pectin nanocomposite films were produced by a wet casting method. The morphological properties of methylcellulose and pectin films were characterized by UV-VIS spectroscopy, FT-IR and Particle size analysis. The structural, thermal properties of the

blended films were characterized by FT-IR, SEM and their anti-microbial activity were also studied by using disc diffusion method against E. Coli, Bacillus, Streptococcus aureus, Klebsiella. The effects of Methylcellulose and Pectin on morphological, thermal, water vapor transmission rate (WVTR), and mechanical properties were evaluated. The biocomposite films showed good water vapor barrier, thermal stabilities, mechanical properties, and anti-microbial properties.

Keywords: Biodegradable films, Methylcellulose, Blended, Antimicrobial.

Corresponding Author: Email ID: r.gangadharaa@gmail.com.

ETCS-2019-28

Isolation of Isoxazol-Pyrimidin Fused Heterocycle Derivative from *Tetrastigmaleucostaphylum* (Dennist) Alston and their Pharmacokinetic Studies

Adarsh Krishna T.P[1, 2]*, Shobha Rani T[1]*, Ajeesh Krishna T.P[1,2], Sanis Julie[1], Reghu Ravindran[4]

[1]*School of Herbal Studies and Naturo Sciences, Department of Organic Chemistry, Dravidian University, Kuppam, Andhra Pradesh-517 426, India.*
[2]*Department of Veterinary Pharmacology and Toxicology, College of Veterinary and Animal Sciences, Wayanad, Kerala-673 576, India.*
[3]*Division of Plant Molecular Biology, Entomology Research Institute, Loyola College, Chennai, Tamil Nadu- 600 024, India*
[4]*Department of Veterinary Parasitology, College of Veterinary and Animal Sciences, Wayanad, Kerala-673 576, India.*

ABSTRACT

Nitrogen-containing heterocycles with an oxygen atom are considered as an important class of compounds in medicinal chemistry because of their diversified biological applications. Isoxazole is an azole with an oxygen atom next to the nitrogen. Isoxazole rings are found in some natural products, such as ibotenic acid and also found in a number of drugs, including COX-2 inhibitor valdecoxib. Furoxan, a nitric oxide donor is containing isoxazolyl group and found in many β-Lactamase resistant antibiotics, such as cloxacillin, dicloxacillin, and flucloxacillin.

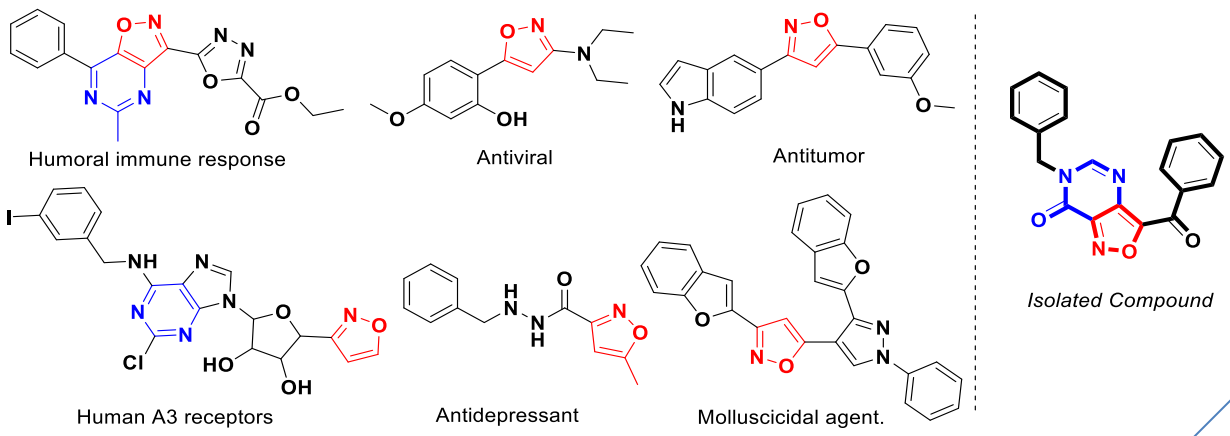

SYNTHESIS AND CHARACTERISATION OF BIO-NANOCOMPOSITE FILMS AND THEIR ANTIMICROBIAL STUDIES

R.Gangadhara[1].,K.P.Satheesh[2].,N.Devanna[3].,T.Vishnu[4]

[1,2,3] Department of chemistry JNTUA,Ananthapuramu.

4 Department of chemistry, MatrusriEngg.College,Hyderabad.

Abstract:

Plastic packaging is essential nowadays.Biodegradable thermoplastic materials offer great potential to be used in food packaging. However, the major problem caused by non-biodegradable polymers in the end of life has to be minimized and eliminated by the use of biopolymers.In this paper we will present review on polysaccharides nanocomposites used in packaging. Nevertheless, with increasing attention and research on this field, it has been possible to place some strategies to overcome the problems ad recognize the solutions. This review summarizes some of the most used polysaccharides in food packaging applications. Finally, the future study will be based on replacement of nonbiodegradable materials with biodegradable materials.

Keywords: polysaccharides, biopolymer derived membranes, microbial polysaccharide, packaging.

1.Introduction:

Plastics are now being used on a large scale for packaging a variety of food stuffs. Food packaging is essential for protection, preservation, contaminant, convenience and to increase the shelf life of food. The packaging material that is in direct contact with food can be in the form of bottles, trays or bags (1).Essentially packaging strategies result from the combination of food science, processing and preservation, once they must extend the shelf life of food products reducing the wastage(2).

Plastic packaging represents almost 40% of the European plastics market and it is essential for processing, protecting,storing,transporting and preserving food (3,4).This success of plastics comes from the fact that many of them can be moulded, extruded, cast and blown in different shapes or films (4,5).The real success of plastics in foodpackaging industry is achieved with combination of all referred characteristics and their use to keep food fresh and free of contamination(6).

This review provides an overview of the application of biodegradable polymers from renewable resources in packaging materials. A wide range of different polysaccharides, their properties, and their state of the art in research and commercial fields are described and discussed.

2.Biodegradable polymers:

For the polymer industry it is important to distinguish between biopolymers and biodegradable materials. While biopolymers are biodegradable,not all biodegradable materials are considered biopolymers.As examples, polycaprolactone(PCL),polyglycolide(PGA) and polybutylene succinate adipate(PBSA) are biodegradable materials, but not classified as biopolymers because they are produced from non-renewable resources (7).

The idea of using biopolymers in packaging, to contribute to sustainable development is recognized, since it is possible to dispose of the plastic waste to be degraded in nature.

3.Polysaccharides in food packaging

Polysaccharides are most abundant macromolecules in the biosphere. These complex carbohydrates constituted by glyosidic bonds are often one of the main structural elements of plants and animal exoskeletons or have an important role in plant energy storage (8).

Polysaccharide based membranes have been widely used in food industry in packaging and edible coatings. These are more attractive due to their good barrier against oxygen and carbon dioxide and good mechanical properties.

3.1. Polysaccharides obtained from plants:

3.1.1. Starch

Starch is the most abundant polysaccharide in plants. It is biodegradable, low cost, easy to handle and exhibit thermoplastic behaviour. The main sources of starch are corn, potato, tapioca.

Starch granules are insoluble in cold water and are composed of two typesof glucose polymers,amylose and amylopectin.Starch has the ability to form membranes and coatings with very low oxygen permeability,however its applicability as packaging material is dependent on its high hydrophilic character and limited mechanical properties.Research has been carried out to overcome these problems mainly by the use of plasticizers, which increase the mobility of chain, improves flexibility with good mechanical properties. The most used plasticizers are polyols such as glycerol, glycol and sorbitol (9,10,11,12).

3.1.2. Galactomannans

Galactomannans are neutral polysaccharides composed of β-(1-4)-D-mannose backbone with a single D-galactose branch linked α-(1-6),they differ fromeach other by the mannose/galactose (M/G) ratio.The three major galactomannans with interest in food and non-food industries are guar gum,tara gum and locust bean gum (13,14).

These natural polysaccharides are commonly used in the food industry, mainly as thickeners, stabilizers, coating etc. The mechanical and barrier properties of galactomannan membranes and coatings are on the basis of their application to improve the shelf-life, safety and quality of food products.

3.1.3. Cellulose

Cellulose is the most abundant occurring natural polymer on earth,being the predominant constituent in cell wallsof all plants.Cellulose is composed of monomer, glucose under its β-D-glucopyranose form (15).Due to its regular structure and array of hydroxyl groups, it tends to form strong hydrogen bonded crystalline microfibrils and fibres and is most familiar in the form of paper, paperboard in packaging context (16,17).

Its great interest is related with specific properties such as low density, high mechanical strength, low cost, durability, renewability, biodegradability, non-toxicity,biocompatibility, chemical stability, good films forming performance and ease of making chemical derivatives(15,18).

3.2. Polysaccharides obtained from Animals

Chitin and Chitosan

Chitin is the secondmost abundant agro-polymer produced in nature.It appears naturally in the exoskeleton of arthropods and in the cell walls of fungi and yeasts. It is an acetylated polysaccharide composed of N-acetyl-D-glucosamine and is produced commercially by chemical extraction processes from prawns and crabs waste.Chitin can also be produced using enzyme hydrolysis or fermentation process, these processes are not economically feasible yet on industrial scale(19,20).

Chitosan membranes are biodegradable, biocompatible,renewable,non-toxic and commercially available. Furthermore, chitosan membranes are reported as being semi permeable to gases presenting low oxygen permeability, essentialfor some foodpreservation,and moderate water vapour barrier(21,22,23,24).

Despite these unique properties of chitosan membranes, much research has been done focused on their improvement.Adding glycerol to chitosan membranes, and applying thermos-mechanical treatment is possibleto obtain a kind of thermoplastic material that grants good mechanical properties(19,25).

3.3. Polysaccharides obtained from Algae

3.3.1. Carrageenan

Carrageenan is naturally occurring hydrophilic, anionic sulphated linear polysaccharide extracted from red seaweeds, specifically from Rhodophyceae family(26,27).Carrageenan is approved as food grade additive, and it has been used mainly as emulsifier and stabilizer in flavoured milks, pet food, dietic formulas, dairy products and infant formulas (28,29).

Carrageenan is also used to produce edible films and coatings, though the reports about its application in coatings are much more common.Carrageenan edible films and coatings and their blends with other polymers were reported to be used in food to preserve fresh cut fruits, by reducing moisture loss and decreasing gas exchange,as well as preventing the discoloration and maintaining texture (30,31).

3.3.2.Alginate

Alginate is a linear polysaccharide that is abundant in nature and is synthesize by brown seaweeds and some soil bacteria.It has an anionic character and is water soluble, consisting of monomeric units of 1-4-linked

α-D-mannuronate(M blocks) and β-l-guluronate(G blocks),as well as segments of alternating mannuronic and glucuronic acids(MG blocks).The physical properties of alginates depends on the relative proportion of these three blocks, which are directly related with the extraction source(32).They are appealing film forming compounds because of their biodegradability, non-toxicity, biocompatibility and low cost.Sodium alginate is the most used in industry and was the first by-product from algal purification(20,27).

3.4.Polysaccharides obtained from Microorganisms

Several polysaccharides with film forming ability can be produced by microorganisms(yeast,fungus or bacteria) such as pullulan,gellan gum, xanthan gum, fucopol,bacterial cellulose or bacterial alginates.

3.4.1. Pullulan

Pullulan is a linear, water soluble and neutral exopolysaccharide,constituted mainly of maltotriose units connected by α-1,6 glycosidic units and produced by yeast like fungus Aureobasidium pullulans using a variety of feedstocks containing simple sugars(17).

Pullulan is biodegradable,non-toxic,tasteless and odourless.It can be used as food additive, ass flocculent agent or even as blood plasma substitute,beyond filmforming agent.Pullulan membranes are edible,homogenous,printable,transparent,flexible,heat sealable, and good barriers to oxygen(33,34,35).However they are water sensitive and mechanically weak(36,37).These properties,and fact of pullulan membranes inhibit fungal growth,make them a good material for food applications.

3.4.2. Gellan gum

Gellan gum is an anionic water-soluble exopolysaccharide, producedby Sphingomonas elodea,also known as Auromonas elodea or Pseudomonas elodea.In food industry,gellan gum is usually used as additive, however the applications of gellan gum may also be extended to membranes and coatings for food industry. These membranes and coatings offer advantages, essentially due to their ability to reduce oil absorption by providing an effective barrier.In batters,for example, product crispness is maintained long after frying or baking,which helps to maintain product quality under heating lamps (38).

3.4.3.Xanthum Gum

Xanthum gum is an exopolysaccharide produced by Xanthomonas campestris using glucose and sucroseassole carbon source. Xanthan is water soluble and non-toxic.It imparts a high viscosity at low concentrations in aqueousmedia,with a strong shear-thinning behaviour. The rheological propertiesofxanthan solutions are quite stable in a widerange of $p^{H,}$ionic strength and temperature values(39,40).

Xanthan gum has been used in a widevariety of industrial applications, suchas food, cosmetic, pharmaceutical, textile, petroleum production.In food industry, it is mainly use as additive.Thus far, there is not much information about xanthan membranes for food packaging,may be caused by the current high cost of xanthan production(41).

3.4.4. Fucopol

Fucopol is a high molecular weight exopolysaccharide produced by Enterobacter A47 using glycerol by-product from biodiesel industry as carbon source. This biodegradable,anionic, water soluble heteropolysaccharide is composed by fructose,maltose,glucose,glucuronic acid and acyl groups, which account for 12-18wt% of the fucopol dry weight(42,43,44).

Fucopol production at lab scalehas shown productivities and yieldscomparableto other commercial microbial bacterial polysaccharides,such as xanthan and gellan (39). Although this polysaccharide is not commercially available yet,the scale upof its production is being developed.

4.Coclusions and Future Perspectives

In this work, the state of the art on polysaccharide based membranes use for food packaging applications was revised. Intensive academic and industry research is being carried out to find new and improved polymers to obtain biopolymers that may replace the conventional synthetic and non-biodegradable ones as packaging material.

References:

1. Coles R., McDowell D., Kirwan M.J. Food Packaging Technology. Taylor & Francis; Oxford, United Kingdom: 2003.

2. 94/62/ec on Packaging and Packaging Waste. European Parliament and Council Directive; European Union: 1994. l0062-en-05.04.2005-001.001.

3. Plastics Europe. Plastic Packaging: Born to Protect. Plastics Europe—Association of plastics manufacturers; Brussels, Belgium: 2012.

4. Plastics Europe. Plastics—The facts 2014/2015. Plastics Europe—Association of plastics manufacturers; Brussels, Belgium: 2015.

5. Plastics Europe Packaging. [(accessed on 2 December 2015)]. Available online:http://www.plasticseurope.org/use-of-plastics/packaging.aspx.

6. American Chemistry Council Lifecycle of a plastic product. [(accessed on 2 December 2015)]. Available online: http://plastics.americanchemistry.com/Life-Cycle#uses.

7. Plackett D. Biopolymers: New Materials for Sustainable Films and Coatings. Wiley; Chichester, UK: 2011. Introductory overview; pp. 1–14.

8. Thakur V.K., Thakur M.K. Handbook of sustainable polymers: Processing and applications. Pan Stanford Publishing; Singapore: 2016.

9. Souza A.C., Benze R., Ferrão E.S., Ditch field C., Coelho A.C.V., Tadini C.C. Cassava starch biodegradable films: Influence of glycerol and clay nanoparticles content on tensile and barrier properties and glass transition temperature. LWT-Food Sci. Technol. 2012; 46:110–117. doi: 10.1016/j.lwt.2011.10.018. [Cross Ref]

10. Müller C.M.O., Yamashita F., Laurindo J.B. Evaluation of the effects of glycerol and sorbitol concentration and water activity on the water barrier properties of cassava starch films through a solubility approach. Carbohydrate. Polymer. 2008; 72:82–87. doi: 10.1016/j.carbpol.2007.07.026. [Cross Ref]

11. Isotton F.S., Bernardo G.L., Baldasso C., Rosa L.M., Zeni M. The plasticizer effect on preparation and properties of etherified corn starches films. Ind. Crops Prod. 2015; 76:717–724. doi: 10.1016/j.indcrop.2015.04.005. [Cross Ref]

12. Abdorreza M.N., Cheng L.H., Karim A.A. Effects of plasticizers on thermal properties and heat sealability of sago starch films. Food Hydrocoll. 2011; 25:56–60. doi:

13. Cerqueira M.A., Bourbon A.I., Pinheiro A.C., Martins J.T., Souza B.W.S., Teixeira J.A., Vicente A.A. Galactomannans use in the development of edible films/coatings for food applications. Trends Food Sci. Technol. 2011; 22:662–671. doi: 10.1016/j.tifs.2011.07.002. [Cross Ref]

14. Pawar H.A., Lalitha K.G. Isolation, purification and characterization of galactomannans as an excipient from senna tora seeds. Int. J. Biol.Macromol. 2014; 65:167–175. doi: 10.1016/j.ijbiomac.2014.01.026.[PubMed] [Cross Ref].

15. Credou J., Berthelot T. Cellulose: From biocompatible to bioactive material. J. Mater. Chem. B. 2014; 2:4767–4788. doi: 10.1039/C4TB00431K. [Cross Ref]

16. Cruz-Romero M., Kerry J.P. Crop-based biodegradable packaging and its environmental implications. CAB Rev. Perspect. Agric. Vet. Sci. Nutr. Nat. Resour. 2008; 3:1–25. doi: 10.1079/PAVSNNR20083074.[Cross Ref]

17. Babu R., O'Connor K., Seeram R. Current progress on bio-based polymers and their future trends. Prog. Biomater. 2013; 2:1–16. doi: 10.1186/2194-0517-2-8. [Cross Ref]

18. Duan J., Reddy K.O., Ashok B., Cai J., Zhang L., Rajulu A.V. Effects of spent tea leaf powder on the properties and functions of cellulose green composite films. J. Environ. Chem. Eng. 2016; 4:440–448. doi: 10.1016/j.jece.2015.11.029. [Cross Ref]

19. Thakur V.K., Thakur M.K. Handbook of sustainable polymers: Processing and applications. Pan Stanford Publishing; Singapore: 2016.

20. Van den Broek L.A.M., Knoop R.J.I., Kappen F.H.J., Boeriu C.G. Chitosan films and blends for packaging material. carbohydratepolymer. 2015; 116:237–242. doi: 10.1016/j.carbpol.2014.07.039. [PubMed][Cross Ref]

21. Rinaudo M. Chitin and chitosan: Properties and applications. Prog. Polym. Sci. 2006; 31:603–632. doi: 10.1016/j.progpolymsci.2006.06.001. [Cross Ref]

22. Pereda M., Aranguren M.I., Marcovich N.E. Water vapor absorption and permeability of films based on chitosan and sodium caseinate. J. Appl. Polym. Sci. 2009; 111:2777–2784. doi: 10.1002/app.29347.[Cross Ref]

23. Elsabee M.Z., Abdou E.S. Chitosan based edible films and coatings: A review. Mater. Sci. Eng. C. 2013; 33:1819–1841. doi: 10.1016/j.msec.2013.01.010. [PubMed] [Cross Ref]

24. Fajardo P., Martins J.T., Fuciños C., Pastrana L., Teixeira J.A., Vicente A.A. Evaluation of a chitosan-based edible film as carrier of natamycin to improve the storability of saloio cheese. J. Food Eng. 2010; 101:349–356. doi: 10.1016/j.jfoodeng.2010.06.029. [Cross Ref]

25. Epure V., Griffon M., Pollet E., Avérous L. Structure and properties of glycerol-plasticized chitosan obtained by mechanical kneading. carbohydrate. Polym. 2011; 83:947–952. doi: 10.1016/j.carbpol.2010.09.003. [Cross Ref]

26. Prajapati V.D., Maheriya P.M., Jani G.K., Solanki H.K. Carrageenan: A natural seaweed polysaccharide and its applications. carbohydrate. Polym. 2014;105:97–112. doi: 10.1016/j.carbpol.2014.01.067. [PubMed][Cross Ref]

27. Tavassoli-Kafrani E., Shekarchizadeh H., Masoudpour-Behabadi M. Development of edible films and coatings from alginates and carrageenan's. carbohydrate. Polym. 2016; 137:360–374. doi: 10.1016/j.carbpol.2015.10.074. [PubMed] [Cross Ref]

28. Necas J., Bartosikova L. Carrageenan: A review. Vet. Med. 2013;58:187–205

29. McHugh D.J. A Guide to the Seaweed Industry—FAO Fisheries Technical Paper 441. Food Agriculture Organization of the United Nations; Rome, Italy: 2003.

30. Bico S.L.S., Raposo M.F.J., Morais R.M.S.C., Morais A.M.M.B. Combined effects of chemical dip and/or carrageenan coating and/or controlled atmosphere on quality of fresh-cut banana. Food Control. 2009;20:508–514. doi: 10.1016/j.foodcont.2008.07.017. [Cross Ref]

31. Plotto A., Narciso J.A., Rattanapanone N., Baldwin E.A. Surface treatments and coatings to maintain fresh-cut mango quality in storage. J. Sci. Food Agric. 2010; 90:2333–2341. doi: 10.1002/jsfa.4095.[PubMed] [Cross Ref]

32. Pawar S.N., Edgar K.J. Alginate derivatization: A review of chemistry, properties and applications. Biomaterials. 2012; 33:3279–3305. doi: 10.1016/j.biomaterials.2012.01.007. [PubMed] [Cross Ref].

33. Freitas F., Alves V.D., Reis M.A., Crespo J.G., Coelhoso I.M. Microbial polysaccharide-based membranes: Current and future applications. J. Appl. Polym. Sci. 2014;131 doi: 10.1002/app.40047. [Cross Ref]

34. Kristo E., Biliaderis C.G. Physical properties of starch nanocrystal-reinforced pullulan films. Carbohydr. Polym. 2007; 68:146–158. doi: 10.1016/j.carbpol.2006.07.021. [Cross Ref]

35. Gniewosz M., Synowiec A. Antibacterial activity of pullulan films containing thymol. Flavour Fragr. J. 2011; 26:389–395. doi: 10.1002/ffj.2063. [Cross Ref]

36. Shih F.F., Daigle K.W., Champagne E.T. Effect of rice wax on water vapour permeability and sorption properties of edible pullulan films. Food Chem. 2011; 127:118–121. doi: 10.1016/j.foodchem.2010.12.096. [Cross Ref]

37. Singh R.S., Kaur N., Kennedy J.F. Pullulan and pullulan derivatives as promising biomolecules for drug and gene targeting. Carbohydr. Polym. 2015; 123:190–207. doi: 10.1016/j.carbpol.2015.01.032.[PubMed] [Cross Ref]

38. CPKelco Kelcogel® gellan gum book 5th edition. [(accessed on 22 February 2016)]. Available online:http://www.appliedbioscience.com/docs/Gellan_Book_5th_Edition.pdf.

39. Freitas F., Alves V.D., Coelhoso I., Reis M.A.M. Production and food applications of microbial biopolymers. In: Teixeira J.A., Vicente A.A., editors. Engineering Aspects of Food Biotechnology. CRC Press; Boca Raton, FL, USA: 2013.

40. Faria S., de Oliveira Petkowicz C.L., de Morais S.A.L., Terrones M.G.H., de Resende M.M., de França F.P., Cardoso V.L. Characterization of xanthan gum produced from sugar cane broth. Carbohydr. Polym. 2011;86:469–476. doi: 10.1016/j.carbpol.2011.04.063. [Cross Ref]

41.Palaniraj A., Jayaraman V. Production, recovery and applications of xanthan gum by xanthomonas campestris. J. Food Eng. 2011; 106:1–12. doi: 10.1016/j.jfoodeng.2011.03.035. [Cross Ref]

42. Torres C.A.V., Marques R., Antunes S., Alves V.D., Sousa I., Ramos A.M., Oliveira R., Freitas F., Reis M.A.M. Kinetics of production and characterization of the fucose-containing exopolysaccharide from enterobacter A47. J. Biotechnol. 2011; 156:261–267. doi: 10.1016/j.jbiotec.2011.06.024. [PubMed][Cross Ref]

43. Alves V.D., Freitas F., Torres C.A.V., Cruz M., Marques R., Grandfils C., Gonçalves M.P., Oliveira R., Reis M.A.M. Rheological and morphological characterization of the culture broth during exopolysaccharide production by *Enterobacter sp.* Carbohydr. Polym. 2010; 81:758–764. doi: 10.1016/j.carbpol.2010.03.048. [Cross Ref]

44. Torres C.A.V., Marques R., Ferreira A.R.V., Antunes S., Grandfils C., Freitas F., Reis M.A.M. Impact of glycerol and nitrogen concentration on enterobacter A47 growth and exopolysaccharide production. Int. J. Biol. Macromol. 2014; 71:81–86. doi: 10.1016/j.ijbiomac.2014.04.012. [PubMed] [Cross Ref]

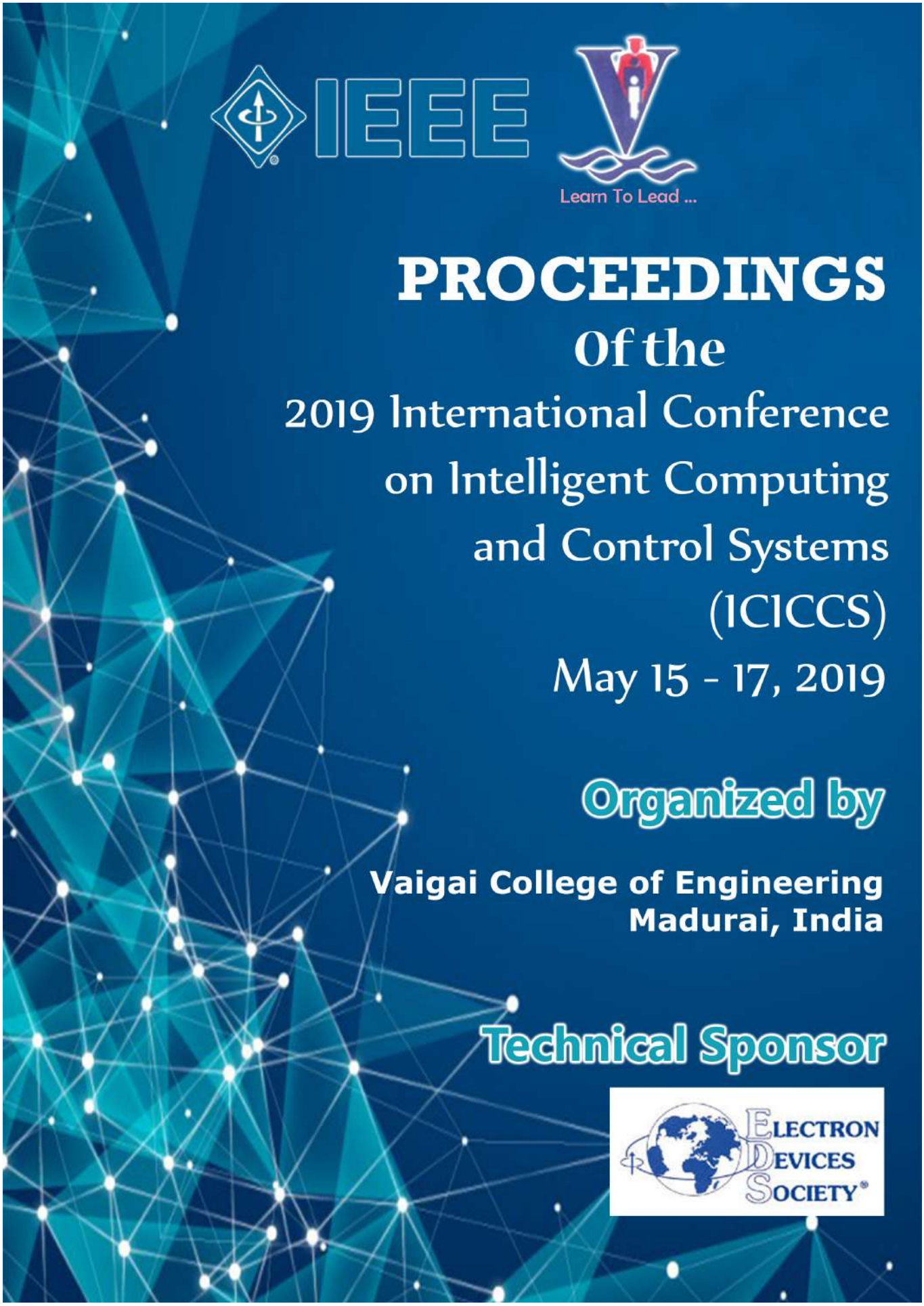
IEEE
Learn To Lead ...
PROCEEDINGS
Of the
2019 International Conference
on Intelligent Computing
and Control Systems
(ICICCS)
May 15 - 17, 2019
Organized by
Vaigai College of Engineering
Madurai, India
Technical Sponsor
ELECTRON DEVICES SOCIETY

Proceedings of the International Conference on Intelligent Computing and Control Systems (ICICCS 2019)
DVD Part Number:CFP19K34-DVD; ISBN: 978-1-5386-8112-1

QWERTY Keyboard in Virtual Domain Using Image Processing

Dr. Pallavi Khare
Associate Professor, Department of ECE
Matrusri Engineering College, Saidabad
Hyderabad, 500059, Telangana state, India
pallavi3386@gmail.com

K. Satya Ram, S. Sourabh, A. Mahender
B.E. students, Department of ECE
Matrusri Engineering College, Saidabad
Hyderabad, 500059, Telangana state, India
swargam.sourabh@gmail.com

***Abstract*—Individuals inside the cutting-edge times are occupied with genuine issues at hand and they don't have even one moment to squander. They battle to reduce their regular work by utilizing standard gadgets like Desktop Computers and Laptops, moreover further developed gadgets like cell phones and PCs. To improve the versatility and utility people will in general cut back the size of the gadgets. In this way the greater part of the cell phones and hand-held gadgets contain tiny keypads. Some of the people who utilize such a device think that it's hard to see the letters on the console. With a cell phone, a full-size physical keypad isn't perfect. Yet, options are accessible as written recognition, speech recognition and so forth but every one of them has severe short comings on the exactness and accommodation of a full-size keypad. This paper displays an imaginative virtual keyboard to beat the previously mentioned issues, which may be a feasible swap for fold-up keypad. The proposed device basically dependent on the vision based human-PC cooperation concept, image capturing and image processing technique that contains virtual keys similar to the size of conventional keys inside the ordinary QWERTY keyboard. This device comprises of 2 fundamental modules, in particular, Image Capturing, Character Identification and Mapping. The final product of the virtual keyboard project was a cost-effective, easy to understand and transportable virtual keyboard, that sends typed characters to any display device.**

Keywords—Interactive Surface, Virtual Keyboard, Image Capturing, Image Processing.

I. INTRODUCTION

As the interest for processing condition advances, new human-PC interfaces have been actualized to give various connections among clients and machines. By the by, the reason for most human-to-PC communications remains the binomial console/mouse. We are exhibiting here a cutting-edge innovation, which is the Virtual Keypad. As the name makes it obvious the virtual keypad has no physical appearance. Virtual console is an application which virtualizes equipment console with various formats consequently enabling client to change the design dependent on application. With different layouts hence allowing user to change the layout based on application. For example, client can choose diverse language for editorial manager or select a particular format for gaming applications. Client can even plan his very own design in hardware variant.

Ancient QWERTY keyboards occupy a comparatively large area and offer little in terms of enhancements [12]. Nowadays wireless keyboards are well-liked and are really popular. These keyboards provide a more robust feel and are more economical. Presently the keyboard technology has become static (remained the same) and their interactivity and usefulness would increase if they were created to be more dynamic. Varied on-screen virtual keyboards have been developed however it's troublesome to facilitate full sized console on the display because it creates obstacle to envision the papers being typewritten. Another major hindrance with on-screen keyboards is that they cannot be customized to suit various needs. Though alternative sorts of Virtual Keyboards exist; by utilizing technologies like 3D cameras. Owing to this, a sensible execution of such keyboards isn't possible. The Virtual Keyboard that we tend to introduce uses solely a regular internet camera, with no extra hardware.

In view of changes and advancements of small cameras in a few electronic devices, human pc interface scientists have explored the opportunity of executing a console style interface utilizing a camera as alternative for real console hardware. A webcam watches the client's hands, which lay on a level surface. The webcam may watch the hands from over the surface, or at associate degree angle. The virtual console's package examines those images in period to see the arrangement of keystrokes picked by the client. This innovation has numerous applications: in certain nations (for instance, India), people speak a few distinct dialects that make fabricating physical consoles for a few unique demographics infeasible. A webcam-based console will basically bolster a few dialects, Smart-phone or tablet clients may at times wish to utilize a full-sized console with their gadget, anyway as a general rule it is all around improbable to convey a physical console wherever an individual goes. Since most cell phones come outfitted with a camera, a camera-based console which uses a product code to investigate the clients

978-1-5386-8113-8/19/$31.00 ©2019 IEEE

input content and after that shows yield keystroke may give a product-based goals for this issue.

II. LITERATURE SURVEY

Keyboards are required in various computerized zones. Not just cell phones need a virtual keypad, additionally gadgets which make virtual zones, for instance computer generated reality or increased reality glasses, need to give content info potential outcomes.

In [1], a novel Interactive Projection System (IPS) was recommended, which allows bare fingers for touch detection on regular planar surfaces (e.g., desks, flat surfaces), with a single camera module and a pattern projector. The problem in uncovered finger contact recognition is getting back the contact data just from the 2-D picture grabbed by the webcam. The graphical UI (GUI) key is anticipated superficially and is altered by the finger while pressing it, and there is a critical positive connection between the key's bending and the finger's position relative to the surface. In this way, a novel, quick, and simple method was proposed which exploits the key's bending to recognize any contact between the finger and the surface. The proposed touch identification method is performed in three phases: 1) area of intrigue extraction through a homography mapping, by which the computational intricacy of the accompanying procedure is decreased; 2) the key's deformation discovery utilizing a unique edge location method, which considerably lessens the mistakes because of the impact of the finger's shadows and edges and 3) contact judgment by the key's deformation. A few innovations (e.g., virtual console, control point seeing), which utilize the proposed touch location technique dependent on the keys, are described in this paper. An assessment is done on the virtual console and the outcomes exhibit that the proposed methodology can recognize uncovered finger contact continuously with the incorrect location rate of 1.00%, false identification rate of 2.08%, and contact recognition rate of 96.92% at the run of the mill anticipated separation.

The aim in [2] was to execute a virtual console utilizing picture examination strategy, in particular, shadow analysis. This framework was actualized by utilizing one low-cost webcam which is fit for the purpose and catches RGB pictures of the client's fingertips, which come in contact with a designed surface or a console layout so as to distinguish a keystroke. In view of this data and an underlying alignment picture of the console layout the framework creates a discrete succession of keystrokes that can be utilized to type or control other programs. Recognizing the client's keystrokes implies playing out the accompanying two undertakings:

(i) Detecting the client's fingertips.

(ii) Determining the shadows in an area of every fingertip.

Changing the picture coordinates of any contact location to console arranges. Shadow analysis requests solid suppositions about the lighting and hand locations that will show up in virtual console pictures. Tragically, these assumptions are not really compensated with trustworthy execution. There were comparable troubles with fingertip ID. Both curves and angles form point procedures which can acceptably distinguish secluded fingertips, yet don't convey trustworthy execution when two fingers are converged into a solitary district or when one finger impedes another. Either method is inclined to allotting false-positives to finger-like items, especially knuckles. A really helpful virtual console dependent on shadow examination couldn't in any way, shape or form be fused into a current versatile working innovation. To accomplish far reaching appropriation, such an innovation must have a far lower error rate and a lot fewer lighting prerequisites.

In [3] proposed topology, a camera is mounted over any desired location. But the only criteria are that the camera should focus the entire keyboard layout and it comes to five important processes and they are, 1. Image Acquisition, 2. Interrupt Detection from Frame Sequence, 3. Finger Extraction using Threshold Algorithm, 4. Finger Tip Analysis by Edge Detection Method and 5. Key Extraction. The following are the drawbacks of this implementation.

1. Performance: By utilizing Java Media Framework as the stage makes the virtual console essentially slower and more memory-devouring than locally assembled languages, for example, C or C++.
2. User Interface: The regular view of GUI applications written in Java utilizing the Swing toolbox is altogether different from local applications.
3. Wastage of RAM: The java compiler allocates the memory in RAM to the program before the runtime, i.e., that is static allocation of memory is done. This might cause wastage of RAM resources and in turn cause the system to become much slower than is desired.

Blob Analysis as described in [4] is a basic strategy of machine vision dependent on investigation of predictable picture areas. All things considered it is a device of decision for applications in which the items being examined are obviously perceivable from the foundation of HSV model. HSL represents hue, saturation and lightness and is regularly likewise called HLS. HSV represents hue, saturation and value, and is likewise regularly called HSB (B for Brightness). A third model, basic in PC vision applications, is

978-1-5386-8113-8/19/$31.00 ©2019 IEEE

HSI, for hue, saturation and intensity. The image is blurred with increasing standard deviations. The difference between two successively images from video feed using back- ground subtraction method and the results are then stacked up. The movement of object will be captured and that object will be detected by the BLOB. The following are the disadvantages associated with this method of implementation.

1. Difficult for amateurs: If the client does not have programming background in C++.
2. Documentation is weak: In C++ programming language the documentation is not up to the mark. Now and then you need to have a decent comprehension of the method, and really read the code, on the grounds that the documentation does not generally clarify what the parameters imply and how they influence the result. The documentation does not generally accompany test code, and that makes it harder to get it.
3. Small machine learning library: A PC vision engineer every now and again needs many machine learning methods. This has a little arrangement of AI calculations contrasted with the functions accessible when you are utilizing Python.
4. Visualization and troubleshooting: Debugging and picturing is troublesome in C++. This is particularly valid in the event that you are thinking of another method starting with no outside help. As this means you can't refer to previously written code in case you come across any errors while compiling the program or any bugs while executing the program. The user needs to have an in-depth knowledge of C++ to be able to do this.

Based on the extensive research done on this subject matter it could be concluded that the virtual keyboard implementation could certainly be improved and the benchmark can be raised to a higher level. This can be achieved by updating the system and using better hardware with the ever-increasing performance of micro-processors and enabling the system with the image processing libraries of python.

III. PROPOSED SYSTEM

Every new invention and innovation start out as an idea which has to conceptualized and then realized. The idea of converting hand movements in the 3D space into actual meaningful data which could be correlated and used to type characters is very intriguing and proved quite challenging. In order to bring about and execute this idea we began by thinking what kind of hardware would support this system while being as small as possible. Once we figured out that the raspberry pi was the obvious choice next, we started to consider the tools that would enable us to realize this idea both hardware as well as software. The versatility offered by python3 and OpenCV in conjunction apart from being freeware seemed to offer the best solution to realizing it.

1. We depict the picture examination strategies used to change over the client's surface-contacts into keystrokes. Best in class camera based virtual console plans are executed utilizing a grouping of picture investigation strategies.
2. The framework's camera takes a picture "I" for processing. By doing skin segmentation on "I", we acquire a threshold picture with a locale "H" indicating the fingertips in the frame.
3. "H" is broken down to decide the areas of the client's fingertips. The reference recorded above decides the contours which converts these values to parameters which indicate the limits of "H" [7]. They translate fingertips with the focuses on the contours that enhance certain geometric values (for instance, shape). We observe two of these geometric methods to deal with finding the fingertips and look at their execution.
4. Given the evaluated fingertip locations, one must ascertain which fingertips are coming into contact with the console's keys.
5. To guide contact focuses to key presses, we expect the keys of the virtual console are portrayed as a regular quadrilateral. We expect the format of the console is informed at assembly time and the console layout has control focuses from which we can infer a point of view adjustment change [8]. At that point we convert the console space directions of the touch focuses to key presses.

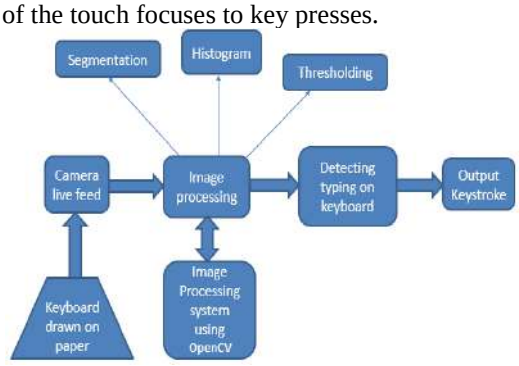

Figure 3.1: Block diagram of the proposed system

After contour detection is done, the compute module is able to determine which character is being pressed relying upon the zone change of the form. The edge estimation should be appropriately balanced with the goal that the framework can effectively, precisely and reliably determine which character is being composed. After extensive experimentation the ideal estimation of the limit form region was observed to be 100 units. When the zone traverses this limit the framework recognizes it as a key being squeezed.

978-1-5386-8113-8/19/$31.00 ©2019 IEEE

Algorithm

1. For the input live stream a steady audiovisual input is acquired from the camera in conjunction to the Raspberry Pi. A camera driver software (API) is utilized for this purpose.
2. Image capturing happens at standard periods of time (around 10 times each second), the present edge from the video is duplicated from one picture to another wherein we can observe and control the pixels.
3. Pre-Processing: An image handling method is utilized on the grabbed frame to enhance it for further handling. Here we either obscure the picture on the off chance that it could be excessively crisp. Otherwise we hone the picture in the event that the input stream is excessively obscured. Consequently, either honing or Gaussian blur method is utilized dependent on the nature of the feed.
4. Selective RGB: The pixels in the grabbed frame are sifted depending on the core components Red, Green and Blue parameters in the frame and the limit values for these parameters are determined.
5. Converting RGB image to HSV model: HSV is an abbreviation for Hue, Value, and Saturation. Hue speaks to shading type. It very well may be portrayed in term of point on the above circle [9]. Saturation speaks to dynamic quality of shading. Value speaks to splendor of shading. Converting the coloured or normal image into this model makes it easier for the system to then threshold the image.
6. A basic histogram for each and every symbol is built. Histogram is the recurrence of mean of the pixels (which will be either totally dark or totally bright in the wake of Thresholding).
7. Various advances in pattern matching and pattern recognition are utilized and connected to coordinate the example being put away and perceive the accurate example with the information given by client.
8. The result which is in the form of a keystroke utilizes the machine learning API, the yield keystroke is examined, which is then produced on the designated gadget.

Flowchart

To begin with, the virtual keyboard hardware is setup. The camera is slanted so that the keyboard setup is visible properly without any distortions and the webcam is focused correctly. The users hand motion is constantly captured by the webcam which sends this information to the Raspberry Pi through the link. The image handling software at that point makes an interpretation of the RGB picture into a threshold picture which makes it less complex for the framework to perform further processing on it. After the processing the system determines the contours of the user's finger, which is tracked and depending on the area of the contour judges that a specific character has been typed. Once the threshold value crosses 100 units the system determines that as the user's finger touching the surface. When this is done the character, which is composed is then shown on the screen. After this procedure is done the framework at that point checks for the following character to be entered. On the off chance that there is no other character to be entered, at that point the procedure arrives at an end.

The virtual keyboard implementation flowchart is shown in the figure 3.2.

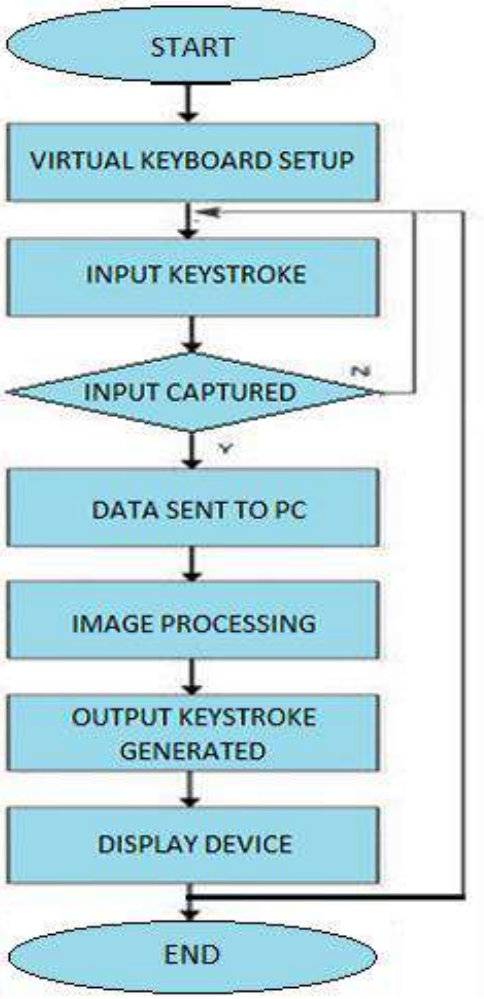

Figure 3.2: Flowchart of the Proposed System

A. Fingertip Detection

The initial phase in Image Processing includes assessing the areas of the fingertips (in picture space) with the assistance of the webcam. Given this geometrical information, we can utilize two methodologies for finding the fingertips in an image as visible in figure 3.3. The principal approach is to ascertain the exact contours, and corelate fingertips with coordinates. The second methodology is to ascertain the angles at which the fingertips are with coordinates [10]. Normally, each methodology requires processing of the grabbed frame by the webcam for distinctive

978-1-5386-8113-8/19/$31.00 ©2019 IEEE

algorithms to be viable and utilized. In any case, in every one of these methodologies image segmentation is done. Image segmentation is the method which parcels a complex picture into discrete but simpler fragments. The objective of this is to improve and additionally change the portrayal of a picture into something that is increasingly significant and simpler to examine. After it has been completed a picture histogram is created. A picture histogram is a sort of data representation method that portrays the tonal dissemination in a computerized picture in the form of a graph. It graphs the quantity of pixels for individual tonal parameter [12]. By taking a glance at the histogram for a particular picture an observer will most likely be able to assimilate whole tonal conveyance.

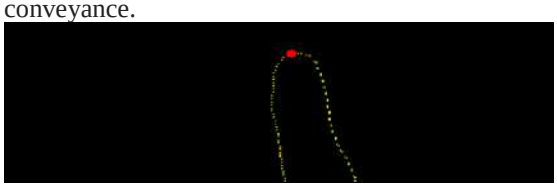

Figure 3.3: Fingertip detected, indicated by the red dot

B. Touch Detection

In this step of preparing, we give the evaluated co-ordinates of the fingertips as info and the yield is information containing data about which of those tips are assessed to be in contact with the interactive surface on which the keyboard layout is placed.

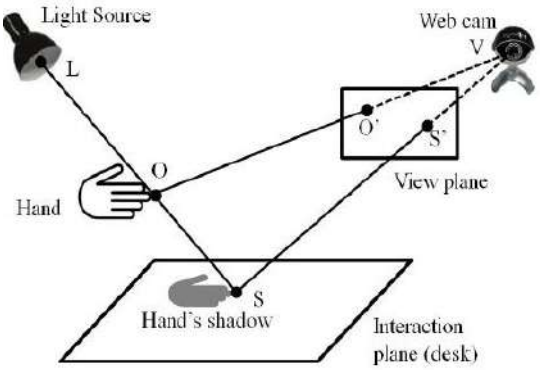

Figure 3.4: Shadow Analysis example

We can utilize a technique known as shadow analysis to take care of this issue of identifying when the hand is in contact with the plane (work area). The initial phase in shadow analysis aims at removing the dark pixels of the hands from the picture. We achieve this by thresholding the picture [11]. The outcome is built up in the wake of inspecting a few test pictures to investigate which fingertip is nearest to which key. We will in general look at a square of 20×20 pixels in the area of 'p' inside the parallel picture 'S'. On the off chance that level of dark pixels inside the area is lower than a standard predefined rate 's'. There is a fixed lower and upper limit of this threshold which determines when contact has taken place. These limits are shifted till the correct limit is found for accomplishing highest precision possible.

C. Mapping Touch Points to Keystroke

The preceding steps of operations yields a database of coordinates that gauge where the hand has interacted with the layout of the console. In this step, we depict how we decipher those image-space coordinates to rectilinear coordinates, and afterward to real keystrokes, rectifying for point of view [5]. Our framework accepts the format of the keyboard and it is comprehended at beforehand which the coordinates are sorted out inside a parallelogram of pre-determined dimensions. Our final layout would comprise of a parallelogram framework with keys, as described in Figure 3.5. We assign the 4-the board point's e_0, e_1, e_2, e_3. Each point has the accompanying co-ordinates $e_i = (a_i, b_i, c_i)$ inside the plane of the layout. We expect the webcam is put at a separation of d, and do the majority of our operations in this picture space [6]. To reduce effort, we expect the majority of our dimensional values have the same units. To get the coordinates of the control-points in picture space, we begin by thresholding the picture which is frame grabbed at the beginning of procedure.

The output thresholded image has four connected elements, we consider that the keyboard-layout is placed in order that the vectors e_1-e_0 and e_2-e_3 are parallel to the coordinate axis with dimension w and therefore the matrix $e_3- e_0$ and e_2-e_1 are orthogonal to the coordinate axis, with length h. The subsequent threshold picture has four associated components, we expect that the keyboard layout is adjusted all together that the vectors e_1-e_0 and e_2-e_3 are parallel to the facilitate hub with length w and accordingly the vectors e_3-e_0 and e_2-e_1 are opposite to the arrange pivot, with length h. These picture space co-ordinates are observed alongside the location of the fingertip which brings about distinguishing which key has been touched and the subsequent keystroke is then shown display screen [6]. The figure 3.5 is really a square shape when it's put on the desk yet in this model when the camera is slanted at a point the square shape appears to be a parallelogram. On the off chance that the camera is put vertically directly over the work area, at that point it shows up as a legitimate square shape.

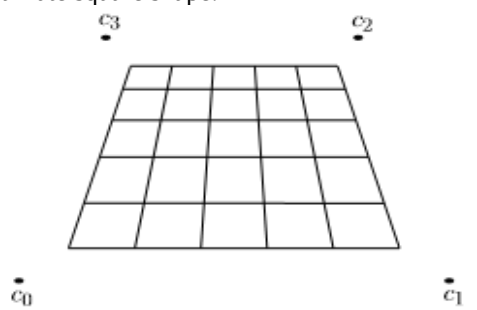

Figure 3.5: An example of the keyboard mat, under perspective projection

978-1-5386-8113-8/19/$31.00 ©2019 IEEE

The implementation of the project design can be divided in two parts.

1. Hardware which includes the interfacing of the Raspberry Pi with the USB webcam.
2. Firmware which constitutes the python code which utilizes the image processing libraries of OpenCV.

IV. CONCLUSION AND FUTURE SCOPE

In contrast to the past fundamental keyboard, Virtual Keyboard has rather more focal points for personalization, accommodation, and suitable for specific situations. For people with handicaps and uses where a few fast keystrokes are required Virtual keyboards can be of incredible use. This console is one of only a handful not many which utilizes microcomputer to actualize the capacities unlike the numerous virtual keyboards currently accessible in market. The exactness and precision of keys has been tried completely. In view of this we unquestionably reached a conclusion that this usage is effectively achievable and useful.

The genuine use of this notion would be in creating virtual consoles for cell phones, which could empower us to utilize a full measured QWERTY console without the requirement for extra occupying area or equipment. Also, the VK can be utilized for applications in virtual reality in the entertainment sector, 3D demonstrating and so on. In a nation like India, which has a rich store of dialects, a Virtual Keyboard can be utilized to accommodate multiple languages, by simply remapping of characters, with no adjustment in equipment. This can make consoles financially practical and can support multiple languages. At last, such a console makes the likelihood of creating particular consoles without extra consumption.

V. ACKNOWLEDGMENT

We would like to express our gratitude to the Head of the Department Dr. N. Srinivasa Rao and Dr. M. Sushant Babu for their timely cooperation while carrying out the paper work. It is their friendliness that made us feel free and learn more from them.

VI. REFERENCES

[1]. “Bare-fingers Touch Detection” by the Button’s Distortion in a Projector-Camera System by Jun Hu, Guolin Li, Xiang Xie, Zhong Lv and Zhihua Wang.

[2]. “A Camera Based Virtual Keyboard with Touch Detection by Shadow Analysis” by Joseph Thomas, December 10,2013.

[3]. “Webcam based virtual keyboard”, by R. Jayachandran, R. Sachidhanandham, at Proceedings of 10th ISERD International Conference, Dubai, UAE, 6th September, 2015.

[4]. “Virtual keyboard using BLOB analysis”, by K. Antara, S. Ayesha, F. Fernandes, C. Shubhangi, at International Journal of Computer Science Trends and Technology (IJCST) – Volume 4 Issue 2, Mar - Apr 2016.

[5]. “Virtual keyboard design: State of the arts and research issues”, by Sayan Sarkar, Soumalya Ghosh, Pradipta Kumar Saha, Debasis Samanta, at IEEE 3 APRIL 2010.

[6]. ”Virtual keyboard”, by Y. Aakansha, S. Chitra, V. Sriraman , S. Pooja, S. Priyanka, at International Journal of Science, Engineering and Technology Research (IJSETR), Volume 3, Issue 3, March 2014.

[7]. Y. Adajania, J. Gosalia, A. Kanade, H. Mehta, Prof. N. Shekokar, “Virtual Keyboard Using Shadow Analysis”, Third International Conference on Emerging Trends in Engineering and Technology, 2010.

[8]. H. Du, T. Oggier, F. Lustenberger and E. Charbon, “A virtual keyboard based on true3D optical ranging,” Proc. British Machine Vision Conference (BMVC), Oxford, pp. 220-229, Sept. 2013.

[9]. M. Hagara and J. Pucik. Fingertip detection for virtual keyboard based on camera. In Radioelektronika (RADIOELEKTRONIKA), 2013 23rd International Conference, page 356 to 360, 2013.

[10]. M. Hagara and J. Pucik. Fingertip detection for virtual keyboard based on camera. In Radioelektronika, 2013 23rd International Conference, page 356 to 360, 2013.

[11]. Baxes, G.A. “Digital Image Processing – Principles and applications” American 1994

[12]. Kolsch, M. and Turk, M. “Keyboards without Keyboard: A survey of virtual keyboards,” n.pag. University of California, November 5 2003.

978-1-5386-8113-8/19/$31.00 ©2019 IEEE

International Conference on Recent Innovations in Electrical, Electronics & Communication Engineering (ICRIEECE)

2.

27th & 28th July 2018

ICRIEECE Conference Proceedings

Organised by

School of Electrical Engineering
Kalinga Institute of Industrial Technology (KIIT)
Bhubaneswar, Odisha India.

(Deemed to be University U/S 3 of the UGC Act, 1956)

ISBN : CFP18P98-PRT/978-1-5386-5994-6

KIIT UNIVERSITY
Bhubaneswar Odisha India

Supported by

IEEE Advancing Technology for Humanity
IEEE Bhubaneswar Sub-Section
PGC
CSTPLI

method of malaria detection that is using microscope is the gold standard. But this method is time consuming and inefficient and results are inaccurate. Hence an automated method based on image classification that can identify malaria parasites present in the blood smear images is developed. This is useful where the expert in microscopic analysis is not available. Thin blood smear images are acquired, preprocessed, relevant features are extracted from them and is further segmented to make the processing faster and finally morphological operations based on shapes and sizes is carried out. Experimental results show that the proposed method is as efficient as the manual method or clinical method.

Power Quality Improvement using FLC based UPQC

Pratik Das, Samikshya Mishra and Santanu Sen

Abstract: The quality of the power is affected by many factors like harmonic contamination, due to the increment of non-linear loads, such as large thyristor power converters, rectifiers, voltage and current flickering due to arc in arc furnaces, sag and swell due to the switching of the loads etc. These problems are partially solved with the help of LC passive filters but cannot solve random variation in the load current and voltage waveform. Active filters can resolve this problem but its cost is high. One of the many solutions is the use of a combined system of shunt and active series filters like unified power quality conditioner which aims at achieving a low cost under highly effective control. In this paper compensation principle and different control strategies based on Fuzzy Logic based controller of the UPQC in detail are used. The control strategies are modeled using MATLAB/SIMULINK. The performance is also observed under influence of utility side disturbances such as harmonics, flicker and spikes. The simulation results are listed in comparison of different control strategies and for verification of results.

PS-DCT Image Functioned Framework for Steganography

Dr. Pallavi Khare, Dr. M. Sushanth Babu and Dr. Akhil Khare

Abstract: This research paper present a unique approach of Image primarily based steganography method wherever pseudorandom sequence generators operate is employed to randomize the mapping sequence in an exceedingly pseudorandom fashion. The embedding method of the key message is completed per the pseudo-random sequence, and extraction is completed exploitation identical sequence at the opposite side. At the bottom level, 2D-DCT is employed to cover the bits of secret message within the stego image by exchange the LSBs of DCT coefficients. Since in previous paper the LSB substitution technique is already used, here during this paper the previous concept is extended and used DCT rather than LSB technique. a replacement text randomization algorithmic rule (4-2 swap text randomization algorithm) is additionally accustomed modify the key message before embedding.

Optimization based Tuning of Fractional PID Controller for Small Hydro Power Plant

Himanshi Verma, K. Dhananjay Rao and Subhojit Ghosh

Abstract: The increased stress on the use of renewable energy has motivated the wide adoption of small hydro power plant for meeting the ever increasing power demand. The present paper proposes the design of fractional order PID controller using TLBO optimization approach for controlling the governor and excitation system of a prototype small hydro power plant. As compared to the classical integer order PID controller, the use of FOPID allows greater flexibility in achieving the controller

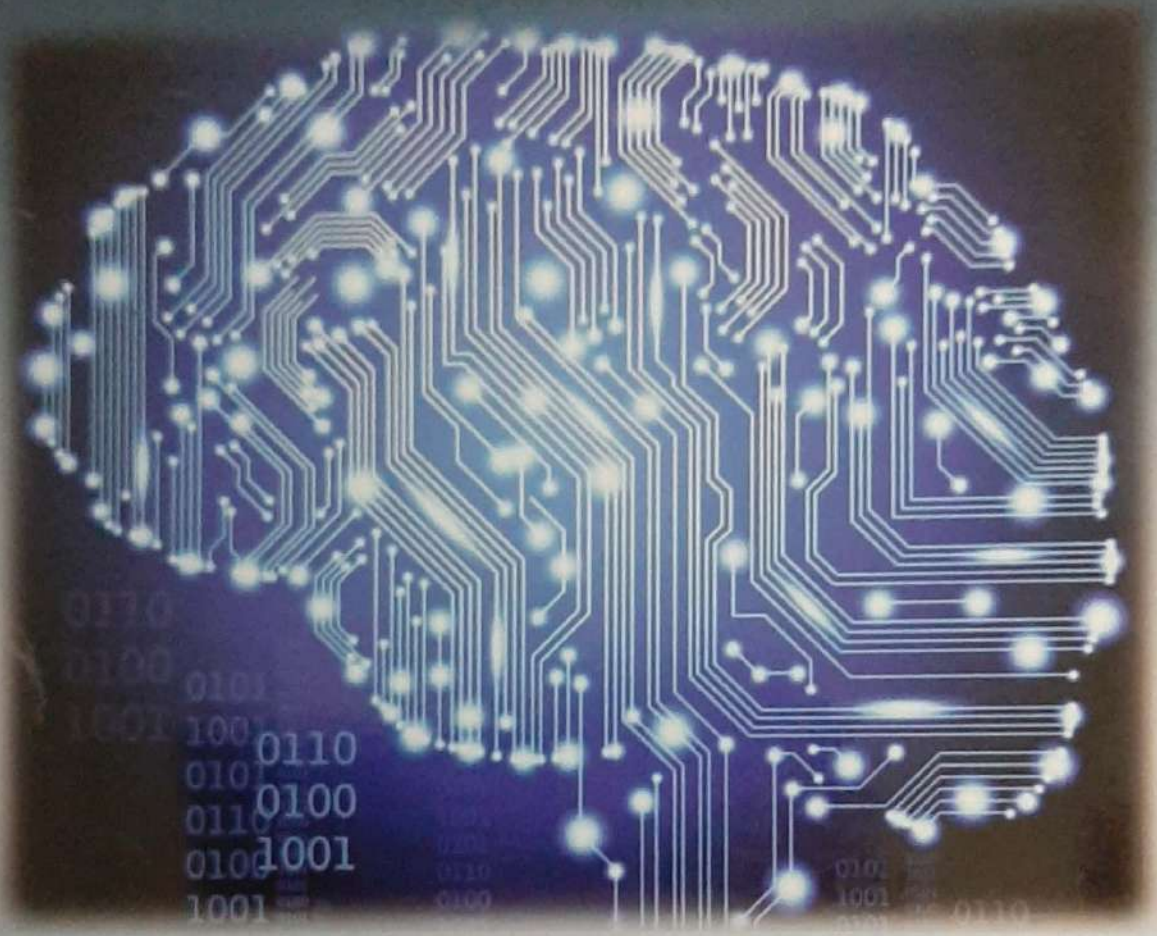

Supported by

IEEE Advancing Technology for Humanity

IEEE Bhubaneswar Sub-Section

PGC

CSTPLI

Website: www.rieece.org | www.pgcinfo.org

Contact: 0891-2761433

PS-DCT image functioned Framework for Steganography

Dr. Pallavi Khare[1] Dr. M. Sushanth Babu[2] Dr. Akhil Khare[3]
[1]Assistant Professor, ECE Dept.,MatrusriEngg. College, Hyderabad India, pallavi3386@gmail.com
[2] Professor, ECE Dept., MatrusriEngg. College, Hyderabad India, sushanth19.m@gmail.com
[3]Professor, CSE Dept., MVSR Engg. College, Hyderabad India, khare_cse@mvsrec.edu.in

***Abstract*-This research paper present a unique approach of Image primarily based steganography method wherever pseudorandom sequence generators operate is employed to randomize the mapping sequence in an exceedingly pseudorandom fashion. The embedding method of the key message is completed per the pseudo-random sequence, and extraction is completed exploitation identical sequence at the opposite side. At the bottom level, 2D-DCT is employed to cover the bits of secret message within the stego image by exchange the LSBs of DCT coefficients. Since in previous paper the LSB substitution technique is already used, here during this paper the previous concept is extended and used DCT rather than LSB technique. a replacement text randomization algorithmic rule (4-2 swap text randomization algorithm) is additionally accustomed modify the key message before embedding.**

Keywords – Steganography, Security, DCT, Pseudorandom.

I. INTRODUCTION

Steganography is the art as well as the science of concealing info into another covering media in such the simplest way that no-one except the supposed recipient is aware of concerning the key message and retrieve it. Steganography (means ―covered writing‖ in Greek) is Associate in nursing previous art that has been used since the golden age of Balkan country wherever some practices were recorded like: writing a message on a wood table then covering it with wax. different techniques use invisible ink, microdots, changing channels and character arrangement. Steganography may be a form of cryptography within which the key message is hidden in a very digital image. Steganography differs from Cryptography within the sense that wherever cryptography focuses on keeping the contents of a message secret, whereas steganography focuses on keeping the terribly existence of the message secret [1-3].

Various image primarily based steganography methodology specifically LSB (least-significant-bit), PVD(pixel-value differencing), GLM(gray level modification) and also the methodology projected by Ahmed et al. has been in brief mentioned within the following section.

A. Data Hiding by Least Significant Bit (LSB)

The most standard and common techniques is predicated on manipulating the least-significant-bit (LSB) [9], [10] and [11] planes by directly replacement the LSBs of the cover-image with the message bits. LSB methods generally come through high capability however unfortunately LSB insertion is susceptible to slight image manipulation like cropping and compression.

B. Data Hiding by Pixel Value Differencing Method

Another method proposed by Wu and Tsai, the pixel-value differencing (PVD) method can successfully provide both high embedding capacity and outstanding imperceptibility for the stego image. Based on PVD method, various approaches have also been proposed. Among them Chang et al. proposes a new method using tri-way pixel-value differencing.

C. Data Hiding by GLM

In 2004, Potdar et al. [11] proposes GLM (Gray level modification) technique which is used to map data by modifying the gray level of the image pixels. Gray level modification Steganography is a technique to map data (not embed or hide it) by modifying the gray level values of the image pixels.

D. Data Hiding by the Method Proposed by AHMAD et al.

In this work a novel Steganography technique for concealing data among the abstraction domain of the grey scale image has been planned. The planned approach works by dividing the quilt into blocks of equal size and so embeds the message within the fringe of the block reckoning on the quantity of ones in left four bits of the pixel. The paper has been organized in some sections. Section i discussed a short introduction and a discussion on the related works in the relevant field. Section II outlined concerning some steganographic strategies. Consequent section III delineates the planned procedure. Section IV delineates the general procedure via associate degree example. Next section V of the paper is concerning analyzing the experimental result. The last section VI concluded on the research paper.

II. STEGANOGRAPHIC METHODS

There are mainly three ways to hide a digital message in a digital cover [5][7][8][9].

A. Injection

Data injection embeds the key message directly within the host medium. The matter with this sort of embedding is that it always makes the host file larger, and so the alteration is less complicated to observe.

B. Substitution

Normal information is replaced or substituted with the key information. This typically leads to little or no size modification for the host file. However, counting on the sort of host file and also the quantity of hidden information, the substitution technique will degrade the standard of the first host file.

C. Generation of New Files

A cover is generated for the sole purpose of concealing a secret message. A sender creates image of one thing innocent that may be passed to receiver; the innocent picture is that the cover that has the mechanism for transference the message.

Digital images will be dealt in two totally different domains. One is that the abstraction domain, wherever the image is taken into account because the two dimensional array of pixels oriented in an exceedingly table format. On the opposite hand, within the frequency domain, Images are thought of as the digital signal transmitted through the physical media. Another method proposed by Wu and Tsai, the pixel-value differencing (PVD) method can successfully provide both high embedding capacity and outstanding imperceptibility for the stego image. Based on PVD method, various approaches have also been proposed. Among them Chang et al. proposes a new method using tri-way pixel-value differencing. During this research paper *2d* discrete cosinetransform (2D-DCT) technique [6] is employed rather than Least significant Bit (LSB) substitution technique as the basic hiding technique [4].

III. THE PROPOSED SCHEME OF STEGANOGRAPHY

In this paper a replacement image primarily based steganography scheme is presented within which both the key message yet because the cover image is split into a number of small but equal sized segments [4]. once that segmentation, separate segments of the key message are embedded by using LSB technique at the DCT coefficients of those image segments, however a selected section of the cover image for a selected section of text is chosen in an exceedingly pseudo-random fashion. This technique makes the embedding or insertion method tough, however imposes additional security [4]. Analysis might facilitate to discover that steganography has been silent on the cover image, however attackers can't be able to extract the key message from the cover image without knowing the parameters employed in this method.

A. Embedding Method

This new steganography technique is block mapping technique. The complete Steganography method has two components. One half is to insert or hide the key text message within a canopy image, desirable coloured image. This method is completed at the sendingend. Another half is employed at the receiving end to extract the first secret text message from the stego-image.

STEP 1:

The secret message is taken as the primary input. This is the secret message to be hidden inside the cover image. Total number of characters (*Ch*) of the secret message is counted.

STEP 2:

A unique integer number named Threshold (*T*) is calculated through a novel message digest mechanism. It takes a one-time password, a set Key (For advanced security purpose) and therefore the secret message as input. looking on the total range of characters and therefore the strength of password, Threshold is calculated.

STEP 3:

This Steganography algorithmic rule segments the entire text into some equal sized blocks known as Cells containing equal range of characters. The size of e a c h cell (denoted as *C*) depends on the amount of characters within the secret message and therefore thevalue of Threshold. the dimensions is calculated by adding the digits of the full range of characters (*Ch*) within the text and Threshold (*T*) i.e. the amount of character per cell or size of cell denoted by

$$C = sum\ of\ digits\ of\ Ch + T \tag{1}$$

STEP 4:

To calculate the entire range of Cell(s) (denoted by C_T), divide the entire no of characters (*Ch*) by the size of each cell (denoted as *C*).the size of every cell(*C*) might not always be an element of the entire range of characters (*Ch*). thus take the ceiling value of the result and add some redundant bit(s) when the last character of the last cell to equalize it with others. Spaces, dots or any other image are often accustomed fill the amount of required characters in each cell. Total numbers of cells are calculated by

$$C_T = \left\lceil {}^{Ch}/_{C} \right\rceil \tag{2}$$

STEP 5:

By considering each character is consisting of 7 bits (ASCII values), total number of bits (*b*) in a cell is calculated by multiplying the size of cell (*C*) with 7. Each bit requires a LSB of 2D-DCT coefficient of each logical block of the cover image for embedding purpose. To hide a cell containing text required *C*×7 bits.

STEP 6:

This calculation depends on stowing away of content into measure up to estimated square pieces of cover picture. That implies, the cover picture must be partitioned or portioned into various equivalent estimated consistent square pieces. Each intelligent piece will shroud a specific cell of content. As in light of the fact that the measurement of each consistent piece of picture is square, discover the square foundation of b and get the entire number closest and bigger than square base of b. This number gives the measurement of each sensible piece of picture that conceals a unit of content, i.e. right roof of foundation of b:

$$D = \lceil \sqrt{b} \rceil \tag{3}$$

STEP 7:

The measurement is then ascertained as D × D. This is the measure of each square formed legitimate piece of the cover picture and 2D-DCT is connected on each of those pieces. To make the concealing procedure fruitful, D × D must be more noteworthy than or equivalent to the quantity of bits in a unit (b), i.e.

$$D \times D \geq b \ \text{ or } \ D2 \geq b \tag{4}$$

STEP 8:

A general limitation is determined to the measurement of the cover picture, for example, cover picture must be a 800 × 600 picture. That implies width of the cover picture *W* is 800 pixels and tallness *H* is 600 pixels. *D* is the measurement of each legitimate square piece. Subsequent to isolating tallness and width of the cover picture by *D*, and overlooking the partial piece of the outcomes, figure $M = H/D$ and $N = W/D$. *M* and *N* are the quantity of intelligent divisions alongside tallness and width of the photo and length of every division is

D. The aggregate number of consistent squares of picture indicated by B = M × N, where B is add up to number of Cells. B must be more noteworthy than CT, i.e. B > CT

$$M = H/D \text{ and } N = W/D \quad \text{and} \quad B = M/N \qquad (5)$$

STEP 9:

In this progression, the whole cover picture is fragmented into *B* number of legitimate square pieces. On each of those legitimate $D \times D$ square pieces, 2D-DCT is connected and coefficients are ascertained.

STEP 10:

After division of the cover picture into *B* number of intelligent squares, relegate some particular block(s) to shroud the mystery message of a specific cell into it. This task of square number is done in a pseudo-arbitrary design utilizing a stomach related mapping capacity. Mapping is done in pseudo-arbitrary mold so that amid extraction, a similar pseudo-irregular grouping can be created, yet it will be hard to foresee any example of mapping. The mapping capacity relies upon size of Cell(*C*), Threshold (*T*) and aggregate number of Blocks (*B*).

$$B_i = F_{mapping}(C, Threshold, B) \qquad (6)$$

To create a pseudo-arbitrary succession that will indicate the specific locales for every unit of content, area recognizable proof numbers or district ID number, likewise called as piece numbers must be remarkable, whatever the quantity of squares ought to be. Another confinement must be kept up here which is the upper bound of the produced number. The qualities must not surpass the aggregate number of squares (*B*). This suggests the capacity must be a modulus capacity of *B* or (*B*+1). To produce the pseudo-arbitrary grouping having adequate spaces between the numbers with the goal that likelihood of getting covered or to maintain a strategic distance from crashes between those numbers, a base separating is presented by including energy of *C* and Threshold esteem. Exploratory outcome demonstrates that the mapping capacity works best if the articulation will be as per the following:

$$B_i = [(T^i \times C^i) mod(B - i)] + i \qquad (7)$$

Where i =1,2,3… C_T. B_i is a pseudo-arbitrary number created for a particular estimation of C_{Ti}. *Bi* is the square number of unit number C_{Ti}.

STEP 11:

Every unit of content is changed over to bit stream and afterward the bit stream is randomized utilizing another randomization system called ―4-2 swap content randomization method‖. Utilizing this randomization strategy, the randomized grouping can be changed over again into the first arrangement. The capacity likewise takes Threshold and Passkey as contribution for doing randomization. This makes the procedure one time and solid.

STEP 12:

Subsequent to doing this randomization of the bit-stream, inserting of the mystery message is finished by supplanting the LSB of each DCT coefficient of each chose intelligent piece of cover picture.

STEP 13:

The stego-picture in the change area is then changed over into the spatial space by applying IDCT. The stego-picture got is like the cover picture and the contrast between the two pictures is not recognizable by the human eye [6]. This picture is really transmitted to the goal over the open and unreliable channel. Fig1 delineates the infusion technique for the mystery message inside the cover picture.

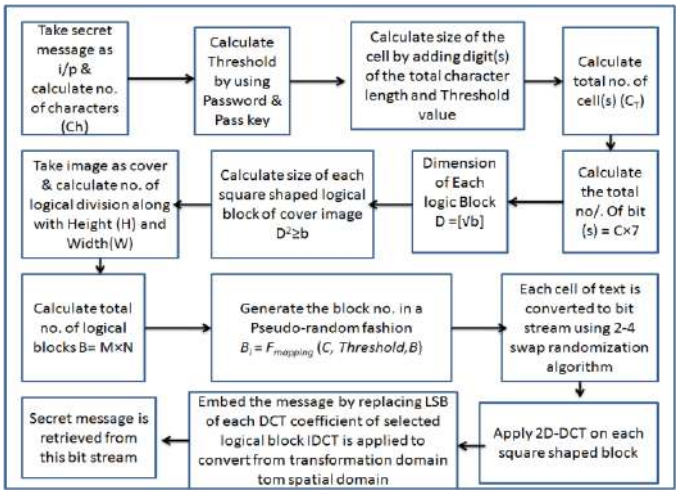

Fig. 1. SP-AM algorithm of embedding of secret message

B. Retrieval Method

The recovery of the mystery message from the stego-picture is finished by following a similar calculation connected for installing the mystery message. Every one of the means depicted before are rehashed for the stego-picture at the less than desirable end with the exception of the IDCT technique, on the grounds that there is no compelling reason to change over the picture from change area to spatial space. After the division of the picture, 2D-DCT is connected on the stego-picture [6]. At that point LSBs are separated from the DCT coefficients of each intelligent square. After extraction of the whole piece stream of the mystery message, the ―4-2 swap‖ randomization work is connected on it.

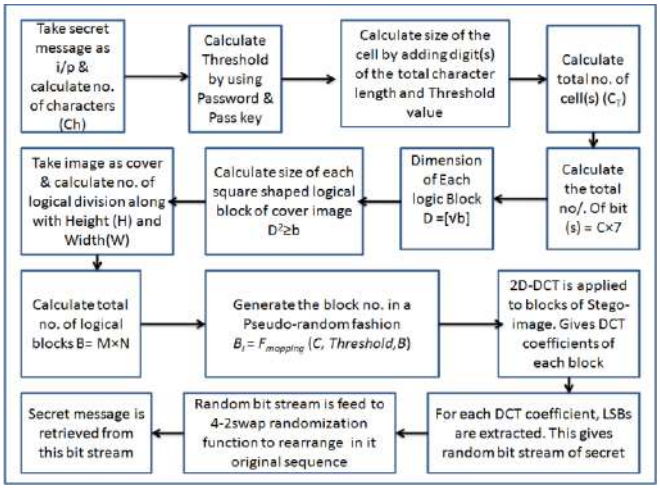

Fig. 2.SP-AM algorithm of retrieval of secret message

As this capacity is a reversible capacity, it re-organizes the bit stream into its unique grouping. Presently from this bit

stream, the mystery message is produced. Fig 2 demonstrates the recovery strategy for the mystery message from the cover picture.

C. Utilization of 2D-DCT on Cover Image

The essential thought to shroud data in the recurrence area is to modify the size of the majority of the DCT coefficients of cover picture. The 2-D DCT change over the picture hinders from spatial space to recurrence area. The schematic piece chart of the entire procedure is given in Fig 3 and Fig 4.

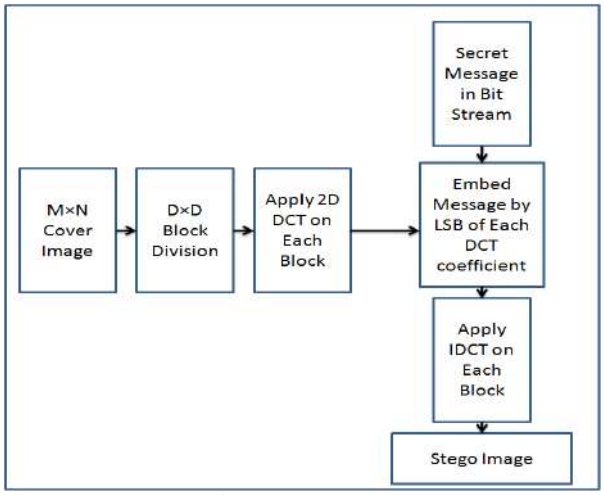

Fig. 3. Insertion of a secret message into a cover image

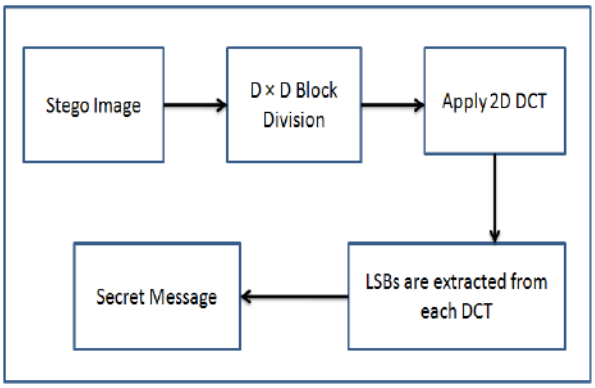

Fig. 4. Retrieval of a secret message into an cover image

Let $I(x,y)$ denote an 8-bit grayscale cover-image with x = 1,2,…….,M and y = 1,2,…….,N. This M×N cover-image is divided into D × D blocks and two-dimensional (2-D) DCT is performed on each of L = M×N / D^2 blocks.
The mathematical definition of DCT is:

Forward DCT:

$$F(u,v) = \frac{1}{4}C(u)C(v)\sum_{x=0}^{7}\sum_{y=0}^{7} f(x,y)Cos\left[\frac{\pi(2x+1)u}{16}\right]Cos\left[\frac{\pi(2y+1)v}{16}\right] \quad (8)$$

For u = 0,…,7 and v = 0,…,7

Where $C(k) = \begin{cases} \frac{1}{\sqrt{2}} & , for\ k = 0 \\ 1 & , otherwise \end{cases}$

Inverse DCT:

$$f(x,y) = \frac{1}{4}\sum_{u=0}^{7}\sum_{v=0}^{7} C(u)C(v)F(u,v) * Cos\left[\frac{\pi(2x+1)u}{16}\right]Cos\left[\frac{\pi(2y+1)v}{16}\right] \quad (9)$$

For $x = 0, \ldots\ldots,7$ and $y = 0, \ldots\ldots,7$.

D. 4-2 Swap Text Randomization Method

The secret message is randomized before the embedding process to impart more security to the entire steganography process. The randomization algorithm is described here.

I. The secret message is taken as input & the length of the message is calculated.
II. The entire message is segmented into some equal sized cells & padding space if required. Number of cells depends on the total no of characters (Ch) & size of cell(C).
III. Evaluate the ASCII values for all characters of each part for the secret message.
IV. Modify the ASCII values by using the Passkey & Threshold value.
V. Convert each ASCII value into its corresponding 8bits binary value for each character.
VI. Swap left most 4bits with the right most 4bits binary value.
VII. Swap first two bits with last two bits for efficient randomization for binary image
VIII. Convert each 8bits binary value into its corresponding hexadecimal value.

The block diagram of Fig 5 depicts the text randomization process applied on the secret message before embedding.

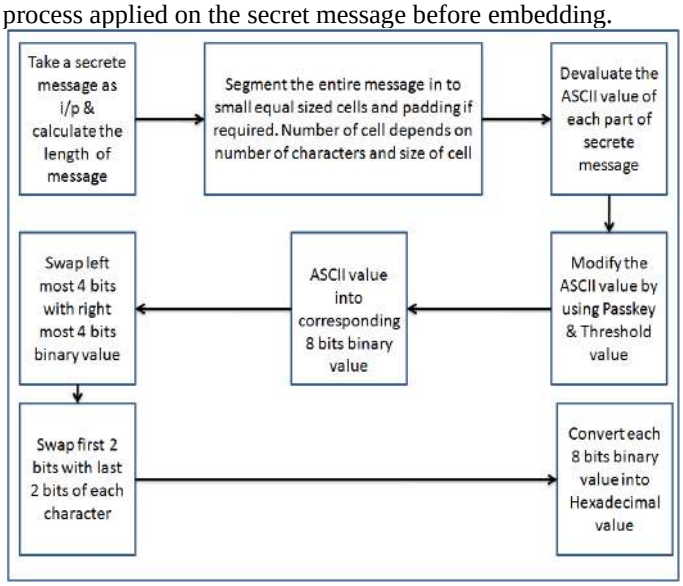

Fig. 5. 4-2 Swap text randomization method

IV. IMPLEMENTATION OF AN EXAMPLE

A. Illustration of 4-2 swap Text Randomization Method

The content randomization strategy is delineated with a case in this area. For instance consider the mystery message as ―the college foundation of innovation at burdwan‖.

Here, add up to number of characters (Ch) = 49
Assume the computed Threshold (T) = 7

The measure of Cell(C) = 4+9+7 = 20
Add up to number of cell required = roof (49/20) = 3
Min number of character must contain every cell = roof (49/3) = 17.
To level every cell with same number of character require ((17*3)- 49) = 2 underscores (_) or spaces( ) to add after the last character of the mystery message.
Presently every one of the cells contain measure up to number of characters.

Cell 1 = "the university in" = 17
Cell 2 = "statute of techno" = 17
Cell 3 = "logy at burdwan_" = 17.

Presently for cell 1 the message is "the university in".

The accompanying table demonstrates that after alteration of each character the comparing ASCII esteems are:

Table 1. Result of 4-2 Swap Text Randomization Method Characters Modified ASCII 8 Bits Binary Equivalent 4 Bits Swapped Binary Equivalent First 2bits swap with Last 2bits Decimal Equivalents

TABLE1 : RESULT OF 4-2 SWAP TEXT RANDOMIZATION METHOD

Character	**Modified ASCII**	**8 Bits Swapped Binary Equivalent**	**4 Bits Swapped Binary equivalent**	**First 2 bits Swap with Last 2 bits**	**Decimal Equivalents**
T	129	10000001	00011000	00011000	024
h	117	01110101	01010111	11010101	213
e	114	01110010	00100111	11100100	228
	45	00101101	11010010	10010011	147
u	130	10000010	00101000	00101000	040
n	123	01111011	10110111	11110110	246
i	118	01110110	01100111	11100101	229
v	131	10000011	00111000	00111000	056
e	114	01110010	00100111	11100100	228
r	127	01111111	11110111	11110111	247
s	128	10000000	00001000	00001000	008
i	118	01110110	01100111	11100101	229
t	129	10000001	00011000	00011000	024
y	134	10000110	01101000	00101001	041
	45	00101101	11010010	10010011	147
i	118	01110110	01100111	11100101	229
n	123	01111011	10110111	11110110	246

In this mold the changed decimal likeness ASCII benefits of comparing characters will produce. Thus another two tables for Cell2 and Cell3 individually will likewise create. So the mystery content is randomized utilizing an interesting capacity which called as 4-2 swap content randomization strategy. In the wake of getting the decimal equal estimations of the considerable number of characters, a bit stream is created from each of them and that bit stream is installed by supplanting the LSBs of all DCT coefficients of the cover picture.

B. Algorithm Used for Embedding the Secret Message

The algorithm used for embedding process is illustrated in this section. Here the calculation of the Threshold value is also shown.

STEP 1

Take a string as input & calculate the length.

STEP 2

Calculate the Threshold T

$$T \leftarrow C \,\%\, 9$$
$$T \leftarrow T + P_L$$
$$T \leftarrow T \,\%\, 9$$
$$T \leftarrow T + \left[(9 - X)\left((P_L - P_M)/P_L\right)\right]$$

(Where P_L=Original Password Length & P_M=Minimum Password Length/Passkey).

STEP 3

Ascertain the measure of unit (u) by including the digit(s) of the string length and the Threshold (T).

STEP 4

Ascertain the aggregate number of unit (U)

$$U \leftarrow [C/u]$$

STEP 5

Ascertain Bits per unit (B)
$B \leftarrow u \times 7$ (Each Character is of 7 bits)

STEP 6

Ascertain the measurement of each legitimate piece (D)

$$D \leftarrow \lceil \sqrt{b} \rceil$$

STEP 7

Figure the Total Dimension *(D^2) and $D^2 \geq B$*

STEP 8

Take a picture as information and compute number of consistent division alongside Height (H) and Width (W)

$$M = H/D \& N = W/D$$

STEP 9

Figure the Total no. of Logical pieces (B)

$$B \leftarrow M \times N$$

STEP 10

Create the piece numbers by

$$B_i \leftarrow [(F^i \times u^i) mod(B - i)] + i$$

Where $i = 1 to\ n$

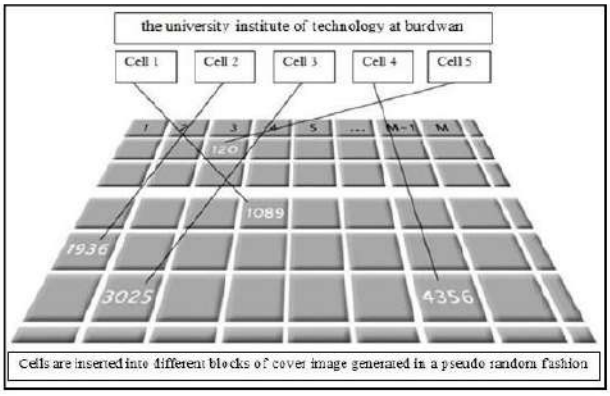

Fig. 6. A realistic view of block mapping process

Modify the ASCII values by using the Passkey & Threshold value.

STEP 11

Evaluate the ASCII values for all characters of each part for the secret message.

STEP 12

Modify the ASCII values by using the Passkey & Threshold value.

STEP 13

Convert each ASCII value into its corresponding 8bits binary value for each character.

STEP 14

Swap left most 4bits with the right most 4bits binary value.

STEP 15

Swap first two bits with last two bits for efficient randomization for each binary value.

STEP 16

Convert each 8bits binary value into its corresponding hexadecimal value.

STEP 17

Get DCT coefficients of all the D x D logical segments of the cover image.

STEP 18

Replace the LSBs of DCT coefficients by the bits of the modified bit stream of secret message generated by the 4-2 swap randomization method. Fig 7, Fig 8 and Fig 9 shows the secret message, cover image and stego-image respectively.

Fig. 7. Secret text

Fig.8.Cover Image

Fig. 9. Stego Image

This algorithm illustrates the whole embedding process at the sending end. After embedding the secret message, IDCT is applied [6] on the image to convert it from transform domain to spatial domain and the output stego-image is generated.

V. RESULT ANALYSIS

Exploratory outcome demonstrates that 2D-DCT grants more unwavering quality and security as opposed to the LSB substitution method. Some assessment parameters are utilized to gauge the execution of the calculation. The regular assessment parameters are [6] [9] MSE, PSNR, Capacity and so on.

Mean Square Error (MSE)

It is defined as the square of error between cover image and stego-image. The distortion in the image can be measured using MSE and is calculated using the following equation

$$MSE = \left[\frac{1}{N \times N}\right]^2 \sum_{i=1}^{N} \sum_{j=1}^{N} (X_{ij} - \overline{X_{ij}})^2 \qquad (10)$$

Where X_{ij}= The intensity value of the pixel in the cover image

$\overline{X_{ij}}$= The intensity value of the pixel in the stego image

N=Size of the image

Peak Signal to Noise Ratio (PSNR)

It is the measure of quality of the image by comparing the cover image with the stego-image, i.e., it measures the statistical difference between the cover and stego-image, and is calculated using the following equation.

$$PSNR = 10 log_{10} \frac{255^2}{MSE} \text{ db} \qquad (11)$$

Capacity

It is the size of the data in a cover image that can be modified without deteriorating the integrity of the cover image. The steganography embedding operation needs to preserve the statistical properties of the cover image in addition to its perceptual quality. Capacity is represented by bits per pixel (bpp) and the Maximum Hiding Capacity (MHC) in terms of percentage [6].

Experimental result shows that the new approach using DCT coefficient is better than that of the earlier method using LSB substitution technique. Taking the picture of Lena and converting it into a 800×600 dimensional image, the following table shows the MSE values for 3 different block sizes.

TABLE 2. EXPERIMENTAL RESULT

Image Block Size	Technique	MHC (%)	PSNR (dB)	MSE
150 ×150	LSB	55	39.56	32.45
	DCT	57	37.82	32.38
200 ×200	LSB	46	38.58	32.28
	DCT	48	32.62	32.14
400 ×400	LSB	34	35.90	28.98
	DCT	34	32.46	26.87

VI. CONCLUSION

This steganography calculation infers a multi-level security in light of the fact that before installing the characters of the mystery instant message into a cover picture utilizing 2D-DCT, the whole content is divided first into different cells and each fragment of mystery message are randomized at bit level. This randomization or change is finished utilizing a one of a kind capacity which is a reversible capacity, i.e. the capacity can re-create the first succession from the randomized yield. Again every one of the fragments of content are arbitrarily embedded into various areas of the cover picture. A bit-stuffing technique is utilized to make the quantity of characters of every unit measure up to. Another pseudo-irregular succession generator work is utilized to produce a pseudo-arbitrary arrangement to install each of the unit of mystery message into the sensible square areas or pieces of the cover picture in a pseudo-arbitrary mold. Utilizing a similar pseudo-arbitrary grouping, extraction should be possible to get the first message. As specified before, the information esteem named Threshold (T) of the pseudo-irregular arrangement generator work relies upon the mystery secret key and a passkey known to the two expected gatherings (sender and beneficiary) as it were. As these are mystery esteems, another level of security is likewise forced here. This technique can be enhanced again by expanding the quality of edge esteem era work, altering the strategy for ascertaining the aggregate number of characters in every unit of message and furthermore by forcing the randomization work (4-2 swap randomization technique) at the character level and in addition at the bit level. Here 2D-DCT strategy is inferred rather than LSB substitution method in this broadened rendition of the past paper.

REFERENCES

[1]. Abdelhamid Awad Attabya, Mona F.M. Mursi Ahmedb, Abdelwahab K. Alsammak "Data hiding inside JPEG images with high resistance to steganalysis using a novel technique: DCT-M3" Ain Shams Eng J (2017) Production and hosting by Elsevier B.V.

[2]. Ahlem Fatnassi ; Hamza Gharsellaoui ; Sadok Bouamama A Novel Approach for Embedding Information in Image Cover Media with Security " World Symposium on Computer Applications & Research (WSCAR), 2016 , added in IEEE explore : 22 December 2016

[3]. S.G. Shelke, S.K. Jagtap A novel approach: Pixel matching based image steganography International Conference on Pervasive Computing (ICPC), 2015 added in IEEE Explorer : Sept 2015.

[4]. Rupali Bhardwaj , Vaishali Sharma Image Steganography Based on Complemented Message and Inverted bit LSB Substitution Elsevier Procedia Computer Science 93 (2016) 832 – 838.

[5]. Huang W, Zhao Y and Rong-Rong Ni, Block-based Adaptive Image Steganography using LSB Matching Revisited, Journal of Electronic Science and Technology, Vol. 9 (4), 2011.

[6]. S. Pujari, S. Mukhopadhyay, ―An Image based Steganography Scheme Implying Pseudo-Random Mapping of Text Segments to Logical Region of Cover Image using a New Block Mapping Function and Randomization Technique‖, International Journal of Computer Applications (0975 – 8887) Volume 50 – No.2, July 2012.

[7]. Yang C and Wang S, Transforming LSB Substitution for Image-based Steganography in Matching Algorithms, Journal of Information Science and Engineering 26, 1199-1212, 2010.

[8]. Shiva Kumar K B, Raja K B, Chhotaray R K, Pattanaik S, Bit Length Replacement Steganography Based On DCT Coefficients, International Journal of Engineering Science and Technology, Vol. 2 (8), 3561-3570, 2010.

[9]. Potdar V.and Chang E. Gray level modification steganography for secret communication. In IEEE International Conference on Industria lInformatics, pages 355–368, Berlin, Germany, 2004.

[10]. HongmeiTang, GaochanJin, Cuixia Wu and Peijiao Song. (2010): ―A New Image Encryption and Steganography Scheme,‖ IEEEInternational Conference on Computer and Communication Security, pp 60 – 63.

[11]. Mahdi Ramezani and Shahrokh Ghaemmaghami. (2010): ―Adaptive Image Steganography with Mod-4 Embedding using Image Contrast‖, IEEE Consumer Communication And Networking Conference.

[12]. Cheng-Hsing Yang, Shiuh-Jeng Wang, ―Transforming LSB Substitution for Image-based Steganography in Matching Algorithms‖, Journal of Information Science and Engineering 26, 1199-1212 (2010).

Shri Vile Parle Kelavani Mandal's

Dwarkadas J. Sanghvi College of Engineering

(Approved by AICTE & Permanently Affiliated to the University of Mumbai)

No. U-15, J.V.P.D. Scheme, Bhaktivedanta Swami Marg,
Opp. Cooper Hospital, Vile Parle (West), Mumbai-400 056.

International Conference on Intelligent Manufacturing and Automation
ICIMA 2018

Certificate

This is to certify that Dr./Mr./Ms. C. Venkateshwar Reddy

has participated/presented a paper titled Effect of Benzoxazine on Epoxy based Carbon Fabric Reinforced Composites for High Strength Applications

in the International Conference on Intelligent Manufacturing and Automation (ICIMA 2018) organised by the Departments of Mechanical Engineering and Production Engineering on 20th and 21st July 2018 at DJSCE, Mumbai.

Dr. K. N. Vijaya Kumar
Joint Convenor

DWARKADAS J. SANGHVI COLLEGE OF ENGINEERING MUMBAI 400 056

Dr. Hari Vasudevan
Convenor

Effect of Benzoxazine on Epoxy Based Carbon Fabric Reinforced Composites for High Strength Applications

C. Venkateshwar Reddy, Ch. Joseph S. Raju, P. Ramesh Babu and R. Ramnarayanan

Abstract Benzoxazine (BZ) is novel class of thermoset polymers exhibiting tailor-made properties in a wide range of structural applications especially in aerospace industries. When BZ is used as hybrid resin in composite preparation, it offers attractive mechanical properties. An attempt was made with combination of DGEBA epoxy resin and an aromatic diamine hardener with different weight proportions of BZ 2, 4, 6, 8 and 10% reinforced with PAN-based carbon fabric, in order to study the mechanical characteristics. The weight proportions of BZ enhanced the properties of tensile strength, Flexural strength and inter-laminar shear strength (ILSS) due to strong interfacial adhesion between fabric and hybrid resin system. The studies reveal that 4% of BZ-reinforced composites possess better properties than those of the reference neat epoxy–amine matrix and other weight percentages of composites. In this study, the mechanical, thermal properties of the hybrid were compared with reference epoxy–amine matrix composite. Optical microscope images ascertain the existence of homogeneous distribution of benzoxazine in the composites. The Glass transition temperature (T_g) was determined by Dynamic Mechanical Analyzer (DMA) technique reveals lowering of T_g in hybrid due to off-stoichiometry by the incorporation of BZ. However, post-curing of the composite enhanced both mechanical and thermal properties.

Keywords Benzoxazine (BZ) · Hybrid resin · Weight proportions · DMA Mechanical properties · Off-stoichiometry · Post-curing

C. V. Reddy (✉)
Matrusri Engineering College, Hyderabad 500059, India
e-mail: cvreddy36@gmail.com

Ch. J. S. Raju · R. Ramnarayanan
Advanced Systems Laboratory, Hyderabad 500069, India

P. R. Babu
University College of Engineering, Osmania University, Hyderabad, India

© Springer Nature Singapore Pte Ltd. 2019

H. Vasudevan et al. (eds.), *Proceedings of International Conference on Intelligent Manufacturing and Automation*, Lecture Notes in Mechanical Engineering,
https://doi.org/10.1007/978-981-13-2490-1_32

1 Introduction

An advanced composite material based on carbon fabric-reinforced thermoset polymers (CFRTP) plays a vital role in aerospace structural applications, as well as high-performance sports goods and windmill structures. However, there are still challenges for CFRTP to achieve the desired mechanical properties [1–3].

Many processing techniques are available to fabricate the laminates to meet the requirements of different applications. The selection of manufacturing process technique depends on size and quality of composites. There are two manufacturing process techniques: autoclave process and out-of-autoclave process. The autoclave process is the only means to fabricate carbon fabric structures with good quality for aerospace applications, whereas the out-of-autoclave processes such as liquid composite moulding (LCM), liquid resin infusion (LRI) and automated tape placement (ATP) are predominant processes having its less-expensive equipment to fabricate composite components. Fabrication of CFRTP is made with autoclave process with pressure bag moulding, by providing heat and pressure to the composite product [4, 5].

Benzoxazine (BZ) is a novel class of thermosetting polymeric material which has various outstanding properties such as zero shrinkage, low-moisture absorption, good thermal and mechanical properties [6]. It possesses an important property, that is their ability to blend with various other resins such as epoxy and polyurethane; therefore, this leads to their easy processability and improved mechanical properties in addition to some unique physical, mechanical properties and application. BZ co-cures with epoxy resin; therefore, in recent years, BZ blends have attracted considerable attention by researchers, engineers and polymer industries. The blending of BZ with epoxy resins was reported [7–10]. The addition of epoxy resin with the BZ forms hybrid resin network which greatly increases the crosslink density of the thermosetting matrix and strongly influences on its mechanical properties. In this work, benzoxazine polymer was blended with epoxy–amine resin in different proportions and the composite laminates prepared by autoclave technique were studied for their physical, mechanical and thermal properties.

2 Experimentation

2.1 Materials

Bisphenol F-based benzoxazine (BZ) is mixed with Bisphenol A-based epoxy resin (DGEBA) and a low-viscosity liquid aromatic hardener Diethyl toluene diamine (DETDA) to form a hybrid resin system. PAN-based high-strength carbon fabric-3 K grade with 8-harness style was used as a reinforcement for making composite laminates. The chemical structures of the polymers used were depicted in the Fig. 1.

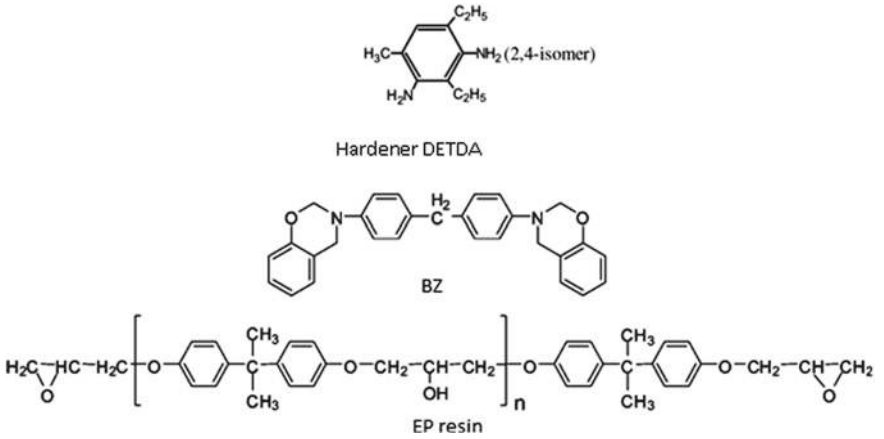

Fig. 1 Chemical structures of the polymer materials

Table 1 Hybrid resin

Laminates	Resin		
	Epoxy DGEBA	Hardener DETDA	Benzoxazine BZ (%)
L0	100	24	0
L1	98	24	2
L2	96	24	4
L3	94	24	6
L4	92	24	8
L5	90	24	10

2.2 Preparation of Benzoxazine/Epoxy Resin Carbon Fabric-Reinforced Composites

Benzoxazine resin provides relatively mild condition for polymerization, very low-melt viscosity, broad processing window, high reactivity and good overall properties. Before preparation of carbon fabric with BZ/epoxy prepreg, the BZ which is in solid powder form that cannot be used directly with epoxy resin was dissolved in acetone solvent in the proportion of 1:2 ratio by weight, which makes BZ to become liquid form. The liquid BZ of different proportions of 2, 4, 6, 8, 10% was mixed with epoxy resin DGEBA-DETDA in parts by weight (pbw) in a vessel and mixed thoroughly with the help of stirrer at room temperature for 10 min to obtain a clear solution of hybrid BZ/epoxy resin. The prepared hybrid resin solution was uniformly spread on the carbon fabric with brush and made to allow for drying at room temperature around 24 h to get tackiness in prepreg. The mechanical properties of carbon fabric with resin DGEBA- and hardener DETDA (100:24)-prepared samples were taken as reference. The following table shows the details of hybrid resin (Table 1).

The prepared prepregs were cut into 15 no. of plies of 300 × 300 mm size, and all plies were placed on a release agent (wax)-coated metallic mould. Autoclave was used to provide heat and pressure to the composite during curing. In this method, prepregs were stacked in a mould in a definite sequence to avoid any relative movement in between the prepreg sheets. After stacking the prepregs, the whole assembly was vacuum bagged to remove any air entrapped in between the layers. After a definite period of time when it was ensured that all air was removed, the entire assembly was transferred to autoclave. Here, heat and pressure were applied for a definite interval of time. In this process, matrix is uniformly distributed and intimate contact was achieved through proper bonding between fibres and matrix. After the processing, the assembly was cooled at a definite rate and then vacuum bag was removed. The composite part was taken out from the mould. Initially, a release gel was applied onto the mould surface to avoid sticking of polymer to the mould surface. This process is mainly used in applications requiring high strength-to-weight ratio components such as aircraft parts, marine, military, spacecraft and missiles. The schematic autoclave-moulding process is shown in Figs. 2 and 3.

Fig. 2 Hybrid resin impregnated on carbon fabric

Fig. 3 Prepreg cut into 300 × 300 mm size

The main advantages of this composite processing method allow high-volume fraction of reinforcement in the composite part, high degree of uniformity in part consolidation, better adhesion characteristics between layers and good control over resin and carbon fabric was achieved. No void content in the finished part due to removing entrapped air through vacuum and complete wetting of fibres was achieved.

2.3 Composite Curing

Autoclave was used for curing the composite as shown in Fig. 4. The oven air temperature was controlled with digital temperature indicator cum controller. The following cure cycle was applied and curing under vacuum and pressure as shown in Fig. 5. The main advantages of this composite processing method allow high-volume fraction of reinforcement in the composite part, high degree of uniformity in part consolidation, better adhesion characteristics achieved between layers and good control over resin and carbon fabric. Due to removing entrapped air through vacuum, no void content found in the finished component and complete wetting of fibres was achieved.

Fig. 4 Curing process using autoclave

Fig. 5 Curing under vacuum and pressure

2.4 Cure Cycle

- Autoclave curing has been carried out under vacuum with the following cure cycle.
- Temperature of the oven increased from room temperature to 80 °C in 30 min. Held the temperature for 4 h. After 4 h applied pressure of 5 bars.
- Increased the temperature after 4 h 80–120 °C in 20 min. Held the temperature for 2 h.
- Further increased the temperature from 120 to 180 °C in 20 min. Held the temperature for 4 h.
- After completion of cure time 4 h switched off the oven and allowed the laminate, cool to room temperature within 4–5 h.
- Extracted the laminates from the mould.

3 Testing, Results and Discussion

3.1 Physical Properties

The strength of any composite material depends on physical properties like fibre volume fraction and density. Estimated the fibre volume fraction and density of the laminates.

3.2 Tensile Strength

The tensile behaviour of prepared samples was determined at room temperature by using universal testing machine (UTM) according to ASTM D3039 standard. Tensile test set-up and specimen tensile failure modes are shown in Figs. 6 and 7, respectively. Six test specimens having dimensions of width 15 mm and thickness 2.0 mm were loaded between two adjustable grips of a 100 KN computerized universal testing machine with data acquisition system. Failure modes observed during the testing were identified. Tensile strength and modulus of specimens shown in Figs. 8 and 9, respectively.

The weight per cent of benzoxazine resin up to 4% (L2 laminate) improved tensile strength and modulus due to strong interfacial adhesion between composite layers and also due to the increased crosslink density. The improvement was compared with the reference epoxy composite. Failure mode of specimens at higher strength is a clean-cut mode in the gauge length, whereas at higher percentage addition of BZ the specimens broken in in-plane mode resulted in lower strength and modulus.

3.3 Flexural Strength

The Flexural strength is determined by three-point bend test in accordance with ASTM D790 (Fig. 10). The size of the test specimens is 10 mm width and 3 mm thickness. Three-point bend test was performed in a servo-controlled UTM machine having load cell capacity of 5 KN. The cross head speed 2 mm/min and span length to specimen depth ratio $s/t = 16$ were selected. Six specimens were tested and average value is considered (Fig. 11).

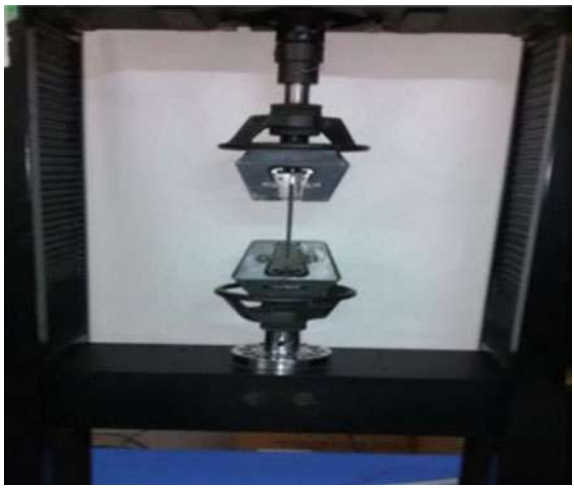

Fig. 6 Tensile test set-up

Fig. 7 Tensile failure modes

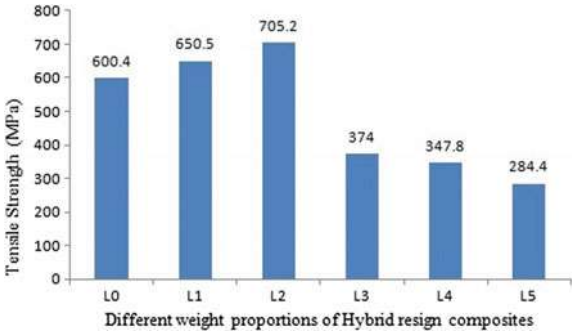

Fig. 8 Tensile strength (MPa)

Flexural strength and modulus for tested specimens were shown in Figs. 12 and 13. Flexural strength and modulus increased up to 4% by parts addition of BZ on reference epoxy–amine due to flexing of composite at higher loads due to strong inter-laminar strength.

3.4 Inter-laminar Shear Strength

The inter-laminar shear strength was calculated by using short-beam shear test as per ASTMD2344. Six samples were tested in electro-mechanical testing machine INSTRON 4505 with the crosshead speed of 1 mm/min, and span length to specimen ratio $s/t = 4$ was maintained. Test set-up and specimen failure modes were shown in Figs. 14 and 15, respectively.

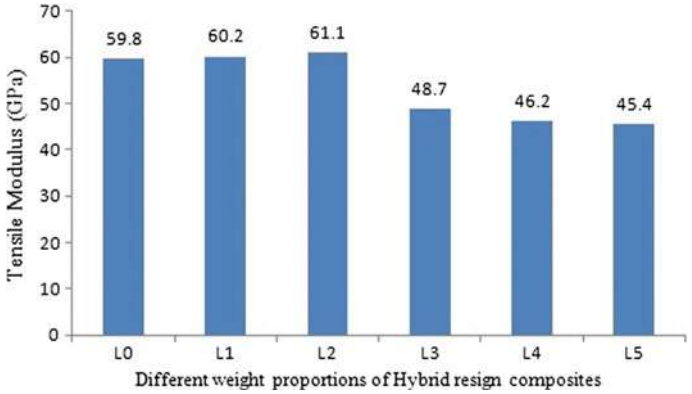

Fig. 9 Tensile modulus (GPa)

Fig. 10 Flexural test set-up

Tested specimens values were shown in Fig. 16. Highest value of ILSS achieved at 4% addition of BZ due to strong interfacial shear property.

3.5 Optical Microscope Images

The following optical images in Figs. 17 and 18 reveal comparative topography of reference epoxy–amine to BZ/epoxy–amine. Homogenous distribution of reinforcement to matrix adhesion of BZ is quite evident.

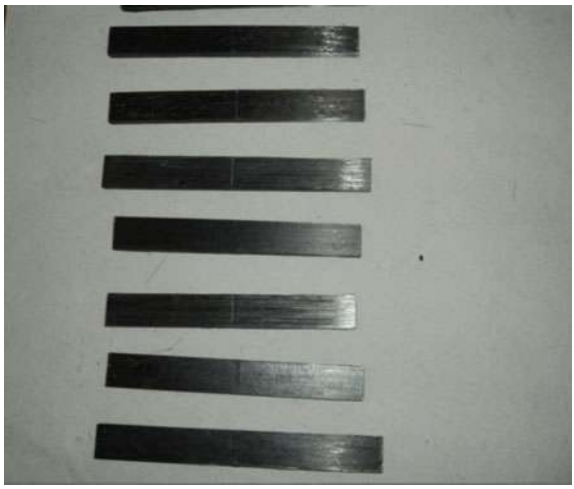

Fig. 11 Failure modes in flexural specimens

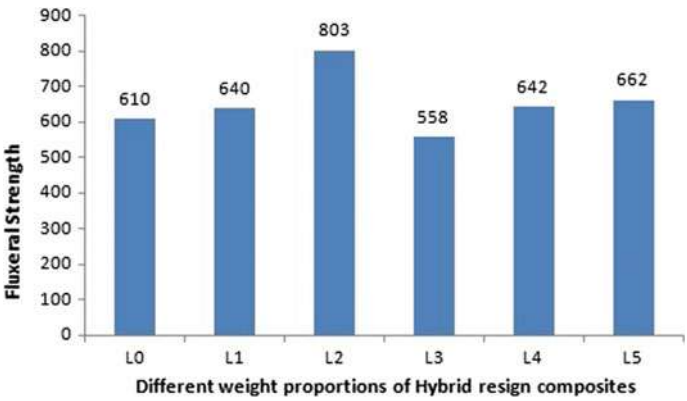

Fig. 12 Flexural strength (MPa)

The amine-hardened EP formed a co-network with the BZ. This contained nanoscaled inclusions of the homopolymerized BZ. Figure 18 reveals the finest dispersion characteristics of the BZ traced to the phase segregation and crosslinking with EP.

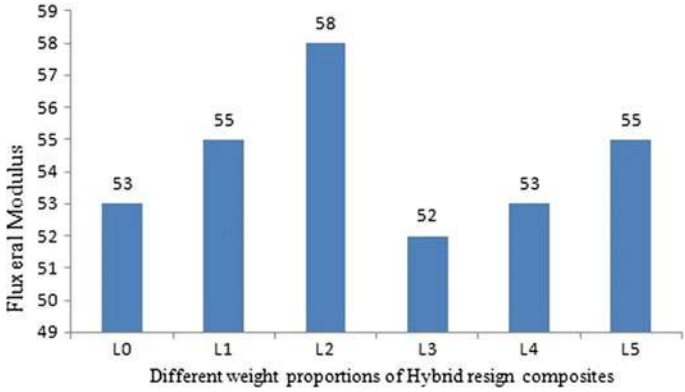

Fig. 13 Flexural modulus (GPa)

Fig. 14 Three-point bend test set-up

3.6 Thermal Properties

3.6.1 Differential Scanning Calorimeter (DSC) Scan

DSC thermograms were registered in the temperature range from $T = 0$ to 300 °C at a heating rate of 10 °C/min under N2 flushing (30 ml/min). The sample weight of around 10 mg was taken for both BZ and EP individually. Exothermic peak for BZ at 250 °C and exothermic peak for EP at 180 °C were observed. DSC curves were shown in Fig. 19.

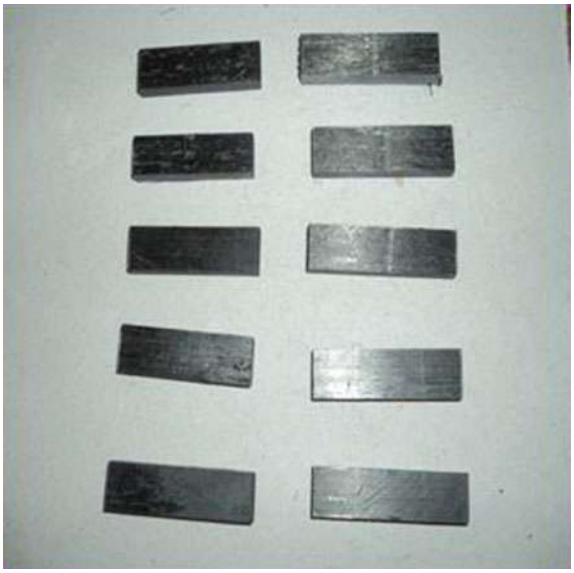

Fig. 15 Failure modes in ILSS specimens

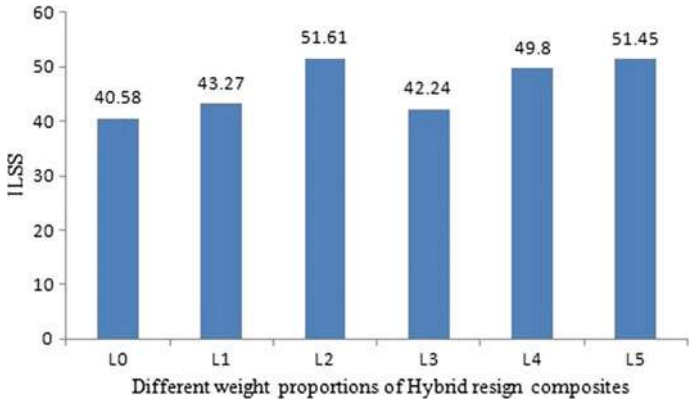

Fig. 16 Inter-laminar shear strength (ILSS)

The individual exothermic peak T_{peak} at 180 °C relates to the complete crosslinking of EP-Amine reaction and which is in line with the Glass transition temperature (T_g) for laminate L_0 composite. T_{peak} at 250 °C relates to homopolymerization of BZ itself. The incorporation of BZ to EP-Amine reduced the T_g in hybrid composites due to off-stoichiometry and increase observed upon post-curing due to homopolymerization and crosslinking with EP-Amine.

Fig. 17 Image of EP-Amine

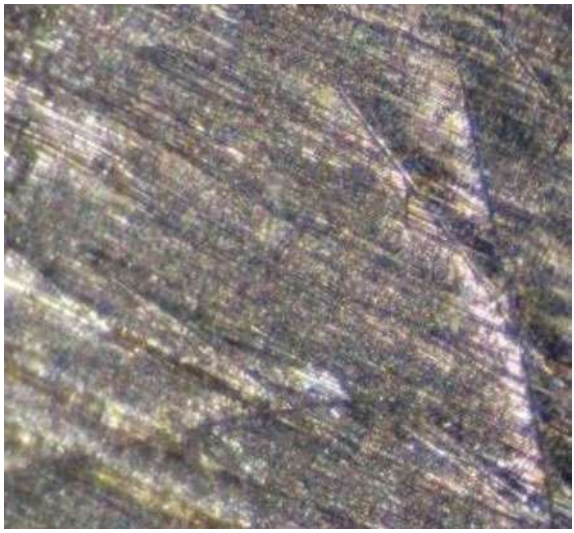

Fig. 18 Image of BZ/EP-Amine

3.6.2 Dynamic Mechanical Analysis (DMA) Scan

T_g is determined by DMA technique for the specimens having dimensions of 35 mm × 10 mm with 3 mm thickness. DMA curves for the laminates L_0 to L_5 were shown in Fig. 20. T_g was reduced by the incorporation of BZ due to off-stoichiometry caused by BZ and epoxy–amine reaction (which is in line with the DSC results). However, upon post-curing, enhancement in T_g was observed (as shown in Table 2) due to further reaction of BZ with epoxy–amine resulting in higher crosslink density.

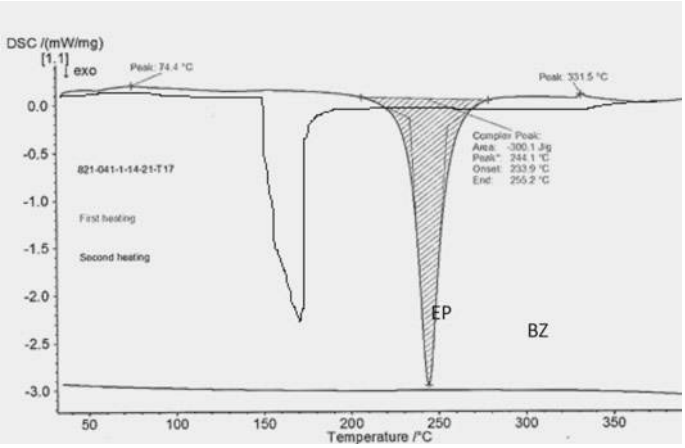

Fig. 19 DSC curves for BZ and EP

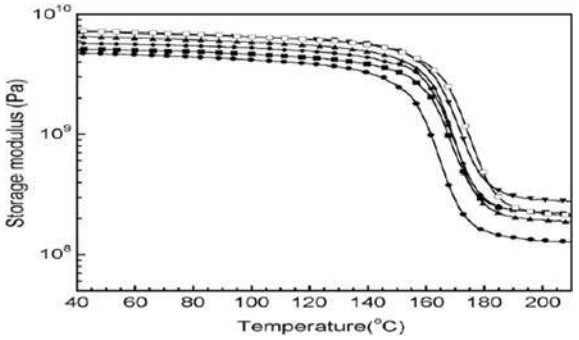

Fig. 20 DMA curves for laminates

Table 2 Glass transition temperatures

Laminate	BZ (%)	T_g	T_g (After post-cure)
L0	0	180	180
L1	2	175	185
L2	4	170	180
L3	6	165	175
L4	8	155	165
L5	10	145	160

4 Conclusion

It was studied the effect of aromatic amine hardener on epoxy modified with benzoxazine at different ratios and the thermal and mechanical properties of the cor-

responding hybrid was determined. It was observed from the results that aromatic amine-hardened epoxy formed a co-network with the benzoxazine resin. The weight per cent of benzoxazine resin up to 4% improved mechanical properties due to strong interfacial adhesion between composite layers and also due to the crosslink density. The improvement was compared with the reference epoxy composite. Thermal properties—the T_g of the hybrid was lower than the reference EP that was traced to off-stoichiometry caused by the amine/oxazine reaction. However, T_g increased upon post-curing due to nanoscaled homopolymerized BZ was well connected to the EP network.

References

1. Hossein Rahmani, S. Heydar Mahmoudi Najafi and Alireza Ashori: Mechanical performance of epoxy/carbon fibre laminated composites, Journal of Reinforced Plastics and Composites, 33(8) (2014) 733–740.
2. Hong-wei He, Feng Gao: Effect of Fibre Volume Fraction on the Flexural Properties of Unidirectional Carbon Fibre/Epoxy Composites, International Journal of Polymer Analysis and Characterization, 20 (2015) 180–189.
3. Umar Farooq, Peter Myler: Preparation of Aerospace Grade Carbon Fibrous Laminated Composite Panels with Improved Performance and Reduced Fabrication Process Defects and Flaws, ARPN Journal of Engineering and Applied Sciences, 12(4) (2017) 1128–1143.
4. D. Purslow, R. Childs: Autoclave moulding of carbon fibre-reinforced epoxies, Composites, 17(2) (1986) 127–136.
5. Timotei Centea, Lessa K. Grunenfelder, Steven R. Nutt: A Review of Out-of-Autoclave Prepregs-Material properties, Process phenomena and Manufacturing considerations, Composite part A, Applied science mfg. 70 (2014) 132–154.
6. S. Rajeshkumar, J. Dhanasekaran, S. Krishna Mohan: Epoxy benzoxazine based ternary systems of improved Thermo-mechanical behaviour for structural composite applications, RSC Advances, (2014), 1–15.
7. Mingzhen Xu, Xulin Yang, Rui Zhao, Xiaobo Liu: Copolymerizing Behaviour and Processability of Benzoxazine/Epoxy Systems and their Applications for Glass Fibre Composite Laminates, Journal of Applied Polymer Science, (2013) 1176–1184.
8. S. Grishchuk, Z. Mbhele, S. Schmitt, J. Karger-Kocsis: Structure, Thermal and Fracture Mechanical Properties of Benzoxazine-Modified Amine-cured DGEBA Epoxy Resins, eXPRESS Polymer Letters, 5(3) (2011), 273–282.
9. K.S. Santhosh Kumar, C.P. Raghunathan Nair, R. Sadhana, K.N. Ninan.: Benzoxazine-bismaleimide blends: Curing and thermal properties, European Polymer Journal, 43(12) (2007) 5084–5096.
10. V. Garcia-Martinez, M.R. Gude, A. Urena: Understanding the Curing Kinetics and Rheological Behaviour of a New Benzoxazine Resin for Carbon Fibre Composites, Reactive and Functional Polymers, Elsevier, February (2017).

ARTIFICIAL INTELLIGENCE AND SOFT COMPUTING RESEARCH LAB - PROCEEDINGS

The **AISCRL** is committed to the publication of proceedings of our conference. Its objectives is to publish original research in various areas of Science and Technology. This will provide good chances for academic and industry professionals to discuss recent progress in areas of Science and Technology

Research papers were strictly peer-reviewed by program committees to make sure that the the papers accepted were high quality and relevant to the current and future issues and trends in Science and Technology

The scope of **AISCRL** includes the entire area of science and technology from the current and future trends.The Language of publication is English.The Authors have to sign the copyright transfer form.

169

AISCRL
ISBN: 978-0-9876174-5-3

AISCRL

Fiaidhi (Ed.) AISCRL Research on Smart Technologies in Drata Scieene and Communications AISCRL

Jinan Fiaidhi (Eds.)
N. Thirupathi Rao
Ch. Sekhar

ARTIFICIAL INTELLIGENCE AND SOFT COMPUTING RESEARCH LAB

Research on Smart Technologies in Data Science and Communications

PROCEEDINGS,
2ND INTERNATIONAL CONFERENCE
SMART DSC - 2018
06TH - 08TH DECEMBER 2018
VIGNAN'S INSTITUTE OF INFORMATION TECHNOLOGY (A)
VISAKHAPATNAM, INDIA.

AISCRL ARTIFICIAL INTELLIGENCE AND SOFT COMPUTING RESEARCH LAB

Prevention of Gas Leakage Hazards in Home

[1]A S Keerthi Nayani, [2]Ch.Sekhar

[1]*Dept of ECE, Matrusri Engineering College, Hyderabad, India.*
[2]*Dept of CSE, Vignan's Institute of Information Technology, Visakhapatnam, India*
naskeerthi@gmail.com,sekhar1203@gmail.com

Abstract

Having the learning important to have the capacity to counteract and recognize a gas release right off the bat is critical with the end goal to avert potential gaseous petrol crises. Understanding what a flammable gas spill crisis is and how to respond is imperative to guarantee you and your family's security. In this paper talking about what a gas spill crisis is and what to do in the event that one happens, yet going to give you a wide-assortment of location and anticipation tips. Having this fundamental information will limit you and your family's dangers for gas spills crises.

Keywords: *LPG, gas sensor, Leakage detection*

1. Introduction

LPG(Liquid petroleum gas) is generally utilized in homes for focaLiquid petroleum gas warming, high temp water, gas-flames, cooking, and in versatile radiators for recreation exercises, for example, vessels, convoys and grills. This vitality source is essentially made out of propane and butane which are exceptionally combustible synthetic mixes. LPG holes can occur, however once in a while, inside a home, business premises or in gas controlled vehicles. Spillage of this gas can be unsafe as it raises the danger of building fire or a blast. The setbacks caused by this peril are as yet regular news in the media. Since the LPG in that capacity does not have any smell, gas organizations/refineries include an odorant, for example, ethanethiol, thiophene or a mercaptan so holes can be recognized effortlessly by the vast majority [2]. In any case, a few people who have a decreased feeling of smell will be unable to depend upon this innate security component. In such cases, a gas spillage locator winds up imperative and shields individuals from the threats of gas spillage. Various research papers have been distributed on gas spillage location strategies. A remote

home wellbeing gas spillage framework has been proposed in [2] where the alert gadget gives versatility inside the house premises.
.

2. Problem Formation

Home flames have been occurring much of the time and the danger to human lives and properties is developing as of late. Fluid oil gas (LPG) is exceedingly inflammable and can consume even at some separation from the wellspring of spillage. Most fire mishaps are caused on account of a low quality elastic cylinder or the controller isn't killed when not being used. Consequently, building up the gas spillage ready framework is exceptionally basic. Subsequently, this paper exhibits a gas spillage ready framework to recognize the gas spillage and to alert the general population locally available.

Gas spillage prompts different mischances bringing about both material misfortune and human wounds. The danger of blast, terminating, suffocation depend on their physical properties such poisonous quality, combustibility, and so on. The quantity of passings because of blast of gas barrels has been expanding as of late. The purpose behind such blast is because of substandard chambers, old valves, exhausted controllers and absence of mindfulness in taking care of gas barrels.

Distinguish Gas Leakage (like LPG spill, Butane spill, Methane spill) or any such oil based vaporous substance that can be recognized utilizing MQ5 Sensor.Unfortunately, when that you truly see a petroleum gas spill from the smell or sound it has just turned into a potential gas crisis. That is the reason it is imperative that you take deterrent measures to forestall spills before they happen.

3. Prevention Methodology

In the event that you presume that there is a gas spill in your home it is important that you respond rapidly or else the outcomes can be extremely hindering. To begin with, leave your home promptly and make a point to not utilize any electrical gadgets, for example, light switches or phones. Power utilization could start or touch off the flammable gas spill. Open blazes could likewise cause this so

make sure to not utilize matches or lighters. Finally, leave the zone and call your service organization to manage the issue. It is in every case best to give experienced experts a chance to fix any gas spills with the end goal to diminish the danger of gaseous petrol blasts. Try not to come back to the zone until the point when your home has been considered safe via prepared experts.

The following are the approaches for manual detection and prevention

- **SMELL the air.** We add a particular scent to flammable gas with the goal that spills are less demanding to distinguish.

- **LISTEN for holes**. A murmuring, shrieking or thundering sound close to a pipeline may show getting away petroleum gas. (Uncommon markers demonstrate the area of most significant pipelines.)

- **LOOK for pieces of information:**

    - A harmed association with a gas apparatus,
    - Dead or kicking the bucket vegetation over or close to a pipeline
    - A fire close to a pipeline
    - Exposed pipeline after a seismic tremor, fire, surge or another debacle Working Mechanism.

The manual approach may lead time taken and less efficient due to human error. To minimize and improve the efficient by automated senor based system. Gas spills or smell can be detected using sensor called MQ- sensor.

	V_c : 5V±0.1 V_H : 5V±0.1 Tao : -20℃-50℃ Sensing Resistance : 3KΩ-30KΩ (1000ppm iso-butane) Temp: 20℃• ±2℃ Humidity: 65%±5%

Figure 1: MQ 2 SENSOR and Specifications

MQ 2 SENSOR

The MQ-2 is a combustible gas and smoke sensor recognizes the convergences of burnable gas noticeable all around and yields its perusing as a simple voltage. The sensor can quantify groupings of combustible gas of 300 to 10,000 ppm. The MQ-2 gas sensor is delicate to LPG, I-butane, propane, methane, liquor, Hydrogen and smoke. They are utilized in gas spillage recognizing types of gear in family and industry and in the compact gas locator.

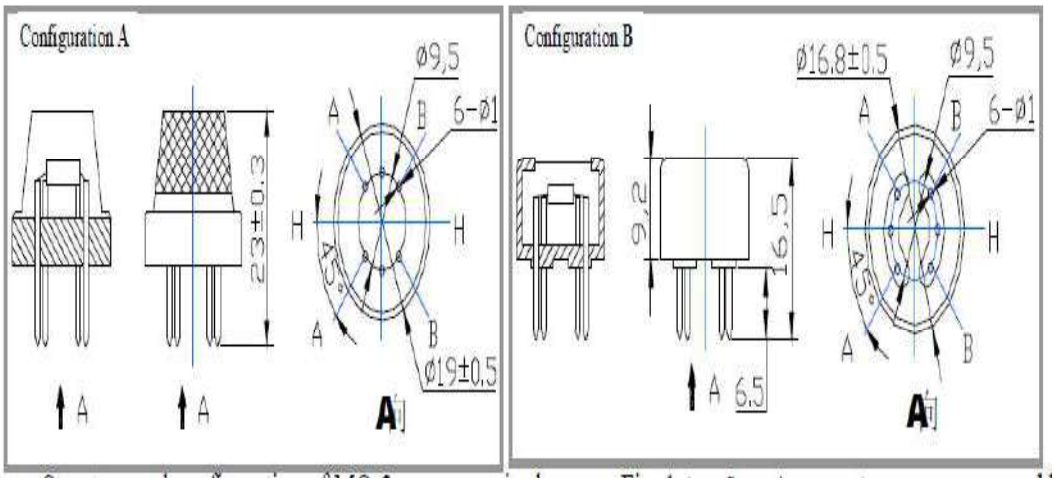

Figure2: Working Mechanism of MQ2 sensor

Structure and arrangement of MQ-2 gas sensor appear as Fig. 1 (Configuration An or B), sensor created by hull made by plastic and treated steel net. The radiator gives important work conditions to work of delicate segments. The wrapped MQ-2 have 6 stick, 4 of them are utilized to bring signals, and other 2 are utilized for giving warming current[3].

Resistance value of MQ-2 is difference to various kinds and various concentration gases. So,When using this components, sensitivity adjustment is very necessary. we recommend that you calibrate the detector for 1000ppm liquified petroleum gas<LPG>,or 1000ppm iso-butane<i- C4H10>concentration in air and use value of Load resistance that(RL) about 20 KΩ(5KΩ to 47 KΩ). When accurately measuring, the

proper alarm point for the gas detector should be determined after considering the temperature and humidity influence.

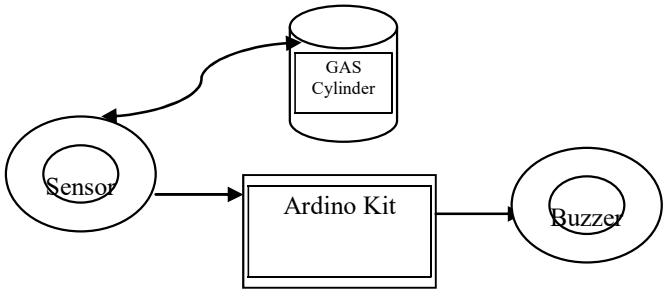

Figure 3: Model Block Diagram

GAS Detection system: If any GAS leakage occurs the system detects all the flammable gases if the gas leakage crosses the Threshold it detects the gases like methane, butane, propane, LPG, and smoke. Upon detecting the gases it turns ON the ventilator fans and sends an alert message to the user or the registered department. The system takes care of everything without a single input from the user.

4. Summary

Gas spillage prompts extreme mischance bringing about material misfortunes and human wounds. Gas spillage happens chiefly because of poor upkeep of gear and lacking familiarity with the general population. Subsequently, LPG spillage identification is basic to needed mishaps and to spare human lives. This paper disused about manual human based detection and how to over improve the performance using sensor based mechanism. In future work we need to develop a product with lesser price and easy to operate by normal human.

5. References

[1] LPG Gas Leakage Detection and Alert System, E. Jebamalar Leavline et.al. International Journal of Electronics Engineering Research. ISSN 0975-6450 Volume 9, Number 7 (2017) pp. 1095-1097

[2] Design and Implementation of an Economic Gas Leakage Detector, A. MAHALINGAM et.al. Recent Researches in Applications of Electrical and Computer Engineering.

[3]Technical Data of MQ Sensor, HANWEI ELETRONICS CO. LTD
[4] Improvement on Gas Leakage Detection and Location System Based On Wireless Sensor Network, Ganesh D, Anilet Bala.A, International Journal of Engineering Development and Research, Volume 3, Issue 2 | ISSN: 2321-9939

IEEE.org IEEE Xplore IEEE-SA IEEE Spectrum More Sites SUBSCRIBE SUBSCRIBECart Create Account Personal Sign In

Browse My Settings Help Institutional Sign In

Institutional Sign In

All

ADVANCED SEARCH

Conferences > 2018 3rd International Confer...

Improvement of Code Utilization CDMA for On-Chip Communication Architecture using Orthogonal Gold Code

Publisher: IEEE

Cite This Cite This PDF

K Ashok Kumar ; P Dananjayan All Authors

26
Full
Text Views

Export to
Collabratec

Alerts

Manage
Content Alerts

Add to Citation
Alerts

Abstract

Document Sections

I. Introduction

II. Related Work

III. Spreading Codes for CDMA

IV. Generation of Orthogonal Gold Code

V. Results and Discussion

Show Full Outline

Authors

Figures

References

Keywords

Metrics

More Like This

Downl
PDF

Abstract: Orthogonal codes are majorly crucial for code division multiple access (CDMA) for suppressing the multiple access interference (MAI). The Walsh based orthogonal codes are... **View more**

Metadata

Abstract:
Orthogonal codes are majorly crucial for code division multiple access (CDMA) for suppressing the multiple access interference (MAI). The Walsh based orthogonal codes are used for data transmission in on-chip communication because of cross correction is zero between adjacent sequences. Though, the code utilization is less of Walsh based codes when compared with Pseudo-random noise (PN) sequences. To provide better code utilization with orthogonality, an orthogonal gold code is proposed in this paper thereby the orthogonal gold code is used for large size of on-chip communication architecture. These codes are suitable for CDMA and show better code utilization than the Walsh based orthogonal codes. For implementation, the Xilinx 14.7 software with Vertex-6 FPGA and is used and simulations of 32-bit are experimented in MATLAB thereby the crosscorrelation performance improved than Walsh based orthogonal codes.

Published in: 2018 3rd International Conference on Inventive Computation Technologies (ICICT)

Date of Conference: 15-16 Nov. 2018 **INSPEC Accession Number:** 19453229

More Like This

Performance of narrowband interference suppression filters in a direct sequence code division multiple access system
Proceedings of ICUPC - 5th International Conference on Universal Personal Communications
Published: 1996

Hardware implementation for fast convolution with a PN code using field programmable gate array
Proceedings of the 33rd Southeastern Symposium on System Theory (Cat. No.01EX460)
Published: 2001

Show More

Date Added to IEEE *Xplore*: 12 March 2020

ISBN Information:

DOI: 10.1109/ICICT43934.2018.9034282

Publisher: IEEE

Conference Location: Coimbatore, India, India

Contents

I. Introduction

A code division multiple access (CDMA) is absolutely suitable to the simultaneous data transmission where the communication system has multiple senders and receivers. It is known that the CDMA needs a large number of spreading codes to minimize the cross correction and capable providing good bandwidth efficiency. It is very attractive for wireless communication medium because of number of advantages than time division multiple access (TDMA) and frequency division multiple access (FDMA). The various forms of spreading spectrum modulation techniques are used for generating different types of spreading codes for efficient CDMA system. A direct sequence spreading spectrum (DS-SS) is one of the popular modulation schemes to generate unique code and spread across wide band frequencies of spectrum [1]. A pseudo-random noise (PN) sequences the sequence of binary digits which looks random statistically but generated deterministically. The PN sequences are satisfy three tests for randomness to improve the efficiency. i.

Balance property: The difference of between the number of zeros and ones is either 0 or 1. The PN sequence of length 2^N contains $2^{N-1}1$'s and $2^{N-1}0'$s.

Sign in to Continue Reading

ii.

Run-length property: A run-length of k is set k succeeding identical digits is bound by different digits on its ends. For a PN sequence, $\frac{1}{2}$ of runlength is 1, $\frac{1}{4}$ of run-length is 2, $\frac{1}{8}$ of run-length is 3 and so on. The number of runs of 0's and number of runs of 1's are same for a sequence.

iii.

Correlation property: Correlation is the measurement of similarity between the sequences. The autocorrelation is similarity between original sequence and cyclically shifted copy of original sequence. The crosscorrelation is the similarity between two different sequences. The autocorrelation of a finite, discrete signal $x(n)$ is defined in eqn. (1) and the crosscorrelation of discrete signals $x(n)$ and $y(n)$ is given in eqn. (2) [2].

Authors

Figures

References

Keywords

Metrics

© Copyright 2021 IEEE - All rights reserved. Use of this web site signifies your agreement to the terms and conditions.

IEEE Account

» Change Username/Password
» Update Address

Purchase Details

» Payment Options
» Order History
» View Purchased Documents

Profile Information

» Communications Preferences
» Profession and Education
» Technical Interests

Need Help?

» **US & Canada:** +1 800 678 4333
» **Worldwide:** +1 732 981 0060
» Contact & Support

About IEEE *Xplore* | Contact Us | Help | Accessibility | Terms of Use | Nondiscrimination Policy | Sitemap | Privacy & Opting Out of Cookies
A not-for-profit organization, IEEE is the world's largest technical professional organization dedicated to advancing technology for the benefit of humanity.
© Copyright 2021 IEEE - All rights reserved. Use of this web site signifies your agreement to the terms and conditions.

Proceedings of the International Conference on Inventive Computation Technologies (ICICT-2018)
DVD Part Number:CFP18F70-DVD; ISBN:978-1-5386-4984-8

Improvement of Code Utilization CDMA for On-Chip Communication Architecture using Orthogonal Gold Code

Ashok Kumar. K
Assistant Professor, Department of ECE, Matrusri Engineering College, Hyderabad, India-500059
Email-kashok483@gmail.com

Dananjayan. P
Professor, Department of ECE, Pondicherry Engineering College, Puducherry, India-605014

***Abstract*-Orthogonal codes are majorly crucial for code division multiple access (CDMA) for suppressing the multiple access interference (MAI). The Walsh based orthogonal codes are used for data transmission in on-chip communication because of cross correction is zero between adjacent sequences. Though, the code utilization is less of Walsh based codes when compared with Pseudo-random noise (PN) sequences. To provide better code utilization with orthogonality, an orthogonal gold code is proposed in this paper thereby the orthogonal gold code is used for large size of on-chip communication architecture. These codes are suitable for CDMA and show better code utilization than the Walsh based orthogonal codes. For implementation, the Xilinx 14.7 software with Vertex-6 FPGA and is used and simulations of 32-bit are experimented in MATLAB thereby the crosscorrelation performance improved than Walsh based orthogonal codes.**

Keywords:-NoC; Crossbar; CDMA; Orthogonal gold codes; FPGA.

I. INTRODUCTION

A code division multiple access (CDMA) is absolutely suitable to the simultaneous data transmission where the communication system has multiple senders and receivers. It is known that the CDMA needs a large number of spreading codes to minimize the cross correction and capable providing good bandwidth efficiency. It is very attractive for wireless communication medium because of number of advantages than time division multiple access (TDMA) and frequency division multiple access (FDMA). The various forms of spreading spectrum modulation techniques are used for generating different types of spreading codes for efficient CDMA system. A direct sequence spreading spectrum (DS-SS) is one of the popular modulation schemes to generate unique code and spread across wide band frequencies of spectrum [1]. A pseudo-random noise (PN) sequences the sequence of binary digits which looks random statistically but generated deterministically. The PN sequences are satisfy three tests for randomness to improve the efficiency.

i. **Balance property:** The difference of between the number of zeros and ones is either 0 or 1. The PN sequence of length 2^N contains 2^{N-1}1's and 2^{N-1}0's.

ii. **Run-length property:** A run-length of k is set k succeeding identical digits is bound by different digits on its ends. For a PN sequence, $\frac{1}{2}$ of run-length is 1, $\frac{1}{4}$ of run-length is 2, $\frac{1}{8}$ of run-length is 3 and so on. The number of runs of 0's and number of runs of 1's are same for a sequence.

iii. **Correlation property:** Correlation is the measurement of similarity between the sequences. The autocorrelation is similarity between original sequence and cyclically shifted copy of original sequence. The crosscorrelation is the similarity between two different sequences. The autocorrelation of a finite, discrete signal $x(n)$ is defined in eqn. (1) and the crosscorrelation of discrete signals $x(n)$ and $y(n)$ is given in eqn. (2) [2].

$$r_{xx}(T) = \sum_{n=0}^{L} x(n)x(n-T) \quad (1)$$

$$r_{xy}(T) = \sum_{n=0}^{L} x(n)y(n-T) \quad (2)$$

where T is the time delay and L is the length of sequence. The eqn. (1) indicates the three different values of autocorrelation. The autocorrelation is positive when signal is exact similar to the cyclic shifted version of original signal. The value is negative when signal is dissimilar to shifted version of original signal. The value is zero when signal is exactly orthogonal to the original signal. The eqn. (2) is also indication three different values of crosscorrelation only difference is signals are different to each other.

The remaining of the paper is as follows. Section-II describes the literature of the different forms orthogonal sequences. Section –III presented generation of spreading sequences for CDMA based communication systems and generation of orthogonal gold code is provided in section-IV.

Section-V gives the results and discussion of orthogonal gold code based CDMA system and a case study of network on chip is presented in section-VI. Finally, this paper concluded in section-VII.

II. Related Work

The orthogonal codes are used in many applications especially in CDMA based communication systems. Donelan, H., and T. O'Farrell [3] proposed a new method for generating orthogonal sequences which provides n-sequences to n-chips of a system. By using new method, the orthogonal sequences are generated from the gold code but need not of preferred pair of m-sequences. The procedural steps are required for generating orthogonal sequences from gold code. The various set of sequences are experimented for peak crosscorrelation and these orthogonal set of sequences are provided good crosscorrelation when size of set increased. To increase the system capacity, Akhavan-Bahabdi, Mehdi, and Mohsen Shiva [4] presented a Double Orthogonal Multi-Carrier Code Division Multiple Access (DO/MC-CDMA). The $\boldsymbol{2N-1}$ codes are supplied for code length of $\boldsymbol{N}$. However, the improved performance is restricted for less value of $\boldsymbol{N}$. Akansu, Ali N., and Radha Poluri [5] proposed a walsh-like nonlinear phase binary orthogonal sequences for both synchronous and asynchronous multiuser communications. The walsh-like and gold sequences are used for nonlinear phase where as Walsh codes are used in linear phase. The capability of communication system is improved when compared with Walsh and gold codes. Though, bit error rate (BER) of the proposed code is high in case of multi-user when compared with Walsh codes. Jos et al. [6] presented a method to generate multiple sets of orthogonal codes for spread spectrum sequences by utilizing any single two level autocorrelation sequences. This multiple set of codes are supplied more number of sequences with low inter-set correction. Still, the orthogonality property is the critical issue because of the sequences is related to different sets. Shufeng et al. [7] proposed a method that using an orthogonal gold code for CDMA to avoid the un-satisfactory performance of m-sequence in case of multi-users. By using of crosscorrelation property of gold code, the orthogonal gold code is generated and used for multi-user CDMA systems. The performance of BER is proven that the orthogonal gold code is perfectly suitable for large size of system.

This work is directed from the literature of orthogonal codes presented in [5] and [7]. The orthogonal codes are generated from the preferred m-sequences thereby applying for large network system on chip (SoC). The new orthogonal codes are implemented on field programmable gate arrays (FPGA) and compared with Walsh codes.

III. SPREADING CODES FOR CDMA

Two types of sequences are popularly used for verity of communication that is one of the group is maximal sequence is known binary PN sequences and another group is orthogonal sequences [8].

A. Maximal Length Sequence

The Maximal length sequences (m-sequences) are generated with linear feedback shift register (LFSR) and duplicate non-zero sequence which is produced with m-length registers thereby the length of sequence is $L = 2^m - 1$. The m-sequences are produces longest codes by LFSR of a given length. The sequential shifting 1 or 0 along the path of sequence will be the output by performing arithmetic addition.

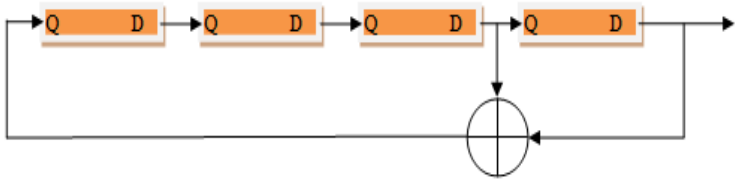

Fig.1 Generation of m-sequence by a LFSR

B. Gold Code

To reduce the crosscorrelation of m-sequences, the gold code is generated with properly selected of two m-sequences that is arithmetic addition of modulo-2 addition [9]. Fig.2 depicts the generation of gold code by preferred pair of m-sequences that each sequence length $2^m - 1$ and shown three crosscorrelation values $\{-1, -T$ and $T-2\}$. The advantage of gold code is generating large set of spreading sequences for the particular system.

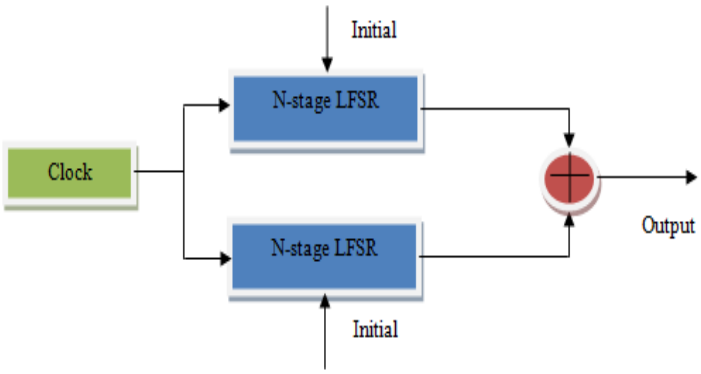

Fig.2 Generation of gold code sequence with correct selection of PN-sequences

C. Kasami Code

Kasami codes are one of the important sequences of m-sequence because of its low correction values. Kasami sequence is having two different set of sequences that are small set and large set. The generating of small set of Kasami code is similar process of generation of gold code with $N = 2^m - 1$ of m-sequence having period of $L = 2^m - 1$. The crosscorrelation of small set of Kasami sequence is $\{-1, -(2^{\frac{m}{2}} + 1), (2^{\frac{m}{2}} - 1)\}$. The large set of Kasami sequence is composed with gold code and small set of

Kasami code whose period is $L = 2^m - 1$. The crosscorrelation of large set of Kasami sequence is $\{-1, -1 \pm 2^{\frac{m}{2}}, -1 \pm 2^{\frac{m+2}{2}}\}$. The maximum crosscorrelation of large set of Kasami code and gold code are equal

D. Orthogonal sequences

An orthogonal sequence improves the bandwidth utilization for spreading spectrum. The crosscorrelation of orthogonal sequence is almost zero. The best way of generating orthogonal code is with Walsh-Hadamard matrix. The Walsh based sequences generated orthogonal codes with power of 2.

$$H_1 = (1) \qquad H_2 = \begin{pmatrix} 1 & 1 \\ 1 & -1 \end{pmatrix}$$

$$H_{2N} = \begin{pmatrix} H_N & H_N \\ H_N & -H_N \end{pmatrix}$$

The row of Hadamard matrix is in the order of 2^N composes the Walsh codes which encode N-bit sequences. Consider 0 in place of 1 and 1 in place of -1 for generating of proper length of orthogonal sequence.

IV. GENERATION OF ORTHOGONAL GOLD CODE

The generation of orthogonal code is needed for variable data rate communication with zero crosscorrelation. These codes are resulted by modifying original gold code which is generated with preferred pair of m-sequences. The gold codes are generated crosscorrelation value equal to -1 for number of time shifts. This indicates the crosscorrelation values of time shifts of gold sequence provides 0 by appending an extra 0 to the original gold codes. For an instance, 7-bit chip gold code 1011100 modifies to get orthogonal gold code 10111000 whose length is 8. These set of K number of orthogonal gold codes having length of $K = N + 1$.

The generation of orthogonal gold code are similar to Walsh based codes for supporting multi-rate data rate transmission. However, the Walsh based code generates $N - 1$ number of spreading codes for N-length sequence where as orthogonal code produces $N \times (N - 1)$ number of sequences. Table 1 depicts the comparison of number of spreading codes between Walsh and orthogonal gold code. From the table, it is clear that the difference at number of sequences is small when the system needs less spreading sequences proportionally the difference is large when system needs high spreading sequences.

TABLE 1 Comparison of number of spreading sequences for Walsh and orthogonal code

Length of code	Number of distinct codes	
	Walsh code	Orthogonal code
4	4	12
16	16	240
64	64	4032
256	256	65280

V. RESULTS AND DISCUSSION

The orthogonal gold code is designed and implemented for CDMA in Xilinx software with Vertex-6 Field Programmable Gated Array (FPGA) device. The orthogonal gold code is used for CDMA based on-chip communication and compared with Walsh code based CDMA. Fig.3 depicts the RTL (register-transfer level) schematic of 16-bit orthogonal CDMA based communication system. Because of space constraint, decoding of CDMA is shown with only two nodes total of 16 nodes. The 16 orthogonal sequences are multiplexed with 16 different senders thereby these multiplexed data added arithmetically before encoding to the channel. In the decoding stage, the encoded data multiplexed with orthogonal gold code thereby original data is re-constructed by comparison module whose inputs are from accumulating registers.

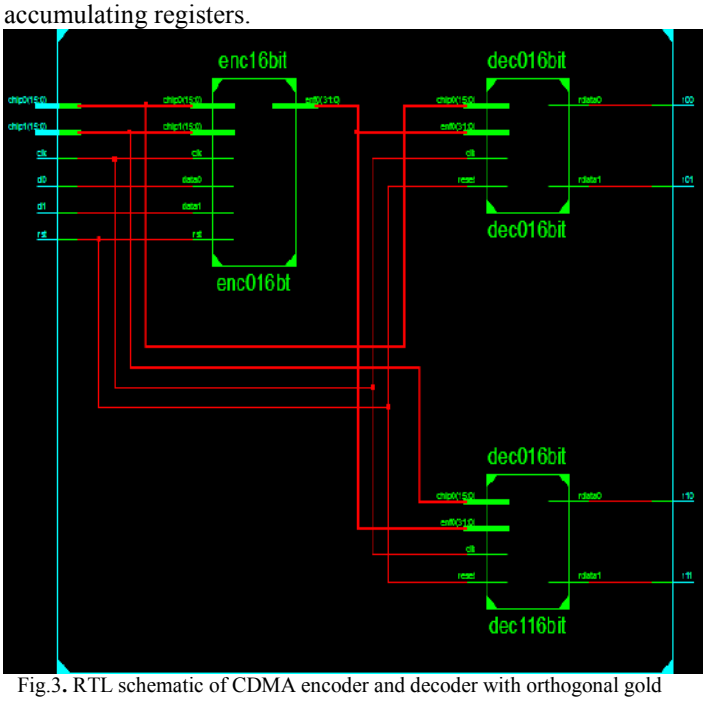

Fig.3. RTL schematic of CDMA encoder and decoder with orthogonal gold code for 16 bit data

Fig.4 shows the simulation result of 16-bit of CDMA with orthogonal gold code which is in blue colour is input data and red colour is output. The different simulations of CDMA are tested and demonstrated for finding of efficiency of orthogonal gold code based system. The all experiments proved that the original data packets are re-constructed accurately by using the orthogonal gold codes.

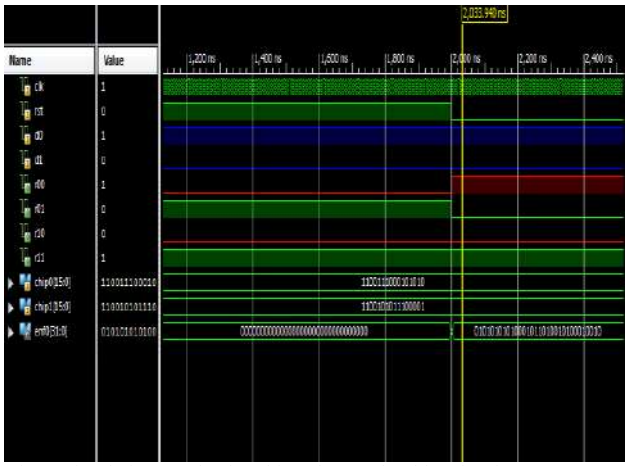

Fig. 4 Simulation result of 16-bit orthogonal gold code of CDMA system with two nodes

The 4,8,16 and 32 bit orthogonal gold code of CDMA is implemented and synthesis results are shown in terms of area utilization (Occupied Slices, LUT-FF pair, Bonded IOBs), latency (delay) and power consumption (dynamic power consumption) are presented Table 2. From table, it infers that the CDMA technique with orthogonal gold code is also attainable for improve performance of communication on-chip.

TABLE 2 Implementation results of CDMA with different orthogonal gold codes

Data width	Occupied Slices	LUT-FF pairs	Bonded IOBs	Delay (ns)	Dynamic Power consumption (mW)
4	31	39	18	2.993	0.98
8	52	76	24	3.873	1.72
16	115	176	40	6.648	6.49
32	157	242	64	9.762	10.34

The crosscorrelation values for 32- bit of orthogonal sequences are evaluated by simulation in MATLAB. The comparison of the gold code, Walsh code and new proposed code (orthogonal gold) are shown in fig.5. From figure, it is clear that the orthogonal gold codes are providing less crosscorrelation than Walsh codes because of good correlation property of gold codes.

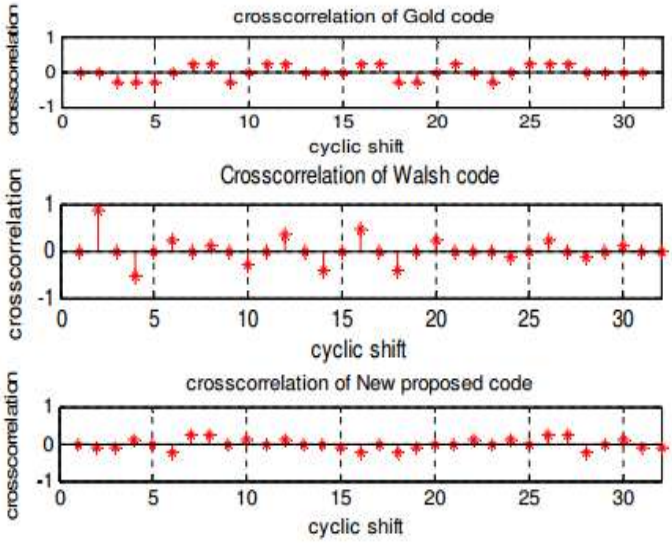

Fig.5 Comparison of crosscorrelation for gold code, Walsh code and orthogonal gold code

VI. CASE STUDY

The CDMA is well suited for network on chip (NoC) communication architecture where the crossbar switch transfers the data packets simultaneously. Each NoC switch composes multi-input ports and multi-output ports to obtain high performance of on-chip communication [10]. To control data transferring in the presence of multiple ports, the design of arbiter and crossbar are critically important to achieve high performance NoC based SoC [11]. The conventional crossbar switch realized with combination of multiplexer and de-multiplexer which suits for multiple data transmission. However, the data transfer speed of typical crossbar switch is not satisfying for NoC based SoC when number of ports are increased thereby the CDMA is now popularly suitable for NoC [12]. The crosstalk errors are also majorly affecting the performance of NoC because of scaling of technology decreases the space between the on-chip interconnects which leads to increase in coupling capacitance [13] hence the strong error control schemes are needed for maintaining high reliability of NoC based SoC systems.

VII. CONCLUSION

Orthogonal codes are considerably constraint for performance of CDMA systems. The Walsh based orthogonal codes popular for CDMA because of low crosscorrelation and orthogonal property. However, the code utilization of Walsh based is less thereby it is not suitable for high port NoC fabric. An orthogonal gold codes exactly suitable for large systems due to high code utilization property. In this paper, the orthogonal gold codes are designed and implemented for CDMA thereby the comparison is provided between Walsh code and orthogonal gold code. The orthogonal gold code shown more code utilization than Walsh code thereby it is used in large size of on- chip networks.

REFERENCES

1. Dinan, Esmael H., and Bijan Jabbari. "Spreading codes for direct sequence CDMA and wideband CDMA cellular networks." *IEEE communications magazine* 36, no. 9 (1998): 48-54.
2. Student, C. S. E. "Walsh Codes, PN Sequences and their role in CDMA Technology."
3. Donelan, H., and T. O'Farrell. "Method for generating sets of orthogonal sequences." *Electronics letters* 35, no. 18 (1999): 1537-1538.
4. Akhavan-Bahabdi, Mehdi, and Mohsen Shiva. "Double orthogonal codes for increasing capacity in MC-CDMA systems." In *Wireless and Optical Communications Networks, 2005. WOCN 2005. Second IFIP International Conference on*, pp. 468-471. IEEE, 2005.
5. Akansu, Ali N., and Radha Poluri. "Walsh-like nonlinear phase orthogonal codes for direct sequence CDMA communications." *IEEE Transactions on Signal Processing* 55, no. 7 (2007): 3800-3806.
6. Jos, Sujit, Jinesh P. Nair, Debarati Sen, and Arun Naniyat. "Method of generating multiple sets of orthogonal codes with wide choice of spreading factors." *IEEE Wireless Communications Letters* 1, no. 5 (2012): 492-495.
7. Shufeng, Li, He Shiyao, and Wu Hongda. "Analysis of DS-CMDA system using orthogonal gold sequence." In *Electronics Information and Emergency Communication (ICEIEC), 2017 7th IEEE International Conference on*, pp. 520-523. IEEE, 2017.
8. Kedia, Deepak, and S. L. Maskara. "Evaluation of Spreading Codes for CDMA Wireless Mobile Communication." In *Proc. National Conf. on Communications*, pp. 498-502. 2002.
9. George, Maria, Mujtaba Hamid, and Andy Miller. "Gold code generators in Virtex devices." *Xilinx Application Note xapp217, v1* 1 (2001).
10. Kumar, K. Ashok, and P. Dananjayan. "A Survey for Silicon on Chip Communication." *Indian Journal of Science and Technology* 10, no. 1 (2017).
11. Ashok Kumar K, Dananjayan P, "Parallel Distributed Round Robin Arbiter for Network on Chip," *Journal of Computational and Theoretical Nanosciences*, 10, pp. 2064-2068, 2018
12. Ashok Kumar K, Dananjayan P, "Parallel Overloaded CDMA Crossbar for Network on Chip," submitted to *Facta Universitatis, Series: Electronics and Energetics*.
13. Ashok Kumar K, Dananjayan P, "Reduction of power consumption using Joint Low Power Code with Crosstalk Avoidance Code in case of crosstalk and random burst errors," *International Journal of Engineering Technology*, 7, no.3.12, (2018).

BIOGRAPHY OF AUTHORS

Ashok Kumar K received Bachelor of Technology from Jawaharlal Nehru Technical University in 2009 and Master of Technology in 2011 from Jawaharlal Nehru Technical University. He worked 3 years as an Assistant Professor in MallaReddy Institute of Engineering and Technology. Currently, he is working as Assistant Professor in the Department of Electronics and Communication Engineering, Matrusri Engineering College, Hyderabad, India. He has 6 publications in International Journals and 1 international conference. His research interests include VLSI system design, Spread Spectrum Techniques, Communication Networks.

P. Dananjayan received Bachelor of Science from University of Madras in 1979, Bachelor of Technology in 1982 and Master of Engineering in 1984 from the Madras Institute of Technology, Chennai and Ph.D. degree from Anna University, Chennai in 1998. He is currently working as a Principal and Professor in the Department of Electronics and Communication Engineering, Pondicherry Engineering College, Pondicherry, India. He is also as a visiting professor to AIT, Bangkok. He has more than 110 publications in National and International Journals. He has presented more than 130 papers in National and International Conferences. He has guided 19 Ph.D candidates and is currently guiding 6 Ph.D students. His research interests include Spread Spectrum Techniques, Wireless Communication, Wireless Adhoc and Sensor Networks.

We are IntechOpen, the world's leading publisher of Open Access books Built by scientists, for scientists

5,200
Open access books available

127,000
International authors and editors

150M
Downloads

Our authors are among the

154
Countries delivered to

TOP 1%
most cited scientists

12.2%
Contributors from top 500 universities

WEB OF SCIENCE™

Selection of our books indexed in the Book Citation Index in Web of Science™ Core Collection (BKCI)

Interested in publishing with us?
Contact book.department@intechopen.com

Numbers displayed above are based on latest data collected.
For more information visit www.intechopen.com

Chapter

Combined Crosstalk Avoidance Code with Error Control Code for Detection and Correction of Random and Burst Errors

Ashok Kumar Kummary, Perumal Dananjayan, Kalannagari Viswanath and Vanga Karunakar Reddy

Abstract

Error correction codes are majorly important to detect and correct occurred errors because of various noise sources. When the technology is scaling down, the effect of noise sources is high. The coupling capacitance is one of the main constraints to affect the performance of on-chip interconnects. Because of coupling capacitance, the crosstalk is introduced at on-chip interconnecting wires. To control the single or multiple errors, an efficient error correction code is required. By combining crosstalk avoidance with error control code, the reliable intercommunication is obtained in network-on-chip (NoC)-based system on chip (SoC). To reduce the power consumption of error control codes, the bus invert-based low-power code is integrated to network interface of NoC. The advanced work is designed and implemented with Xilinx 14.7; thereby the performance of improved NoC is evaluated and compared with existing work. The 8×8 mesh-based NoC is simulated at various traffic patterns to analyze the energy dissipation and average data packet latency.

Keywords: NoC, CAC, ECC LPC, SoC, FPGA

1. Introduction

As technology is scaling up, a number of circuits are integrated in on-chip. The intercommunication among the on-chip devices is majorly important because of millions of integrated devices in the system on chip (SoC). The communication architectures of SoC are not efficient to provide high performance; thereby network-on-chip (NoC) is the new paradigm introduced [1]. Because of parallelism, the NoC is providing high performance in terms of scalability and flexibility even in the case of millions of on-chip devices. Still, NoC suffers with design parameters that affect the performance of NoC. As technology is scaling up, the performance of NoC is mainly affected with coupling capacitance. The effect of crosstalk capacitance is more in horizontal than in vertical; thereby the crosstalk errors frequently occur in on-chip interconnecting wires [2]. An efficient error correction code is required to control the crosstalk error that may occur once or multiple times. The crosstalk avoidance codes (CAC) are popularized to control the error in on-chip interconnects; thereby a reliable communication is obtained.

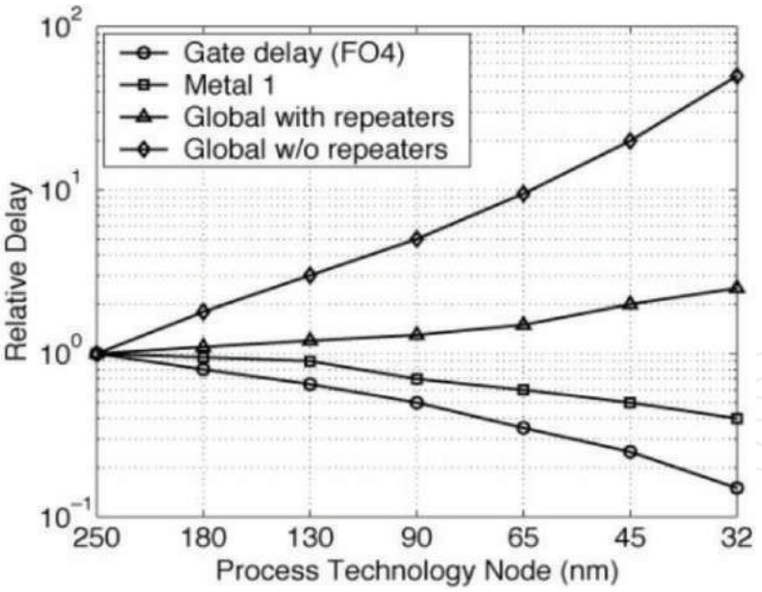

Figure 1.
Trend of relative delay with scaling of technology [3].

The CAC reduced the worst-case switching capacitance in on-chip interconnects by avoiding the switching transitions of data that is 010-101. This condition reduced the worst-case capacitance from $(1 + 4\lambda)\, C_L$ to $(1 + 2\lambda)\, C_L$; hence, the energy dissipation is reduced from $(1 + 4\lambda)\, C_L \alpha V_{dd}^2$ to $(1 + 2\lambda)\, C_L \alpha V_{dd}^2$ where λ is the ratio of coupling capacitance to total capacitance, C_L is the self-capacitance of interconnection wire, α is the transition factor, and V_{dd} is the supply voltage for the system. The energy dissipation is reduced by reducing the transition activity of interconnection wires for the data packet. The behavior of relative delay with scaling of technology is shown in **Figure 1**.

International Technology Roadmap for Semiconductor (ITRS-2011) predicted that when the delay from the gates is reduced, the delay from wires is increased with scaling of technology because the interconnecting wires are affected more when scaling of technology is less than 45 nm [3]. Hence, the interconnecting wires affected the performance of NoC-based SoC in terms of delay as well as energy consumption, and it is huge in case of the errors.

The errors mainly occur in interconnecting wires because of coupling capacitance; thereby strong error correction code (ECC) is required to detect and correct errors [4]. The error may occur once or multiple times, and also multiple errors occurred in interconnection wires; hence, the ECCs are not enough to detect and correct errors. In literature, different techniques are proposed for detection and correction of multiple errors. The parity check, dual rail (DR), modified dual rail (MDR), boundary shift code (BSC), and CAC are popularized among various techniques for control of multiple errors in interconnection wires.

The remaining chapter is as follows: Section 2 includes the related work of error control methods and also discussed the merits and demerits. Section 3 presented the proposed encoder and decoder of combined CAC-ECC method. Section 4 gives the advanced encoding and decoding of NoC router with combined LPC-CAC-ECC scheme. Section 5 discussed the implementation of proposed work in NoC architecture, and finally, Section 6 concludes the chapter.

2. Related work

The detection and correction of errors present in the on-chip interconnects are majorly important because it leads to drop or block data packet; hence the performance

of NoC architecture is reduced. Huge research is going on for the error detection and correction of on-chip interconnects. Parity code is used to detect 1-bit error in data packet. It is simple but errors are not corrected. Hamming code is proposed for detection of 2-bit errors and also correction of 1-bit error [5]. Various error control codes are introduced with the help of hamming code because it is easy to implement.

To reduce delay in on-chip interconnects, forbidden overlap condition (FOC), forbidden transition condition (FTC), and forbidden pattern condition (FPC) of crosstalk avoidance code are used [6]. The crosstalk avoidance codes are reduced delay from $(1 + 4\lambda) C_L$ to $(1 + 2\lambda) C_L$ and also energy dissipation. Still, the area utilization has increased because the extra bits are added to the original data packet. To control multiple errors, duplicate parity (DAP) is proposed by duplicating data packets, and then hamming code is used for transmission of duplicated data [7]. The average data packet latency is reduced by DAP-based method, although the power consumption has increased because the number of interconnecting wires is increased. To reduce the power consumption in the case of crosstalk avoidance codes, Sridhara and Shanbhag [8] proposed and combined a low-power code (LPC) with crosstalk avoidance codes.

The FOC, FTC, and FPC are used for detection and correction of errors due to crosstalk; thereby the data packet latency is reduced. To reduce power consumption, bus invert-based technique is used and combined with error control codes. The joint LPC-CAC code improved the performance of NoC, but still, area utilization has increased. To obtain reliable on-chip communication, Single Error Correcting-Burst Error Detecting (SEC-BED) with Hybrid Automatic Repeat reQuest (HARQ) is proposed. The single random error is detected and corrected, whereas the retransmission is requested when double random and burst errors are detected. The SEC-BED scheme detected errors efficiently, although the delay, area, and power consumption have increased because of Ex-Or-based tree structure used in calculating parity check bits and go-back-N-based retransmission used in HARQ.

To reduce worst-case bus delay, joint crosstalk avoidance with triple error correction (JTEC) code is proposed. In encoding operation, the code word is used with hamming code and then duplicated. Because hamming code is duplicated, the decoder detected 4-bit errors and corrected 3-bit errors. Because JTEC required large area, JTEC is advanced as JTEC-simultaneous quadruple error detection (JTEC-SQED). The JTEC-SQED replaced hamming codes into Hsiao codes; thereby the performance is improved when compared with JTEC. To increase error control capability, triplicate add parity (TAP) is used for encoding data and compared with sent parity bit in decoder to detect and correct the errors in interconnecting wires [9]. The TAP-based error control scheme efficiently detected and corrected 1-bit, 2-bit, and some 3-bit errors. Still, the power consumption has increased because the required number of interconnecting wires increases.

To reduce the power consumption with TAP-based scheme, this chapter proposes joint LPC-CAC-ECC scheme to detect and correct 1-bit, 2-bit, and some 3-bit burst errors efficiently, and also the power consumption of codec module is reduced with the help of BI technique. The proposed work is mainly concentrated on controlling of multiple errors and also improving of NoC communication architecture.

3. Joint CAC-ECC

The ability of error control method is determined by the reliable communication which is provided in the presence of errors. By embedding the error control schemes, the performance of the system is reduced when compared with error control scheme-less system. The data packet latency and power consumption

affect more in the presence of error control schemes. To detect and correct multiple errors efficiently, the CAC-ECC methods are combined. In this chapter, the 1-bit and 2-bit errors due to crosstalk are detected and corrected and also some of the 3-bit errors.

Triplicate add parity (TAP)-based encoder is used to transfer the data from source to destination through the interconnection wires. **Figure 2** depicts TAP-based encoder of joint CAC-ECC scheme. The 32-bit data triplicates to encode to the destination through interconnection wires. In the advanced encoder, each data bit triplicates and also calculates overall parity of 32-bit data; hence, a total of 97-bits of data are encoded to the decoder section. By triplication, the errors are efficiently controlled in the interconnecting wires.

The parity bit is also measured with Ex-Or operation and encoded to the decoder section to check the parity of received data. By the comparison of parity, the errors are detected and corrected efficiently. The decoder structure of joint CAC-ECC scheme is shown in **Figure 3**.

The decoder divides encoded data into three groups, and parity of each group is calculated and compared with sent parity bit. The encoded data are divided into three groups of 32-bit data with the help of group separator, and sent parity bit (p0) is used to compare with the parity of each group (p1, p2, p3). The 1-bit and 2-bit errors are detected when parity of group changed from sent parity. **Table 1** depicts the different possibilities of errors at data bits in interconnection wires. The 1-bit errors are detected with its parity. The 2- and 3-bit errors are identified by considering the following instances:

Instance I: p1 = p2 and p2 ≠ p3.

To find out error-less group, the parity of group 1 is compared with sent parity (p0). If p0 is equal to p1, then group 1 is considered as error-less, otherwise group 3 is considered as error-less.

Instance II: p1 ≠ p2 and p2 = p3.

To find out error-less group, the parity of group 1 is compared with sent parity. If p0 is equal to p1, then group 1 is considered as error-free, otherwise group 2 is error-free.

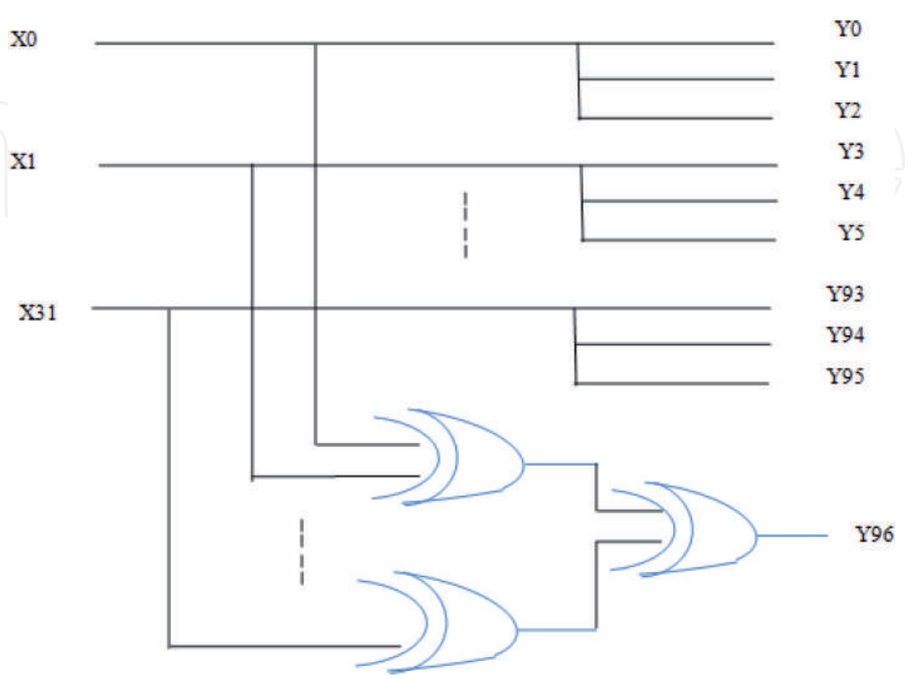

Figure 2.
TAP-based encoder of proposed scheme.

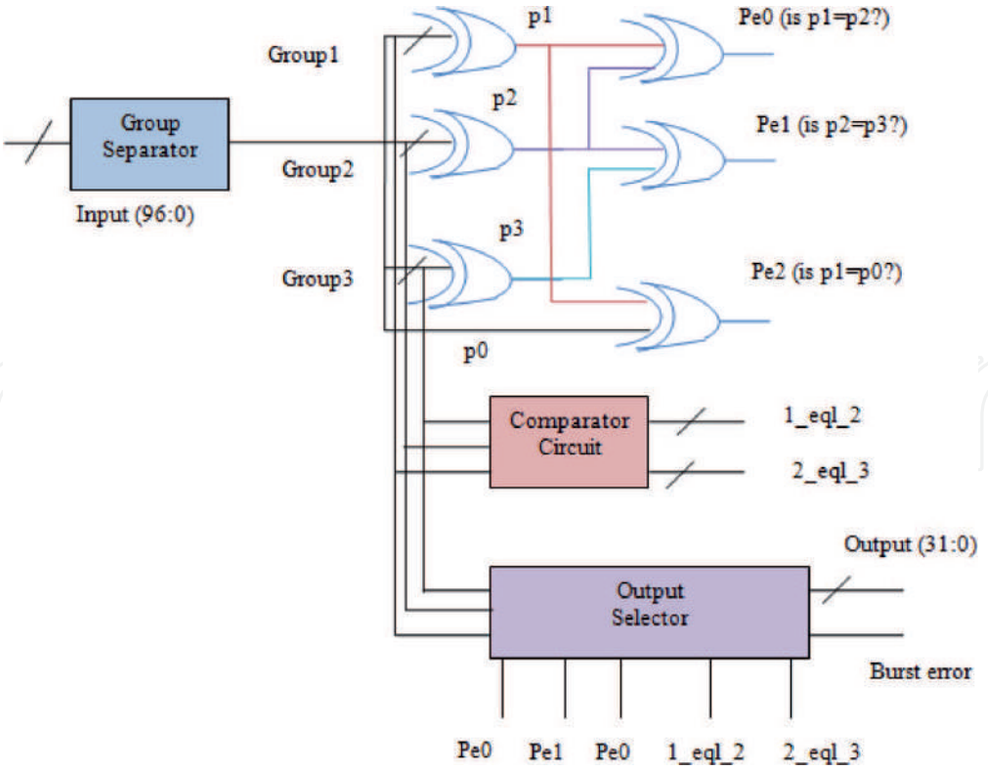

Figure 3.
Decoder structure of joint CAC-ECC scheme.

Instance III: p1 ≠ p2 and p2 ≠ p3.

To find out error-less group, the parity of group 1 is compared with sent parity. If p0 = p1, then the group is considered as error-free, otherwise group 2 is error-free.

Instance IV: p1 = p2 and p2 = p3.

The error bits highlighted in **Table 1** are considered for this instance. Because of not detecting the even parities, the error bits having even parities are divided into two categories. (i) 1-bit error in three groups is called burst error. When p0 = p1 and p1 = p2, then burst error is detectable or else consider another category.
(ii) The original data of group 1, group 2, and group 3 are compared to select error-free group. When group 1 is equal to group 2, then group 2 is selected as error-free or else group 2 and group 3 are compared again. When group 2 is equal to group 3, then group is considered as error-free or else group-1 is considered as error-free.

The number of detection and correction bits of ECC depended on the hamming distance of technique. The hamming distance of TAP-based scheme is four; that is, the triplication of data is presented, the hamming distance is three, and also one is from added parity bit. If the hamming distance of original data packets is k, then

	1-bit error				**2-bit errors**								**3-bit errors**						
Group 1 (p1)	1	0	0	1	0	1	**2**	**0**	**0**	**1**	0	1	0	3	0	0	1	2	2
Group 2 (p2)	0	1	0	1	1	0	**0**	**2**	**0**	**1**	1	0	2	0	3	0	2	1	0
Group 3 (p3)	0	0	1	0	1	1	**0**	**0**	**2**	**1**	2	2	1	0	0	3	0	0	1
	Correct				Correct								Correct					Incorrect	

Table 1.
Different possible error bits in interconnecting wires.

the number of detection error bits is k – 1 and the number of correction bits is $\frac{k-1}{2}$; hence, CAC-ECC scheme detected three error bits and corrected two error bits.

Though the CAC-ECC scheme has detected and corrected crosstalk errors efficiently, the power consumption and data packet latency have huge increase because more number of interconnecting wires are used in the advanced error control scheme. Because of triplication of original data, the combined CAC-ECC scheme used more number of wires; thereby the power consumption of advanced method has increased.

4. Advanced NoC router

The errors affect more on the performance of NoC-based SoC because of more number of interconnection links involved for parallel processing. The combined CAC-ECC scheme is embedded in the network interface (NI) of router; thereby the errors are controlled and also avoided to propagate to remaining network. The encoder of error control scheme is embedded to transmit NI (TX-NI), and decoder of error control scheme is added to the receive NI (RX-NI); thereby the original data are transferred efficiently. Because of embedded combined CAC-ECC in the NI, the router of NoC presented huge power consumption; hence, there is a need of reducing the power consumption in NoC. By analyzing various error control schemes in NI, flexible unequal error control (FUEC) methodology is introduced and generalized to any kind of error control codes [10].

4.1 Combined LPC-CA-ECC scheme

To reduce power consumption in NoC architecture in the case of error control schemes, the low-power code is added to the error control codes; thereby the power consumption is reduced and also errors are corrected efficiently. Bus invert (BI) method is used to reduce the transition activity of interconnecting wires; thereby the power consumption is reduced. The power consumption is given in eq. (1).

$$P_d = \alpha C_L f_c V_{dd}^2 \tag{1}$$

where α is the transition activity, C_L is the load capacitance, f_c is the maximum clock frequency, and V_{dd} is the supply voltage. From Eq. (1), it is known that the dynamic power consumption is directly proportional to the transition activity.

The bus invert-based low-power code (LPC) is shown in **Figure 4**. The BI technique reduced the number of transitions by using the hamming distance of original data packet; thereby the original data are inverted before encoding. The original data are inverted when the hamming distance is more than half, otherwise it is sent to encoder without inverting. The majority of voter circuit with combination of Ex-Or gates inverted the data when it is required. The majority of voter circuit is composed of a number of full-adders, which increases the size of circuit.

4.2 HARQ

The combined LPC-CAC-ECC scheme detected and corrected multiple crosstalk errors and also reduced the power consumption of on-chip interconnects. The error control scheme does not correct some of the 3-bit errors; hence, the hybrid automatic retransmission request (HARQ) is enabled to retransfer the data from source to destination. The HARQ resend the data packets when the receiver asserted continuous three negative acknowledgments (NACK).

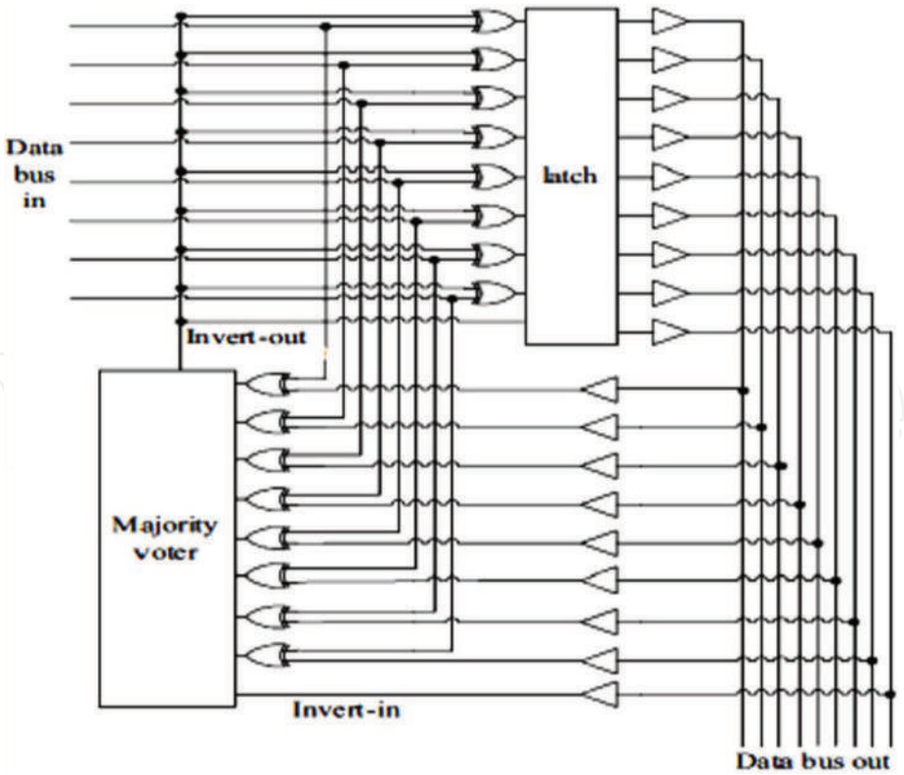

Figure 4.
Bus invert method of low-power code.

The advanced work of error control scheme is embedded in the NI of the NoC, and also codec module is responsible for encoding and decoding of the data without errors. To improve the data transfer speed of NoC, each router is added with an extra PE; thereby the number of router required to complete data transfer is reduced. To control arbitration among ports of router, the advanced scheduling algorithms are used in arbiter. The selected port transferred the data to the output through crossbar switch. To avoid deadlock error, each port of router is composed of buffer memory and its controller. A store and forward packet switching (SF) and minimal routing algorithm are used to improve the performance of mesh-based NoC architecture [11].

5. Implementation

The advanced error control scheme is designed in Xilinx 14.7 and implemented on Virtex-6 Field Programmable Gate Array (FPGA) target device. The simulation and synthesis are demonstrated for each module of NoC. The performance of NoC is evaluated in terms of area utilization (occupied slices, LUT-FF pairs, and bonded IOBs), latency (delay), and power consumption. **Table 2** shows the performance of encoder and decoder of joint CAC-ECC scheme. The area utilization and delay of codec module are increased linearly with the increase of data width because of the number of interconnection wires in encoder and also the number of cycles required to detect and correct error in decoder.

The data transfer of the encoder is more than the decoder because of the number of rounds required to detect and correct. The required cycles increase more in the case of more number of error bits and also higher data width. **Tables 3** and **4** show the performance of NoC router with CAC-ECC scheme and joint CAC-ECC-LPC scheme. From **Table 3**, it is inferred that the data transfer speed of NoC in the presence of soft errors decreased with the increase of data width because more number of interconnecting

Family	Number of occupied slices		Number of slice LUTs		Number of bonded IOBs		Delay (ns)	
	Encoder	Decoder	Encoder	Decoder	Encoder	Decoder	Encoder	Decoder
8-bit	1	15	2	39	35	36	1.01	2.82
16-bit	3	24	2	42	67	68	1.37	3.15
32-bit	7	49	7	79	131	132	1.53	3.20

Table 2.
Area utilization and delay of codec module of CAC-ECC scheme.

Family	Number of slice registers	Number of slice LUTs	Number of fully used LUT-FF pairs	Latency (ns)	Power consumption (mW)
8-bit	814	566	375	3.70	9.56
16-bit	952	636	453	5.52	47.42
32-bit	1858	1485	676	6.06	89.55

Table 3.
Performance of NoC router with CAC-ECC scheme.

wires are required for encoder of CAC-ECC scheme and also more number of cycles are required in decoder to detect and correct the soft errors in on-chip interconnecting wires. Hence, the power consumption is huge when data width is large.

From **Table 4**, it is clear that the low-power code is reducing the total power consumption even in the case of error control schemes. It is observed that the data transfer speed of NoC maintained the same and the power consumption is reduced from little to huge when data width is increased. Still, the area utilization is increased in joint LPC-CAC-ECC scheme because of a number of combinational circuits required in BI method to reduce the power consumption.

As BI code worked based on hamming distance of original data, the area utilization is increased. Still, it is reduced when hamming distance of original data is less than half; hence, the performance of NoC is improved.

Table 5 shows the comparison of proposed error control scheme with recent schemes for 32-bit of data width. From **Table 5**, it is observed that the proposed method shows better results than the existing error control methods. The comparison is shown with various parameters such as number of wires used, number of error detection and correction, swing voltage of interconnect, delay for detection and correction, and also power consumption. Among all methods, CADEC provided better results than the proposed work. Still, detection and correction of CADEC are limited to 2-bit errors. The power consumption of proposed work has improved to 11% than JTEC.

Family	Number of slice registers	Number of slice LUTs	Number of fully used LUT-FF pairs	Latency (ns)	Power consumption (mW)
8-bit	823	635	440	3.70	9.40
16-bit	996	764	518	5.52	46.90
32-bit	1926	1599	1014	6.06	81.64

Table 4.
Performance of NoC router with joint LPC-CAC-ECC method.

S. no.	Coding scheme	Data width	Number of wires used	Error detection	Error correction	Link swing voltage (V)	Delay	Power consumption (μW)
1	Hamming	32	38	Double	Single	1.02	1 + 4λ	49.30
2	Hsiao SEC-DED [12]	32	39	Double	Single	1.02	1 + 4λ	51.60
3	DAP [13]	32	65	Double	Single	1.02	1 + 2λ	16.22
4	CADEC [7]	32	77	Random and burst error of two	1-bit and 2-bit errors	0.89	1 + 2λ	26.77
5	JTEC [14]	32	77	Random and burst error of three	1-bit and 2-bit errors	0.81	1 + 2λ	39.49
6	Joint LPC-CAC-ECC	32	97	Random and burst error of three	1-bit, 2-bit errors, and some of 3	0.61	1 + 2λ	34.86

Table 5.
Comparison of advanced error control scheme with recent work.

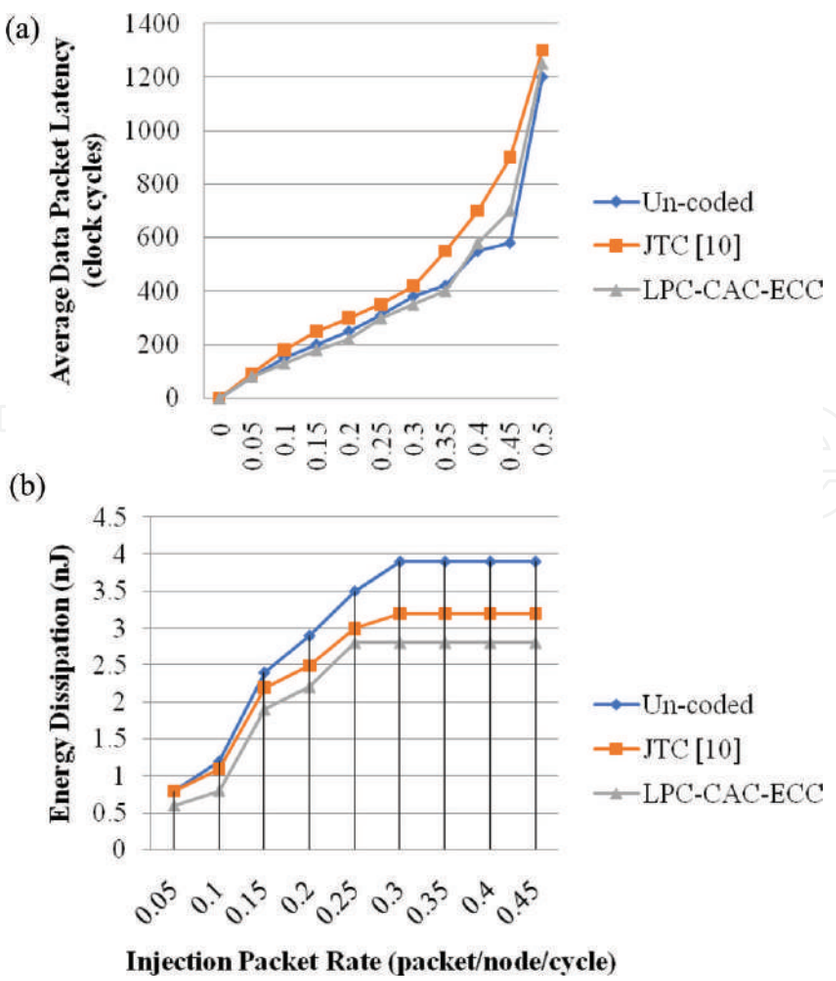

Figure 5.
Simulation results of data packet latency (a) and energy dissipation (b) of advanced NoC with others.

To analyze the data packet latency and energy dissipation, the advanced NoC architecture is simulated 32 times at uniform-random traffic in Riviera-pro windows version. Each experiment of simulation showed less latency and less energy dissipation. The 8×8 mesh-based NoC is simulated and compared with recent NoC, that is, JTC [14], and also uncoded NoC. From **Figure 5**, it is clear that the advanced NoC has lesser data packet latency and has greater than uncoded because the advanced router transfers the data with joint CAC-ECC scheme in case of occurred errors; otherwise it transfers without error control scheme. The energy dissipation of advanced NoC is lesser than both existing works because the BI-based LPC is utilized in router in case of error control code being embedded in the NI.

6. Conclusion

The scaling of technology introduces number of errors in on-chip interconnects. The crosstalk errors majorly affected the performance of NoC communication architecture due to the coupling capacitance between the interconnecting wires. This chapter discussed number of errors and their control schemes. To control multiple errors, joint CAC-ECC scheme is embedded in NI; hence the errors are controlled and avoided to propagate remaining network. As error control scheme presented more power consumption, the BI-based method of low-power code used to reduce the case of error control scheme is used. The performance of advanced NoC is simulated and compared with recent work; thereby 11% improvement is shown when compared with JTC. To analyze the data packet latency and energy dissipation, the 8×8 mesh-based NoC architecture is simulated and compared with recent work; thereby the advanced NoC architecture shows better results than the recent NoC.

Conflict of interest

It is declared that this article has no "conflict of interest."

Author details

Ashok Kumar Kummary[1*], Perumal Dananjayan[2], Kalannagari Viswanath[3] and Vanga Karunakar Reddy[1]

1 Matrusri Engineering College, Hyderabad, Telangana, India

2 Pondicherry Engineering College, Puducherry, India

3 R.L. Jalappa Institute of Technology, Bangalore, India

*Address all correspondence to: kashok483@gmail.com

IntechOpen

© 2019 The Author(s). Licensee IntechOpen. This chapter is distributed under the terms of the Creative Commons Attribution License (http://creativecommons.org/licenses/by/3.0), which permits unrestricted use, distribution, and reproduction in any medium, provided the original work is properly cited. CC BY

References

[1] Benini L, De Micheli G. Networks on chips: A new SoC paradigm. Computer-IEEE Computer Society. 2002;**35**:70-78. DOI: 10.1109/2.976921

[2] Patel KN, Markov IL. Error-correction and crosstalk avoidance in DSM busses. In: Proceedings of the 2003 International Workshop on System-Level Interconnect Prediction 2003 Apr 5; ACM. pp. 9-14. DOI: 10.1145/639929.639933

[3] The International Technology Roadmap for Semiconductors [Internet]. 2011. Available from: http://www.itrs2.net/2013-itrs.html

[4] Fu B, Ampadu P. Error Control for Network-on-Chip Links. New York; Springer Science & Business Media, Verlag; 2011. DOI: 10.1007/978-1-4419-9313-7

[5] Hamming RW. Error detecting and error correcting codes. Bell System Technical Journal. 1950;**29**(2):147-160. DOI: 10.1002/j.1538-7305.1950.tb00463.x

[6] Pande PP, Zhu H, Ganguly A, Grecu C. Energy reduction through crosstalk avoidance coding in NoC paradigm. In: Digital System Design: Architectures, Methods and Tools, 2006. DSD 2006. 9th EUROMICRO Conference on 2006 Sep; IEEE. pp. 689-695. DOI: 10.1109/DSD.2006.49

[7] Ganguly A, Pande PP, Belzer B, Grecu C. Design of low power & reliable networks on chip through joint crosstalk avoidance and multiple error correction coding. Journal of Electronic Testing. 2008;**24**(1-3):67-81. DOI: 10.1007/s10836-007-5035-1

[8] Sridhara SR, Shanbhag NR. Coding for system-on-chip networks: A unified framework. IEEE Transactions on Very Large Scale Integration (VLSI) Systems. 2005;**13**(6):655-667. DOI: 10.1109/TVLSI.2005.848816

[9] Maheswari M, Seetharaman G. Design of a novel error correction coding with crosstalk avoidance for reliable on-chip interconnection link. International Journal of Computer Applications in Technology. 2014;**49**(1):80-88. DOI: 10.1504/IJCAT.2014.059097

[10] Gracia-Morán J, Saiz-Adalid LJ, Gil-Tomás D, Gil-Vicente PJ. Improving error correction codes for multiple-cell upsets in space applications. IEEE Transactions on Very Large Scale Integration (VLSI) Systems. 2018;**26**:2132-2142. DOI: 10.1109/TVLSI.2018.2837220

[11] Kumar K A, Dananjayan P. Reduction of power consumption using joint low power code with crosstalk avoidance code in case of crosstalk and random burst errors. International Journal of Engineering & Technology. 2018;**7**(3.12):62-68. DOI: 10.14419/ijet.v7i3.12.15864

[12] Fu B, Ampadu P. Burst error detection hybrid ARQ with crosstalk-delay reduction for reliable on-chip interconnects. In: Defect and Fault Tolerance in VLSI Systems, 2009. DFT'09. 24th IEEE International Symposium on 2009; IEEE. pp. 440-448. DOI: 10.1109/DFT.2009.45

[13] Pande PP, Ganguly A, Feero B, Belzer B, Grecu C. Design of low power & reliable networks on Chip through joint crosstalk avoidance and forward error correction coding. In: Null 2006 Oct 4; IEEE. pp. 466-476. DOI:10.1109/DFT.2006.22

[14] Ganguly A, Pande PP, Belzer B. Crosstalk-aware channel coding schemes for energy efficient and reliable NOC interconnects. IEEE Transactions on Very Large Scale Integration (VLSI) Systems. 2009;**17**(11):1626-1639. DOI: 10.1109/TVLSI.2008.2005722

→ 15% off orders of all print products | Use Code: BOOKLOVER15 | Ends February 12th at 11:59 PM UTC | Details

lulu Menu

Search

Show Bookstore Categories

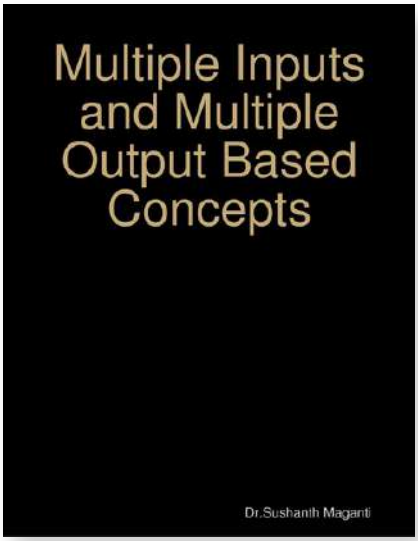

Multiple Inputs and Multiple Output Based Concepts

By Dr.M.Sushanth Babu

Ebook
GBP 7.18

Add to Cart

Share

n radio, multiple-input and multiple-output, or MIMO (pronounced /ˈmaɪmoʊ/ or /ˈmiːmoʊ/), is a method for multiplying the capacity of a radio link using multiple transmit and receive antennas to exploit multipath propagation.[1] MIMO has become an essential element of wireless communication standards including IEEE 802.11n (Wi-Fi), IEEE 802.11ac (Wi-Fi), HSPA+ (3G), WiMAX (4G), and Long Term Evolution (4G). More recently, MIMO has been applied to power-line communication for 3-wire installations as part of ITU G.hn standard and HomePlug AV2 specification.

Details

Publication Date	1/21/2017
Language	English
ISBN	9781365697760
Category	Engineering
Copyright	All Rights Reserved - Standard Copyright License
Contributors	By (author): Dr.M.Sushanth Babu

Specifications

Format	EPUB

Keywords

MIMO WSN LTE

Report This Content to Lulu

Ratings & Reviews

Write a review

Did you love this book? Leave a review for other readers!

About Us
Work at Lulu
English
Help Center
GBP

blog

Get exclusive Publishing & Marketing tips to help you create and sell your books more effectively! You can unsubscribe at any time.

Your Email
Submit

lulu
lulu api
Lulu JUNIOR
glasstree

Privacy Policy
Terms & Conditions
Copyright © 2021 Lulu Press, Inc. All rights reserved.

50% OFF CALENDARS & PLANNERS

Add to Wishlist

Low Power Transmission System Based On Smart Technologies

by Dr.M.Sushanth babu

★★★★★ (0)

NOOK Book (eBook)

$8.99

ADD TO CART

Sign in to Purchase Instantly

Available on Compatible NOOK Devices and the free NOOK Apps.

WANT A NOOK? Explore Now

Get Free NOOK Book Sample

Buy As Gift

LEND ME® See Details

Overview

lectric power transmission is the bulk movement of electrical energy from a generating site, such as a power plant, to an electrical substation. The interconnected lines which facilitate this movement are known as a transmission network. This is distinct from the local wiring between high-voltage substations and customers, which is typically referred to as electric power distribution. The combined transmission and distribution network is known as the "power grid" in North America, or just "the grid". In the United Kingdom, the network is known as the "National Grid"

Manage Preferences

Accept All Cookies

Barnes & Noble uses cookies to offer you a better user experience. By clicking “Accept All Cookies” you agree to the storing of cookies on your device in accordance with our **Cookie Policy**

REVIEWS

★★★★★
Click here to be the first to review this product

Recently Viewed

Clear All

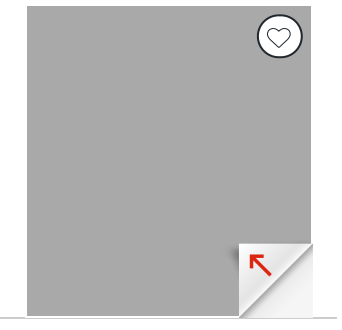

Low Power Transmission System Based On Smart ...
by Dr.M.Sushanth babu
★★★★★

Related Searches

book by charles f haanel
book by christopher hand
book by ahmed mousa
transmission of electrical power
book by happy caldwell
book by phil rourk

Explore More Items

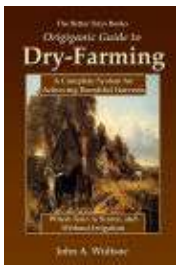

The Better Days Books Origiganic Guide to Dry-Farming:
Nearly 60% of the earth's land surface receives twenty inches or less of annual rainfall- ...
Quick View

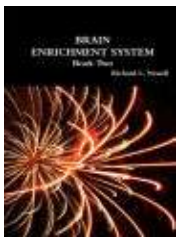

BRAIN ENRICHMENT SYSTEM Book Two
Experience this Unique and Humorous mode of systematically reinforced learning. Increase Your Mental Powers and ...
Quick View

Control System Analysis & Design in MATLAB and
Control System Analysis & Design in MATLAB and SIMULINK is blueprinted to solve undergraduate control ...
Quick View

Barnes & Noble Press
Publish your book with B&N
Learn More ›

The B&N Mastercard®
5% Back on All B&N Purchases
Learn More ›

Download the Free NOOK App

Become a B&N Member

Manage Preferences

Accept All Cookies

Barnes & Noble uses cookies to offer you a better user experience. By clicking “Accept All Cookies” you agree to the storing of cookies on your device in accordance with our **Cookie Policy**

Store name, location, or ZIP code

Sign up for savings, news, and updates

Email Address

Submit your email address to receive Barnes & Noble offers & updates. You can view Barnes & Noble's Privacy Policy here. Unsubscribe from our emails at any time.

Terms of Use Copyright & Trademark Privacy Do Not Sell My Personal Information Accessibility Cookie Policy Sitemap

©1997-2021 Barnes & Noble Booksellers, Inc.

33 East 17th Street, New York, NY 10003

Manage Preferences

Accept All Cookies

Barnes & Noble uses cookies to offer you a better user experience. By clicking "Accept All Cookies" you agree to the storing of cookies on your device in accordance with our **Cookie Policy**

We are IntechOpen, the world's leading publisher of Open Access books Built by scientists, for scientists

5,200
Open access books available

127,000
International authors and editors

150M
Downloads

Our authors are among the

154
Countries delivered to

TOP 1%
most cited scientists

12.2%
Contributors from top 500 universities

WEB OF SCIENCE™

Selection of our books indexed in the Book Citation Index in Web of Science™ Core Collection (BKCI)

Interested in publishing with us? Contact book.department@intechopen.com

Numbers displayed above are based on latest data collected.
For more information visit www.intechopen.com

Chapter

Combined Crosstalk Avoidance Code with Error Control Code for Detection and Correction of Random and Burst Errors

Ashok Kumar Kummary, Perumal Dananjayan, Kalannagari Viswanath and Vanga Karunakar Reddy

Abstract

Error correction codes are majorly important to detect and correct occurred errors because of various noise sources. When the technology is scaling down, the effect of noise sources is high. The coupling capacitance is one of the main constraints to affect the performance of on-chip interconnects. Because of coupling capacitance, the crosstalk is introduced at on-chip interconnecting wires. To control the single or multiple errors, an efficient error correction code is required. By combining crosstalk avoidance with error control code, the reliable intercommunication is obtained in network-on-chip (NoC)-based system on chip (SoC). To reduce the power consumption of error control codes, the bus invert-based low-power code is integrated to network interface of NoC. The advanced work is designed and implemented with Xilinx 14.7; thereby the performance of improved NoC is evaluated and compared with existing work. The 8×8 mesh-based NoC is simulated at various traffic patterns to analyze the energy dissipation and average data packet latency.

Keywords: NoC, CAC, ECC LPC, SoC, FPGA

1. Introduction

As technology is scaling up, a number of circuits are integrated in on-chip. The intercommunication among the on-chip devices is majorly important because of millions of integrated devices in the system on chip (SoC). The communication architectures of SoC are not efficient to provide high performance; thereby network-on-chip (NoC) is the new paradigm introduced [1]. Because of parallelism, the NoC is providing high performance in terms of scalability and flexibility even in the case of millions of on-chip devices. Still, NoC suffers with design parameters that affect the performance of NoC. As technology is scaling up, the performance of NoC is mainly affected with coupling capacitance. The effect of crosstalk capacitance is more in horizontal than in vertical; thereby the crosstalk errors frequently occur in on-chip interconnecting wires [2]. An efficient error correction code is required to control the crosstalk error that may occur once or multiple times. The crosstalk avoidance codes (CAC) are popularized to control the error in on-chip interconnects; thereby a reliable communication is obtained.

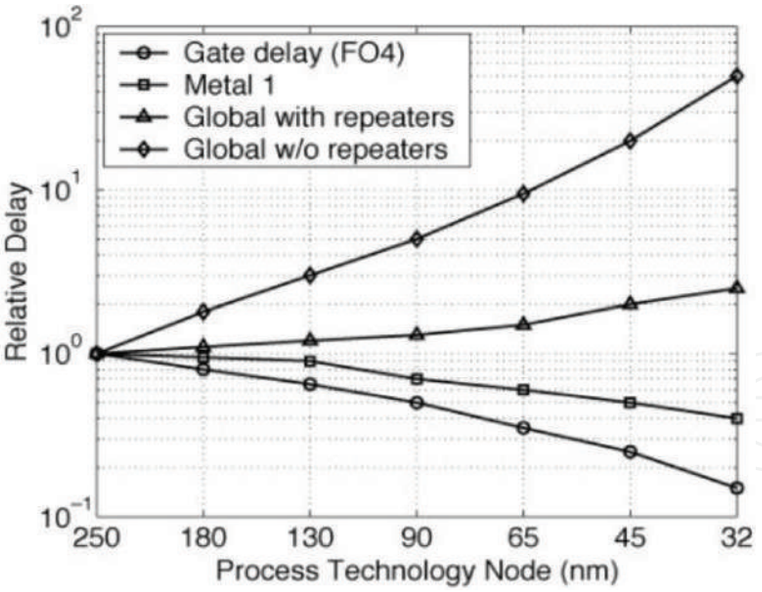

Figure 1.
Trend of relative delay with scaling of technology [3].

The CAC reduced the worst-case switching capacitance in on-chip interconnects by avoiding the switching transitions of data that is 010-101. This condition reduced the worst-case capacitance from $(1 + 4\lambda)\, C_L$ to $(1 + 2\lambda)\, C_L$; hence, the energy dissipation is reduced from $(1 + 4\lambda)\, C_L \alpha V_{dd}^2$ to $(1 + 2\lambda)\, C_L \alpha V_{dd}^2$ where λ is the ratio of coupling capacitance to total capacitance, C_L is the self-capacitance of interconnection wire, α is the transition factor, and V_{dd} is the supply voltage for the system. The energy dissipation is reduced by reducing the transition activity of interconnection wires for the data packet. The behavior of relative delay with scaling of technology is shown in **Figure 1**.

International Technology Roadmap for Semiconductor (ITRS-2011) predicted that when the delay from the gates is reduced, the delay from wires is increased with scaling of technology because the interconnecting wires are affected more when scaling of technology is less than 45 nm [3]. Hence, the interconnecting wires affected the performance of NoC-based SoC in terms of delay as well as energy consumption, and it is huge in case of the errors.

The errors mainly occur in interconnecting wires because of coupling capacitance; thereby strong error correction code (ECC) is required to detect and correct errors [4]. The error may occur once or multiple times, and also multiple errors occurred in interconnection wires; hence, the ECCs are not enough to detect and correct errors. In literature, different techniques are proposed for detection and correction of multiple errors. The parity check, dual rail (DR), modified dual rail (MDR), boundary shift code (BSC), and CAC are popularized among various techniques for control of multiple errors in interconnection wires.

The remaining chapter is as follows: Section 2 includes the related work of error control methods and also discussed the merits and demerits. Section 3 presented the proposed encoder and decoder of combined CAC-ECC method. Section 4 gives the advanced encoding and decoding of NoC router with combined LPC-CAC-ECC scheme. Section 5 discussed the implementation of proposed work in NoC architecture, and finally, Section 6 concludes the chapter.

2. Related work

The detection and correction of errors present in the on-chip interconnects are majorly important because it leads to drop or block data packet; hence the performance

of NoC architecture is reduced. Huge research is going on for the error detection and correction of on-chip interconnects. Parity code is used to detect 1-bit error in data packet. It is simple but errors are not corrected. Hamming code is proposed for detection of 2-bit errors and also correction of 1-bit error [5]. Various error control codes are introduced with the help of hamming code because it is easy to implement.

To reduce delay in on-chip interconnects, forbidden overlap condition (FOC), forbidden transition condition (FTC), and forbidden pattern condition (FPC) of crosstalk avoidance code are used [6]. The crosstalk avoidance codes are reduced delay from $(1 + 4\lambda) C_L$ to $(1 + 2\lambda) C_L$ and also energy dissipation. Still, the area utilization has increased because the extra bits are added to the original data packet. To control multiple errors, duplicate parity (DAP) is proposed by duplicating data packets, and then hamming code is used for transmission of duplicated data [7]. The average data packet latency is reduced by DAP-based method, although the power consumption has increased because the number of interconnecting wires is increased. To reduce the power consumption in the case of crosstalk avoidance codes, Sridhara and Shanbhag [8] proposed and combined a low-power code (LPC) with crosstalk avoidance codes.

The FOC, FTC, and FPC are used for detection and correction of errors due to crosstalk; thereby the data packet latency is reduced. To reduce power consumption, bus invert-based technique is used and combined with error control codes. The joint LPC-CAC code improved the performance of NoC, but still, area utilization has increased. To obtain reliable on-chip communication, Single Error Correcting-Burst Error Detecting (SEC-BED) with Hybrid Automatic Repeat reQuest (HARQ) is proposed. The single random error is detected and corrected, whereas the retransmission is requested when double random and burst errors are detected. The SEC-BED scheme detected errors efficiently, although the delay, area, and power consumption have increased because of Ex-Or-based tree structure used in calculating parity check bits and go-back-N-based retransmission used in HARQ.

To reduce worst-case bus delay, joint crosstalk avoidance with triple error correction (JTEC) code is proposed. In encoding operation, the code word is used with hamming code and then duplicated. Because hamming code is duplicated, the decoder detected 4-bit errors and corrected 3-bit errors. Because JTEC required large area, JTEC is advanced as JTEC-simultaneous quadruple error detection (JTEC-SQED). The JTEC-SQED replaced hamming codes into Hsiao codes; thereby the performance is improved when compared with JTEC. To increase error control capability, triplicate add parity (TAP) is used for encoding data and compared with sent parity bit in decoder to detect and correct the errors in interconnecting wires [9]. The TAP-based error control scheme efficiently detected and corrected 1-bit, 2-bit, and some 3-bit errors. Still, the power consumption has increased because the required number of interconnecting wires increases.

To reduce the power consumption with TAP-based scheme, this chapter proposes joint LPC-CAC-ECC scheme to detect and correct 1-bit, 2-bit, and some 3-bit burst errors efficiently, and also the power consumption of codec module is reduced with the help of BI technique. The proposed work is mainly concentrated on controlling of multiple errors and also improving of NoC communication architecture.

3. Joint CAC-ECC

The ability of error control method is determined by the reliable communication which is provided in the presence of errors. By embedding the error control schemes, the performance of the system is reduced when compared with error control scheme-less system. The data packet latency and power consumption

affect more in the presence of error control schemes. To detect and correct multiple errors efficiently, the CAC-ECC methods are combined. In this chapter, the 1-bit and 2-bit errors due to crosstalk are detected and corrected and also some of the 3-bit errors.

Triplicate add parity (TAP)-based encoder is used to transfer the data from source to destination through the interconnection wires. **Figure 2** depicts TAP-based encoder of joint CAC-ECC scheme. The 32-bit data triplicates to encode to the destination through interconnection wires. In the advanced encoder, each data bit triplicates and also calculates overall parity of 32-bit data; hence, a total of 97-bits of data are encoded to the decoder section. By triplication, the errors are efficiently controlled in the interconnecting wires.

The parity bit is also measured with Ex-Or operation and encoded to the decoder section to check the parity of received data. By the comparison of parity, the errors are detected and corrected efficiently. The decoder structure of joint CAC-ECC scheme is shown in **Figure 3**.

The decoder divides encoded data into three groups, and parity of each group is calculated and compared with sent parity bit. The encoded data are divided into three groups of 32-bit data with the help of group separator, and sent parity bit (p0) is used to compare with the parity of each group (p1, p2, p3). The 1-bit and 2-bit errors are detected when parity of group changed from sent parity. **Table 1** depicts the different possibilities of errors at data bits in interconnection wires. The 1-bit errors are detected with its parity. The 2- and 3-bit errors are identified by considering the following instances:

Instance I: p1 = p2 and p2 ≠ p3.

To find out error-less group, the parity of group 1 is compared with sent parity (p0). If p0 is equal to p1, then group 1 is considered as error-less, otherwise group 3 is considered as error-less.

Instance II: p1 ≠ p2 and p2 = p3.

To find out error-less group, the parity of group 1 is compared with sent parity. If p0 is equal to p1, then group 1 is considered as error-free, otherwise group 2 is error-free.

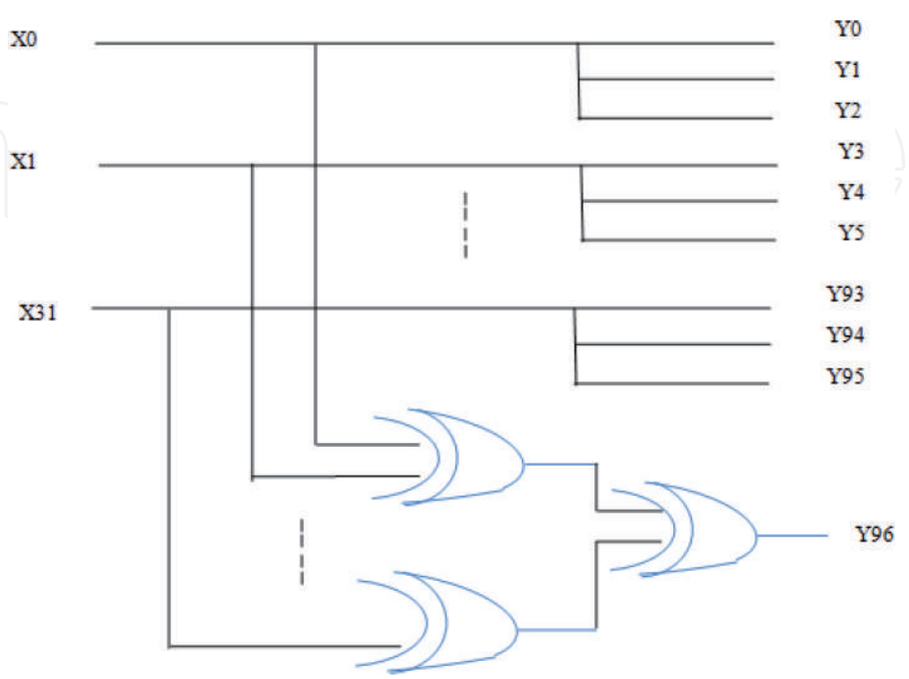

Figure 2.
TAP-based encoder of proposed scheme.

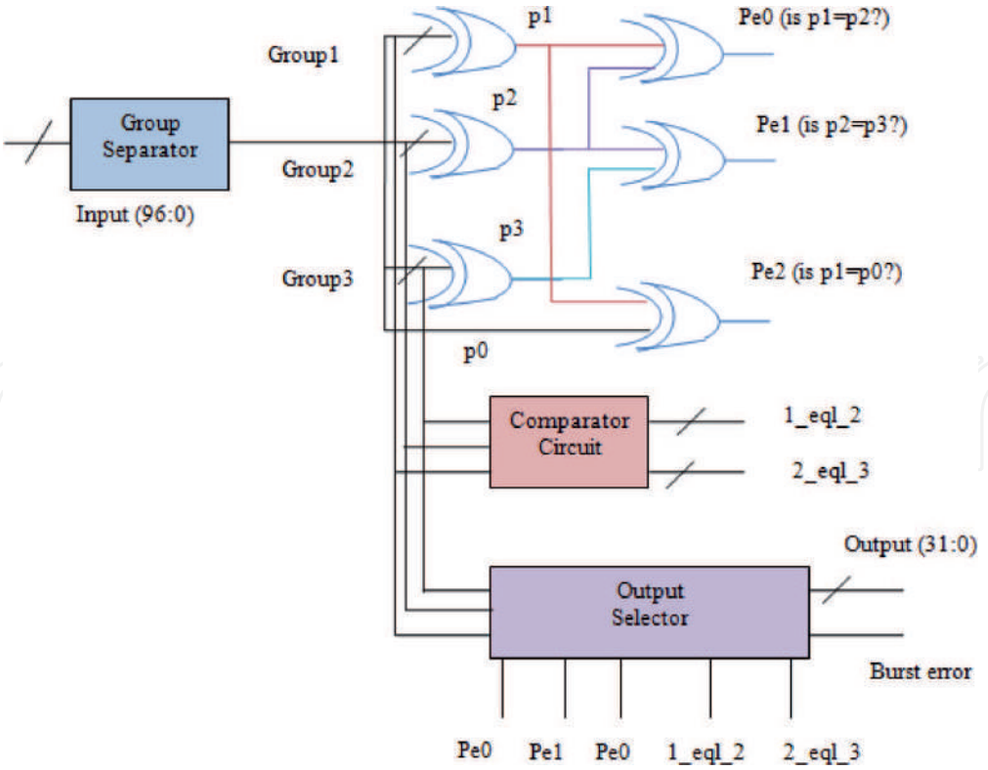

Figure 3.
Decoder structure of joint CAC-ECC scheme.

Instance III: p1 ≠ p2 and p2 ≠ p3.

To find out error-less group, the parity of group 1 is compared with sent parity. If p0 = p1, then the group is considered as error-free, otherwise group 2 is error-free.

Instance IV: p1 = p2 and p2 = p3.

The error bits highlighted in **Table 1** are considered for this instance. Because of not detecting the even parities, the error bits having even parities are divided into two categories. (i) 1-bit error in three groups is called burst error. When p0 = p1 and p1 = p2, then burst error is detectable or else consider another category.
(ii) The original data of group 1, group 2, and group 3 are compared to select error-free group. When group 1 is equal to group 2, then group 2 is selected as error-free or else group 2 and group 3 are compared again. When group 2 is equal to group 3, then group is considered as error-free or else group-1 is considered as error-free.

The number of detection and correction bits of ECC depended on the hamming distance of technique. The hamming distance of TAP-based scheme is four; that is, the triplication of data is presented, the hamming distance is three, and also one is from added parity bit. If the hamming distance of original data packets is k, then

	1-bit error				**2-bit errors**								**3-bit errors**						
Group 1 (p1)	1	0	0	1	0	1	**2**	**0**	**0**	**1**	0	1	0	3	0	0	1	2	2
Group 2 (p2)	0	1	0	1	1	0	**0**	**2**	**0**	**1**	1	0	2	0	3	0	2	1	0
Group 3 (p3)	0	0	1	0	1	1	**0**	**0**	**2**	**1**	2	2	1	0	0	3	0	0	1
	Correct				Correct								Correct					Incorrect	

Table 1.
Different possible error bits in interconnecting wires.

the number of detection error bits is k – 1 and the number of correction bits is $\frac{k-1}{2}$; hence, CAC-ECC scheme detected three error bits and corrected two error bits.

Though the CAC-ECC scheme has detected and corrected crosstalk errors efficiently, the power consumption and data packet latency have huge increase because more number of interconnecting wires are used in the advanced error control scheme. Because of triplication of original data, the combined CAC-ECC scheme used more number of wires; thereby the power consumption of advanced method has increased.

4. Advanced NoC router

The errors affect more on the performance of NoC-based SoC because of more number of interconnection links involved for parallel processing. The combined CAC-ECC scheme is embedded in the network interface (NI) of router; thereby the errors are controlled and also avoided to propagate to remaining network. The encoder of error control scheme is embedded to transmit NI (TX-NI), and decoder of error control scheme is added to the receive NI (RX-NI); thereby the original data are transferred efficiently. Because of embedded combined CAC-ECC in the NI, the router of NoC presented huge power consumption; hence, there is a need of reducing the power consumption in NoC. By analyzing various error control schemes in NI, flexible unequal error control (FUEC) methodology is introduced and generalized to any kind of error control codes [10].

4.1 Combined LPC-CA-ECC scheme

To reduce power consumption in NoC architecture in the case of error control schemes, the low-power code is added to the error control codes; thereby the power consumption is reduced and also errors are corrected efficiently. Bus invert (BI) method is used to reduce the transition activity of interconnecting wires; thereby the power consumption is reduced. The power consumption is given in eq. (1).

$$P_d = \alpha C_L f_c V_{dd}^2 \tag{1}$$

where α is the transition activity, C_L is the load capacitance, f_c is the maximum clock frequency, and V_{dd} is the supply voltage. From Eq. (1), it is known that the dynamic power consumption is directly proportional to the transition activity.

The bus invert-based low-power code (LPC) is shown in **Figure 4**. The BI technique reduced the number of transitions by using the hamming distance of original data packet; thereby the original data are inverted before encoding. The original data are inverted when the hamming distance is more than half, otherwise it is sent to encoder without inverting. The majority of voter circuit with combination of Ex-Or gates inverted the data when it is required. The majority of voter circuit is composed of a number of full-adders, which increases the size of circuit.

4.2 HARQ

The combined LPC-CAC-ECC scheme detected and corrected multiple crosstalk errors and also reduced the power consumption of on-chip interconnects. The error control scheme does not correct some of the 3-bit errors; hence, the hybrid automatic retransmission request (HARQ) is enabled to retransfer the data from source to destination. The HARQ resend the data packets when the receiver asserted continuous three negative acknowledgments (NACK).

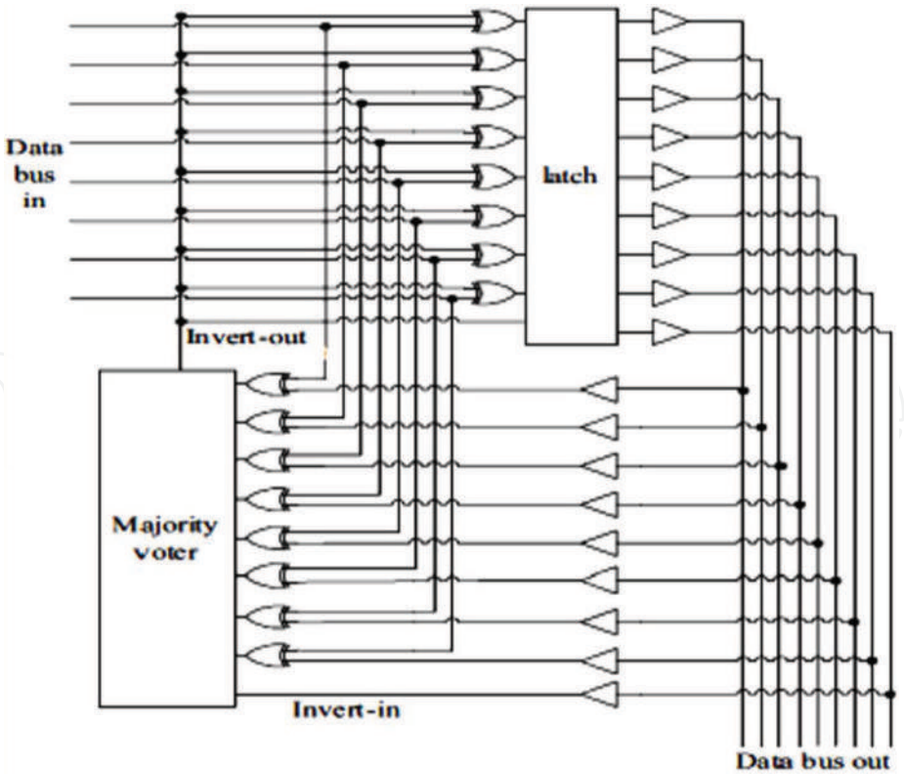

Figure 4.
Bus invert method of low-power code.

The advanced work of error control scheme is embedded in the NI of the NoC, and also codec module is responsible for encoding and decoding of the data without errors. To improve the data transfer speed of NoC, each router is added with an extra PE; thereby the number of router required to complete data transfer is reduced. To control arbitration among ports of router, the advanced scheduling algorithms are used in arbiter. The selected port transferred the data to the output through crossbar switch. To avoid deadlock error, each port of router is composed of buffer memory and its controller. A store and forward packet switching (SF) and minimal routing algorithm are used to improve the performance of mesh-based NoC architecture [11].

5. Implementation

The advanced error control scheme is designed in Xilinx 14.7 and implemented on Virtex-6 Field Programmable Gate Array (FPGA) target device. The simulation and synthesis are demonstrated for each module of NoC. The performance of NoC is evaluated in terms of area utilization (occupied slices, LUT-FF pairs, and bonded IOBs), latency (delay), and power consumption. **Table 2** shows the performance of encoder and decoder of joint CAC-ECC scheme. The area utilization and delay of codec module are increased linearly with the increase of data width because of the number of interconnection wires in encoder and also the number of cycles required to detect and correct error in decoder.

The data transfer of the encoder is more than the decoder because of the number of rounds required to detect and correct. The required cycles increase more in the case of more number of error bits and also higher data width. **Tables 3** and **4** show the performance of NoC router with CAC-ECC scheme and joint CAC-ECC-LPC scheme. From **Table 3**, it is inferred that the data transfer speed of NoC in the presence of soft errors decreased with the increase of data width because more number of interconnecting

Family	Number of occupied slices		Number of slice LUTs		Number of bonded IOBs		Delay (ns)	
	Encoder	Decoder	Encoder	Decoder	Encoder	Decoder	Encoder	Decoder
8-bit	1	15	2	39	35	36	1.01	2.82
16-bit	3	24	2	42	67	68	1.37	3.15
32-bit	7	49	7	79	131	132	1.53	3.20

Table 2.
Area utilization and delay of codec module of CAC-ECC scheme.

Family	Number of slice registers	Number of slice LUTs	Number of fully used LUT-FF pairs	Latency (ns)	Power consumption (mW)
8-bit	814	566	375	3.70	9.56
16-bit	952	636	453	5.52	47.42
32-bit	1858	1485	676	6.06	89.55

Table 3.
Performance of NoC router with CAC-ECC scheme.

wires are required for encoder of CAC-ECC scheme and also more number of cycles are required in decoder to detect and correct the soft errors in on-chip interconnecting wires. Hence, the power consumption is huge when data width is large.

From **Table 4**, it is clear that the low-power code is reducing the total power consumption even in the case of error control schemes. It is observed that the data transfer speed of NoC maintained the same and the power consumption is reduced from little to huge when data width is increased. Still, the area utilization is increased in joint LPC-CAC-ECC scheme because of a number of combinational circuits required in BI method to reduce the power consumption.

As BI code worked based on hamming distance of original data, the area utilization is increased. Still, it is reduced when hamming distance of original data is less than half; hence, the performance of NoC is improved.

Table 5 shows the comparison of proposed error control scheme with recent schemes for 32-bit of data width. From **Table 5**, it is observed that the proposed method shows better results than the existing error control methods. The comparison is shown with various parameters such as number of wires used, number of error detection and correction, swing voltage of interconnect, delay for detection and correction, and also power consumption. Among all methods, CADEC provided better results than the proposed work. Still, detection and correction of CADEC are limited to 2-bit errors. The power consumption of proposed work has improved to 11% than JTEC.

Family	Number of slice registers	Number of slice LUTs	Number of fully used LUT-FF pairs	Latency (ns)	Power consumption (mW)
8-bit	823	635	440	3.70	9.40
16-bit	996	764	518	5.52	46.90
32-bit	1926	1599	1014	6.06	81.64

Table 4.
Performance of NoC router with joint LPC-CAC-ECC method.

S. no.	Coding scheme	Data width	Number of wires used	Error detection	Error correction	Link swing voltage (V)	Delay	Power consumption (μW)
1	Hamming	32	38	Double	Single	1.02	1 + 4λ	49.30
2	Hsiao SEC-DED [12]	32	39	Double	Single	1.02	1 + 4λ	51.60
3	DAP [13]	32	65	Double	Single	1.02	1 + 2λ	16.22
4	CADEC [7]	32	77	Random and burst error of two	1-bit and 2-bit errors	0.89	1 + 2λ	26.77
5	JTEC [14]	32	77	Random and burst error of three	1-bit and 2-bit errors	0.81	1 + 2λ	39.49
6	Joint LPC-CAC-ECC	32	97	Random and burst error of three	1-bit, 2-bit errors, and some of 3	0.61	1 + 2λ	34.86

Table 5.
Comparison of advanced error control scheme with recent work.

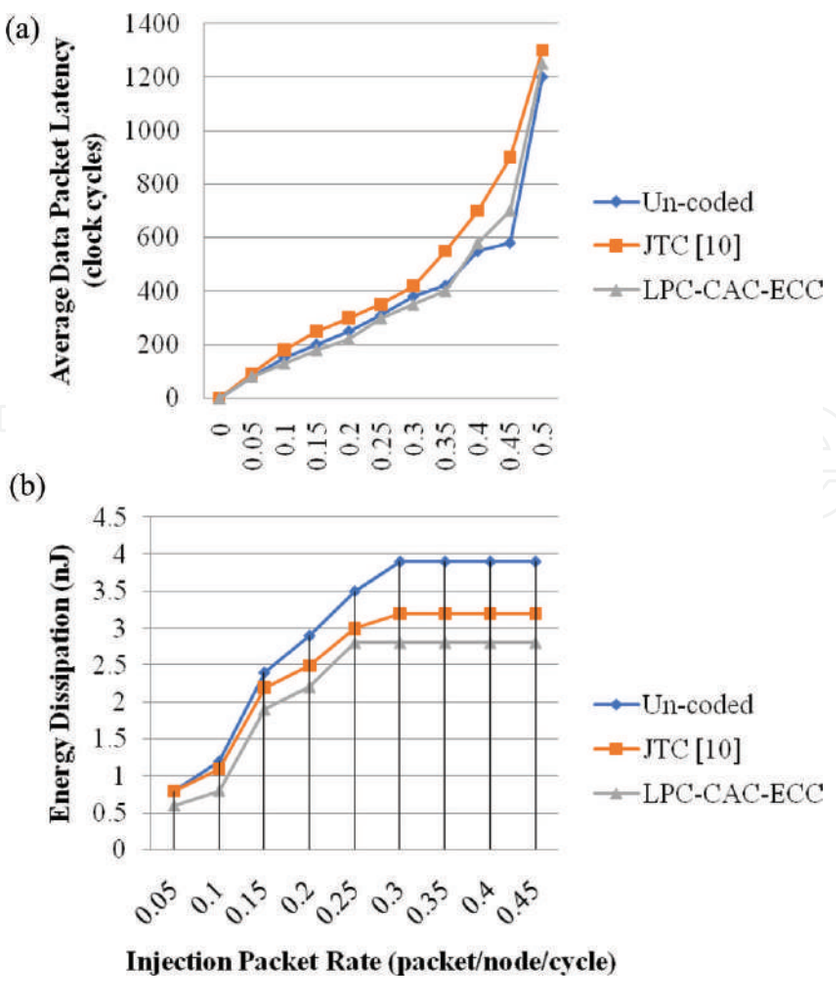

Figure 5.
Simulation results of data packet latency (a) and energy dissipation (b) of advanced NoC with others.

To analyze the data packet latency and energy dissipation, the advanced NoC architecture is simulated 32 times at uniform-random traffic in Riviera-pro windows version. Each experiment of simulation showed less latency and less energy dissipation. The 8×8 mesh-based NoC is simulated and compared with recent NoC, that is, JTC [14], and also uncoded NoC. From **Figure 5**, it is clear that the advanced NoC has lesser data packet latency and has greater than uncoded because the advanced router transfers the data with joint CAC-ECC scheme in case of occurred errors; otherwise it transfers without error control scheme. The energy dissipation of advanced NoC is lesser than both existing works because the BI-based LPC is utilized in router in case of error control code being embedded in the NI.

6. Conclusion

The scaling of technology introduces number of errors in on-chip interconnects. The crosstalk errors majorly affected the performance of NoC communication architecture due to the coupling capacitance between the interconnecting wires. This chapter discussed number of errors and their control schemes. To control multiple errors, joint CAC-ECC scheme is embedded in NI; hence the errors are controlled and avoided to propagate remaining network. As error control scheme presented more power consumption, the BI-based method of low-power code used to reduce the case of error control scheme is used. The performance of advanced NoC is simulated and compared with recent work; thereby 11% improvement is shown when compared with JTC. To analyze the data packet latency and energy dissipation, the 8×8 mesh-based NoC architecture is simulated and compared with recent work; thereby the advanced NoC architecture shows better results than the recent NoC.

Conflict of interest

It is declared that this article has no "conflict of interest."

Author details

Ashok Kumar Kummary[1*], Perumal Dananjayan[2], Kalannagari Viswanath[3] and Vanga Karunakar Reddy[1]

1 Matrusri Engineering College, Hyderabad, Telangana, India

2 Pondicherry Engineering College, Puducherry, India

3 R.L. Jalappa Institute of Technology, Bangalore, India

*Address all correspondence to: kashok483@gmail.com

IntechOpen

© 2019 The Author(s). Licensee IntechOpen. This chapter is distributed under the terms of the Creative Commons Attribution License (http://creativecommons.org/licenses/by/3.0), which permits unrestricted use, distribution, and reproduction in any medium, provided the original work is properly cited. CC BY

References

[1] Benini L, De Micheli G. Networks on chips: A new SoC paradigm. Computer-IEEE Computer Society. 2002;**35**:70-78. DOI: 10.1109/2.976921

[2] Patel KN, Markov IL. Error-correction and crosstalk avoidance in DSM busses. In: Proceedings of the 2003 International Workshop on System-Level Interconnect Prediction 2003 Apr 5; ACM. pp. 9-14. DOI: 10.1145/639929.639933

[3] The International Technology Roadmap for Semiconductors [Internet]. 2011. Available from: http://www.itrs2.net/2013-itrs.html

[4] Fu B, Ampadu P. Error Control for Network-on-Chip Links. New York; Springer Science & Business Media, Verlag; 2011. DOI: 10.1007/978-1-4419-9313-7

[5] Hamming RW. Error detecting and error correcting codes. Bell System Technical Journal. 1950;**29**(2):147-160. DOI: 10.1002/j.1538-7305.1950.tb00463.x

[6] Pande PP, Zhu H, Ganguly A, Grecu C. Energy reduction through crosstalk avoidance coding in NoC paradigm. In: Digital System Design: Architectures, Methods and Tools, 2006. DSD 2006. 9th EUROMICRO Conference on 2006 Sep; IEEE. pp. 689-695. DOI: 10.1109/DSD.2006.49

[7] Ganguly A, Pande PP, Belzer B, Grecu C. Design of low power & reliable networks on chip through joint crosstalk avoidance and multiple error correction coding. Journal of Electronic Testing. 2008;**24**(1-3):67-81. DOI: 10.1007/s10836-007-5035-1

[8] Sridhara SR, Shanbhag NR. Coding for system-on-chip networks: A unified framework. IEEE Transactions on Very Large Scale Integration (VLSI) Systems. 2005;**13**(6):655-667. DOI: 10.1109/TVLSI.2005.848816

[9] Maheswari M, Seetharaman G. Design of a novel error correction coding with crosstalk avoidance for reliable on-chip interconnection link. International Journal of Computer Applications in Technology. 2014;**49**(1):80-88. DOI: 10.1504/IJCAT.2014.059097

[10] Gracia-Morán J, Saiz-Adalid LJ, Gil-Tomás D, Gil-Vicente PJ. Improving error correction codes for multiple-cell upsets in space applications. IEEE Transactions on Very Large Scale Integration (VLSI) Systems. 2018;**26**:2132-2142. DOI: 10.1109/TVLSI.2018.2837220

[11] Kumar K A, Dananjayan P. Reduction of power consumption using joint low power code with crosstalk avoidance code in case of crosstalk and random burst errors. International Journal of Engineering & Technology. 2018;**7**(3.12):62-68. DOI: 10.14419/ijet.v7i3.12.15864

[12] Fu B, Ampadu P. Burst error detection hybrid ARQ with crosstalk-delay reduction for reliable on-chip interconnects. In: Defect and Fault Tolerance in VLSI Systems, 2009. DFT'09. 24th IEEE International Symposium on 2009; IEEE. pp. 440-448. DOI: 10.1109/DFT.2009.45

[13] Pande PP, Ganguly A, Feero B, Belzer B, Grecu C. Design of low power & reliable networks on Chip through joint crosstalk avoidance and forward error correction coding. In: Null 2006 Oct 4; IEEE. pp. 466-476. DOI:10.1109/DFT.2006.22

[14] Ganguly A, Pande PP, Belzer B. Crosstalk-aware channel coding schemes for energy efficient and reliable NOC interconnects. IEEE Transactions on Very Large Scale Integration (VLSI) Systems. 2009;**17**(11):1626-1639. DOI: 10.1109/TVLSI.2008.2005722

UMA PUBLICATIONS

C PROGRAMMING

CODING & APTITUDE APPROACH

DR. G. SHYAMA CHANDRA PRASAD

Scanned with CamScanner

Uma Publications

ISBN	:	978-81-920425-5-8
C Programming – Coding and Aptitude Approach		
Publisher	:	Himanshu Kulkarni,
		Uma Publications
		C/O R.B.Karkare, KarkareNiwas,
		Mill Road, Kalamandir, Nanded.
Cell	:	+91 9421850831
Mail	:	umapublicationsned@gmail.com
Website	:	umapublishinghouse.com
Cover Design	:	Sriram Kulkarni
Cell	:	+91 9975477661
Layout	:	Ms.Swati Karkare
Printed by	:	Pooja Printers, Pune
Edition	:	2018 Vol-1

All rights reserved by Uma Publications, Nanded.

No part of the publication may be reproduced or distributed.

Rs.220/-

Scanned with CamScanner

C PROGRAMMING

CODING AND APTITUDE APPROACH

Dr G Shyama Chandra Prasad
Matrusri Engineering College, Hyderabad

Scanned with CamScanner